UNIVERSITY OF NAPLES FEDERICO II

DEPARTMENT OF PHARMACY

Ph.D. programme in Pharmaceutical Sciences

Grape seed extract as a source of proanthocyanidins with potential effects on human health

Ph.D. student

Fortuna Iannuzzo

Coordinator
Prof.
ROSARIA MELI

Tutor
Prof.
GIAN CARLO TENORE

XXXV CYCLE (2020-2022)

Preface

This Ph.D. thesis is submitted as a requirement for obtaining the Ph.D.Degree at the University of Naples Federico II (Italy). It is written based on three-years research conducted by the author, Fortuna Iannuzzo, at the Department of Pharmacy in Naples, under the supervision of Prof. Gian Carlo Tenore, at the Department of Galenic Technique of the company S.I.I.T. S.R.L.-INNOVATIVE HEALTHCARE PRODUCTS in Milan (Italy), under the supervision of Dr. Elena Madaro and at the Department of Nutrition and Bromatology, University of Granada (Spain), under the supervision of Prof. José Ángel Rufián-Henares.

Fortuna Iannuzzo

Naples, March 2023

TABLE OF CONTENTS

Chapter 4

Evaluation of Antibacterial Activity of GSE and ATGSE against Escherichia coli in Bladder Epithelial Cell Cultures

Chapter 5

Development of a Potential Nutraceutical Formulation for the Treatment of Urogenital Diseases

List of Publications

- Schiano, E., Annunziata, G., Ciampaglia, R., **Iannuzzo, F.**, Maisto, M., Tenore, G.C., Novellino, E. Bioactive Compounds for the Management of Hypertriglyceridemia: Evidence From Clinical Trials and Putative Action Targets. *Frontiers in Nutrition*. **2020**, 7,586178.

- Maisto, M., Annunziata, G., Schiano, E., Piccolo, V., **Iannuzzo, F.**, Santangelo, R., Ciampaglia, R., Tenore, G.C., Novellino, E., Grieco, P. Potential Functional Snacks: Date Fruit Bars Supplemented by Different Species of Lactobacillus spp. *Foods.* **2021**, 10(8),1760.

- Schiano, E., Piccolo, V., Novellino, E., Maisto, M., **Iannuzzo, F.**, Summa, V., Tenore, G. C. Thinned Nectarines, an Agro-Food Waste with Antidiabetic Potential: HPLC-HESI-MS/MS Phenolic Characterization and In Vitro Evaluation of Their Beneficial Activities. *Foods.* **2022**, 11(7), 1010.

- Maisto, M., Schiano, E., Novellino, E., Piccolo, V., **Iannuzzo, F.**, Salviati, E., Summa, V., Annunziata, G., Tenore, G.C. Application of a Rapid and Simple Technological Process to Increase Levels and Bioaccessibility of Free Phenolic Compounds in Annurca Apple Nutraceutical Product. *Foods.* **2022**, 11(10), 1453.

- Schiano, E., Maisto, M., Piccolo, V., Novellino, E., Annunziata, G., Ciampaglia, R., Montesano, C., Croce, M., Caruso, G., **Iannuzzo, F.**, Summa, V., Tenore, G.C. Beneficial Contribution to Glucose Homeostasis by an Agro-Food Waste Product Rich in Abscisic Acid: Results from a Randomized Controlled Trial. *Foods.* **2022**, 11(17), 2637.

- Maisto, M., Piccolo, V., Novellino, E., Schiano, E., **Iannuzzo, F.**, Ciampaglia, R., Summa, V., Tenore, G.C. Optimization of Phlorizin Extraction from Annurca Apple Tree Leaves Using Response Surface Methodology. *Antioxidants.* **2022**, 11(10), 1933.

- Maisto, M., **Iannuzzo, F.**, Schiano, E., Ciampaglia, R., Labanca, A., Montesano, D., Piccolo, V., Rossi, P., Tenore, G.C. Effects of Fortified Laying Hen Diet with Moringa oleifera Leaves and Goji Berries on Cholesterol and Carotenoid Egg Content. *Foods.* **2022**, 11(20), 3156.

- **Iannuzzo, F.**, Piccolo, V., Novellino, E., Schiano, E., Salviati, E., Summa, V., Campiglia P., Tenore G.C., Maisto, M. A Food-Grade Method for Enhancing the Levels of Low Molecular Weight Proanthocyanidins with Potentially High Intestinal Bioavailability. *International Journal of Molecular Sciences*. **2022**, 23(21), 13557.

- Maisto, M., Piccolo, V., Novellino, E., Schiano, E., **Iannuzzo, F.**, Ciampaglia, R., Summa, V., Tenore, G.C. Optimization of Ursolic Acid Extraction in Oil from Annurca Apple to Obtain Oleolytes with Potential Cosmeceutical Application. *Antioxidants.* **2023**, 12(2), 224.

- Maisto, M., **Iannuzzo, F.**, Novellino, E., Schiano, E., Piccolo, V., Tenore, G. C. Natural Polyphenols for Prevention and Treatment of Urinary Tract Infections. *International Journal of Molecular Sciences*. **2023**, 24(4), 3277.

- Schiano, E., Neri, I., Maisto, M., Novellino, E., **Iannuzzo, F.**, Piccolo, V., Summa, V., Grumetto, L., Tenore, G.C. Validation of an LC-MS/MS Method for the Determination of Abscisic Acid Concentration in a Real-World Setting. *Foods*. **2023**, 12(5), 1077.

- Musto, G., Schiano, E., **Iannuzzo, F.**, Tenore, G.C., Novellino, E., Stornaiuolo, M. Genotoxicity Assessment of Nutraceuticals Extracted from Thinned Nectarine (*Prunus persica* L.) and Grape Seed (*Vitis Vinifera* L.) Waste Biomass. *Foods*. **2023**, 12(6), 1171.

List of Figures

List of Tables

List of Equations

List of Abbreviations

AA: Arachidonic acid

ABTS: 2,2'-azino-bis(3-ethylbenzothiazoline-6-sulfonic acid)

ACN: Acetonitrile

AMPK: AMP-activated protein kinase

AMR: Antimicrobial resistance

ANOVA: Analysis of variance

AR: Androgen receptor

ATCC: American-type culture collection

ATGSE: Alkaline treatment of grape seed extract

BLC: B lymphocyte chemoattractant

BMI: Body mass index

BPH: Benign prostatic hyperplasia

BW: Body weight

C/EBP: CCAAT/enhancer-binding protein

C5a: Fifth complement cascade protein a

CFU: Colony forming units

CH_3COOH: Acetic acid

Cmax: Maximum plasma concentrations

COMT: Catechol-O-methyltransferases

COX: Cyclooxygenase

Ctrl: Control

CV: Coefficient of variation

CVD: Cardiovascular diseases

DHT: Dihydrotestosterone

DMSO: Dimethyl sulfoxide

DP: Degree of polymerization

DPPH: 2,2-diphenyl-1-pycrylhydrazyl

EC50: Half maximal effective concentration

EDTA: Ethylenediaminetetraacetic acid

EGTA: Egtazic acid

ELISA: Enzyme-linked immunosorbent assay

ESI: Electrospray ionization

$FeCl_3$: Ferric chloride

FSB: Fetal bovine serum

GAE: Gallic acid equivalents

GCSF: Granulocyte colony-stimulating factor

GLP-1: Glucagon-like peptide-1

GLUT-4: Glucose transporter- 4

GSE: Grape seed extract

GSP: Grape seed proanthocyanidins

GSPE: Grape seed proanthocyanidins extract

H_2SO: Sulfuric acid

HCl: Hydrochloric acid

HDL: High-density lipoprotein

HESI: Heated electrospray ionization

HF: High fat

HRMS: High-Resolution Mass Spectrometry (HRMS)

HRP: Horseradish peroxidase

IC: Inhibitory concentration

IC50: Half-maximal inhibitory concentration

ICAM-1: Intercellular adhesion molecule 1

IL-1ra: Interleukin-1 receptor antagonist

KC: Keratinocyte chemoattractant

LDL: Low-density lipoprotein

LOX: Lipoxygenase

LPS: Lipopolysaccharide

LUTS: Lower urinary tract symptoms

m/z: mass/charge

MAPK: Mitogen activated protein kinase

MCSF: Macrophage colony-stimulating factor

MeOH: Methanol

MIC: Minimum Inhibitory Concentration

MIP-2: Macrophage-inflammatory protein-2

MN: Molecular networking

MOI: Multiplicity of infection

MS: Mass spectrometry

MTT: 3-(4,5-Dimethylthiazol-2-yl)-2,5-diphenyltetrazolium bromide

Na_2CO_3: sodium carbonate

NaOH: Sodium hydroxide

NCE: Normalized collision energy

NO: Nitric oxide

PAC: Proanthocyanidin

PC: Procyanidin

PCA: Principal component analysis

PD: Prodelphinidin

Ph. Eur.: European Pharmacopoeia

PIMT: Mass tolerance of the precursor ion

PMSF: Phenylmethylsulfonyl fluoride

PP: Properlargonidin

PPAR-γ: Peroxisome proliferator-activated receptor gamma

PSA: Prostate specific antigen

RANTES: Regulated on activation, normal T Cell expressed and secreted

RID: Refractive index detector

ROS: Reactive oxygen species

RP: Reverse phase

RT: Retention time

SCFA: Short-chain fatty acids

SD: Standard deviation

SDF-1: Stromal cell-derived factor-1

SIRT1: Sirtuin 1

SULT: Sulphotransferases

TE: Trolox equivalent

TIMP-1: Tissue inhibitor of metalloproteinases 1

TMPD: N, N, N', N'-tetramethyl-p-phenylenediamine

TPC: Total polyphenolic content

TPTZ: 2,4,6-tris(2-pyridyl)-s-triazine

Trolox: 6-hydroxy-2,5,7,8- tetramethylchromane-2-carboxylic acid

UCP: Uncoupling proteins

UGT: Uridine 50-diphosphate glucuronosyltransferase

UHPLC: Ultra-High-Performance Liquid Chromatography

UPEC: Uropathogenic *Escherichia coli*

UTI: Urinary tract infection

WAT: White adipose tissue

Abstract

Proanthocyanidins (PACs) are a group of bioactive molecules found in a variety of plants and foods that have numerous beneficial effects on human health. Their bioavailability and metabolism depend on their molecular size. Although studies in the literature are quite contradictory, it is generally reported that monomers and dimers of PACs are more bioavailable than those with a higher degree of polymerization (DP). High molecular weight PACs are converted by the colon microflora into lower molecular weight and absorbable metabolites with health-promoting properties. In this regard, if polymeric PACs could be depolymerized into oligomeric ones, their bioaccessibility and bioavailability could also significantly increase. Several depolymerization methods of PACs are described in the literature, but none of them is applicable in the agri-food industry due to the difficulty of execution, high costs and the impossibility to produce food-grade nutraceutical products. One of the most typical sources of PACs is represented by grapes, especially its seeds. Grape skins and seeds are waste products of wine production, nevertheless, they represent a still rich source of bioactive molecules, especially antioxidants. This aspect is part of the green-economy concept and involves the use of agri-food waste as an alternative raw material for the extraction of bioactive compounds to be included in nutraceuticals and dietary supplements. In light of these considerations, this Ph.D. thesis aimed to develop a food-grade, as well as, rapid and economical method for the large-scale production of PACs with high bioavailability and bioaccessibility from a grape seed extract (GSE) (*Vitis Vinifera* L.). Therefore, GSE was subjected to alkaline treatment to depolymerize PAC polymers into low molecular weight monomers and oligomers. The different chemical composition of GSE and its version processed under alkaline conditions (ATGSE) was evaluated

using a molecular networking (MN) approach based on results obtained from HPLC-ESI HRMS/MS characterization analysis. The network analysis mainly noted the PAC cluster with about 142 PAC compounds identified. In particular, the obtained results showed a higher content of monomeric and dimeric PACs in ATGSE compared to GSE, with 58% and 49% monomers and 31% and 24% dimers, respectively. Conversely, trimeric (9%), polymeric (4%), and galloylated PACs (14%) were more abundant in GSE than in ATGSE (6%, 1%, and 4%, respectively). Moreover, *in vitro* antioxidant and anti-inflammatory activities were investigated, showing the high beneficial potential of both extracts. In addition, to evaluate the different intestinal bioactivity and bioaccessibility, GSE and ATGSE were subjected to a human gastrointestinal digestion-colonic fermentation process *in vitro*, carried out at the Department of Nutrition and Bromatology, University of Granada (Spain). Fermentation was carried out using fecal material from five different donors (healthy adults and children, obese, celiac, and cow's milk protein allergic children). For this purpose, the antioxidant profile and short-chain fatty acid (SCFA) production were determined. After *in vitro* gastrointestinal digestion, the bioaccessible polyphenol fraction and antioxidant capacity were higher in the ATGSE sample than in the GSE, while this trend was reversed after *in vitro* fermentation. Nevertheless, ATGSE fermentation showed a higher modulatory effect on the composition and functionality of the gut microbiota of healthy and pathological subjects, which was reflected in a greater increase in SCFA concentration. Literature studies show that structural variations of PACs seem to play an important role in determining their effectiveness. However, it is not possible to make broad generalizations about the structure-bioactivity correlation of PACs, as it is highly dependent on the biological systems in which these molecules act. Therefore, the second part of my Ph.D. project aimed to investigate the potential biological effects of the two extracts with different PAC compositions on human health disorders. In particular, the interest was directed toward diseases of the urogenital system. One of the most important diseases of the

urogenital system in men is benign prostatic hyperplasia (BPH), which leads to non-physiological enlargement of the prostate, especially in old age. Therefore, a first evaluation of the different bioactivity of the two extracts was performed through a study on an animal model of BPH induced by subcutaneous administration of testosterone. At the end of the four weeks of treatment, the weight of the prostates removed microsurgically from the mice was evaluated and hematological and biochemical analyses of blood and tissues were performed. The data showed that oral administration of ATGSE (250 mg/kg) was more effective in reducing prostate weight, PSA levels, and expression of major pro-inflammatory cyto-chemokines in the prostate homogenate. On the other hand, the most common pathology of the urogenital system in women is cystitis, which is caused mainly by the attack of uropathogenic *Escherichia coli* (UPEC) in the bladder epithelium. Therefore, the different bioactivity of the two extracts was tested in an *in vitro* model to evaluate their ability to inhibit the growth and invasion of UPEC (ATCC 700928) in human bladder cells (HT-1376). ATGSE at a dose of 25 mg/mL proved to be more effective than GSE in inhibiting bacterial invasion, showing colony forming units (CFU) of 10^5 and 10^7, respectively. Considering these promising biological effects of ATGSE, the Ph.D. project included a research period at the Department of Galenic Technique of the company S.I.I.T. S.R.L.-INNOVATIVE HEALTHCARE PRODUCTS in Milan, where the most appropriate technological process was developed to obtain a nutraceutical formulation based on ATGSE, through the best possible selection of excipients, ingredients, and strategies for releasing the active ingredient. This technological process allowed to significant increase the density of ATGSE and turn it into a compressible powder. Considering the nature of this PAC-rich food matrix and its sensitivity to gastric pH, the gastro-resistant tablet proved to be the most appropriate choice to increase the bioaccessibility of the active ingredient in the

small intestine. In conclusion, the results obtained suggest that ATGSE could represent an innovative nutraceutical formulation rich in bioavailable and bioaccessible PACs with potential beneficial properties on human health. However, our results highlight the need for further *in vitro* and *in vivo*, before efficacy can be tested in humans.

Introduction

Proanthocyanidins

Structure and Classification

Proanthocyanidins (PACs) are polyphenolic compounds belonging to the class of flavanoids. Specifically, they are oligomers or polymers resulting from the condensation of two or more flavan 3-ol units, consisting of two aromatic benzene rings (A and B) connected by an oxygenated heterocyclic ring (C) (Forbes *et al.*, 2014). The general chemical structure of flavan-3-ol monomers is shown in **Figure 1**.

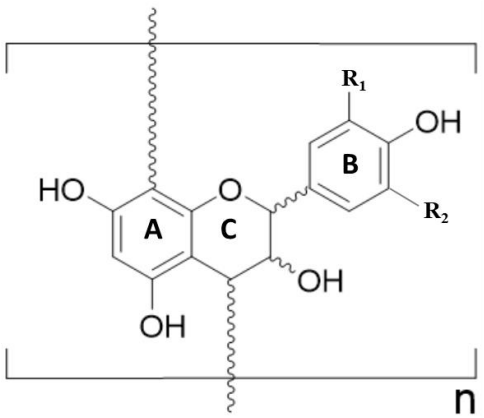

Figure 1. General chemical structure of flavan-3-ol monomers.

Oligomers are formed by the condensation of 2-4 flavan-3-ol units, while polymers are much larger and are formed by the condensation of 5-60 units. The name PACs does not refer to their biosynthetic origin, but to their chemical behavior. They are converted into anthocyanidins when incubated in hot mineral acid (Porter *et al.*, 1986). In contrast to oligomers or polymers, the resulting compounds have a characteristic color ranging from red to blue. They differ in their constituent units, the position of the hydroxyl groups, the interflavanic bonds, and the degree of

polymerization (DP) (Zeng *et al.*, 2020). Depending on the DP, PACs can be classified as monomeric (DP=1), oligomeric (DP=2-4), and polymeric (DP > 4) derivatives. Based on the interflavanic bonds linking monomeric flavan-3-ol units, PACs can belong to A-type or B-type (**Figure 2**). The most common B-type bonds are stable C-C bonds between the C4 of a flavan-3-ol unit and the C8 or C6 of another unit. When binding between two units, the hydroxyl group bonded to the C-ring of each flavan-3-ol can be in the S or R position. As a result, four different B-type PACs can be formed from C4-C8 bonds and four more from C4-C6. In addition to the C-C bond, A-type PACs contain an additional ether bond (C-O-C) between the monomer units, usually a C2-O-C7 ether bond or a C2-O-C5 ether bond.

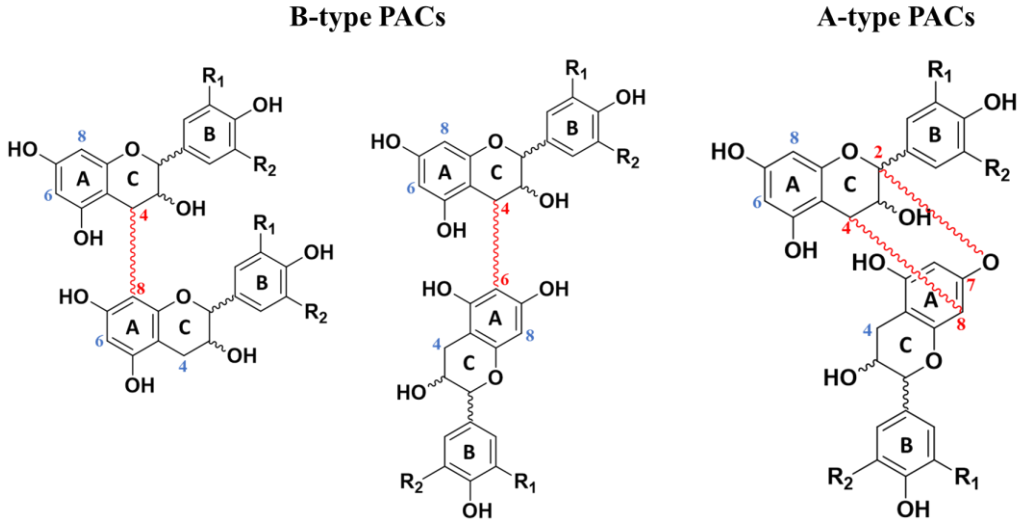

Figure 2. Linkage (red) that allows the polymerization of two monomers of flavan-3-ols, leading to the formation of B-type or A-type PACs.

For the same reasons as described above, four A-type PACs can be formed in this case. Furthermore, galloyl substituents were found in position C3, which are very common in grape seeds (Rigaud *et al.*, 1993; Santos-Buelga *et al.*, 1995). PAC oligomers can consist exclusively of A-type or B-type or both A and B bonds. Based on the position of the hydroxyl groups, three main types of PACs can be

distinguished: propelargonidins (with one hydroxyl group), procyanidins (with two hydroxyl groups), and prodelphinidins (with three hydroxyl groups) (**Figure 3**).

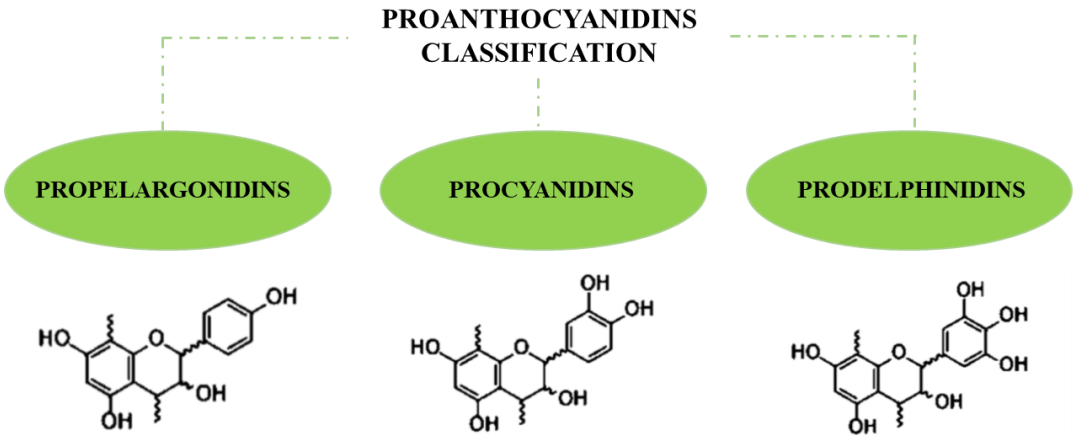

Figure 3. Proanthocyanidins classification.

Procyanidins (PCs) are the most abundant subgroup in food and are a homogeneous group consisting exclusively of (epi)catechin units. When PCs are incubated in warm mineral acid, the extension units are converted to cyanidins, and the terminal unit is released as flavan-3-ol (epi)catechin. Another subgroup is represented by the prodelphinidins (PDs), a heterogeneous group, that contains (epi)gallocatechin unit as well as at least one (epi)catechin unit. When PDs are incubated in warm mineral acid, the extension units (epigallocatechin and epicatechin) are released as delphinidin and cyanohydrin, respectively, while the terminal unit is released as flavan-3-ol (epi)gallocatechin. The third subgroup found in food is propelargonidins (PPs). As with PDs, it is a heterogeneous group, that contains at least one (epi)afzelechin unit in addition to the (epi)catechin units. Therefore, depending on the position of the monomer units, acid depolymerization can lead to the anthocyanidins pelargonidin and/or cyanidin (from the extension units) and the flavan-3-ols (epi)afzelechin or (epi)catechin (from the terminal unit).

Absorption and Metabolism of Proanthocyanidins

The degree of polymerization (DP) and molecular size appears to play an important role in determining the bioavailability and metabolism of PACs. Monomers and dimers are absorbed and present in relatively small amounts in the blood, while those with a high DP cannot be directly absorbed by humans (Donovan *et al.*, 2002; Holt *et al.*, 2002). However, larger oligomers produce smaller and more absorbable molecules when they are metabolized by the colonic microflora, with health-promoting properties (Monagas *et al.*, 2010; Deptez *et al.*, 2000). The main organs involved in the absorption and metabolism of PACs are shown in **Figure 4**.

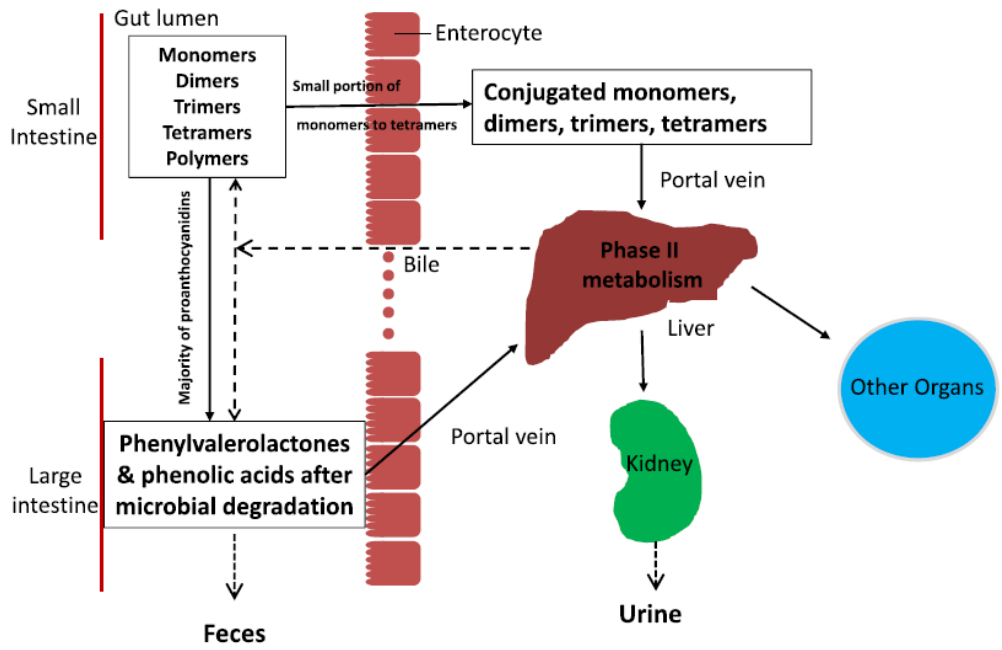

Figure 4. Schematic representation of organs involved in the absorption and metabolism of proanthocyanidins (Ou and Gu, 2014).

- **Absorption and Bioavailability**

The uptake of flavan-3-ol monomers has been studied in detail. Both *in vitro* and *in vivo* studies have shown that monomers and oligomers (DP>4) are more bioavailable than the higher polymeric units, and are rapidly absorbed in the small intestine. In contrast, polymeric PACs have poor absorption and low permeability compared to the corresponding flavan-3-ol monomers, and consequently, oligomeric PACs are also absorbed more slowly than monomeric flavan-3-ols (Holt *et al.*, 2002; Zhang *et al.*, 2016). Thus, the absorption rate of these compounds decreases with increasing molecular weight and structure, which also affects their absorption in different parts of the intestine. *In vitro* studies have demonstrated that the epithelial permeability of dimeric and oligomeric PACs in cultured Caco-2 intestinal cells is higher (Zumdick *et al.*, 2012; Hemmersbach *et al.*, 2013) than that of polymeric PACs, gradually decreasing as the number of monomeric units of which they are composed increases (Zumdick *et al.*, 2012). Similarly, Deprez *et al.* (2011) observed that catechin monomers and dimeric and trimeric PCs had similar permeability coefficients to mannitol, a marker of paracellular transport, on Caco-2 cells of human intestinal epithelial. In contrast, PC polymers with a DP of 7 were not permeable (Deprez *et al.*, 2001). The results of the *in vitro* studies appear to be consistent with the *in vivo* scientific evidence reported in the literature. Serra *et al.* (2020) demonstrated that after oral administration to rats of a grape seed extract (GSE), monomers, dimers, and trimers of PCs are rapidly absorbed into the plasma, reaching a maximum concentration 1 hour after ingestion (Serra *et al.*, 2010). Similarly, a study conducted by Shoji *et al.* (2006) showed that after administration of 1g/kg of apple to rats, the maximum plasma concentrations (Cmax) of epicatechin, dimeric procyanidin B2, and trimeric procyanidin C1 in plasma were 1.3 μM, 0.4 μM, and 0.14 μM, respectively. Specifically, dimer and trimer concentrations peaked 2 hours after administration, while monomer concentrations peaked 1 hour after

administration (Shoji *et al.*, 2006). Moreover, the maximum plasma concentration of PACs in plasma is dose-dependent. In this context, Stoupi *et al.* (2010) conducted a study in an animal model in which they administered two different doses of pure procyanidin B2 at 10.5 mg/kg and 21 mg/kg respectively and found maximum plasma concentrations of 1.38 µg/ml and 2.6 µg/ml, respectively. Furthermore, human studies also seem to confirm the better and easier absorption of monomers and oligomers of PACs in the human intestinal tract. Literature studies report that dimeric PCs are detected mainly in the serum and plasma of patients who eat foods rich in PACs (Holt *et al.*, 2002; Sano e*t al.*, 2003). Furthermore, a study by Wiese *et al.* (2015) showed that after ingestion of a single dose of 1 mg epicatechin and procyanidin B1/kg body weight, both intact molecules and their metabolites were detected in plasma within 8 hours. On the contrary, ingestion of polymeric PCs at a dose of 2 mg/kg of body weight did not show the presence of metabolites or derived dimeric and oligomeric PCs in plasma (Wiese *et al.*, 2015). A recent study compared the plasma concentration of (-)-epicatechin in human blood and urine after volunteers were given a cocoa drink containing monomers of (-)-epicatechin and PC polymers with a DP of 2 to 10. All (-)-epicatechin absorbed into the blood or urine was from ingested (-)-epicatechin. No (-)-epicatechins were derived from ingested oligomers and polymers (Ottaviani *et al.*, 2012). These studies provide further evidence that the biological activity of different flavanols varies according to their molecular size and DP. The higher uptake of monomers and oligomers compared to polymers with higher DP has led to increased interest in oligomer-rich food sources with low DP PACs. However, as foods souces of PACs are more likely to contain polymeric molecules, research efforts have focused on developing processing methods to convert the naturally occurring and more abundant high DP oligomers into low DP monomers and oligomers.

- **Metabolism in the Small Intestine and Liver**

PACs can be absorbed in the small intestine or as intact molecules or they can be metabolized by conjugation reactions such as glucuronidation, sulphation, and methylation. The small intestine is the primary site of glucuronidation, which occurs in the luminal part of the endoplasmic reticulum through the action of uridine 50-diphosphate glucuronosyltransferase (UGT) (Monagas *et al.*, 2010b). Sulphation and methylation occur mainly in the liver via cytosol sulphotransferases (SULT) and catechol-O-methyltransferases (COMT) (Monagas *et al.*, 2010b). However, it has been reported that a high concentration of PAC dimers and their galloyl fractions can inhibit the activity of COMT and reach the plasma in an unchanged form. Generally, part of the monomeric or oligomeric flavan-3-ols is absorbed into the blood in the small intestine, while the other part is transported into the liver and undergoes phase II metabolism, producing glucuronide, sulfate and/or methylated metabolites, which are then returned to the small intestine in conjugated forms via the bile (Ou *et al.*, 2014). After ingestion, PACs and their metabolites travel through the bloodstream to the various organs and tissues, where they are further metabolized or can directly exert their beneficial effects. However, which PAC molecules reach the intestine unchanged and which are metabolized is not yet fully understood. To this end, Shrestha *et al.*(2012) have demonstrated that when the B2 dimer is incubated with liver microsomes, only minor glucuronidated products are detected in the liver microsomes, while most of the B2 remains unmetabolized. In contrast, Baba *et al.* (2002) found that procyanidin B2 is partially degraded *in vivo* to epicatechin, which was found conjugated or methylated in rat plasma. This result was confirmed by Bittner *et al.* (2014), who showed that high concentrations of the conjugated forms of 3'O-methyl-epicatechin and 4'-O-methyl-epicatechin are found in the plasma of pigs after oral administration of procyanidins B4. Furthermore, glucuronidated conjugates of these metabolites were also detected, suggesting that procyanidin B4

could be degraded into monomeric subunits in pigs and then further metabolized to methylated and glucuronidated conjugates (Bittner *et al.*, 2014). A similar experiment was conducted in humans, showing that ingestion of epicatechin and procyanidin B1 resulted in the appearance of the conjugated forms of epicatechin (3'O-methyl-epicatechin and 4'-O-methyl-epicatechin) and procyanidin B1 (methyl-O-procyanidin B1) in plasma and urine within 8 hours (Wiese *et al.*, 2015). Therefore, epicatechin and procyanidin B1 could be absorbed in humans and converted into conjugated and methylated metabolites (Wiese *et al.*, 2015). As the above studies show, monomeric and oligomeric PCs can be readily absorbed in the small intestine as metabolites or intact molecules. Although polymeric PACs are less bioavailable in the intestine, they reach the colon where they are metabolized by the gut microbiota into low molecular weight metabolites that can be absorbed in the gastrointestinal tract, indicating a potential role of gut microbiota metabolites in exerting adverse effects. pharmacological.

- **Microbial Metabolism**

Most PACs, especially the polymeric ones, reach the colon after passing through the small intestine, where only small amounts are absorbed. Polymeric PACs in the colon are further depolymerized by the gut microflora into low molecular weight monomers and oligomers or metabolized into low molecular weight aromatic metabolites, such as phenolic acids, phenylvalerolactones, and phenylacetic acids, and absorbed in the intestine (Tao *et al.*, 2019; Ou *et al.*, 2014; Cires *et al.*, 2017). The colonic metabolites formed could contribute to the health-promoting effects of PACs (Russell *et al.*, 2013). The role of the gut microbiota in the catabolism of PACs has often been studied using a static anaerobic incubation system in which they were fermented with freshly harvested human colonic fecal bacteria. Using this system, Deprez *et al.* (2000) demonstrated that the polymeric PCs of willow were completely degraded after 48 hours of incubation. The main catabolites included 3-(3'-

hydroxyphenyl)propionic acid, 4-hydroxyphenyl acetic acid, 3-(4'-hydroxyphenyl)propionic acid, and 3-phenyl propionic acid (Deprez *et al.*, 2000). Another *in vitro* study demonstrated that the major metabolites identified after fermentation of dimeric PACs purified with human fecal microbiota were 2-(3,4-dihydroxyphenyl) acetic acid and 5-(3,4-dihydroxyphenyl)-γ-valerolactone (Appeldoorn *et al.*, 2009). However, the microbial metabolism of PACs varies depending on the different compositions of the food matrix in which they are contained. In this regard, a recent study demonstrated that the ingestion of PACs-rich extracts from red wine and grape seeds in rats resulted in the presence of 35 metabolites in plasma and urine, including structurally related metabolites of (epi)catechin and 5-carbon side chain ring fission metabolites (phenyl-γ-valerolactone and phenylvaleric acids), and 50 metabolites, including phenolic acids and aromatic catabolites (Pereira-Caro *et al.*, 2020). However, in another study, the presence of metabolites such as m-hydroxyphenyl propionic acid, ferulic acid, 3,4-dihydroxyphenylacetic acid, m-hydroxyphenyl acetic acid, vanillic acid, and hydroxybenzoic acid was detected in urine samples from human volunteers after cocoa intake (Rios *et al.*, 2003). However, several studies have described phenylvalerolactones as the major metabolites of tea catechins produced by gut microorganisms and detected in human urine and blood (Ou et al., 2014). However, the ability of bacteria to catabolize PACs in the gut decreases with increasing molecule size. Therefore, DP is an important factor influencing the microbial metabolism of these compounds. Gonthier *et al.* (2003) demonstrated that the yield of phenolic acids in the urine of rats after consumption of foods containing monomers and oligomers of PCs was 10% and 7% for monomers and dimers, while it decreased to 0.7% and 0.5% for trimers and polymers, respectively. This result was confirmed by Goodrich *et al.* (2015) who demonstrated that after GSE ingestion in rats, the concentration of monomers was statistically lower in the distal colon after 6 hours, while the concentration of dimers and oligomers, was not statistically

different in the distal colon after 3h and 6h, suggesting that dimers and oligomers may be more difficult to degrade by the gut microbiota than monomers (Goodrich *et al.*, 2015).

Food Sources of Proanthocyanidins

PACs are usually found in flowers, leaves, fruits, barks, nuts, grains, and seeds of various plants, as a defense against biotic and abiotic stress factors. Their astringency protects plants from pathogens and predators. Berries and fruits are the best sources of PACs, Lingonberry, cranberry, black elderberry, black chokeberry, blackcurrant, and blueberry are some of the edible berries with the highest content of PACs (Kren *et al.*, 2007). Commonly consumed foods rich in PACs include wine, grape seeds, cranberries, red goji berries, pomegranates, red rice, cocoa, chocolate, and tea (Hellstrom *et al.*, 2009). According to a study conducted, the highest contents per fresh weight were found in chokeberry, rosehip, and cocoa products (Hellstrom *et al.*, 2009; Patel, 2007). PACs are also present in medlar, mulberry, plum, apricot, and walnut, so they are ubiquitous in almost all fruits (Qin *et al.*, 2009). Furthermore, the content, composition, and nature of PACs vary greatly between different plants. A few foods, such as cashews and black beans, contain only PAC monomers and dimers, while most foods, including cranberries, cranberries, strawberries, grapes, and pinto beans contain PACs with different DPs (Gu *et al.*, 2004). B-type PACs are abundant in grapes, blueberries, cocoa, and apples, while plums, avocados, peanuts, curry, cinnamon, and cranberries have been identified as potential sources of A-type PACs (Gu *et al.*, 2003). The content, the type of interflavanic bonds, and the DP of PACs in some selected foods are shown in **Table 1**.

Table 1. Proanthocyanidins (PACs) content of selected food (mg/100g food) (Adapted from Gu et al., 2004).

Food/spice	Dimers	DP3-10[a]	DP>10[a]	Total	Type[b]
Apple, red delicious, with peel	14	64	38	116	B, PC
Blueberries	7	40	129	176	B, PC
Chocolate, baking	207	680	551	1438	B, PC
Chocolate, milk	26	105	33	164	B, PC
Cinnamon, ground	256	5319	2509	8084	A, B, PC, PP
Cranberries	26	152	234	412	A, B, PC
Grape seed (dry)	417	1354	1100	2871	B, PC
Grapes, red	2	19	59	80	B, PC
Pecans	42	211	223	476	B, PC, PD
Plums, black	16	100	115	231	A, B, PC

[a]DP3-10 indicates values for trimers through decamers summed; DP> 10 indicates values for polymers DP >10, which eluted as a single chromatographic peak.
[b]Linkage type (A, B) and PACs subclasses (PC-procyanidin, PD- prodelphinidin, PP-propelargonidin) identified.

Biological Properties of Proanthocyanidins

The beneficial properties of PACs on human health have been extensively studied. Previous studies have found a positive correlation between PACs consumption and disease risk, as well as their antiradical, anticancer, and anti-inflammatory effects due to the presence of a large number of phenyl hydroxyl groups (Gonthier *et al.*, 2003). These properties may be related to the structure of the PAC units and their DP. However, the correlation between DP and the biological activities of PACs cannot be extensively summarized, as it strictly depends on the different biological systems in which they act (Bitzer *et al.*, 2015). In most cases, PAC activities are proportional to DP, but in some cases, a reverse trend is observed. In some systems, there appears to be an optimal DP above or below which PAC activity is reduced (Dorenhott *et al.*, 2014). However, *in vitro* studies conducted to evaluate the bioactivity of condensed tannins could lead to contradictory results, as most of the ingested PACs could exert their effects only at the level of the gastrointestinal tract due to their low bioavailability. They could exert their

biological effects in two different ways: as complex and non-absorbable molecules with binding properties that can cause local effects in the gastrointestinal tract, or as small absorbable compounds. The low molecular weight metabolites derived from the microbial degradation of PACs in the colon could easily pass the intestinal barrier and reach numerous tissues and organs via blood and lymphatic circulation (Cires *et al.*, 2017). Some main biological effects of PACs are described in the following paragraphs and reported in **Figure 5**.

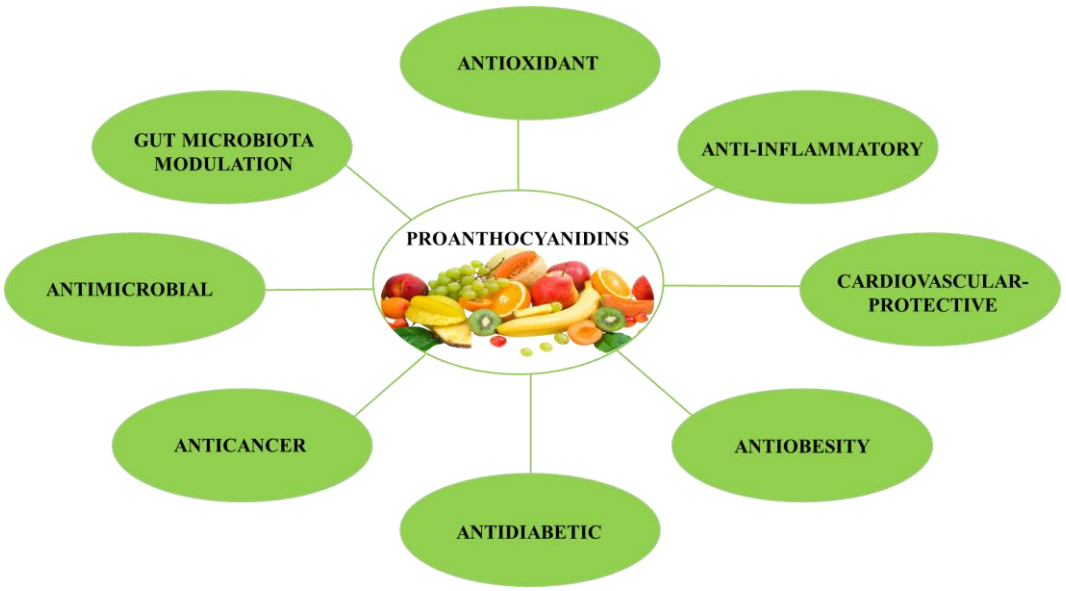

Figure 5. Main health benefits of proanthocyanidins.

- **Antioxidant Activity**

Oxidative stress is a major cause of cell damage even under normal physiological conditions. The cellular damage and metabolic disorders caused by oxidative stress can be effectively counteracted by antioxidants, which counteract the effects of free radicals and protect against molecular and cellular damage (Pandey and Rizvi, 2009). PACs have been extensively studied for their potential activities as antioxidants. The smaller PACs were found to be more effective than the larger

PACs as scavengers of superoxide anions, free radicals, and oxidized xanthine inhibitors (Arimboor and Arumughan 2012; Lee *et al.*, 2007). In this regard, one study examined the ability of A-type oligomeric PCs from the pericarp of *Litchi chinensis* to scavenge 2,2-diphenyl-1-picrylhydrazyl (DPPH) radicals, showing that the antioxidant activity significantly reduced with increase in the molecular weight of the compounds (Li *et al.*, 2012). Another study showed that the antioxidant activity of mangosteen pericarp tannins increases when the mDP (mean degree of polymerization) is 2,71-9,27 but decreases when it is 16,80 (Zhou *et al.*, 2011). On the other hand, some highly polymerized tannins containing several hydroxyl groups were found to have stronger antioxidant activity than monomeric phenols. Thus, polymeric PACs showed a higher protective effect against oxidative stress-induced cytotoxicity in liver cells compared to oligomeric ones (Kim *et al.*, 2013). In addition, other studies have shown that high molecular weight PCs are more effective when oxidation begins in the lipid domains, probably because these molecules insert into the lipid membrane and provide better protection against oxidative stress in the hydrophobic domains than in the hydrophilic domains. However, monomers, dimers, and trimers are most effective as antioxidants when the liposomes begin to oxidize in the aqueous phase (Lotito *et al.*, 2000).

- **Anti-inflammatory Activity**

Inflammation, together with oxidative stress, is a mechanism underlying many diseases, and PACs have been proposed in many studies as bioactive ingredients for the prevention or treatment of disorders and infections, thanks to their high antioxidant and anti-inflammatory activity. PACs have been shown to improve inflammation through a range of activities: inhibition of cyclooxygenase (COX) and lipoxygenase (LOX); modulation of cytokine secretion; regulation of the pro-inflammatory NF-κB pathway and regulation of mitogen activated protein kinase (MAPK) phosphorylation (Zeng *et al.*, 2020). Studies have shown that polymeric

PACs from pistachio showed a significant reduction in NF-κB activation and secretion of pro-inflammatory eicosanoids (PGE2) and cytokines (TNF-α) in LPS-stimulated mouse macrophages compared to oligomeric PACs (Gentile *et al.*, 2012). Oligomeric PACs from persimmon and green tea (mDP ~3.3) showed a greater reduction of oxidative stress, and kidney and liver inflammation than polymeric ones in diabetic rats (Gentile *et al.*, 2012). In human peripheral blood mononuclear cells (lymphocytes, monocytes, macrophages), only cocoa PACs with DP ≥ 4 were able to stimulate the secretion of anti-inflammatory IL-4. In contrast, only monomeric cocoa PACs were able to increase IL-4 secretion in the same cells stimulated with mitogen (phytohaemagglutinin) (Mao *et al.*, 2000). In human monocytes, A-type PACs from peanuts effectively inhibited inflammation in response to LPS stimulation, with dimers and trimers more active than monomers or tetramers (Tatsuno *et al.*, 2012). In human colon cells, polymeric B-type PACs inhibited inflammation and the loss of barrier integrity more effectively than monomers and oligomers (Bitzer *et al.*, 2015).

- **Cardiovascular-Protective Activity**

Among the most studied protective cardiovascular effects of PACs is their ability to improve vascular function by stimulating nitric oxide (NO) production and vasorelaxation. DP appears to have a significant impact on the vascular effects of PACs. Studies have shown that low-molecular-weight PCs from grape seeds reduce hypertension in hypertensive rats, and the mechanism may be related to an increase in the bioavailability of endothelial NO, thereby improving endothelial dysfunction (Belcaro *et al.*, 2013; Draijer *et al.*, 2015). In human endothelial cells, oligomeric PACs from apples (mDP ~3.9) induce cell cycle arrest and inhibit cell proliferation and migration more effectively than monomeric and dimeric PACs (Garcıa-Conesa *et al.*, 2009). In rat aortic endothelial cells, trimeric PACs induce the production of NO, while monomeric and dimeric PACs have no effect (Byun *et al.*, 2012). In rat

aortic rings, grape PACs with DP > 2 induce endothelium-dependent vasorelaxation more effectively than monomeric and dimeric PACs, and galloylation also enhances the activity of grape PACs regardless of their DP (Fitzpatrick *et al.*, 2000). In rat thoracic aorta, monomeric and oligomeric red wine PACs (DP ≤ 4) induce NO-dependent endothelial relaxation more effectively than polymeric PACs (DP > 4) (Andriambeloson *et al.*, 1998). In porcine coronary arteries, oligomeric PACs (DP 2-4) stimulate NO production and induce vasorelaxation to a greater extent than monomeric PACs (Taubert *et al.*, 2002). Further research has shown that PACs play an important role in the prevention of atherosclerosis and the regulation of lipid metabolism. PACs can inhibit the binding of oxidized LDL to the lectin-like oxidized LDL receptor-1, which is involved in the development of atherosclerosis (Mizuno et al., 2017). Furthermore, oligomeric PACs from grapes (DP 2-4) significantly reduced total cholesterol and VLDL and increased HDL in cholesterol-fed mice, while monomeric PACs had no effect (Tebib *et al.*, 1994).

- **Anticancer Activity**

Cancer is the uncontrolled growth of transformed cells, and their ability to invade tissue and metastasize can be controlled by a diet rich in antioxidants. The major effects of PACs in inhibiting carcinogenesis include their antiproliferative and cytotoxic activities, cell cycle inhibition, and induction of tumor cell apoptosis. Studies have shown that oligomeric PACs can alter genes involved in the cell cycle and DNA replication. In addition, they showed a significant effect in reducing tumor growth in xenografts and inhibiting organoid formation in colorectal cancer (Ravindranathan *et al.*, 2018). In an Italian case-controlled study, high consumption of PCs was shown to reduce the risk of endometrial cancer in normal-weight women. In particular, PCs with a DP > 3 derived from beans soups, chocolate, legume, and grapes were more effective than other classes of flavonoids in reducing the risk of uterine cancer (Rossi *et al.*, 2013). In this regard, other studies have also shown that

oligomeric and polymeric PCs have a stronger antiproliferative effect in contrast to monomeric and dimeric PCs. In a study conducted by Lizagarra *et al.* (2007), it was shown that the antiproliferative effect of grape and pine bark PCs in colon carcinoma HT 29 tumor cells increased with increasing DP and galloylation rate (Lizarraga *et al.*, 2007). Therefore, higher molecular weight compounds showed more effective inhibition of cell proliferation and induction of cell cycle arrest or apoptosis. In another study, a fraction of PACs with an mDP of ~5.2 was shown to exert a stronger antiproliferative and cytotoxic effect on prostate and liver cancer cells than fractions of PACs with a lower mDP (Schmidt *et al.*, 2004). Conversely, other scientific evidence reports that the beneficial effect of PCs decreases with increasing DP. In this regard, a study conducted by Shoji and collaborators (2005) demonstrated that PCs isolated from apples drastically suppressed melanin production in melanoma cells, with the inhibitory effect of PCs being greater for the trimer than for the tetramer and pentamer (Shoji *et al.*, 2005). In a pilot study in humans, it was shown that three-month treatment with oligomeric PCs of lower size significantly reduce the risk of lung cancer (Mao *et al.*, 20019; Xue *et al.*, 2018). Thus, it is not possible to make generalizations about the bioactivity of PACs in cancer treatment, as it is influenced not only by their structure and DP but also by the diversity of the biological systems in which they act.

- **Antimicrobial Activity**

Given the development of antibiotic resistance in microbes and the widespread side effects of conventional pharmaceutical antibiotics, polyphenols are gaining increasing interest as natural antimicrobial agents. Numerous clinical studies have shown that cranberry PACs juice has an important effect on the prophylaxis of recurrent urinary tract infections (UTIs) (Jepson *et al.*, 2012). The mechanisms of action of PACs on UTIs are adhesion inhibition of microbial pathogens to uroepithelial cells, reduction of bacterial swarm motility and biofilm formation, and

reduction of infection-related inflammation. A-type PACs from cranberries have been shown to inhibit bacterial adhesion and reduce UTIs symptoms, while B-type PACs from grapes and other sources have little or no effect (Foo *et al.*, 2000; Howell, 2007; Howell *et al.*, 2005). In this regard, Nicolosi *et al.* (2014) investigated the anti-adhesion activity of procyanidin A2 on pathogenic strains such as uropathogenic *Escherichia coli* (UPEC) and *Proteus mirabilis* using a human bladder cancer cell line (HT1376). A significant reduction in the adhesion rate of both UPEC and *Proteus mirabilis* strains was observed compared to the control. Other authors, to evaluate the anti-adhesive effect of two potential procyanidin-based products, a cranberry powder (containing 9 mg PAC/g of extract) and a cranberry extract, on P-fimbriated UPEC, developed two *in vitro* models: the first with bladder epithelial cells and the second with vaginal epithelial cells. The anti-adhesion effect was evaluated before and after treatment with these products. Cranberry powder reduced the mean adhesion of UPEC to vaginal epithelial cells from 18.6 to 1.8 bacteria per cell ($p < 0.001$). The mean adherence of *Escherichia coli* to primary cultured bladder epithelial cells was reduced from 6.9 to 1.6 bacteria per cell in a dose-dependent manner by treatment with 50 µg/ml PACs extract ($p < 0.001$) (Gupta *et al.*, 2007). These studies provide further evidence of the biological relevance of cranberry PAC products in the prevention of UTIs. However, the ability of A-type PACs to inhibit bacterial adhesion was shown to be greater for molecular compounds with $DP \geq 3$, while monomeric and dimeric PACs were found to be relatively effective in the treatment of UTIs. Other studies reported the antibiofilm properties of cranberry PACs on *Pseudomonas aeruginosa*, suggesting that condensed tannins could be a useful therapy against biofilm-mediated infections caused by *P. aeruginosa* (Ulrey *et al.*, 2014). Moreover, cranberry A-type PACs have been shown to effectively alleviate oral candidiasis by reducing *Candida albicans* adhesion and attenuating the inflammatory response by inhibiting NF-κB p65 activation and phosphorylation of specific kinases intracellular signaling (Feldman *et al.*, 2012). Other food sources

rich in PACs, such as grape extract, have been shown to be effective in reducing the number of viable cells for *Listeria monocytogenes* (Bisha *et al.*, 2010*).* Some studies have highlighted the beneficial effect of products based on A-type and B-type PCs in oral cavity infections. An example of such a beneficial effect has been found in dental caries models, including improvement of the mechanical strength of dentin, prevention of bacterial adhesion and biofilm formation by oral bacteria, inhibition of dentin demineralization, inhibition of dentin degradation by matrix metalloproteinases, inhibition of caries formation in animals and reduction of salivary load by *Streptococcus mutans* in humans (Girardot *et al.*, 2014; Xie *et al.*, 2008; Epasinghe *et al.*, 2013; Koo *et al.*, 2010; Weiss *et al.*, 2004). Furthermore, PACs appear to exert beneficial activities in periodontal disease models, including inhibition of oral bacteria growth, inhibition of bacterial lipopolysaccharide (LPS)-induced gingival inflammation, and reduction of periodontitis in animals and humans.

- **Antidiabetic Activity**

Diabetes is a chronic metabolic disease in which glucose metabolism is impaired due to a toxic effect on the pancreatic gland and a resulting insulin deficiency. A severe diabetic condition can lead to neuropathy, retinopathy, or nephropathy. Dietary PACs exert their antihyperglycemic effects through several mechanisms: stimulation of glucose uptake in insulin-sensitive tissues; action on glycolytic and gluconeogenic liver enzymes to reduce glucose production; modulation of various pancreatic β cell functions, such as preventing oxidative stress, increasing insulin secretion and promoting β cell survival. The positive effect of grape seed proanthocyanidins (GSP) in the treatment and prevention of diabetes is described in numerous scientific evidence. A study conducted by Ding *et al.* (2013) showed that GSP can increase normal insulin levels and reduce the number of apoptotic cells in rats with type 2 diabetes. Similarly, a study by Cedo *et al.* (2013) demonstrated that

PCs from grape seeds can modulate apoptosis and proliferation of β cells, improve insulin resistance, and counteract insulin synthesis in rats. Furthermore, supplementation with GSPE attenuated oxidative stress by inhibiting lipid peroxidation, restoring endothelial function, and reducing the risk of vascular disease in diabetes (Okudan *et al.*, 2011). Other studies have shown that A-type oligomeric PCs from lychee pericarp and B-type oligomeric PCs from lotus seed improve glucose homeostasis in diabetic mice by increasing the expression of glucose transporter- 4 (GLUT-4) and insulin receptor protein α in liver and muscle tissues, and activating several enzymes related to glucose metabolism (Liu *et al.*, 2016). In general, the studies conducted have shown that oligomeric and polymeric PCs exert their antidiabetic effects by stimulating glycogen synthesis and glucose uptake in skeletal muscle (Bowser *et al.*, 2017). However, the literature shows that PACs with different sizes exert distinct effects on the central signaling pathways of type 1 and type 2 diabetes mellitus. In experiments on an animal model, tetrameric PACs were shown to stimulate glucagon-like peptide-1 (GLP-1) secretion and insulin secretion levels more effectively than monomers and trimers (Yamashita *et al.*, 2013). In a study conducted by Yamashita *et al.* (2012b), low DP (DP ≤ 3) and high DP (DP ≥ 4) PC fractions from cocoa liquor were evaluated for the prevention of hyperglycemia *in vitro*. PACs with DP ≥ 4 showed more effective stimulation of glucose uptake by the glucose transporter (GLUT-4) in skeletal muscle cells than smaller PACs (DP ≤ 3), while the high DP fraction showed a greater inhibitory effect on α-glycosidase activity in small intestinal skeletal muscle than the low DP fraction, thereby slowing intestinal glucose uptake more effectively (Yamashita *et al.*, 2012b). In diabetic mice, B-type PACs oligomers were more effective than A-type oligomers in lowering fasting blood glucose, while A-type oligomers were more effective in increasing pancreatic insulin expression, blood insulin, and insulin sensitivity (Chen *et al.*, 2012). In a mouse model of obesity and type 2 diabetes, oligomeric cocoa PCs were shown to be more effective than monomeric and polymeric PCs in inhibiting

the onset of obesity and pre-diabetes following a high-fat (HF) diet, thereby improving weight gain, fat mass, glucose tolerance, and insulin resistance (Dorenkott *et al.*, 2014). Similarly, another study in diabetic rats showed that oligomeric PACs (mDP ~3) reduced blood glucose levels more effectively than polymeric PACs.

- **Antiobesity Activity**

Obesity is a metabolic disease with a high probability of developing metabolic syndrome in which cholesterol, lipid, and glucose levels increase, thus leading to diabetes and heart diseases. PACs exert their antiobesity effects through several molecular mechanisms, such as the reduction of weight and body mass, the reduction of energy intake, the regulation of glucose and lipid metabolism, and the increase of energy expenditure (Salvadó *et al.*, 2015). In a study by Zhou *et al.*, a PAC extract from bay leaves was shown to alleviate obesity in an obese rat model fed a high-fat (HF) diet. The rats treated with the bay leaf extract showed a significant weight reduction compared to the HF group. The antiobesity effect of PACs is probably due to the upregulation of SIRT1 expression, inducing PPAR-γ deacetylation, upregulation of C/EBP-γ and BMP 4 expression, and increasing brown fat content (Zhou *et al.*, 2017). Another study conducted by Yamashita *et al.*, investigated the antiobesity and hypoglycemic effect of a cocoa liquor extract rich in PC (containing 4.3% catechin, 6.1% epicatechin, and 39, 4% PCs) in a model of obese C57BL/6 mice fed an HF diet. The results showed a significant reduction in hyperglycemia, glucose intolerance, and fat accumulation in white adipose tissue (WAT). In addition, this extract has been shown to promote the translocation of glucose transporter 4 (GLUT4) and phosphorylation of AMP-activated protein kinase (AMPKa), by upregulating the expression of uncoupling proteins (UCPs) in skeletal muscle and adipose brown tissue and increasing the secretion of adiponectin in WAT (Yamashita *et al*., 2012a). In other animal studies, the effect of GSPE on body weight and fat deposition was investigated in hamsters fed both a standard diet and an HF

diet. At the end of the experiment, a significant decrease in body weight, adiposity index, and weight of all WAT depots examined, especially the retroperitoneal WAT, was observed in both groups treated with GSPE. However, it has been widely reported in the literature that the antiobesity activity of PACs is strictly dependent on their size and DP. Studies conducted have demonstrated the antiobesity effect of PC apple extract through *in vitro* studies on the inhibition of digestive enzymes, such as pancreatic lipase, and through *in vivo* studies on the reduction of triglyceride absorption. These inhibitory effects of PCs increase progressively depending on their DP. In this regard, pentameric or oligomeric PCs showed the maximum inhibitory effects on pancreatic lipase both *in vitro* and *in vivo* in mice and humans, leading to a reduction in plasma triglyceride levels (Sugiyama *et al.*, 2007). In another study conducted by Dorenkott *et al.*, the antiobesity effects of cocoa flavanols were evaluated in C57BL/6J mice. The cocoa extract was fractionated into three fractions with different PC compositions: a monomeric fraction, an oligomeric fraction, and a polymeric fraction. Mice were divided into six groups (n=9) receiving either a low-fat control diet, an HF control diet, or an HF control diet supplemented with 25 mg/kg*BW/day of cocoa extract and with 25 mg/kg*BW/day of cocoa fractions (monomer-rich fraction, oligomer-rich fraction and polymer-rich fraction). After 12 weeks of treatment, the weight of the mice decreased in all groups, in particular, the oligomer-rich fraction was found to be more effective in preventing weight gain (Dorenkott *et al.*, 2014). Furthermore, some recent studies have reported that the effects of PACs on obesity are associated with intestinal microbial species. In this regard, treatment with apple PACs with a high non-absorbable polymers content has been shown to prevent the increase in body weight and visceral fat, and reduce inflammation and intestinal permeability by regulating the expression of genes related to lipid metabolism in C57BL/6J mice fed an HF and high-sugar diet. In addition, polymeric PACs showed significant modulation of the gut microbiota by improving the *Firmicutes/Bacteroidetes* ratio and increasing the proportion of

Akkermansia (Masumoto *et al.*, 2016). In this regard, a recent study has shown that procyanidin B2 can modulate the gut microbiota by improving the proportions of *Bacteroidetes* at the phylum level and *Akkermansia* at the genus level, and preventing weight gain in an animal model with a high-cholesterol diet (Xing *et al.*, 2019).

- **Gut Microbiota Modulation**

The gut microbiota has a profound impact on the nutritional, developmental, and immune functions of the host, and the interaction between PACs and the gut microbiota has been shown to play an important role in human health (Chen *et al.*, 2022). Therefore, a careful analysis of the mechanisms underlying these interactions allows a better understanding of the beneficial effects of PACs on gut health. PACs contain numerous hydroxyl groups, which help inhibit bacterial adhesion and coaggregation, and possess antimicrobial properties against several specific microbes, including commensal and pathogenic microorganisms (Ghouila *et al.*, 2017; Baydar *et al.*, 2006). In addition to their antimicrobial activity, PACs have a prebiotic effect by interacting with the intestinal microflora and stimulating the growth of specific bacterial populations. As reported in the previous paragraph, colonic microorganisms express a large number of enzymes that can metabolize PACs and produce a range of metabolites. The reactions catalyzed by bacterial enzymes are hydrolysis, dehydroxylation, demethylation, decarboxylation, and deconjugation (Walle *et al.*, 2003). *Clostridium* and *Eubacterium* have been proposed as the major bacterial genera involved in the metabolism of flavan-3-ols (Selma *et al.*, 2009). In addition to the metabolites produced by the previously described PACs in the colon, the gut microbiota is also responsible for the production of metabolites resulting from the fermentation of dietary fiber in the colon, i.e. short-chain fatty acids (SCFA), including acetate, propionate, and butyrate (Laparra *et al.*, 2010). Several literature studies report the ability of PACs to increase the production

of SCFA in the colon, although the molecular mechanism underlying this effect is not fully understood (Chen *et al.*, 2022). This mechanism is likely due to their ability to modulate the composition of the gut microbiota. Studies have shown that PACs can stimulate the growth of a variety of probiotics, such as *Bifidobacterium spp*. and *Lactobacillus spp*. Thus, incubation of apple PACs with the human colonic microbiota showed a significant increase in the relative abundance of *Bifidobacteria* and *Faecalibacterium prausnitzii*, which may be associated with potential human health benefits (Koutsos *et al.*, 2019). In a similar model, PAC extracts from grape seeds led to a significant increase in the number of *Bifidobacterium spp*. and the *Lactobacillus-Enterococcus* group and growth inhibition of the *Clostridium histolyticum* group and the *Bacteroides-Prevotella* group (Zhou *et al.*, 2016). Other PAC-rich foods have also been shown to improve diet-induced obesity, metabolic syndrome, and insulin resistance, by increasing the proportion of *Akkermansia* and decreasing the *Firmicutes/Bacteroidetes* ratio (Chen *et al.*, 2022). The effect of PACs on modulating the gut microbiota depends on the nature of the food matrix and the concentration of molecules in the food matrix. In an *in vitro* model of colon fermentation, the addition of (+)-catechin (150 mg/l) for 48 hours significantly increased the growth of *Clostridium coccoides–Eubacterium rectale*, *Bifidobacterium spp.*, and *Escherichia coli* and inhibited that of *Clostridium histolyticum*. The same incubation conditions with epicatechin alone showed an increase in the growth of *Clostridium coccoides-Eubacterium rectale (*Tzounis *et al.*, 2008). In a similar model, GSE with 28% PCs (600 mg/l) significantly increased the growth of the *Lactobacillus/Enterococcus* group after 5 and 10 hours of *in vitro* fermentation, while GSE with 78% PCs at the same concentration significantly reduced *Clostridium histolyticum* after 10 hours. These data suggest that the flavan-3-ols profile of a particular food source could influence the microbiota composition, inducing changes that could in turn affect the bioavailability and potential bioactivity of these compounds (Cueva *et al.*, 2013). In addition, these findings support the

potential prebiotic effect of PACs in improving host health through modulation of the gut microbiota.

Proanthocyanidins in Grape Seeds

Several pharmaceutical companies are currently evaluating the use of agri-food waste as an alternative raw material for the extraction of bioactive compounds to be included in nutraceuticals and food supplements. The reuse of food waste has several economic advantages: low cost, large quantities, high content of bioactive molecules, and financial support from governments that want to promote environmentally eco-friendly practices (Musto *et al.*, 2022). In this regard, research interest in recent decades has focused on the study of bioactive molecules contained in food waste obtained from wine production (Unusan, 2020). Wine production is one of the major agro-industrial activities in the world and *Vitis vinifera* L. is most commonly used for industrial wine production, with a global production of about 77.8 million tonnes for year. Grapes are harvested in temperate zones, where hot summers and rather mild winters are the typical climatic conditions. About 50% of the grapes are processed into wine, one third is used as fresh fruit and the rest is refined into food products such as jams, grape seed extract (GSE) juice, jellies, grape seed oil, dried grapes, and vinegar (Baroi *et al.*, 2022). However, the wine industry produces large quantities of waste and by-products, which represent about 30% of the initial weight of the grapes. The accumulation of this waste can cause economic and environmental problems due to the organic matter, acid pH, salinity, and heavy metal content (Ahmad *et al.*, 2020). The growing demand for grapes has led to a significant increase in both the area and value of the vineyards. Therefore, the accumulation of organic and inorganic waste causes major problems related to their economic and ecological management (Beres *et al.*, 2917). The accumulation of viticultural waste has a negative impact both on the environment and human health through water pollution, oxygen consumption in the soil and groundwater, as well as through the

attraction of vectors of diseases spread (Dwyer *et al.*, 2014). Globally, there is a growing demand for healthy, natural food ingredients that can replace synthetic antioxidants and food preservatives (Garrido *et al.*, 2011). Several scientific studies confirm the presence of polyphenolic substances (antioxidants) in grapevine and its by-products (pomace, grape seeds, stalks, lees, and shoots) as well as their potential applicability as a natural added value in the food, pharmaceutical, and cosmetic industries due to their nutritional benefits (Kalli *et al.*, 2018). Indeed, these antioxidant compounds exhibit a range of biological activities such as immunoprotective and anticancer properties, as well as the prevention of cardiovascular and neural diseases (Kori et al., 2018). Recently, it has been discovered that polyphenols are found in abundance in grape seeds, in particular, PACs represent the most abundant class (Zhou *et al.*, 2022). Indeed, GSE is widely available commercially as dietary supplements for disease prevention and health promotion due to their numerous pharmacological effects, such as antioxidant, anti-inflammatory, anticancer, neuroprotective, hypolipidemic, bacteriostatic, and hypotensive (Chen *et al.*, 2020). **Figure 6** the main steps involved in the production of GSE.

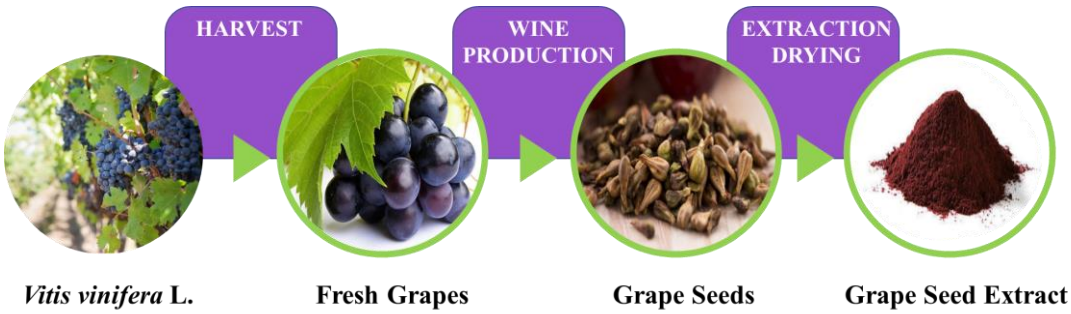

Figure 6. Main steps involved in the production of grape seed extract.

General Objectives

This Ph.D. thesis aimed to investigate the different bioavailability and bioactivity of oligomeric and polymeric proanthocyanidins (PACs) from a grape seed extract (GSE) (*Vitis vinifera* L.). Literature indicates that the biological activity of PACs can vary depending on their composition and degree of polymerization (DP). Many studies have focused on low molecular weight (DP < 3) PAC oligomers, which are completely absorbed in the gastrointestinal tract. The low bioavailability and bioaccessibility of high molecular weight PACs, especially polymeric, have led to the need to develop new methods that can improve these important parameters. Although several methods for the depolymerization of PACs have been described in the literature, they are hardly applicable in the agri-food industry because they are difficult to execute, costly, and not "food-grade". In this context, the main novelty of this project was to subject GSE to a food-grade, rapid, and economical depolymerization method for the large-scale production of high bioavailable PAC. Therefore, the bioactivity and intestinal bioaccessibility of GSE and the extract obtained from the food-grade depolymerization method of GSE (ATGSE) were evaluated through *in vitro* and *in vivo* studies with a particular interest in urogenital tract diseases. A technological process was also carried out to develop a potential nutraceutical formulation with beneficial effects on human health.

Specific Objectives

Each chapter has been designed for a specific objective, as shown below:

- **Chapter 1**

This chapter describes the food-grade chemical method to depolymerize the polymeric PACs of GSE into low molecular weight oligomers and monomers by alkaline treatment. The different chemical composition of GSE and its version processed under alkaline conditions (ATGSE), was evaluated using a molecular network (MN) approach based on the results obtained from HPLC-ESI HRMS/MS characterization analysis. Furthermore, the antioxidant and anti-inflammatory activities were investigated *in vitro*.

- **Chapter 2**

To evaluate the different intestinal bioaccessibility and bioactivity, GSE and ATGSE were subjected to an *in vitro* simulated human gastrointestinal digestion-colonic fermentation. For this purpose, total polyphenol content (TPC), antioxidant capacity, and short-chain fatty acids (SCFA) production were determined. This study was conducted at the Department of Nutrition and Bromatology, University of Granada (Spain).

- **Chapter 3**

In this chapter, the biological effects of GSE and ATGSE were tested on an animal model of benign prostatic hyperplasia (BPH) induced by subcutaneous administration of testosterone. At the end of the treatment, the weight of the prostates removed microsurgically from the mice was evaluated and hematological and biochemical analyses of blood and tissues were performed.

- **Chapter 4**

In this chapter, the antibacterial effect of GSE and ATGSE against uropathogenic *Escherichia coli* (UPEC) in bladder epithelial cells was investigated. For this purpose, the inhibition of bacterial invasion activity was tested in an *in vitro* model of epithelial bladder cells (HT-1376) infected by UPEC (ATCC 700928).

- **Chapter 5**

This chapter describes the technological process carried out at the company S.I.I.T. S.R.L.-INNOVATIVE HEALTHCARE PRODUCTS in Milan to develop a nutraceutical formulation based on ATGSE for the treatment of urogenital system disorders through the best possible selection of excipients, active ingredients and release strategies of the active ingredients.

Chapter 1

A Food-grade Method for Enhancing the Content of Low Molecular Weight Proanthocyanidins

1.1. Introduction

Proanthocyanidins (PACs) are oligomers and polymers composed of flavan-3-ol units found in many plant sources, including fruits, seeds of some plants, flowers, nuts, or barks (Dixon *et al.*, 2005). These molecules have many biological activities, including antimicrobial, anti-inflammatory, radical-scavenging, antioxidant, and anticancer activities (Smeriglio *et al.*, 2017; Hummer and Schreier *et al.*, 2008). The bioavailability of PACs depends on the size of the molecule, with monomers and dimers absorbed and present in the blood at relatively low levels, while those with a higher degree of polymerization (DP) cannot be directly absorbed by humans (Donovan *et al.*, 2002; Holt *et al.*, 2002). However, larger oligomers produce smaller and more absorbable molecules, when they are metabolized by the microflora of the colon, producing metabolites with health-promoting properties (Monagas *et al.*, 2010b; Deprez *et al.*, 2000). In this regard, if polymeric PACs could be depolymerized into oligomeric ones, their bioaccessibility and bioavailability could also significantly increase (Meeran and Katiyar *et al.*, 2007; Tomas-Barberan *et al.*, 2007). The chemical methods investigated for the depolymerization of polymeric PACs include the use of stable composite catalysts or alcoholic solutions of mineral acids, with the addition of (+)-catechin, (−)-epicatechin, and (−)-epigallocatechin gallate as a chain breaker (Zhu *et al.*, 2020; Liu *et al.*, 2013). The main limitations in their use are not only the difficulty of their execution and their high costs but also, above all, the impossibility of using them for the formulation of nutraceutical products, as they are not “food-grade”. Depolymerization methods

of acid-catalyzed PACs in the presence of nucleophiles, such as toluene-α-thiol, benzyl mercaptan, 2-mercaptoethanol or phloroglucinol, have been examined (Liang *et al.*, 2016; Zhang *et al.*, 2017). Nevertheless, these methods are difficult to use in the food industry as they produce flavan-3-ols with nucleophilic adducts that could alter the biological properties of PACs naturally present in the food matrix. Furthermore, acidic or basic methods for the depolymerization of PACs in food matrixes are described in the literature (Imran *et al.*, 2021; Zhang *et al.*, 2017; Maisto *et al.*, 2022b; Hernes and Hedges *et al.*, 2000). In particular, a study published by White and Howard (2010) conducted on cranberry pomace showed that NaOH treatment resulted in an increase in low-molecular-weight procyanidins (PCs) under high temperatures and short times. The oligomeric PACs obtained from released hydrolysis had *in vitro* antioxidant and anti-inflammatory activities and have been implicated in numerous health benefits (Ma *et al.*, 2020; Luca *et al.*, 2020). The best-known sources of PACs are cranberry, apples, grapes, strawberries, cocoa, almonds, cinnamon, peanuts, and tea (Nie and Sturzenbaum, 2019). Among these, grape seeds are waste products of great importance in the agro-food industry because they are the most commonly produced fruit crops in the world and because they represent sources still rich in bioactive compounds (Unusuan, 2020; Schiano *et al.*, 2022b). Furthermore, PACs from grape seeds showed extensive pharmacological and therapeutic activities on health against cardiovascular diseases (CVD), diabetes mellitus, obesity, or cancer-related oxidative stress and inflammatory processes (Nunes *et al.*, 2016; Bagchi *et al.*, 2014). In light of what is stated above, the first aim of my Ph.D. project was to develop a rapid, economical, and food-grade alkaline treatment to depolymerize grape seed extract (GSE) (*Vitis vinifera* L.) PAC polymers into lower-molecular-weight monomers and oligomers, named ATGSE (alkaline treatment of GSE). Therefore, to investigate the components present in GSE, a qualitative analysis of the polyphenolic profile was performed

using UHPLC-ESI HRMS/MS. Additionally, a molecular networking (MN) approach was conducted to analyze and define the chemical composition in terms of PAC differences in both GSE and ATGSE. Finally, *in vitro* antioxidant and anti-inflammatory assays were carried out to evaluate the potential biological activity of GSE and ATGSE

1.2. Results

1.2.1. UHPLC-ESI HRMS/MS and Molecular Networking (MN) Analysis of GSE and ATGSE

To evaluate the polyphenolic composition of GSE and ATGSE extracts, a UHPLC-ESI HRMS/MS analysis was performed. Compounds were identified using a molecular networking (MN) approach, which compares the MS/MS spectra of studied compounds and clusters them based on similarities between the spectra of the fragments within the dataset. MN analysis based on the compounds grouped and detected in GSE and ATGSE is shown in Appendix (**Figure A1**). This bioinformatic approach proved to be a high throughput dereplication of complex matrixes to identify different groups of structural analogs. The analysis of the structural similarity demonstrated that the PAC cluster is the main cluster present in the two extracts. Therefore, the use of the network allowed the identification and characterization of 78 compounds of the PAC cluster, in addition to the identification of other compounds obtained by comparison with literature data. **Table A1** and **Figure A2** in Appendix report the UHPLC-ESI HRMS/MS analysis of PAC compounds present in GSE and ATGSE and the Full MS chromatograms of the two extracts, respectively. A total of 142 PAC molecules were identified, including PACs with single, double, and triple charges, and with various DP. Furthermore, analogs substituted on the flavanic scaffold with galloyl groups and monomers, such as afzelechin and gallocatechin, were identified. **Figure 7** reports the PAC cluster obtained from MN of GSE and ATGSE. These nodes confirmed the presence of

multiple PACs, from oligomers to polymers with higher molecular weight. The result of the networking analysis showed that more polymeric PACs were present in GSE, while oligomeric PACs were predominantly present in both extracts. The difference in PAC composition was expressed as a percentage of area, as shown in **Figure 8**. The data showed that the content of monomeric and dimeric PACs was higher in ATGSE than in GSE, with 58% and 49% monomers and 31% and 24% dimers, respectively. The trimeric PACs were slightly higher in GSE than in ATGSE, with 9% and 6%, respectively. Furthermore, no differences in the composition of tetrameric PACs were observed in the two extracts. Finally, the GSE sample showed an elevated content of polymeric PACs with a degree of polymerization (DP) greater than 4 (4%) and galloylated PACs (14%), compared to the ATGSE sample (1% and 4%, respectively).

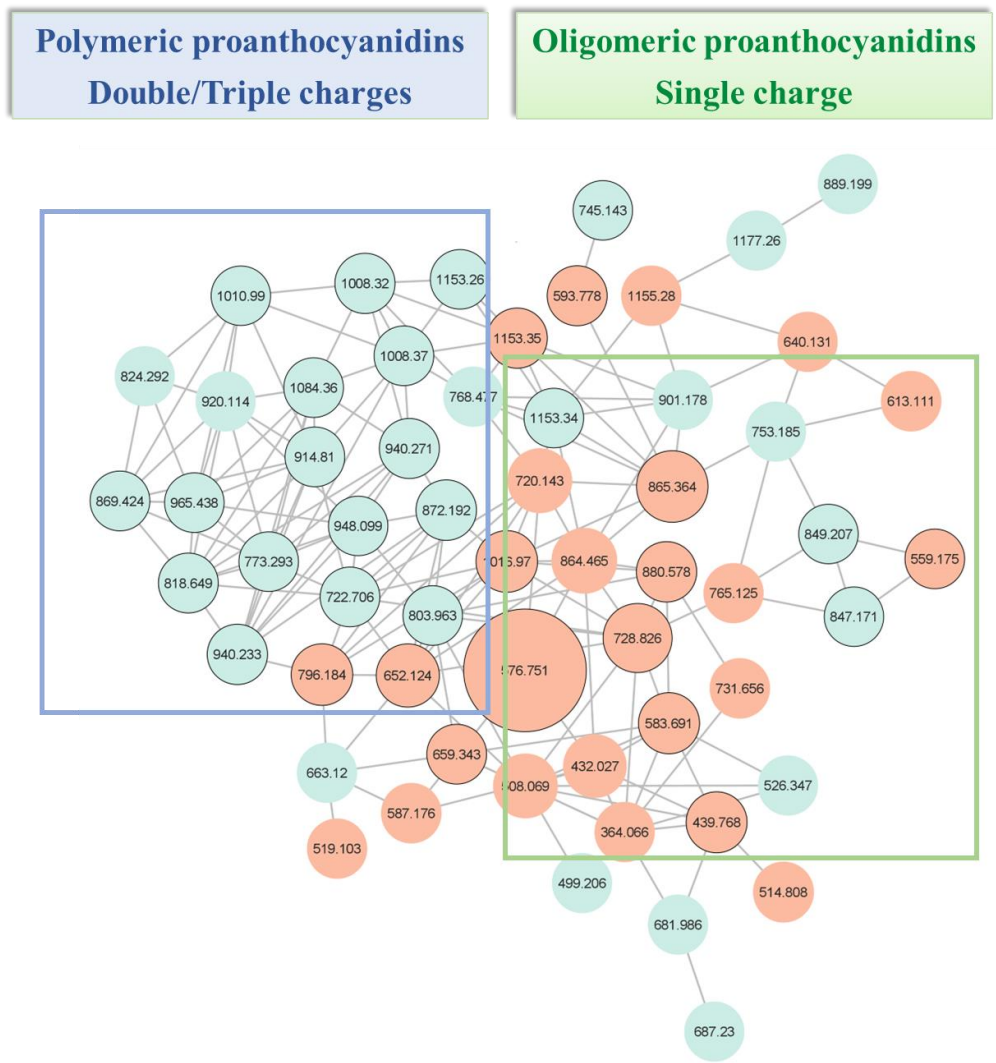

Figure 7. Proanthocyanidin (PAC) cluster obtained by molecular networking (MN) of grape seed extract (GSE) and its alkalinized version (ATGSE). The nodes (circles) represent a consensus MS/MS spectrum having identical precursor mass obtained from the samples, and the colors of the nodes refer to the unique property of the compound present or absent in the two samples. Blue nodes were identified in the GSE extract. Instead, red nodes represent compounds in common in the two extracts. The edges (lines) connect the nodes based on the "cosine score" (fragment match/similarity score ranging from 0.7 to 1), and the thickness of the edges reflects and measures the positive relatedness of the MS/MS spectra of the compounds within a network.

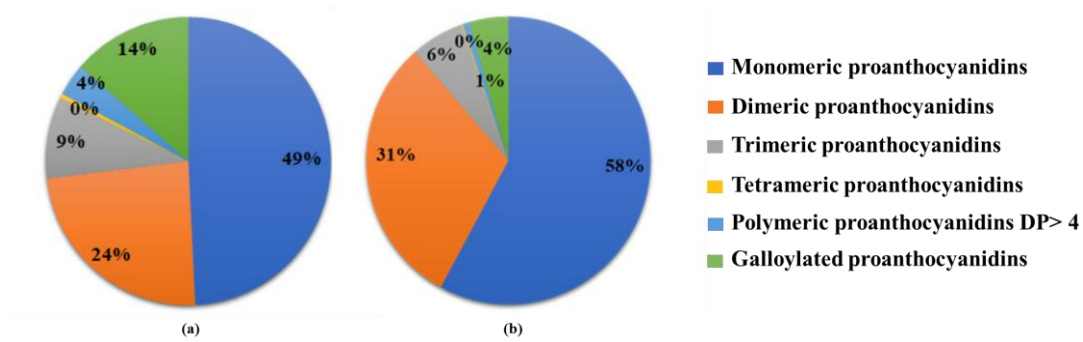

Figure 8. Percentage composition (area %) of proanthocyanidins (PACs) identified in (a) GSE sample and (b) ATGSE sample by UHPLC-ESI HRMS/MS analysis.

1.2.2. Total Polyphenol Content (TPC) and In Vitro Antioxidant Activity of GSE and ATGSE

The Folin-Ciocalteau assay was conducted on hydroalcoholic GSE and ATGSE extracts to evaluate their TPC. The GSE sample showed a TPC of 789 ± 0.046 mg GAE/g of extract, and ATGSE showed a TPC of 611 ± 0.004 mg GAE/g of extract ($p < 0.001$ GSE *vs* ATGSE). Furthermore, the antioxidant activity of GSE and ATGSE was measured by DPPH, ABTS, and FRAP methods. The results obtained were expressed as mol TE/100 g of extract (**Table 2**).

Table 2. Antioxidant activity of grape seed extract (GSE) and its alkalinized version (ATGSE) evaluated by DPPH, ABTS, and FRAP assays.

Compound	DPPH (mol TE/100 g ± SD)	ABTS (mol TE/100 g ± SD)	FRAP (mol TE/100 g ± SD)
GSE	0.39 ± 0.04	0.52 ± 0.02	0.20 ± 0.02
ATGSE	0.32 ± 0.03	0.48 ± 0.02	0.18 ± 0.02

Abbreviations: DPPH, 2,2-diphenyl-1-picrylhydrazyl; ABTS, 2,2′-azino-bis (3-ethylbenzothiazoline-6-sulfonic acid); FRAP, ferric reducing antioxidant power; TE, Trolox equivalent. Values are the mean ± standard deviation (SD) of three replications. Statistical significance was calculated by Student′s t-test analysis, but no significant data were found.

Furthermore, the results obtained by DPPH and ABTS assays of GSE and ATGSE were also expressed as EC50, which is the antioxidant concentration effective in producing 50% of the maximum response, and compared with Trolox, the reference standard. As shown in **Figure 9**, GSE, ATGSE, and Trolox showed EC50 values of 0.01 mg/mL, 0.02 mg/mL, and 0.11 mg/mL for DPPH assay and of 0.01 mg/mL, 0.02 mg/mL, and 0.02 mg/mL for ABTS assay, respectively.

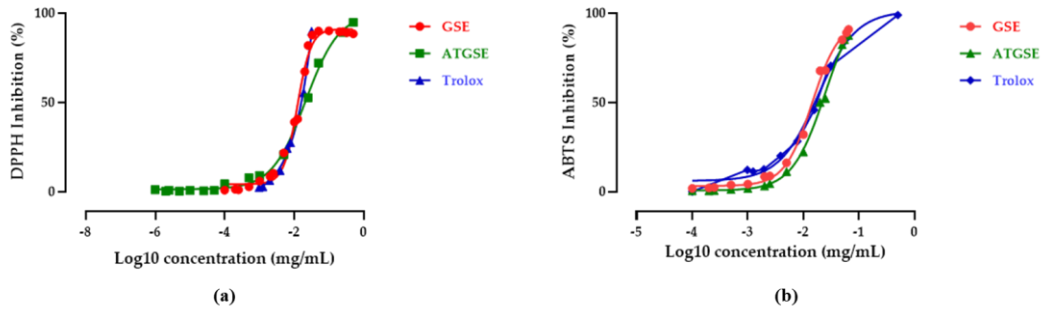

Figure 9. Antioxidant activity of GSE, ATGSE, and Trolox expressed as (a) EC50 of DPPH assay and (b) EC50 of ABTS assay. Values are the mean ± standard deviation (SD) of three replications.

1.2.3. Anti-inflammatory Activity

The anti-inflammatory activity of GSE and ATGSE was tested by *in vitro* 5-lipoxygenase (LOX) inhibition assay and cyclooxygenase (COX-1 and COX-2) inhibition assay. **Figure 10** and **Table 3** show the percentage of 5-LOX inhibition for GSE and ATGSE expressed as IC50, which is the concentration of a compound that provides a semi-maximal inhibitory effect. The results obtained revealed that GSE and ATGSE inhibited 5-LOX in a concentration-dependent manner. Zileuton was used as the reference standard, with an IC50 value of 0.12 ± 0.01 µg/mL. **Table 3** shows the percentage of COX-1 and COX-2 inhibition for GSE and ATGSE expressed as IC50. The results again showed that GSE and ATGSE inhibited COX in a concentration-dependent manner. Naproxen, used as the reference standard,

showed an IC50 value of 0.004 ± 0.001 mg/mL for COX-1 and 0.003 ± 0.015 mg/mL for COX-2.

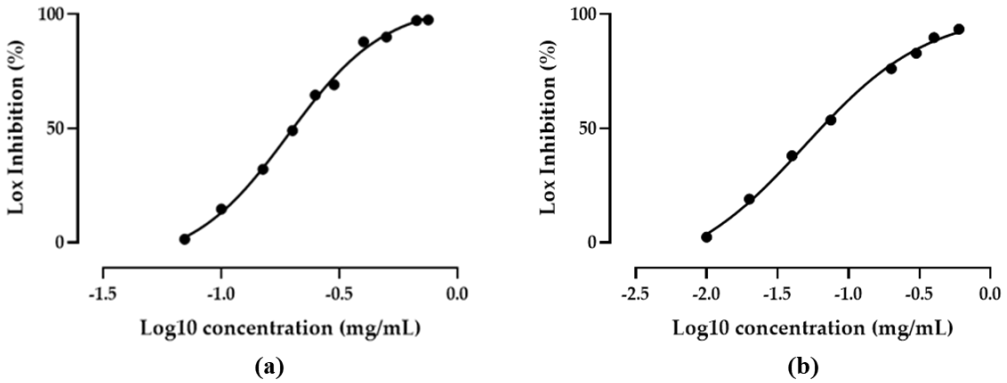

Figure 10. Anti-inflammatory activity evaluated by inhibition of 5-LOX activity (expressed as %) of (a) GSE and (b) ATGSE. Values are the mean ± standard deviation (SD) of three replications.

Table 3. Anti-inflammatory activity evaluated by inhibition of COX-1 and COX-2 activity (expressed in %) of (a) GSE and (b) ATGSE.

Compound	COX-1 Inhibitory Activity (IC_{50} mg/mL ± SD)	COX-2 Inhibitory Activity (IC_{50} mg/mL ± SD)	5-LOX Inhibitory Activity (IC_{50} mg/mL ± SD)
GSE	0.30 ± 0.30	0.21 ± 0.29	0.20 ± 0.01
ATGSE	1.16 ± 0.25*	0.8 ± 0.2*	0.05 ± 0.07*

Values are the mean ± standard deviation (SD) of three replications. Statistical significance is calculated by Student's t-test analysis: $^{*}p< 0.05$ GSE *vs* ATGSE

1.3. Discussion

Proanthocyanidins (PACs) are widely present in various foods, including fruits, vegetables, and plant-based foods with potential health benefits (Smeriglio *et al.*, 2017; Valencia-Hernandez *et al.*, 2021). However, their biological activity can change according to their composition and the degree of polymerization (DP). Many

literature studies have focused on PAC oligomers with a low molecular weight (DP < 3), which are completely absorbed in the gastrointestinal tract (Yang *et al.*, 2021). The low bioavailability of high-molecular-weight PACs, especially polymeric ones (Serra *et al.*, 2010), has led to the need to develop new methods that could improve this important parameter. Although several methods for depolymerization of PACs are described in the literature, only some of them are applicable in the agri-food industry. In a study published by Zhu *et al.* (Zhu *et al.*, 2019), it was reported that ruthenium/carbon-catalyzed depolymerization of polymeric PACs from larch bark resulted in a valuable increase in terms of oligomeric PACs. Moreover, Zhang *et al.* (2021a) have described an innovative method based on the steam explosion treatment of grape seeds aimed at depolymerizing polymeric PACs into oligomeric ones. Other authors have studied the depolymerization of polymeric PACs from grape seeds using a nucleophilic reagent (Wen *et al.*, 2019). However, not all methods described so far can be considered food-grade, and thus these methods are hardly suitable for industrial production. In this context, the main novelty of the present project is the development of a food-grade, as well as a rapid and economical, method for large-scale production of PACs with high bioavailability. One of the main sources of PACs is grape seeds (Rodriguez-Perez *et al.*, 2019). A study published by Gu *et al.* (Gu *et al.*, 2004) reported that the total content of PACs in grape seeds is 35.3 mg/g of dry seed d.w. and that monomers (catechin and epicatechin) and polymers with DP > 10 were the most abundant. Although methods for depolymerization of PACs have already been described in the literature, the results reported in the previous paragraph showed that alkaline treatment of grape seed extract (GSE) proved to be effective in releasing PAC monomers and oligomers from the high-molecular-weight ones. Therefore, an analysis of molecular networking (MN) was carried out to compare the qualitative profile of GSE and its alkalinized version (ATGSE) in terms of the qualitative distribution of PACs. MN based on tandem mass spectrometry (MS/MS) is a recent analytical approach used

to visualize and interpret the data complex from mass spectrometry analysis by grouping the MS/MS spectra based on their similarities in the fragmentation route (Esposito *et al.*, 2017). Subsequently, the metabolites with similar fragmentation are correlated within a network, which facilitates the identification of unknown but related molecules. In the network, PACs were identified as the main cluster with 142 identified compounds, 78 of which belong to the PAC cluster, and the others were characterized by comparison with literature data. In the ESI-MS/MS spectra of the two extracts, oligomers and polymers of A-type and B-type PAC were observed with a DP ranging from 2 to 10. In addition, analogs substituted on the flavanic scaffold with galloyl groups and monomers, such as afzelechin and gallocatechin, were identified. According to the study published by Monagas *et al.* (2010a), the PACs detected were essentially B-type, with an abundance of about 72% compared to 8% of the corresponding A-type species. The proposed mechanism to explain the observed release of low-molecular-weight PACs in ATGSE (monomeric PACs 58%, dimeric PACs 31%), under alkaline conditions and in combination with high pH and temperature, is probably due to the cleavage of the C-C interflavan bond of polymeric PACs (White and Howard, 2010). Furthermore, the decrease in the content of galloylated PACs (4%) could be due to the hydrolysis of the bond of the galloylated esters with the release of gallic acid and the corresponding PAC (Aydin *et al.*, 2019). The higher content of oligomeric PACs in ATGSE seems to be of great importance for potential *in vivo* bioactivity at the systemic level, as several studies have reported that oligomeric PACs are more bioavailable than higher oligomers (Ou and Gu, 2014). Considering the nature of the GSE food matrix, rich in antioxidant PACs, the attention was focused on the evaluation of *in vitro* antioxidant activity. In this regard, Folin-Ciocalteu, DPPH, ABTS, and FRAP assays were performed on GSE and ATGSE samples. The results obtained are in agreement with studies conducted on GSE (*Vitis vinifera* L.), confirming the high antioxidant power of these food waste matrixes (Yemis *et al.*, 2008). Interestingly, it was shown that although

the alkaline treatment resulted in a significant reduction in the polyphenol content in ATGSE ($p < 0.001$ *vs* GSE), probably due to the different reactivity of the PACs with different molecular weights on Folin-Ciocalteu, their antioxidant potential was not significantly modified. In this respect, the results obtained showed a high antioxidant capacity of both extracts studied, comparable to the antioxidant activity of Trolox (used as the reference standard). This activity is probably attributable to the high content of PACs in grape seeds (Karami *et al.*, 2018). Based on this scientific evidence, the potential anti-inflammatory activity of two matrixes was evaluated. It is well known that inflammation is a defense response of the organism, activated by various types of tissue damage (cell injury, irritation, invasion of pathogens), as well as a process to neutralize damaged and necrotic cells (Chen *et al.*, 2018). The development of this process relies on the involvement of numerous factors and mediators, including the release of soluble mediators (e.g., cytokines and chemokines) that recruit immune system cells to the damaged tissue, the release of arachidonic acid with the activation of the cyclooxygenase/lipoxygenase axis for the release of pro-inflammatory prostaglandins and leukotrienes, and the release of reactive oxygen species (ROS) (Forrester *et al.*, 2018; Astudillo *et al.*, 2012). In this context, the inhibition effect of GSE and ATGSE on the three main enzymes involved in the development of an inflammatory process (COX-1, COX-2, and 5-LOX) was investigated. The data obtained demonstrated that the activities of lipoxygenase (5-LOX), cyclooxygenase-1 (COX-1), and cyclooxygenase-2 (COX-2) were effectively inhibited by both extracts. In particular, ATGSE showed significant inhibition of 5-LOX ($p < 0.05$ *vs* GSE), while GSE showed significantly greater COX inhibitory activity ($p < 0.05$ *vs* ATGSE). The high COX inhibitory activity of GSE could potentially be due to the high content of trimeric PACs, which have been shown in the literature to have potent inhibitory activity against these two inflammatory isoenzymes (Mansoor *et al.*, 2016). Furthermore, Sies *et al.* (2005) have shown that oligomeric PCs can inhibit LTA4 synthase, which is the

recombinant form of human 5-lipoxygenase, with a dose-dependent activity, modulating the conversion of arachidonic acid (AA) into various proinflammatory leukotrienes (Samuelsson *et al.*, 1987). This could explain the greater 5-LOX inhibitory activity of ATGSE. Therefore, these results suggest that the supplementation with ATGSE and GSE could contribute to the reduction in inflammatory conditions and the prevention or treatment of oxidative stress-related diseases.

1.4. Conclusions

In conclusion, the performed food-grade alkaline treatment of GSE could represent a reliable and suitable method to increase the low-molecular-weight fraction of PACs in ATGSE. In addition, this treatment has not altered the bioactivity of the two extracts, as evidenced by their high antioxidant and anti-inflammatory activity *in vitro*. Therefore, although both GSE and AGTSE have shown high antioxidant and anti-inflammatory activities, the potential supplementation with ATGSE could ensure greater intestinal bioaccessibility and systemic absorption due to its high content of oligomeric PACs. The results obtained could represent a starting point for further *in vitro* and *in vivo* studies aimed to evaluate intestinal bioaccessibility and bioavailability of the ATGSE low-molecular-weight PACs to assess the potential nutraceutical application of ATGSE. In addition, future studies will be aimed to evaluate the potential biological effect of the two matrixes in the prevention and treatment of inflammatory diseases.

1.5. Experimental Section

1.5.1. Reagents

All chemicals, reagents, and standards used were either analytical or LC-MS grade reagents. Water was treated in a Milli-Q water purification system (Millipore, Bedford, MA, USA) before use. All standards and solvents for chemical analysis and *in vitro* studies were purchased from Sigma-Aldrich (Milan, Italy). The COX Activity Assay Kit was purchased from Cayman Chemical (Cayman Chemical Company, Ann Arbor, MI, USA) (cat No. 701050). Grape seed extract (GSE) 95% proanthocyanidins from *Vitis vinifera* L. was purchased from MB-Med S.r.l (Turin, Italy).

1.5.2. Alkaline Treatment of GSE (ATGSE)

The alkaline treatment of GSE followed the method described by White *et al.* (2010), with slight modifications. GSE (0.5 g) was weighed and placed in glass, screw-top tubes. Then, 20 mL of distilled water and 600 uL di NaOH 1 M were added to the tubes, and the tubes were subsequently vortexed. The tubes were then placed in a shaking bath (200 rpm) set at 45 °C for 4 h. After that, samples were removed from the water bath, frozen at −80 °C, and freeze-dried.

1.5.3. Sample Solution Preparation for UHPLC-ESI HRMS/MS Analysis

One gram of samples (GSE and ATGSE) was treated with 30 mL of MeOH/H_2O (70:30) + 0.1% HCl 12 M with constant stirring for 30 min, at room temperature. The extracts were centrifuged at 4 °C and 6000 rpm for 10 min. The supernatants were filtered through a 0.45 µm PTFE filter and analyzed.

1.5.4. UHPLC-ESI HRMS/MS Analysis of GSE and ATGSE

UHPLC-HRMS analyses were performed on a Thermo Ultimate RS 3000 coupled online to a Q-Exactive hybrid quadrupole Orbitrap mass spectrometer (Thermo Fisher Scientific, Bremen, Germany) equipped with a heated electrospray ionization probe (HESI II) operated in negative mode. The MS was calibrated with a Thermo calmix (Pierce) calibration solution. Separation was performed in RP mode using a Kinetex TM EVO C18 (150 mm × 2.1 mm; 2.6 μm) (Phenomenex, Bologna, Italy). The column temperature was set at 45 °C and the flow rate was 0.4 mL/min. The mobile phase was (A) H_2O + 0.1% CH_3COOH (v/v) and (B) ACN + 0.1% CH_3COOH (v/v). The following gradient was used: 0 min, 2% B; 0.01–15 min, 25% B; 15.01–25 min, 55% B; 25.01–26 min, 98% B; 98% held for 1 min; return to 2% in 0.1 min. Four microliters were injected. Full MS (100–1500 m/z) and data-dependent MS/MS were performed at a resolution of 35,000 and 15,000 FWHM, respectively, and normalized collision energy (NCE) values of 10, 20, and 30 were used. Source parameters were: sheath gas pressure, 50 arbitrary units; auxiliary gas flow, 13 arbitrary units; spray voltage, +3.5 kV; capillary temperature, 310 °C; auxiliary gas heater temperature, 300 °C, and s-lens, 50. Two replicates of each sample were performed. Metabolite annotation was based on accurate mass measurement, MS/MS fragmentation pattern, and comparison with in silico spectra using an MS database search.

1.5.5. Molecular Networking (MN) Analysis

Mass spectra generated by HPLC-MS/MS analysis of GSE and ATGSE extracts were converted from the original ".raw" format to the "mzXML" format. The conversion was performed using MSConverter software (ProteoWizard, Palo Alto, CA USA). The data files were submitted on the GNPS platform server using the WinSCP software (Aron *et al.*, 2020). The molecular network data generated by

GNPS software were obtained with a mass tolerance of the precursor ion (PIMT) and MS/MS fragment ion tolerance set at 0.02 Da and 0.5 Da, respectively. Consensual spectra including fewer than two similar spectra and four fragments of identical masses were removed. To reduce the complexity of the network, the spectra similarity score between clusters (cosine pairs) ranged between 0.7 and 1. MS/MS spectra were filtered by choosing the six most significant fragments to a 50 Da spectral window. The connection between clusters was provided if the individual clusters occurring in the 10 respective clusters were similar to each other, with the maximum size of a spectral family being limited to 100 clusters. The spectra in the network were searched in comparison to GNPS spectral libraries. The library spectra were filtered in the same manner as the input data. The nodes (circles) represent a consensus MS/MS spectrum having identical precursor mass obtained from the samples, and the colors of the nodes refer to the unique property of the compound present or absent in the two samples. Blue and green nodes were identified in GSE and ATGSE extracts, respectively. Instead, red nodes represent compounds in common in the two extracts. Molecular networks created were analyzed online on the GNPS platform (https://gnps.ucsd.edu/accessed on 27 December 2021), and Cytoscape 3.9.0 was used to visualize the generated networks (Wang *et al.*, 2016).

1.5.6. Total Polyphenol Content (TPC)

The TPC was measured by the Folin-Ciocalteau method, using gallic acid as a standard (Sigma-Aldrich, St. Louis, MO, USA). Briefly, 0.125 mL of the sample (properly diluted with water to obtain an absorbance value within the linear range of the spectrophotometer) was added to 0.5 mL of distilled water and 0.125 mL of Folin-Ciocalteau reagent (Sigma-Aldrich, St. Louis, MO, USA). The mixture was incubated at room temperature for 6 min, and then 1.25 mL of an aqueous solution of Na_2CO_3 7.5% (w/v%) was added and adjusted to 3 mL with deionized water. The absorbance was measured at 760 nm after 90 min of incubation in the dark at room

temperature. Samples were analyzed in triplicate, and the results were expressed as mg of gallic acid equivalents (GAE)/g of the sample (Maisto *et al.*, 2022a).

1.5.7. Antioxidant Activity

- **DPPH Radical Scavenging Activity Assay**

The antioxidant activity of the extracts (GSE and ATGSE) was evaluated using a 2,2-diphenyl-1-picrylhydrazyl (DPPH) (Sigma-Aldrich St. Louis, MO, USA) radical scavenging assay, as described by Maisto *et al.* (2021). DPPH is a stable organic nitrogen radical capable of absorbing radiation in the UV-Vis region. The reaction between DPPH and an antioxidant compound capable of donating a hydrogen atom to the radical compound leads to the decolorization of the methanolic DPPH solution due to the disappearance of the radical. A solution of 0.05 mM DPPH in methanol was prepared, and 1000 µL of this solution was mixed with 200 µL of extract in methanol at different concentrations. After mixing, the absorbance of the samples was determined spectrophotometrically at 517 nm. The percentage of DPPH inhibition was calculated according to **Equation 1**:

Equation 1. Percentage of DPPH radical scavenging activity

$$\% \text{ ABTS} = [(A0 - A1) / A0] \times 100$$

where A0 is the absorbance of the control and A1 is the absorbance of the extracts. The 6-hydroxy-2,5,7,8-tetramethylchroman-2-carboxylic acid (Trolox) was used as the antioxidant standard, and the results were expressed in mol Trolox equivalent (TE)/100 g of the sample. Moreover, results were also expressed as EC50, which is the antioxidant concentration required to achieve a 50% reduction in the

initial DPPH• concentration. The experiment was repeated three times at each concentration.

- **ABTS Radical Scavenging Activity Assay**

ABTS radical cation ($ABTS^{\bullet+}$) scavenging activity was determined according to Re *et al.* (Re *et al.*, 1999), with slight modifications. The reaction mixture was prepared with 2.5 mL of ABTS 7.0 mM solution and 44 uL of potassium persulfate 140 mM solution and left in the dark for 7 h to allow radical development. The solution was diluted with ethanol–water to achieve absorbance values of 0.7–0.75 at 734 nm. Analysis was conducted by adding 100 µL of each sample to 1 mL of the ABTS•+ solution. The absorbance was measured after 2.5 min of reaction at 734 nm. Ethanol was used as a blank. The scavenging effect was calculated according to **Equation 2**:

Equation 2. Percentage of ABTS radical scavenging activity

$$\% \text{ ABTS} = [(A0 - A1) / A0] \times 100$$

where A0 is the absorbance of the control and A1 is the absorbance of the extracts. Trolox was used as the antioxidant standard. Results were expressed both as mol of TE/100 g of the sample and EC50, which is the antioxidant concentration required to achieve a 50% reduction in the initial ABTS+ concentration. The experiment was repeated three times at each concentration.

- **Ferric Reducing Antioxidant Power (FRAP) Assay**

The FRAP assay was conducted spectrophotometrically according to the method of Schiano *et al.* (Schiano *et al.*, 2022a), with slight modifications. The method is

based on the ability of electron-donating antioxidants to reduce the Fe^{3+} TPTZ complex (colorless complex) to Fe^{2+} tripyridyltriazine (blue-colored complex), at low pH. The FRAP solution was prepared by adding 5 mL of TPTZ (2,4,6-tris(2-pyridyl)-s-triazine) solution (10 mM) in HCl (40 mM), 5 mL of $FeCl_3$ (20 mM) in water, and 50 mL of acetate buffer (0.3 M, pH 3.6). All solutions were used on the day of preparation. The mixture was preheated at 37 °C. This reagent (2.85 mL) was mixed with 0.15 mL diluted test samples at different concentrations. The absorbance was measured after 4 min at 593 nm. All determinations were performed in triplicate. A standard curve was prepared using Trolox, and the results were expressed as mol TE/100 g of sample.

1.5.8. *Anti-inflammatory Activity*

- **Lipoxygenase Inhibitory Activity Assay**

The lipoxygenase inhibitory activity assay was performed according to the method reported by Sharifi-Rad *et al.* (Sharifi-Rad *et al.*, 2016), with slight modifications. Briefly, 125 µL of the extract at various concentrations was added to 125 µL of soybean lipoxidase enzyme solution (final concentration of 1250 U/mL). This mixture was incubated at 25 °C for 5 min. Then 500 µL of linoleic acid solution (358 µM) was added and the mixture was incubated again for 10 min at 25 °C. A 0.2 M borate buffer solution (pH 9) was used to dissolve all components of the assay, and 750 µL of buffer was also used to dilute the final mixture. After thorough mixing, the absorbance was measured at 234 nm. The percentage (%) inhibition was calculated according to **Equation 3**:

Equation 3. Percentage of LOX inhibition

$$\% \text{ LOX inhibition} = [(\text{Activity of LOX Activity} - \text{Activity of LOX with sample}) / \text{Activity of LOX}] \times 100$$

The results were expressed as IC50 (inhibitory concentration), which is the concentration of inhibitor at which the inhibition percentage reaches 50%. Zileuton was used as the reference anti-inflammatory compound.

- **Cyclooxygenase (COX-1 and COX-2) Inhibitory Activity Assay**

The cyclooxygenase 1 (COX-1) and cyclooxygenase 2 (COX-2) inhibitory activity assays were performed using a Cayman Chemical COX Colorimetric Inhibitor Screening Assay Kit (Cayman Chemical, Ann Arbor, MI, USA). The method assesses the peroxidase activity of COXs by colorimetrically monitoring the appearance of oxidized N, N, N',N'-tetramethyl-p-phenylenediamine (TMPD) at 590 nm. Samples were divided into a positive control (100% of COX activity), containing 150 µL of 0.1 M Tris–HCl buffer (pH 8.0), 10 µL of heme, and 10 µL of the enzyme, and inhibitory samples, containing 150 µL of buffer, 10 µL of heme, 10 µL of the enzyme, and 10 µL of sample solution at different concentrations. Samples were incubated at 25 °C for 5 min, and then 20 µL of arachidonic acid (AA) solution and 20 µL of a colorimetric substrate solution (TMPD) were added. After 2 min of incubation at 25 °C, the absorbance at 590 nm was read. The COX-1 and COX-2 inhibitory activities were calculated as follows:

Equation 4. Percentage of COX inhibition

$$\% \text{ COX inhibition} = [(\text{Activity of COX Activity} - \text{Activity of COX with sample}) / \text{Activity of COX}] \times 100$$

Results were expressed as IC50 (inhibitory concentration), which is the concentration of inhibitor required to inhibit COX activity by 50% (Zielinska *et al.*, 2017). Naproxen was used as the reference anti-inflammatory compound.

1.5.9. *Statistical Analysis*

Each experiment was performed in triplicate. Values were expressed as mean ± standard deviation. Graphs were constructed and IC50 values were determined using GraphPad Prism 8 software. Statistical analysis of the data was performed using the Student's t-test to assess significant differences between a pair of variables. p values below 0.05 were considered significant.

Chapter 2

Study of Antioxidant Capacity and Metabolization of GSE and ATGSE through In Vitro Gastrointestinal Digestion-colonic Fermentation

2.1. Introduction

Proanthocyanidins (PACs) are a class of polyphenols found in various parts of many botanical species and have a variety of beneficial effects on human health (Beecher, 2004). Chemically, PACs are condensed compounds consisting of two or more flavan-3-ol units linked by interflavanic bonds. The degree of polymerization (DP) and molecular weight of PACs influence their absorption and bioavailability (Tomas-Barberan *et al.*, 2007; Meeran and Katiyar *et al.*, 2007). Monomeric and oligomeric PACs are readily absorbed in the small intestine, whereas polymers cannot be directly assimilated by humans and reach the colon where they are further fermented by the gut microbiota, producing low molecular weight metabolites that can be systemically absorbed into the bloodstream (Tao *et al.*, 2019; Cires *et al.*, 2019). Consequently, the depolymerization of polymeric PACs is an important process for their uptake. The intestinal microbiota represents the total of living microorganisms that colonize the digestive tract, especially the intestine. It plays an important role in the metabolic, nutritional, physiological, and immunological processes that occur in humans (Thursby and Juge, 2017; Gentile and Weir, 2018). Namely, it is involved in the regulation of host nutrition and performs an important digestive function to enable the absorption of nutrients supplied with food. It exerts metabolic activities by extracting energy from otherwise indigestible dietary polysaccharides such as resistant starch and dietary fibers, producing important nutrients, such as short-chain fatty acids (SCFA), vitamins, and essential aminoacids

(Skrypnik and Suliburska, 2018; Zheng *et al.*, 2022; Blaak *et al.*, 2020). It is responsible for the fermentation of food components, as it can produce various compounds, including antioxidants, which are transformed by the intestinal microbiota and play an important role in human health (Leeuwendaal *et al.*, 2022). In addition, the intestinal microbiota exerts a protective function against the proliferation of pathogenic bacteria and intervenes in the regulation of intestinal function (Zheng *et al.*, 2022; Iacob S. and Iacob D.G., 2019). It is capable of performing all these functions, as long as it is in a state of equilibrium, known as eubiosis. A large body of scientific evidence has shown that PACs have an important influence on the intestinal microbiota, as they could contribute to its modulation (Ferreira *et al.*, 2023; Chen *et al.*, 2022). They are metabolized by the gut microbiota and converted into metabolites, such as procyanidins (PCs), which have antioxidant, anti-inflammatory, anti-obesogenic, and cardioprotective effects (Rauf *et al.*, 2019). Furthermore, PACs have a prebiotic and antimicrobial role by promoting the homeostasis of the intestinal environment, by reducing the survival of gram-negative bacteria, and significantly increasing the relative abundance of probiotics such as *Bifidobacteria and Lactobacillus*, which have been associated with beneficial effects on host health (Kautos *et al.*, 2017; Zhou *et al.*, 2016). In addition, thanks to their antioxidant and anti-inflammatory properties, PACs and their bacterial metabolites can exert protective effects on the gastric mucosa and the intestinal immune system, by regulating immune cell function and reducing inflammation triggered by pathogens (Andersen-Civil *et al.*, 2021; Ganesan *et al.*, 2021; Nunes *et al.*, 2019). The contribution of PACs to the enrichment of the gut microbiota and maintenance of the intestinal barrier may increase colonic fermentation and the formation of SCFA, which perform various physiological and beneficial functions for human health (Blaak *et al.*, 2020; Wu *et al.*, 2019; Han *et al.*, 2016). However, these effects may be very dependent on interindividual differences in the bacterial community of the gastrointestinal tract. One of the most typical sources of PAC is grapes, and the

seeds in particular represent the richest part (Unusan, 2020; Rodriguez-Perez *et al.*, 2019). They are waste products of wine production, but they are nevertheless a rich source of bioactive molecules, especially antioxidants (Baroi *et al.*, 2022; Schiano *et al.*, 2022a). Based on this consideration, in the results previously described in Chapter 1, we have shown that a simple and food-grade treatment allows the depolymerization of polymeric PACs occurring in grape seed extract (GSE) (*Vitis Vinifera* L.) into low molecular weight monomers and oligomers by alkaline treatment. Mass spectrometry analysis associated with a molecular networking approach showed a higher presence of polymeric PACs from GSE, while monomers and oligomers were predominantly present in the formulation obtained from alkaline treatment of GSE (ATGSE) (Iannuzzo *et al.*, 2022). Therefore, the following two objectives of this Ph.D. project were: firstly, to evaluate the different bioaccessibility of the two extracts through an *in vitro* gastrointestinal digestion-fermentation process; secondly, to evaluate their effects on the composition and functionality of the gut microbiota obtained from fecal material of five different donors (healthy adults and children, and obese, celiac and cow's milk protein allergic children). For this purpose, *in vitro* assays to evaluate total polyphenol content (TPC) and antioxidant capacity were performed, and SCFA production through UHPLC-RID analysis was determined.

2.2. Results

Grape seed extract (GSE) and its version processed under alkaline conditions (ATGSE) were subjected to *in vitro* gastrointestinal digestion, which consists of an oral, gastric, and duodenal phase followed by an intestinal fermentation which simulates the conditions that occur in humans. To evaluate the influence of digestion and fermentation on the samples, the total polyphenol content (TPC) and the antioxidant capacity were analyzed before and after the *in vitro* gastrointestinal digestion-fermentation process. In particular, the fermentation process was

performed on two different types of populations (adults and children), considering healthy and pathological conditions (cow's milk protein allergies, obesity, and celiac disease). Furthermore, the production of short-chain fatty acids (SCFA) of GSE and ATGSE following fermentation was evaluated and compared with the control sample (fecal inoculum). This analysis was carried out to evaluate the capacity of the two extracts to modify the composition and functionality of the intestinal microbiota.

2.2.1. Total Polyphenol Content (TPC) and In Vitro Antioxidant Activity before In Vitro Gastrointestinal Digestion-Fermentation

The Folin- Ciocâlteu assay was performed on the methanolic solution of the GSE and ATGSE extracts to evaluate their TPC, before *in vitro* gastrointestinal digestion-fermentation process. As shown in **Table 4**, the GSE sample showed a TPC of 92.2 g GAE/100g of extract, while the ATGSE showed a TPC of 70.8 g GAE/100g of extract ($p<0.001$ GSE *vs* ATGSE). In addition, three methods were conducted to evaluate the antioxidant capacity of the two extracts: FRAP to measure the ferric-reducing capacity, ABTS, and DPPH to measure radical scavenging activity. The results obtained were expressed in mol TE/100g of extract (**Table 4**). Accordingly, the antioxidant capacity of GSE and ATGSE was 254.70 and 263.4 mol TE/100g of extract, respectively, for the DPPH assay. For the ABTS assay, the antioxidant capacity was 184.6 and 177.3 mol TE/100g of extract, respectively. Finally, the FRAP assay showed that the antioxidant activity was 156.0 and 148.3 mol TE/100g of extract, respectively. The comparison between the antioxidant capacity of the two extracts showed no statistically significant differences, except for the FRAP method ($p< 0.05$ GSE *vs* ATGSE).

Table 4. Total polyphenol content (TPC) and antioxidant activity of grape seed extract (GSE) and its alkalized version (ATGSE) evaluated by Folin-Ciocâlteu, DPPH, ABTS, and FRAP assays.

Sample	Folin-Ciocalteau (g GAE/100g of extract ± SD)	DPPH (mol TE/100g of extract ± SD)	ABTS (mol TE/100g of extract ± SD)	FRAP (mol TE/100g of extract± SD)
GSE	92.2 ± 1.0	254.70 ± 5.4	184.6 ± 3.5	156.0 ± 3.5
ATGSE	70.8 ± 1.9**	263.4 ± 3.4	177.3 ± 3.9	148.3 ± 2.9*

Abbreviations: DPPH, 2,2-diphenyl-1-picrylhydrazyl; ABTS, 2,2'-azino-bis (3-ethylbenzothiazoline-6-sulfonic acid); FRAP, ferric reducing antioxidant power; TE, Trolox equivalent. Values are the mean ± standard deviation (SD) of three replications. Statistical significance is calculated by Student's t-test analysis: $^{*}p < 0.05$; $^{**}p<0.001$ GSE *vs* ATGSE.

2.2.2. Total Polyphenol Content (TPC) and In Vitro Antioxidant Activity after In Vitro Gastrointestinal Digestion- Fermentation

After *in vitro* gastrointestinal digestion of GSE and ATGSE, the TPC in the digestion supernatants was determined (**Figure 11**). Therefore, the Folin-Ciocâlteu results showed that the TPC of the GSE sample after *in vitro* digestion corresponded to 15.5 g of GAE/100 g of extract in contrast to the ATGSE sample where this content was significantly higher and corresponded to 51.6 g of GAE /100 g of extract ($p<0.001$ GSE *vs* ATGSE). As for the fermentation process, the TPC in the GSE sample was significantly lower than in the digestion, corresponding to 8.4 and 5.8 g GAE/100 g of extract in allergic and celiac children, respectively. The exceptions were healthy adults and children, and obese children (TPC of 15.7, 13.2, and 12.7 g GAE/100 g of extract, respectively), where this reduction was not significant. On the other hand, TPC in fermented ATGSE was significantly lower than in the digestion under all conditions studied, with values of 7.3, 6.2, 3.0, 4.5, and 2.2 mol TE/100g of extract respectively in healthy adults and children, allergic, obese and celiac children. Furthermore, the fermented GSE was significantly higher than the fermented ATGSE in all subjects.

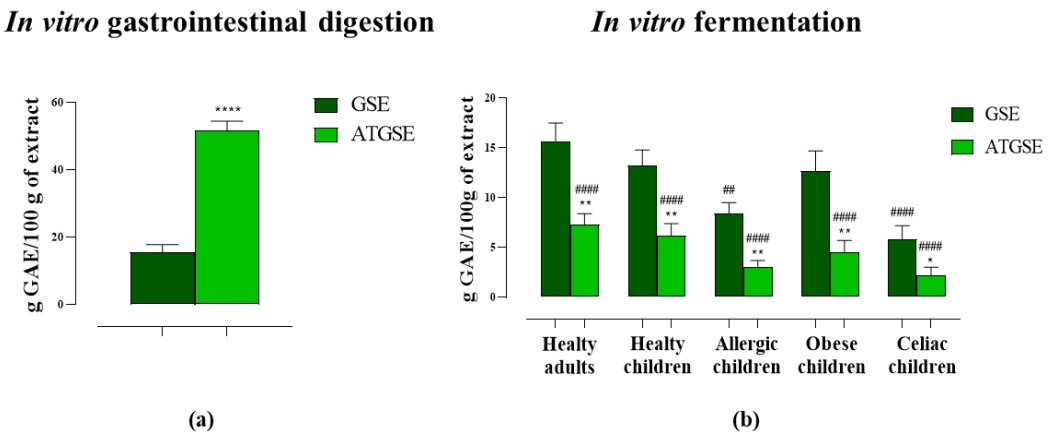

Figure 11. Total polyphenol content (TPC) of grape seed extract (GSE) and its alkalized version (ATGSE) after *in vitro* gastrointestinal (a) and *in vitro* fermentation in healthy and pathological subjects (b). Statistical significance was calculated by Student's t-test analysis: $^{*}p< 0.05$, $^{**}p< 0.01$, $^{***}p< 0.005$, $^{****}p< 0.001$ *vs* GSE; $^{\#}p< 0.05$, $^{\#\#}p< 0.01$, $^{\#\#\#}p< 0.005$, $^{\#\#\#\#}p< 0.001$ *vs* digestion.

The assays performed to assess *in vitro* antioxidant activity show a similar trend to the Folin-Ciocâlteu (**Figure 12**). Thus, the DPPH test showed that the radical scavenging activity after *in vitro* digestion corresponds to 70.7 mol TE/100g of extract for the GSE sample, while this activity was significantly higher for the ATGSE sample ($p<0.001$ *vs* GSE). After, the fermentation process, both extracts showed a statistically significant reduction in radical scavenging activity compared to digestion under all conditions investigated. In particular, the radical scavenging activity in GSE was significantly higher than in ATGSE. This activity expressed as mol TE/100g of extract, was 19.4, 20.0, 9.7, 8.5, 3.2 mol TE/100 g of extract in the GSE sample and 14.1, 10.9, 8.4, 4.5, 1.5 mol TE/100 g of extract in the ATGSE sample, in healthy adults and children, and allergic, obese and celiac children, respectively. The ability to scavenge radicals was also tested against ABTS, a water-soluble organic radical. The ABTS test showed that the radical scavenging activity after *in vitro* digestion was 52.8 and 126.1 mol TE/100g of extract in the GSE and ATGSE samples, respectively ($p<0.001$ GSE *vs* ATGSE). Similar to the DPPH

assay, *in vitro* fermentation of both samples resulted in a statistically significant decrease in antioxidant activity respect to *in vitro* digestion, but the antioxidant activity of the fermented GSE was statistically higher than in the fermented ATGSE. Thus, this activity was determined in healthy adults and children, allergic, obese, and celiac children, with values of 12.5, 10.2, 8.5, 11.7, 4.5 mol TE /100 g of GSE extract and 6.2, 4.3, 3.5, 7.7, 2.4 mol TE /100 g of ATGSE extract, respectively. Finally, the reduction power was determined by a FRAP assay. In agreement with previous results, *in vitro* digestion showed significantly higher reducing activity in the ATGSE sample than in the GSE sample (35.4 and 109.8 mol TE/100 g of extract, respectively). *In vitro* fermentation of both samples led to a statistically significant reduction in antioxidant activity compared to *in vitro* digestion under all the conditions analyzed. In the GSE sample, the reduction corresponded to 7.4, 3.4, 3.2, 6.7, and 2.5 mol TE/100 g of extract, while in the ATGSE sample, the reduction was 4.1, 0.7, 1.4, 2.2, 1.3, in healthy adults and children, allergic, obese and celiac children, respectively. In addition, the FRAP test showed that the reduction power after *in vitro* fermentation was significantly higher in GSE than in its alkalized version.

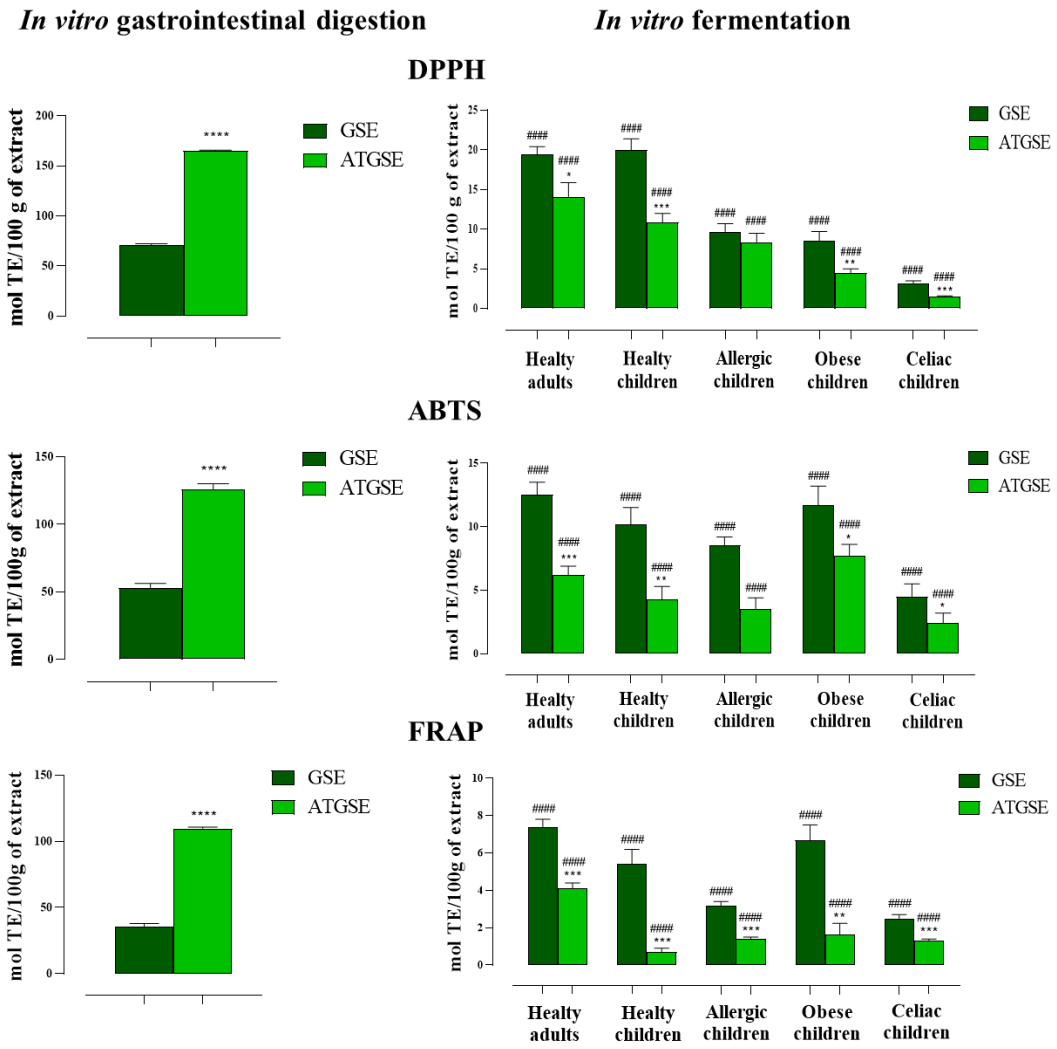

Figure 12. Antioxidant capacity of GSE and ATGSE after *in vitro* digestion-fermentation in healthy and pathological subjects. Statistical significance was calculated by Student's t-test analysis: $^{*}p< 0.05$, $^{**}p< 0.01$, $^{***}p< 0.005$, $^{****}p< 0.001$ *vs* GSE; $^{\#}p< 0.05$, $^{\#\#}p< 0.01$, $^{\#\#\#}p< 0.005$, $^{\#\#\#\#}p< 0.001$ *vs* digestion.

2.2.3. Production of Short-chain Fatty Acids (SCFA) from Gut Microbiota

After the digestion-fermentation process of GSE and ATGSE, SCFA in the fermentation supernatant were determined by coupled chromatography method with RID detection (UHPLC-RID). The SCFA identified and quantified in the samples

were lactic, acetic, succinic, propionic, and butyric acid. The concentrations of the above fatty acids in the GSE and ATGSE samples were compared with those of the respective controls (fecal inoculum). **Figure A3** in Appendix shows the elution chromatogram of the SCFA studied obtained by UHPLC-RID analysis. The results indicate that GSE and ATGSE significantly increased SCFA production compared to control samples, thus exerting an enhancing effect on SCFA-producing bacteria (Appendix, **Table A2**). In general, the increase in lactic, acetic, and succinic acid production was higher than the induced increase in butyric and propionic acid concentrations, regardless of the gut microbiota used for fermentation. In particular, propionic acid concentrations increased significantly in GSE and ATGSE compared to control only in obese children, while they decreased in all other conditions. **Table 5** shows the coefficient of percentage variation of SCFA concentration of GSE and ATGSE, compared to the control. The general trend showed that the percentage of increase was higher in the ATGSE sample than in the GSE sample.

Table 5. Coefficient of variation (%) of short-chain fatty acids (SCFA) concentration in healthy and pathological subjects compared to control, containing fecal inoculum of the different microbiota types without extracts.

Subjects	**Sample**	**Lactic acid**	**Acetic acid**	**Succinic acid**	**Propionic acid**	**Butyric acid**
		CV% *vs* Control	**CV% *vs* Control**	**CV% *vs* Control**	**CV% *vs* Control**	**CV% *vs* Control**
Healthy adults	GSE	85.08 %	148.93 %	0.96 %	-45.44 %	- 14.73 %
	ATGSE	1026.003 %	414.60 %	18.65 %	- 39.97 %	1.03 %
Healthy children	GSE	188.85 %	894.93 %	12.56 %	- 38.17 %	19.77 %
	ATGSE	13710.61 %	1072.12 %	185.09 %	-37.94 %	40.20 %
Allergic children	GSE	529.90 %	816.89 %	286.69 %	- 21.36 %	33.47 %
	ATGSE	3280.24 %	1472.55 %	305.00 %	-49.27 %	30.09 %
Obese children	GSE	2683.18 %	1292.39 %	209.78 %	73.11 %	87.55 %
	ATGSE	9539.21%	2810.83 %	68.59 %	335.19 %	96.34 %

Celiac children	GSE	4457.87 %	508.78 %	254.89 %	-60.00%	115.89 %
	ATGSE	7581.79 %	206.82 %	191.14 %	-61.00 %	82.92 %

However, to better evaluate the quantitative SCFA profile, a principal component analysis (PCA) of the dataset was performed to visualize and investigate the influence of the samples (control, GSE, and ATGSE) on SCFA production by the gut microbiota of healthy and pathological subjects. As shown in **Figure 13**, PC1, PC2, and PC3 accounted for 50.77%, 23.23%, and 14.64% of the total change, respectively. The biplot revealed a large dispersion of SCFA among the different samples and explained 74% and 61.8% of the variability for the first and second biplot, respectively. Considering the first and second PC, the analysis shows that the addition of GSE and ATGSE changed the production of SCFA, as the control samples were grouped in a different sector than the fermented samples, except for the healthy adult. Furthermore, the trend of their distribution was closely related to the production of butyric and propionic acid in the control samples, and to the production of acetic, lactic, and succinic acid in the fermented samples. The second and third PCs confirm the trend described earlier. In this case, all control samples, including the healthy adults, were distributed in a different sector than the treated samples. Their correlation with the type of fatty acids produced was similar to the first and second PC.

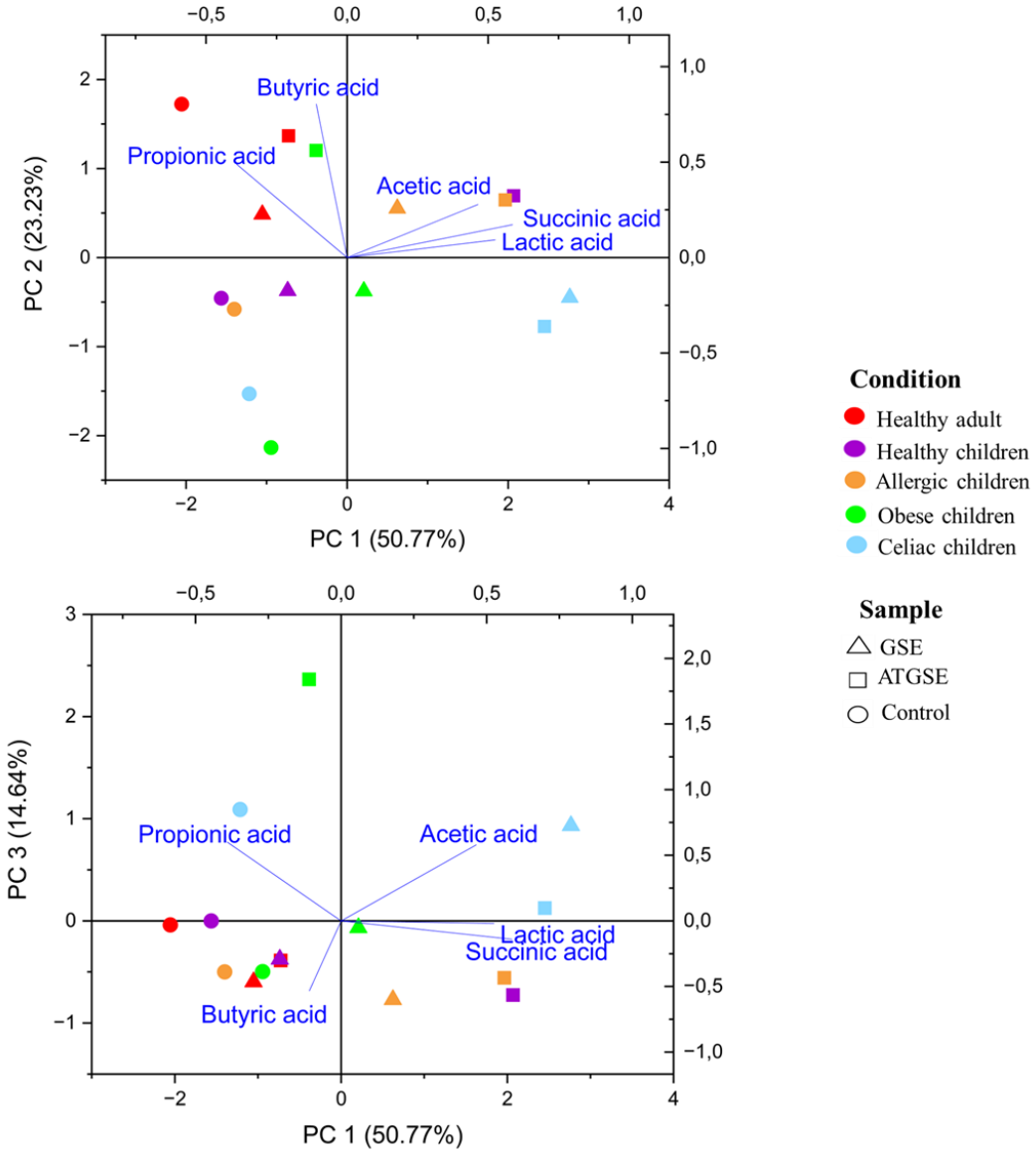

Figure 13. Biplot of the first three principal component analysis (PCA) based on the dissimilarity of short-chain fatty acid (SCFA) production in healthy and pathological subjects among control (fecal inoculum) and extracts (GSE and ATGSE).

Figure 14 shows the heatmap of the analysis of the concentrations of SCFA in the control, GSE, and ATGSE samples by the intestinal microbiota of healthy and pathological subjects. This was consistent with the biplot of the first three PCA. The

different color variations showed a different distribution of the production of SCFA in the treated samples compared to the control samples, increasing especially in the GSE and ATGSE samples. The dendrogram shows that the trend in the production of lactic, acetic, and succinic acid was similar and higher in the treated samples, as was the trend in the production of butyric and propionic acid but higher in the control samples.

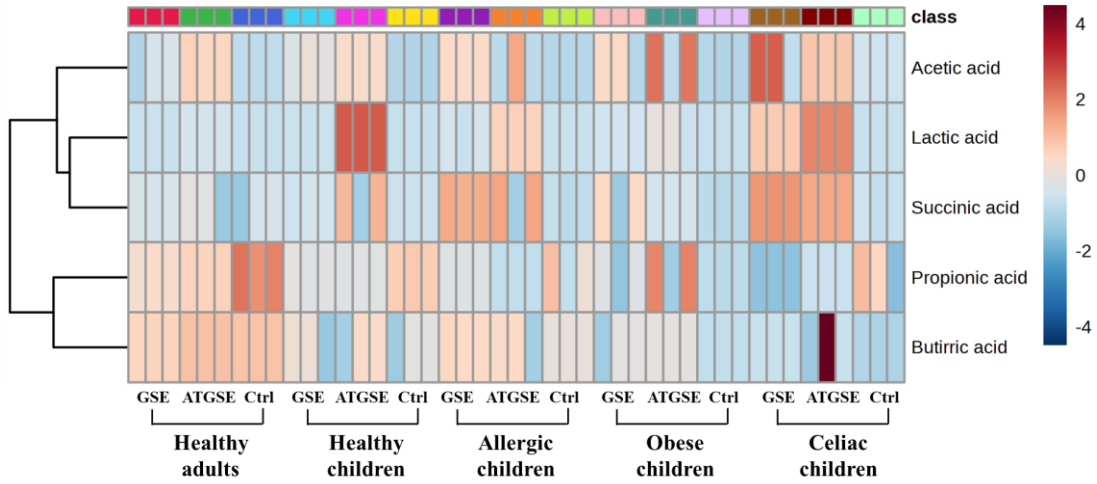

Figure 14. Heatmap of the correlation between the concentrations of SCFA produced by control (fecal inoculum) and extracts (GSE and ATGSE) in healthy and pathological subjects.

2.3. Discussion

Proanthocyanidins (PACs) are found in a wide variety of plants and have beneficial effects on health, including the prevention of cardiovascular disease, cancer, urinary tract infections, and diabetes (Izumi and Terauchi, 2020). The bioavailability of PACs is largely influenced by their DP. It has been shown that the absorption rate of these molecules usually decreases with increasing molecular weight, which also affects their absorption in different parts of the intestine (Ou and

Gu, 2014). Therefore, the previous chapter (Chapter 1) described the developed rapid and food-grade method for the depolymerization of the polymeric PACs of a grape seed extract (GSE) (*Vitis vinifera* L.) into low molecular weight monomers and oligomers under alkaline conditions (ATGSE). The aim of the study, described in this chapter, was to evaluate the different intestinal bioaccessibility, in terms of total polyphenol content (TPC) of the two extracts, using an *in vitro* gastrointestinal digestion-fermentation protocol and their different bioactivity, in terms of antioxidant capacity, after these processes. *In vitro* fermentation was performed using fecal material from five different donors (healthy adults and children, and obese, celiac, and milk protein allergic children). Firstly, to achieve this objective the TPC and antioxidant capacity of the two extracts were determined before *in vitro* digestion-fermentation process. Although Folin-Ciocâlteu showed a statistically significant reduction of TPC in ATGSE ($p<0.001$ *vs* GSE), no statistically significant difference between GSE and ATGSE was found as regards antioxidant activity from DPPH and ABTS assays. These results show once again that the alkaline treatment did not alter the antioxidant capacity of the GSE extract, as evidenced by the high antioxidant activity of both matrixes (Iannuzzo *et al.*, 2022). After *in vitro* gastrointestinal digestion, the bioaccessible polyphenolic fraction in the small intestine was 17% for GSE and 73% for ATGSE. The reduction of TPC compared to the undigested extract is due to the degradation of PACs at the gastrointestinal level (Sanchez-Valezquez *et al.*, 2021), while the higher intestinal bioaccessibility of ATGSE could be due to its higher content of PACs oligomers. In this regard, these hypotheses are consistent with studies demonstrating the best systemic absorption of monomers and oligomers of flavan-3-ols (Chen *et al.*, 2022; Serra et al., 2010). Actually, monomeric, dimeric, and trimeric PACs are rapidly absorbed in the intestine, whereas larger polymers are not absorbed and accumulate in the intestinal lumen (Cires *et al.*, 2019). In this context, Deprez *et al.* (2001), investigated the different intestinal permeability of oligomeric and polymeric PACs using colon

cancer cells (Caco-2) of human origin. These authors found that catechin, dimeric and trimeric PACs had permeability coefficients on monolayers of human intestinal epithelial Caco-2 cells similar to mannitol, a marker of paracellular transport. In contrast, the polymeric PACs (DP>7) were not permeable. This evidence could explain the better intestinal bioaccessibility of the ATGSE extract. As regards the effect of fermentation on the TPC of GSE and ATGSE, the results reported in this chapter show further degradation of polyphenols, with slight differences depending on the origin of the fecal inoculum, probably due to the different ability of the microorganisms to use PACs as substrates for their metabolism. The reduction in TPC in fermented samples has been attributed to the degradation of polyphenols by gut microbiota to bioactive metabolites that can affect regular host intestinal homeostasis (Ou and Gu, 2014). However, the TPC of the fermented GSE was found to be significantly higher than ATGSE. In this context, several studies have shown that once polymeric PACs reach the colon, they are further depolymerized by the intestinal microflora into low molecular weight monomers and oligomers or metabolized into low molecular weight aromatic metabolites, such as phenolic acids, phenyl valerolactones, and phenylacetic acids, and absorbed at intestinal level (Pereira-Caro *et al.*, 2020; Gonthier *et al.*, 2003). However, higher TPC in GSE could be due to the greater release of the more easily absorbed low-molecular metabolites in the colon. As for the antioxidant activity evaluated by DPPH, ABTS, and FRAP tests, the results obtained were in agreement with the trend observed by the Folin-Ciocâlteu assay. Thus, the results showed that the radical scavenging activity and the ferric-reducing capacity of GSE and ATGSE decreased after digestion. After fermentation, a further decrease was observed, which varied depending on the origin of the intestinal microbiota used. In addition, antioxidant activity was higher in the digested GSE than in the digested ATGSE, while in the fermented products, the trend was reversed. The hypotheses on the mechanisms underlying these activities have already been described above, as TPC and antioxidant activity are closely linked.

Overall, these results confirmed the high antioxidant potential of PACs from GSE *in vivo*, as described in several previous studies (Rodriguez-Perez *et al.*, 2019; Busserolles *et al.*, 2006). Finally, to evaluate the effect of the two extracts on the composition and functionality of gut microbiota, their influence on the production of short-chain fatty acids (SCFA) by the gut microbiota of healthy and pathological subjects was analyzed. The identified and characterized SCFA were lactic, acetic, succinic, propionic, and butyric acids. They are produced by intestinal microbiota from the fermentation of dietary polysaccharides (which are not otherwise digested) and absorbed in the intestine, serving as an energy source for the host. They exert regulatory functions on intestinal physiology, metabolism, and immunity (Koh *et al.*, 2016), and act as regulators of energy intake and inflammation (Prasad and Bondy, 2019; Terrapon and Henrissat, 2014). In addition, the interaction between gut microbiota and polyphenols is widely known in the literature, suggesting that polyphenols and the metabolites generated by intestinal microbes can modify and produce variations in the microflora community by exhibiting prebiotic effects and antimicrobial activity against pathogenic gut microflora (Parkar *et al.*, 2013; Kumar Singh *et al.*, 2019). In addition, several literature studies reported the ability of polyphenols and their metabolites to increase SCFA production in the colon (Tzounis *et al.*, 2008; Wang *et al.*, 2021), although the molecular mechanism underlying this activity is not fully understood yet. This mechanism is likely due to their ability to modulate the composition of gut microbiota, by increasing the local anaerobic bacteria through the reduction of oxidative molecules in the intestinal environment (Wang *et al.*, 2021). In this regard, our results showed that PACs both in GSE and ATGSE determined an increase in the total concentration of SCFA compared to controls. This increase was variable based on the origin of the fecal inoculum and the bacterial community present. However, a significantly higher SCFA production was found in the ATGSE sample than in the GSE sample. This result could be because PACs release metabolites at the colonic level that have a greater impact on

the composition of the gut microbiome and increase SCFA production. However, our results cannot be confirmed so far as no further studies have been conducted on the composition of the intestinal microbial community and the metabolites produced in the colon. Additionally, studies will therefore be necessary to investigate the molecular mechanisms underlying these activities.

2.4. Conclusions

In conclusion, the food-grade alkaline treatment performed on GSE could be considered a suitable and reliable method to favor a better intestinal bioavailability of ATGSE, due to its high content of oligomeric PACs. Moreover, ATGSE proved to be a bioactive product with a high antioxidant activity at the intestinal level, and, specifically, with a high capacity to increase SCFA concentration at the colonic level. Our results encourage further studies to investigate ATGSE potential beneficial effects on human health.

2.5. Experimental Section

2.5.1. Chemicals and Sample

The *in vitro* digestion-fermentation reagents used were: salivary α-amylase, pepsin from porcine gastric mucosa, porcine bile acids, tryptone, sodium dihydrogen phosphate, resazurin, cysteine, and sodium sulfide were provided by Sigma-Aldrich (Darmstadt, Germany); pancreatin from porcine pancreas was purchased from Alpha Aesar (United Kingdom). The *in vitro* antioxidant assays reagents were: Folin–Ciocâlteu reagent, sodium carbonate, gallic acid, 2,2 diphenyl-1-picrylhydrazyl (DPPH), 2,4,6-tri(2-pyridyl)-s-triazine (TPTZ), iron (III) chloride hexahydrate, sodium, HCl, acetate, 6-hydroxy-2,5,7,8-tetramethylchroman-2-carboxylic acid (Trolox), 2,2'-azino-bis(3-etilbenzotiazolin-6-solfonico) (ABTS), potassium persulfate were purchased from Sigma-Aldrich (Darmstadt, Germany). Grape seed

extract (GSE) 95% proanthocyanidins from *Vitis vinifera* L. was purchased from MB-Med S.r.l (Turin, Italy).

2.5.2. In Vitro Gastrointestinal Digestion

Grape seed extract (GSE) and its version processed under alkaline conditions (ATGSE) were subjected to *in vitro* gastrointestinal digestion to simulate physiological human intestinal processes as described by Navajas-Porras *et al.* (2022a). 1.25 grams of sample were weighed into centrifuge tubes in triplicate for *in vitro* digestion. The *in vitro* digestion was carried out in three steps: oral, gastric, and intestinal steps. First, 1.25 grams of sample were mixed with 1.25 mL of simulated salivary fluid containing α-amylase 150 U/mL, for 5 min at 37 °C and in oscillation. After 2.5 mL of simulated gastric fluid containing 4000 U/mL of pepsin was added into the tube, the pH was lowered to 3 and kept at 37 °C for 2 h in oscillation. Finally, 5 mL of simulated intestinal fluid containing 200 U/mL of pancreatin and 20 mM bile salts were added into the tube, the pH increased to 7, and kept at 37 °C for 2 h. Enzyme activity was stopped by immersion in ice for 15 min. Afterward, tubes were centrifuged at 4000 rpm for 10 min and the supernatant (fraction available for absorption at the small intestine) was used for *in vitro* antioxidant assays and the pellet (fraction not digested that would reach the colon) was used for *in vitro* fermentation. A tube not containing samples to account for the enzymes (control) was also run.

2.5.3. In Vitro Fermentation

This process was carried out following a protocol described by Pérez-Burillo *et al.* (2018), using fecal material from different 5 donors: 3 healthy adults (Body Mass Index [BMI] = 21.3), and 12 children (5–10 years old): 3 healthy children (percentile 95), 3 obese children (percentile 90), 3 celiac children and 3 children with food

allergies. None of the donors had taken antibiotics in the last 3 months. Fecal material from the same population was pooled together to account for interindividual variability. *In vitro* fermentation was carried out using 15 mL centrifuge tubes. To each tube, 0.5 g of the solid residue of the digestion was added and mixed with 10% of the final volume of the digestion, since physiologically this quantity reaches the large intestine. A control tube without extract and containing only fecal inoculum was analyzed for each of the different types of microbiota. Each of the tubes also contained 7.5 mL of fermentation medium, composed of 14 g/L of peptone, cysteine 312 mg/L, hydrogen sulfide 312 mg/L, and resazurin 0.1% v/v and 2 mL of fecal inoculum, composed of fecal material in phosphate saline buffer at a concentration of 33%. Nitrogen was bubbled into the tubes until anaerobic conditions were reached and kept at 37 °C in oscillation for 20 h. Microbial activity was halted by immersion in ice for 15 min. Tubes were centrifuged at 4000 rpm for 10 min and the obtained supernatant was aliquoted for the antioxidant capacity and the SCFA analysis.

2.5.4. In Vitro Antioxidant Assays

GSE and ATGSE extracts were subjected to *in vitro* assays to evaluate antioxidant capacity. After that, the antioxidant capacity was studied both in the supernatant obtained from *in vitro* gastrointestinal digestion and the supernatant obtained from *in vitro* fermentation. The respective blanks (chemical reagents, enzymes, and fecal inoculum) were considered to correct the antioxidant capacity values of each method.

- **Total Polyphenol Content (TPC)**

The protocol followed was determined quantitatively using the Folin-Ciocâlteu reagent, with gallic acid as the standard. Firstly, 30 µL of the sample was added in triplicate to the 96-well plate and mixed with 60 µL of Na_2CO_3 10% (w/v), 195 µL

of ultra-pure water, and 15 µL of Folin-Ciocâlteu reagent. The antioxidant reaction was monitored for 60 min at 37 °C on a FLUOStar Omega microplate reader (BMG Labtech, Germany). The absorbance of the samples was determined spectrophotometrically at 725 nm. The calibration curve was prepared with gallic acid at concentrations from 0.01 to 1.00 mg/mL. The results obtained were expressed as g of gallic acid equivalents (GAE)/100g of extract (Iannuzzo *et al.*, 2022).

- **DPPH Radical Scavenging Activity Assay**

The antioxidant activity of the extracts (GSE and ATGSE) was evaluated using a 2,2-diphenyl-1-picrylhydrazyl (DPPH) radical scavenging assay, as described by Navajas-Porras *et al.* (2022b). Therefore, 20 µL of sample and 280 µL of DPPH reagent were mixed in a 96-well plate. The DPPH reagent was prepared freshly each day by dissolving 3.7 mg of DPPH in 50 mL of MeOH. The reaction was monitored for one hour at 37 °C on a FLUOStar Omega microplate reader (BMG Labtech, Germany). The absorbance of the samples was determined spectrophotometrically at 520 nm. Each sample was tested in triplicate. A calibration curve was prepared with Trolox ranging from 0.01 to 0.4 mg/mL. The results were expressed as mol Trolox equivalent (TE)/100g of extract.

- **ABTS Radical Scavenging Activity Assay**

ABTS radical cation ($ABTS^{\bullet+}$) scavenging activity was determined according to Schiano *et al.* (2022b), with slight modifications. Briefly, ABTS stock solution was prepared with ABTS (7.0 mM) solution and potassium persulfate 2.45 mM solution and left in the dark for 12-16 h to allow radical development. This solution is stable for one week. The ABTS stock solution was diluted with ethanol: water mixture (50:50) to an absorbance of 0.70 ± 0.02 at 730 nm. This solution was used on the day of preparation. Then, 20 µL of sample and 280 µL of diluted ABTS solution were

mixed in a 96-well plate. The reaction was monitored for 20 min at 37 °C on a FLUOStar Omega microplate reader (BMG Labtech, Germany). A calibration was performed with Trolox stock solution ranging from 0.01 to 1.00 mg/mL. The results obtained are expressed as mol Trolox equivalents (TE)/100g of extract.

- **Ferric Reducing Antioxidant Power (FRAP) Assay**

The ferric-reducing ability of each sample solution was estimated according to the procedure described by Maisto *et al.* (2022a) and adapted to a microplate reader. Briefly, FRAP solution was prepared with acetate buffer (0.3 M; pH 3.6), TPTZ solution (10mM) in HCl (40mM), and FeCl3 • 6H20 (20 mM) in a ratio of 10:1:1. This solution must be kept in the dark and was used on the day of preparation. Then, 20 µL of sample and 280 µL of FRAP solution were mixed in a 96-well plate. The reaction was monitored for 30 min at 37 °C on a FLUOStar Omega microplate reader (BMG Labtech, Germany). A calibration was performed with Trolox stock solution ranging from 0.01 to 0.4 mg/mL. The results obtained are expressed as mol Trolox equivalents (TE)/100g of extract.

2.5.5. Sample Solution Preparation and UHPLC-RID Analysis of Short-chain Fatty Acid (SCFA)

For UHPLC analysis, fermentation supernatants were centrifuged at 13300 rpm for 5 minutes, filtered on a syringe filter of 0.22 µm, and diluted 1:10 with HCl 1M. The UHPLC used for the determination of SCFA was an Agilent 1290 Infinity II (Agilent, USA) equipped with a quaternary pump, an autosampler, and a refractive index detector (RID) set at 35 °C. The analysis was carried out isocratically with a mobile phase composed of H_2SO_4 5 mM solution with a flow rate of 0.5 mL/min. The column was an Infinity Lab Poroshell 120 SB-AQ (3.0x150mm, 2.7 µm; Agilent, USA) set at 35 °C. The injection volume was 5 µL. The identification of

SCFA was confirmed by comparison of the retention time of analytical standard and by coinjection with internal standard. For quantitative analysis, standard curves for each SCFA were prepared over a concentration range of 0.04–100 ppm. The analysis was performed in duplicate, and the data presented are the mean values expressed as millimolar concentration (mM) of each SCFA (Bandini *et al.*, 2022).

2.5.6. Statistical Analysis

Each experiment was performed in triplicate. Values were expressed as mean ± SD. Graphs were constructed using GraphPad Prism 8 software. Statistical analysis of the data was performed using the Student's t-test to assess significant differences between a pair of variables. The statistical significance of the data was tested by one-way analysis of variance (ANOVA), followed by the Bonferroni test to assess significant differences between more pairs of variables. p values below 0.05 were considered significant. Principal component analysis (PCA) was generated using OriginPro 2021b (OriginLab Corporation, Northampton, MA, USA). The heatmap graphic was created with the MetaboAnalystTM software.

Chapter 3

Effect of GSE and ATGSE on a Mouse Model of Testosterone-induced Benign Prostatic Hyperplasia

3.1. Introduction

Benign prostatic hyperplasia (BPH) is a common chronic disease of the urinary tract that occurs mainly in men over 40 years of age and whose incidence increases progressively with age (Roehrborn, 2011). It is characterized by increased proliferation of smooth muscle cells, stromal cells, and epithelial cells, resulting in an enlarged prostate. This can lead to obstruction of the urethra and the development of lower urinary tract symptoms (LUTS) such as urinary urgency, increased urinary frequency, nocturia, dysuria, weak urine stream, and incomplete bladder emptying (Sarma and Wei, 2012; Barkin, 2011). Although the cause of BPH remains unclear, evidence suggests that prostate size in older men is influenced by circulating androgen hormones, such as testosterone and dihydrotestosterone (DHT) (Kim *et al.*, 2015; Tong and Zhou, 2020). DHT is the ultimate mediator of prostate growth and is synthesized in the prostate from circulating testosterone by the action of the enzyme type 2 5-α reductase (Andriole *et al.*, 2004). It is more potent androgen than testosterone because it binds more strongly to the androgen receptor (AR), which regulates the expression of genes that promote the growth and survival of stromal and epithelial cells in the prostate (Roehrborn *et al.*, 2002). However, the excessive proliferation of these cells by androgens, especially DHT, is considered by several researchers to be an important cause of BPH (Choi *et al.*, 2016). Several researchers argue that androgen-dependent excessive proliferation of epithelial and stromal cells in the prostate is an important cause of BPH. In this context, a study conducted by Pejčić *et al.* (2017) showed that testosterone and DHT accumulate in the prostate stroma in patients with BPH and that there is a linear correlation between the

concentration of testosterone and DHT in the prostate tissue and prostate size. Another important process involved in the development of prostatic diseases is inflammation, which is a protective mechanism against tissue damage or pathogens. In this regard, previous studies have shown that the degree of an inflammatory process triggered at the prostate level in patients with BPH is related to the size of the prostate (Tong and Zhou, 2020). This process causes an increase in the synthesis and secretion of inflammatory cytokines and macrophages in response to inflammatory damage, as well as an increase in mediators involved in the biosynthesis of arachidonic acid (AA) (thromboxanes, prostaglandins, and leukotrienes) and oxidative stress (Olivas and Price, 2021; Hamid *et al.*, 2011). The most commonly used test to date for the diagnosis and treatment of BPH is the determination of the PSA value, whose serum level enables a distinction to be made between normal and pathological conditions (Chen *et al.*, 1996). Furthermore, the main pharmacological therapies used for the treatment of BPH include α1-adrenergic receptor antagonists (doxazosin, terazosin, and tamsulosin) and 5α-reductase inhibitors (finasteride and dutasteride). The first one relieves lower urinary tract symptoms (LUTS) and improves urethral obstruction by causing smooth muscle relaxation in the prostate and bladder. Conversely, 5-α reductase inhibitors inhibit the conversion of testosterone to DHT in the prostate, thereby reducing the size of the enlarged prostate (Oelke and Martinelli, 2016). However, the use of these drugs can lead to side effects, such as erectile dysfunction, decreased sexual desire, and reduction of seminal volume in the ejaculate (for 5-α reductase inhibitors) and orthostatic hypotension, asthenia, dizziness, impotence and retrograde ejaculation (for α1-adrenergic receptor antagonists) (Csikos *et al.*, 2021). However, to reduce these side effects, researchers have focused on the development of alternative therapeutic strategies based on the use of natural remedies for the prevention and treatment of various diseases. Among the natural agents studied, polyphenols have recently obtained increasing interest. In this regard, several studies report the

beneficial effects of polyphenolic compounds, such as proanthocyanidins (PACs), in the treatment and prevention of diseases affecting prostate health (Csikos *et al.*, 2021; Eleazu *et al.*, 2017; Mitsunari *et al.*, 2021). PACs are polymers formed by the condensation of monomeric units of flavan-3-ols, which are particularly abundant in grape seeds and have a variety of biological effects (Rauf *et al.*, 2019; Baroi *et al.*, 2022). However, the bioactivity and bioavailability of these molecules can be variable depending on their degree of polymerization (DP). Monomeric and oligomeric PACs are more bioavailable than those characterized by a higher DP (Holt *et al.*, 2002; Donovan *et al.*, 2002; Tomas-Barberan *et al.*, 2007). Based on this consideration, in our previous results we have shown that a simple, food-grade treatment allows PACs polymers from grape seed extract (GSE) (*Vitis vinifera* L.) to be depolymerized into lower molecular weight oligomers and monomers by alkaline treatment (Iannuzzo *et al.*, 2022; Chapter 1). The formulation obtained, named ATGSE, with a high content of oligomeric PACs, showed an elevated intestinal bioavailability with a high antioxidant activity compared to the GSE extract (Chapter 2). Therefore, our research objective, described in this chapter, was to investigate the beneficial potential of GSE and ATGSE in the prevention and treatment of diseases affecting human health, such as BPH. However, to test the bioactivity of GSE and ATGSE on BPH, an animal model study with BPH induced by subcutaneous administration of testosterone was conducted. At the end of the treatment, blood samples were obtained by intracardiac sampling to evaluate PSA values, while the prostate, seminal vesicles, and testicles were microsurgically removed from mice and weighed. Finally, an ELISA SPOT assay was performed on the lysates of the prostate and seminal vesicles to evaluate the modulation of the main pro-inflammatory cyto-chemokines.

3.2. Results

To evaluate the effect of GSE and ATGSE in the treatment of BPH, a study was conducted in an animal model with BPH induced by the administration of subcutaneous testosterone (1 mg/mouse). The experimental groups were divided into a control group (vehicle, olive oil), a BPH group (testosterone 1 mg/mouse), and four treatment groups. The first treatment group was administered GSE at a dose of 500 mg/kg by oral gavage. The other three groups were treated with different doses of ATGSE (125, 250, and 500 mg/kg). The treatment lasted 28 days. During the four-week treatment, the weight of the mice was monitored, and no statistically significant changes were observed in the experimental groups (Appendix, **Figure A4**). To investigate the direct effect of GSE and ATGSE on BPH prostates were weighed at the end of the treatment after being isolated from mice by microsurgery and blood samples were taken by intracardiac sampling to evaluate PSA levels. Considering the association between BPH and infertility, testicular and seminal vesicle weights were also examined. Finally, an Elisa Spot was performed on prostate and seminal vesicle homogenates to assess the modulation of the main pro-inflammatory cyto-chemokines.

3.2.1. Prostate Weight after Four Weeks of Treatment

In the testosterone-treated group (BPH) mean prostate weight increased significantly after 28 days of treatment compared to the vehicle-treated group (control), as shown in **Figure 15**. Furthermore, the group treated with testosterone and GSE at the dose of 500 mg/kg showed a significant increase compared to the control group ($p<0.01$), but no significant difference was observed compared to the BHP group. In the three experimental groups administered with testosterone concomitantly with ATGSE (125mg/kg, 250mg/kg, and 500mg/kg), a significant reduction in prostate weight was observed only at the doses of 250 mg/kg and 500

mg/kg compared to the BPH ($p<0.01$ for 250 mg/kg and $p<0.05$ for 500 mg/kg group) and compared to the group BPH + GSE 500 mg/kg ($p<0.01$ for 250 mg/kg and $p<0.05$ for 500 mg/kg). In particular, it was found that the most effective dose of ATGSE was equivalent to 250 mg/kg, at which a greater reduction in prostate weight was observed, which was almost comparable to the control group.

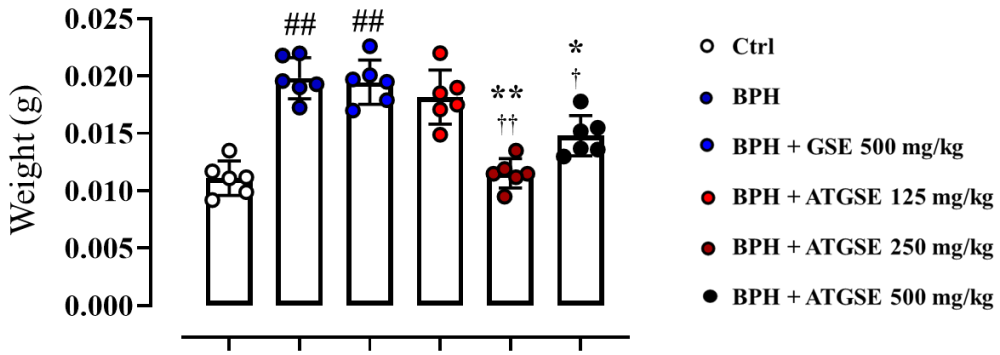

Figure 15. Evaluation of prostate weight after four weeks of treatment. Values are presented as the mean ± S.D. (n = 6 for each experimental group). Statistical significance was calculated by one or two-way ANOVA followed by Bonferroni's or Dunnett's for multiple comparisons: $^{\#\#}p \leq 0.01$ *vs* ctrl; $^{\dagger}p \leq 0.05$, $^{\dagger\dagger}p \leq 0.01$ *vs* BPH, $^{*}p \leq 0.05$, $^{**}p \leq 0.01$ *vs* BPH + GSE 500mg/kg.

3.2.2. Measurement of Prostate Specific Antigen (PSA) Values after Four Weeks of Treatment

The PSA value was measured in the serum of the animals in the different experimental groups using the PSA ELISA kit (**Figure 16**). The normal PSA value in the control group was found to be 0.772 ± 0.201. In the BPH group, a statistically significant increase in PSA value of 3.037 ± 0.849 was observed compared to the control group ($p<0.01$). Similarly, the experimental group treated with testosterone and GSE at the dose of 500 mg/kg showed a statistically significant increase in PSA levels of 3.023 ± 1.025 compared to the control group ($p<0.01$), but no statistically

significant difference was observed compared to BPH group. In the animals receiving simultaneous testosterone and ATGSE at the doses of 250 and 500 mg/kg (with a PSA value of 2.766 ± 0.860 and 0.945 ± 0.258, respectively), a statistically significant reduction in PSA levels was found compared to the BPH group ($p<0.01$) and to BPH + GSE 500 mg/kg group ($p<0.01$). The administration of testosterone and ATGSE at a dose of 125 mg/kg resulted in a PSA value of 2.766 ± 0.860, but no statistically significant difference was found compared to the other experimental groups. In line with the results obtained for prostate weight, treatment with ATGSE at a dose of 250 mg/kg proved to be the most effective in reducing the PSA levels and bringing them almost back to the level of the control group.

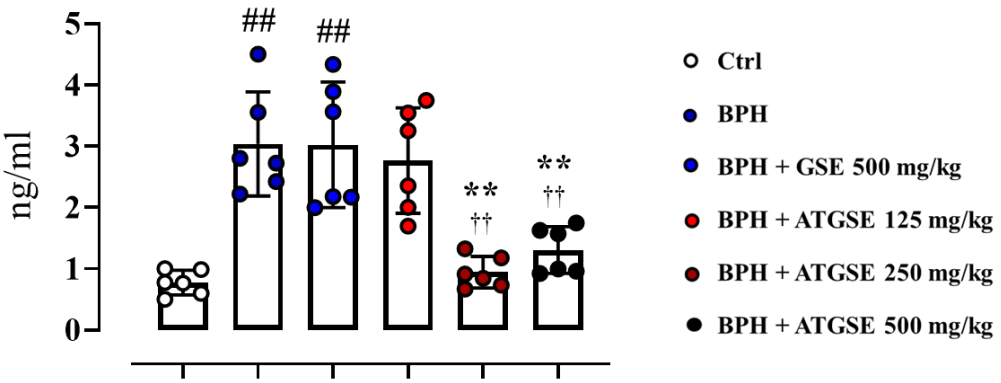

Figure 16. Measurement of PSA concentration (ng/ml) after four weeks of treatment. Values are presented as the mean ± S.D. (n = 6 for each experimental group). Statistical significance was calculated by one or two-way ANOVA followed by Bonferroni's or Dunnett's for multiple comparisons: $^{\#\#}p \leq 0.01$ *vs* ctrl; $^{\dagger}p \leq 0.05$, $^{\dagger\dagger}p \leq 0.01$ *vs* BPH, $^{**}p \leq 0.01$ *vs* BPH + GSE 500mg/kg.

3.2.3. Seminal Vesicles and Testicles Weight after Four Weeks of Treatment

The evaluation of testicle and seminal vesicle weight was performed in the following experimental groups: control, BPH + GSE 500 mg/kg, and BPH + ATGSE

at three different doses (125, 250, 500 mg/kg). Since in the experiments above on prostate weight and PSA levels, the BPH experimental group showed no statistically significant differences compared to the BPH + GSE 500 mg/kg group, and to compare the efficacy of GSE *vs* ATGSE, the BPH group was not included in this analysis. The results obtained are shown in **Figure 17**. In the group treated with testosterone and GSE at a dose of 500 mg/kg, the mean weight of the seminal vesicles increased significantly after 28 days of treatment compared to the control group ($p<0.01$). Furthermore, in the three experimental groups administered with testosterone concomitantly with ATGSE (125 mg/kg, 250 mg/kg, and 500 mg/kg), a significant decrease in seminal vesicle weight was observed only at the doses of 250 and 500 mg/kg compared to the PBH + GSE 500 mg/kg group ($p<0.05$). In particular, the most effective dose of ATGSE was 250 mg/kg, which showed the greatest reduction in seminal vesicle weight, almost comparable to the control group. On the other hand, the analysis of testicle weight showed a statistically significant reduction in the group treated with testosterone and GSE at the dose of 500 mg/kg ($p< 0.01$), but none of the three doses chosen for ATGSE was able to reverse this pathological condition.

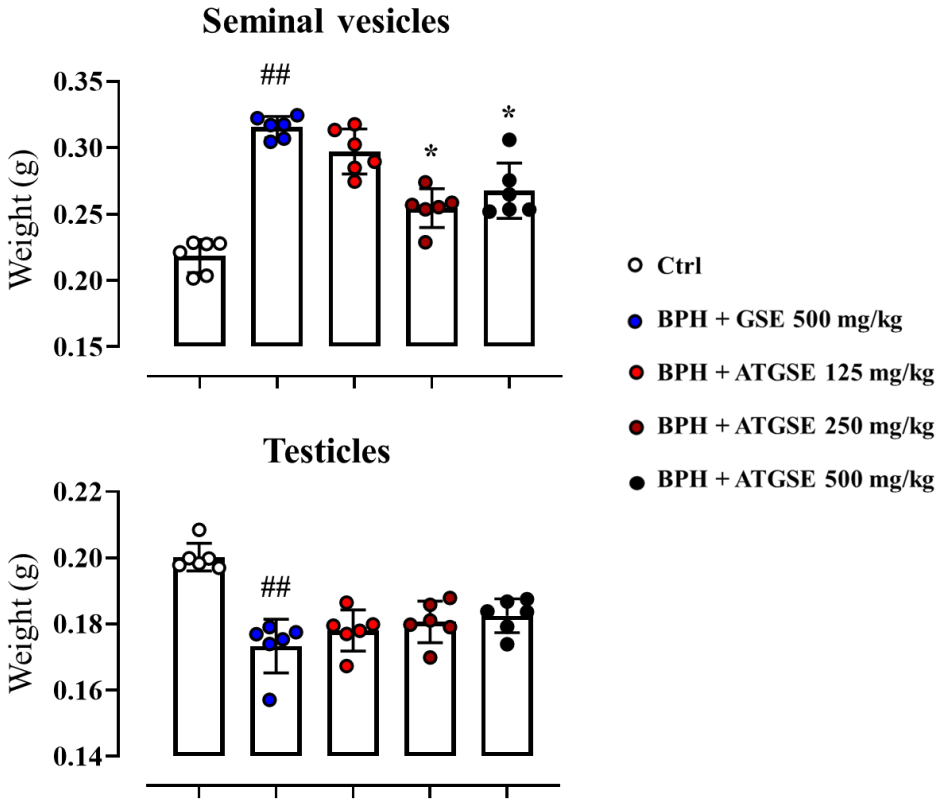

Figure 17. Evaluation of seminal vesicles and testicle weight after four weeks of treatment. Values are presented as the mean ± S.D. (n = 6 for each experimental group). Statistical significance was calculated by one or two-way ANOVA followed by Bonferroni's or Dunnett's for multiple comparisons: $^{\#\#}p \leq 0.01$ *vs* ctrl; $^{*}p \leq 0.05$ *vs* BPH + GSE 500 mg/kg.

3.2.4. Analysis of Proinflammatory Cyto-chemokine Profile in Prostate and Seminal Vesicle Homogenates

Considering the important role of inflammation in the development of BPH pathogenesis, the cytokine and chemokine profiles of prostate and seminal vesicle homogenates were analyzed with the Proteome Profiler cytokine array in the following experimental groups: control, BPH + GSE 500 mg/kg, BPH + ATGSE at three different doses (125, 250, 500 mg/kg). As reported in the previous paragraph,

the BPH group was not included in this analysis. **Figure 18** and **Figure 19** showed the results of the analysis of cytokine and chemokine expression in prostate and seminal vesicle homogenates, respectively. Consistent with the previously described experiments, administration of ATGSE selectively reversed the pro-inflammatory onset in both homogenates analyzed. In particular, analysis of the cyto-chemokine profile of the prostate homogenates (**Figure 18**) showed that the BPH + GSE 500 mg/kg group significantly increased the expression of all the cyto-chemokines analyzed, except for sICam-1. Furthermore, the group treated with testosterone and ATGSE at doses of 250 and 500 mg/kg induced specific modulation of the following factors: C5a ($p<0.01$ for 250 mg/kg), IL-1ra ($p<0.005$ and $p<0.01$ for 250 and 500 mg/kg, respectively), KC ($p< 0.05$ for 250 mg/kg, $p< 0.05$ for 500 mg/kg), MSCF ($p<0.01$ for 250 mg/kg and 500 mg/kg, respectively), SDF-1 ($p<0.01$ for 250 mg/kg and 500 mg/kg, respectively), TIMP-1 ($p<0.05$ for 250 mg/kg, $p<0.005$ for 500 mg/kg). Also, in this case, there was no significant modulation of sICam-1.

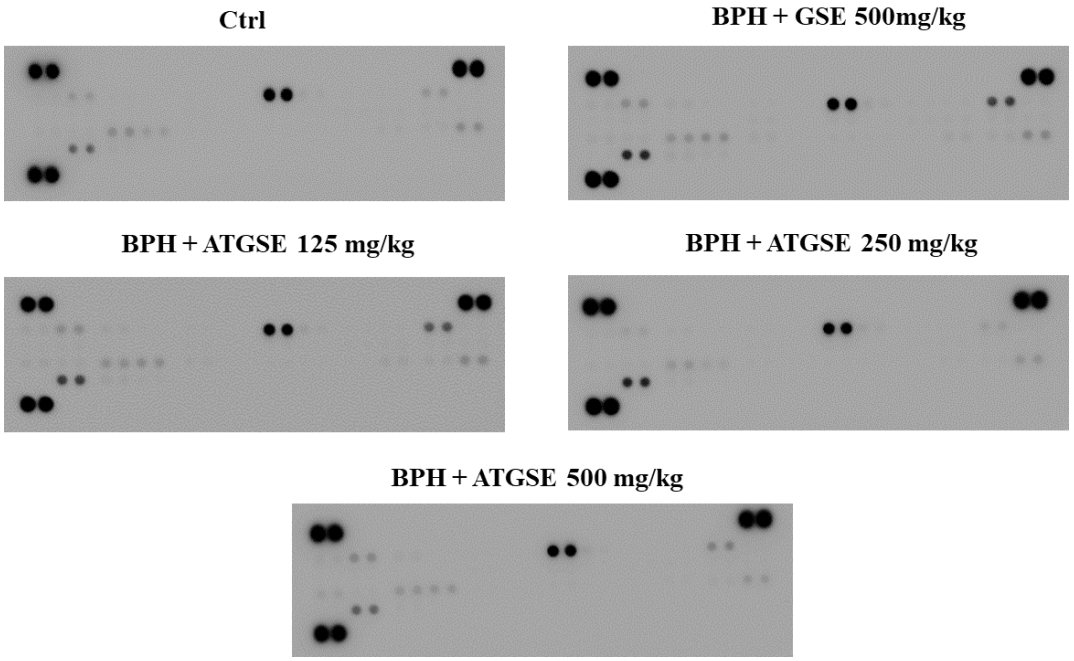

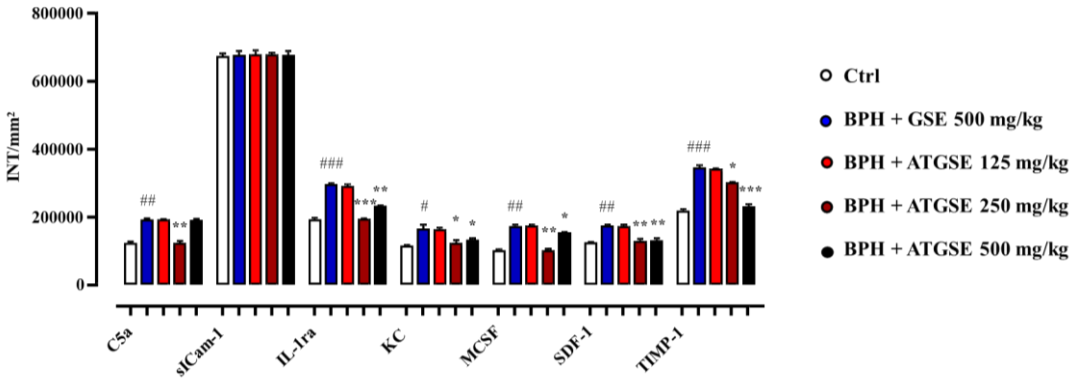

Figure 18. Inflammatory supernatants from prostate homogenates were assayed using Proteome Profiler cytokine array (ARY006, R&D System, Milan, Italy). Values are presented as the mean ± S.D. (n = 6 for each experimental group). Densitometric analysis is expressed as INT/mm^2. Statistical significance was calculated by one or two-way ANOVA followed by Bonferroni's or Dunnett's for multiple comparisons: $^{\#}p \leq 0.05$, $^{\#\#}p \leq 0.01$, $^{\#\#\#}p \leq 0.005$ *vs* ctrl; $^{*}p \leq 0.05$, $^{**}p \leq 0.01$, $^{***}p \leq 0.005$ *vs* BPH + GSE 500mg/kg.

Furthermore, the analysis of the cyto-chemokine profile of the seminal vesicle homogenates (**Figure 19**) showed the expression of the same inflammatory mediators of the prostate homogenates, in addition to the expression of other mediators such as (BLC, GCSF, JE, MIP-2, RANTES). The group treated with testosterone and ATGSE at doses of 250 and 500 mg/kg induced specific reduction of the following factors: BLC ($p< 0.01$ for 250 mg/kg), C5a ($p<0.05$ for 250 mg/kg), GCSF ($p< 0.01$ for 250 mg/kg), IL-1ra ($p<0.005$ for 250 mg/kg and $p < 0.01$ for 500 mg/kg), KC ($p< 0.005$ for 250 mg/kg and 500 mg/kg, respectively), MSFC ($p< 0.05$ for 250 mg/kg), JE ($p<0.005$ for 250 mg/kg and 500 mg/kg, respectively), MIP-2 ($p< 0.005$ for 250 mg/kg and 500 mg/kg, respectively), RANTES ($p< 0.005$ for 250 mg/kg). Conversely, the group treated with BPH + GSE 500 mg/kg showed a significant increase in the expression of the pro-inflammatory cyto-chemokines mentioned. In addition, no significant modulation of SDF-1, TIMP-1, and sICam-1 was observed. In general, these results confirmed that ATGSE at a dose of 250 mg/kg was more effective in reducing the expression of proinflammatory mediators.

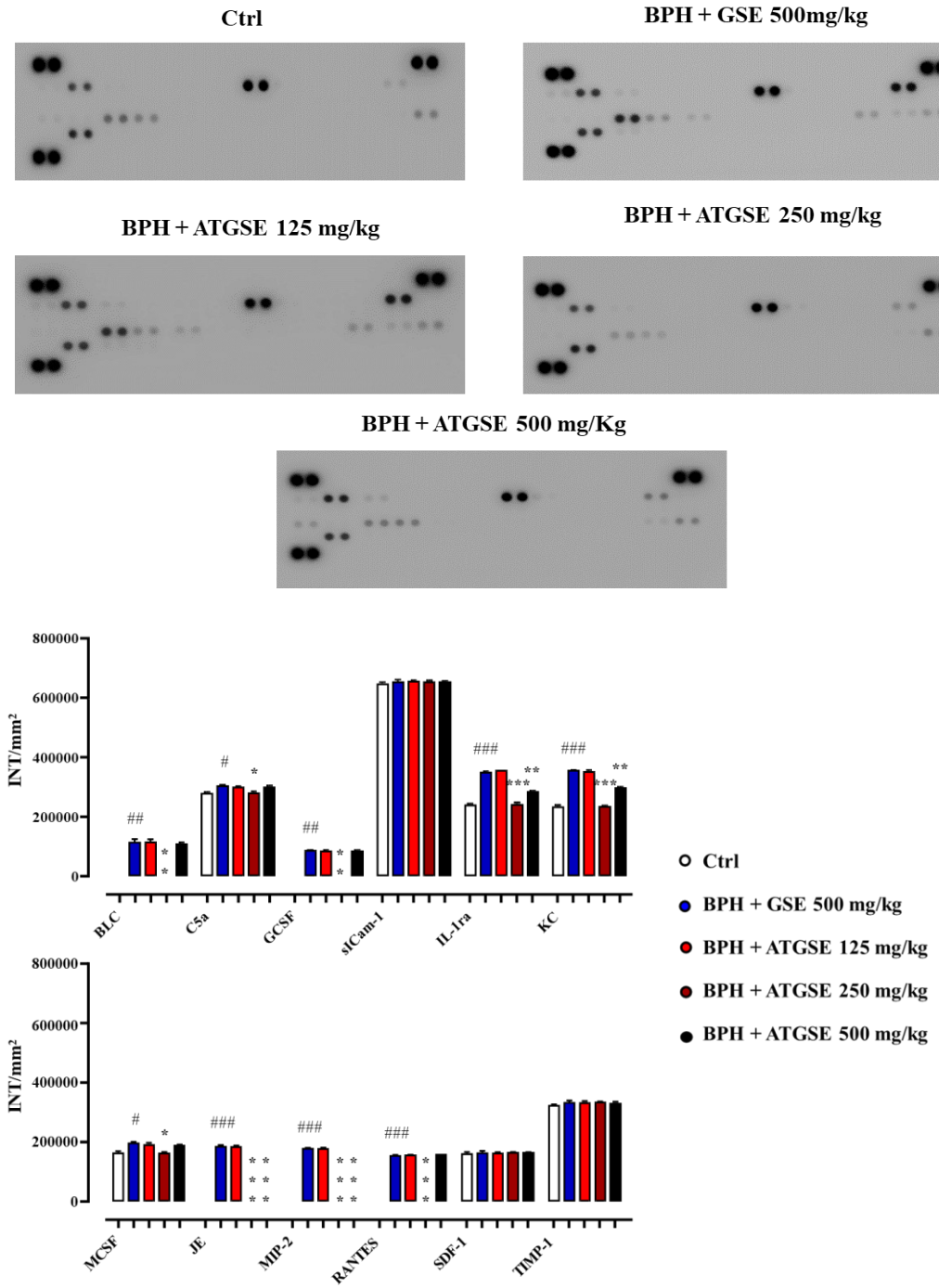

Figure 19. Inflammatory supernatants obtained from seminal vesicle homogenates were assayed using Proteome Profiler cytokine array (ARY006, R&D System, Milan, Italy).

Densitometric analysis is expressed as INT/mm^2. Values are presented as the mean ± S.D. (n = 6 for each experimental group). Statistical significance was calculated by one or two-way ANOVA followed by Bonferroni's or Dunnett's for multiple comparisons: $^{\#}p \leq 0.05$, $^{\#\#}p \leq 0.01$, $^{\#\#\#}p \leq 0.005$ *vs* ctrl; $^{*}p \leq 0.05$, $^{**}p \leq 0.01$, $^{***}p \leq 0.005$ *vs* BPH + GSE 500mg/kg.

Figure 20 shows the heatmap of densitometric analysis of pro-inflammatory cyto-chemokine expression in prostate and seminal vesicle homogenates, expressed as INT/mm^2. This is consistent with the histograms shown above. The different color variations show a different modulation of pro-inflammatory cyto-chemokines expression in the different experimental groups. The heatmap confirms that the group treated with BPH + ATGSE 250 mg/kg showed a significant reduction in the expression of pro-inflammatory cyto-chemokines, as evidenced by the similar color bands compared to the control group.

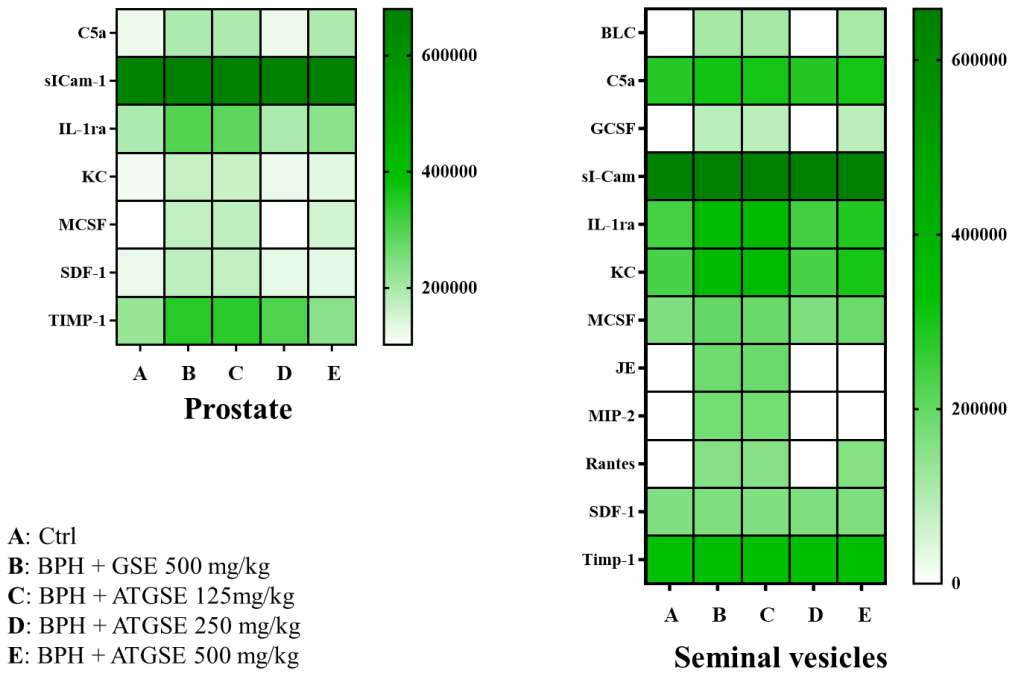

Figure 20. Heatmap of the correlation between the densitometric analysis (expressed as INT/mm^2) of pro-inflammatory cyto-chemokine expression in prostate and seminal vesicle homogenates and the different experimental groups, Ctrl (A), BPH + GSE 500 mg/kg (B),

BPH + ATGSE 125 mg/kg (C), BPH + ATGSE 250 mg/kg (D), BPH + ATGSE 500 mg/kg (E).

3.3. Discussion

BPH is a serious chronic disease of the urinary tract and is one of the most common complaints in older men (Langan, 2019). Pharmacological therapies conventionally used for the treatment of BPH include α1-adrenergic receptor antagonists and 5α-reductase inhibitors (Oelke and Martinelli, 2016). However, the side effects associated with their use have led to an increased search for alternative means to manage this disease (Yu *et al.*, 2020). In this regard, research has focused on the study of effective and safe natural products, including polyphenols, for the treatment of various diseases (Eleazu *et al.*, 2017; Mitsunari *et al.*, 2021; Rauf *et al.*, 2019). In particular, several studies reported the role of proanthocyanidins (PACs) from grape seeds in the treatment of diseases affecting prostate health (Raina *et al.*, 2007; Lei *et al.*, 2014; Lei *et al.*, 2014). However, literature studies have shown that the molecular size and degree of polymerization (DP) of these molecules have a major impact on their bioavailability and bioactivity, which are usually higher for low molecular-weight compounds (Unusan, 2020). In this regard, another aim of the Ph.D. project was to evaluate the heath beneficial effects of a grape seed extract (GSE) (*Vitis vinifera* L.), with a high content of polymeric PACs and its version processed under alkaline conditions (ATGSE), with high content of oligomeric PACs. For this purpose, GSE and ATGSE were tested in a mouse model of BPH induced by subcutaneous administration of testosterone during four weeks of treatment. At the end of the treatment, prostate, testicles, and seminal vesicle were weighed, and serum PSA levels were analyzed. Furthermore, the anti-inflammatory effect of the two extracts in the treatment of BPH was evaluated by the modulation of the main pro-inflammatory cyto-chemokines. The results regarding prostate weight showed that oral administration of ATGSE 250 mg/kg significantly reduced

prostate weight compared to the BPH group and the BPH + GSE 500mg/kg group. Although the latter group did not show statistically significant differences compared to the BPH group, several studies have been reported in the literature highlighting the beneficial potential of GSE in the treatment of BPH. In this regard, Lei *et al.* (2014), conducted a study in rats with testosterone-induced BPH, which showed that treatment with 400 mg/kg/day of grape seed-derived polyphenols effectively reduced prostate size, improved high androgen levels induced by testosterone and regulated the expression of pro-inflammatory cytokines. However, it should be considered that, in our previous results (Chapter 2), GSE extract was shown to have low intestinal bioavailability, probably due to its high content of polymeric PACs compared to ATGSE extract, which is rich in oligomeric PACs, leading to better bioavailability (Iannuzzo *et al.*, 2022). Therefore, the greater beneficial effect of ATGSE could be due to a higher fraction of bioactive PACs or their metabolites reaching the target tissue and being available for systemic absorption. The results obtained for prostate weight are consistent with the results for PSA evaluation, confirming the known relationship between serum PSA levels and BPH progression. PSA has been established as a marker of prostate cancer over the last two decades but has more recently been recognized as an equally important marker in BPH progression (Levitt and Slawin, 2007). In this regard, elevated serum PSA levels have been frequently detected in patients with male reproductive system pathologies, such as prostate cancer, BPH, and inflammatory prostate disease (Amayo and Obara, 2004; Elzanaty *et al.*, 2016). Therefore, the results obtained showed that the BPH group causes a statistically significant increase in PSA levels ($p< 0.001$ *vs* ctrl), which significantly decreases after administration of testosterone and ATGSE at a dose of 250 mg/ kg. Also in this case, the BPH + GSE 500 mg/kg group showed no significant differences compared to the BPH group. Although the etiology of BPH has not been fully elucidated so far, the important role of androgens in prostate growth has been widely demonstrated (Mirone *et al.*, 2006). Therefore, many

researchers believe that the progression of BPH is mediated by DHT, which binds to nuclear androgen receptors and stimulates the transcription of mitogenic growth factors in epithelial and stromal cells, leading to prostatic hyperplasia (Lei *et al.*, 2014). Several clinical observations support the importance of DHT in the development of nodular hyperplasia. Therefore, a study conducted by Briganti *et al. (*Briganti *et al.*, 2009), showed that the therapeutic use of 5-α reductase inhibitors significantly reduced the DHT content of the prostate, thus, reducing the prostate volume and the symptoms of BPH. Based on these considerations, it can be hypothesized that the reduction in prostate weight after treatment with ATGSE may be due to a reduction in testosterone-induced DHT levels, in addition to a reduction in serum PSA levels. It is well known that the prostate, along with testicles and seminal vesicles, contributes to the proper functioning of the male reproductive system. These organs play a key role in the production of seminal fluid, so their dysfunction can increase the risk of infertility, which is an important consequence of BPH (Bearelly and Avellino, 2021). Therefore, analysis of testicle weight showed a significant reduction in the BPH + GSE 500 mg/kg group compared to the control group. Since this experimental group showed no significant differences in prostate and PSA results, compared to the BPH group, it is likely that the administration of GSE also did not affect testicle weight. Therefore, the significant reduction in testicle weight in the group treated with BPH + GSE 500 mg/kg is probably due to the contribution of testosterone exclusively, which is consistent with the literature (Zhang *et al.*, 2013). Furthermore, none of the three ATGSE doses tested was able to reverse this pathological condition. Conversely, analysis of seminal vesicle weight showed a significant reduction in BPH + ATGSE 250 mg/kg, compared to the group treated with BPH + GSE at the dose of 500 mg/kg. Therefore, also in this case, the differences in the chemical composition of the two extracts seemed to strongly influence their bioavailability and bioactivity. Another important factor involved in the progression of BPH is inflammation, an immunological defense mechanism by

which the tissues respond to an insult (Tong and Zhou, 2020). Studies have shown that there is a significant association between prostate size and acute or chronic inflammation (Di Silverio *et al.*, 2003). Furthermore, the anti-inflammatory role of polyphenols in the treatment of inflammatory conditions is widely reported in the literature (Yahfoufi *et al.*, 2018). Therefore, to analyze the anti-inflammatory effects of GSE and ATGSE on BPH, the levels of pro-inflammatory cyto-chemokines, which are normally up-regulated during disease onset and progression, were monitored (Saylor *et al.*, 2012; Djavan *et al.*, 2009; Begley *et al.*, 2008). As a result, increased expression of several inflammatory mediators such as C5a, sICAM-1, MSCF, SDF-1, IL-1α, KC, and TIMP-1 was observed in prostate homogenates after testosterone administration. In addition, high expression of other mediators such as BLC, G-CSF, IL-1Ra, JE, MIP-2, and RANTES was observed in seminal vesicle homogenates. In this regard, the different expression of the cyto-chemokine profile of the prostate and seminal vesicles is attributable to the different cell populations (neutrophils, macrophages, and lymphocytes) which intervene in the different anatomical districts during the inflammatory process underlying BPH (Borish and Steinke, 2003). However, oral administration of ATGSE 250 mg/kg again demonstrated a significant reduction in the expression of pro-inflammatory cyto-chemokines, suggesting a key role in the modulation of inflammatory mediators which intervene following tissue damage.

3.4. Conclusions

In conclusion, oral administration of ATGSE (250 mg/kg), rich in oligomeric PACs, showed a significant decrease in prostate and seminal vesicle weights, and PSA levels in a mouse model of BPH induced by subcutaneous testosterone administration. Furthermore, ATGSE also revealed a protective effect against the inflammatory process triggered during the development of the pathology, by reducing the expression of pro-inflammatory cyto-chemokines in the involved

anatomical districts. These results suggest that ATGSE could represent a potential natural therapeutic agent for the treatment of BPH. However, the molecular mechanisms underlying must be elucidated. Further *in vitro* and *in vivo* studies are needed to evaluate its efficacy and safety in humans.

3.5. Experimental Section

3.5.1. Materials

Testosterone propionate (cat T1875) and olive oil (cat 75348) were purchased from Sigma-Aldrich Co. (Milan, Italy); Mouse Prostate Specific Antigen (PSA) ELISA Kit (cat E-EL-M0961) was purchased from Elabscience (Milan, Italy); Proteome profiler mouse cytokine array kit (cat ARY006) was purchased from R&D System (Milan, Italy). Grape seed extract (GSE) 95% proanthocyanidins from *Vitis vinifera* L. was purchased from MB-Med S.r.l (Turin, Italy). Unless otherwise stated, all the other reagents were from BioCell (Milan, Italy).

3.5.2. Animals

All animal care and experimental procedures complied with international and national law and policies (EU Directive 2010/63/EU for animal experiments, and the Basel declaration including the 3Rs concept). CD-1 male mice (10–14 weeks of age, 25–30 g of weight) were purchased from Charles River (Milan, Italy) and kept in an animal care facility under controlled temperature, humidity, and on a light: dark cycle, with ad libitum access to water and standard laboratory chow diet. All procedures were carried out to minimize the number of animals used (n=6 per group) and their suffering.

3.5.3. In Vivo Model and Drug Administration

After acclimatization, animals were randomly assigned into six groups, six animals per group, as follows: (i) Control group, (ii) Benign prostatic hyperplasia (BPH), (iii) BPH + GSE 500 mg/kg, (iv) BPH + ATGSE 125 mg/kg, (v) BPH + ATGSE 250 mg/kg, and (vi) BPH + ATGSE 500 mg/kg group (**Table 6**). The animals in the BPH groups were subcutaneously injected with testosterone propionate (1 mg/mouse) dissolved in olive oil for 28 days (Zhang *et al.*, 2013; Li *et al.*, 2018; Zhang *et al.*, 2021b), whereas the control group was only injected with olive oil. GSE and ATGSE were dissolved in distilled water (vehicle) and administered by oral gavage (p.o., 300 µl/mouse) once a day for 28 days. Body weights were taken a day before starting the treatment (baseline) and were assessed once a week. At the experimental endpoint, blood was collected by intracardiac puncture before mice were sacrificed. The prostate gland, testicles, and seminal vesicles were freed from connective tissues, excised, and weighed (Huang *et al.*, 2017). Whole blood samples were left to settle for 30 min at room temperature and then centrifugated at 10000 rpm for 5 min. The obtained sera were transferred into a 1.5 mL tube, stored at −80 °C, and used with other collected tissues (prostates and seminal vesicles) for further *ex vivo* analysis.

Table 6. Schematic representation of *in vivo* experimental groups and drug administration.

Exp. group	Group name	Testosterone	GSE	ATGSE
I	Control	-	-	-
II	BPH	1 mg/mouse	-	-
III	BPH + GSE	1 mg/mouse	500 mg/kg	-
IV	BPH + ATGSE	1 mg/mouse	-	125 mg/kg
V	BPH + ATGSE	1 mg/mouse	-	250 mg/kg
VI	BPH + ATGSE	1 mg/mouse	-	500 mg/kg

3.5.4. Measurement of PSA

PSA levels were measured to find the extent of hyperplasia induced in the prostate by testosterone treatment. For this purpose, PSA levels in the serum were quantified using an ELISA kit following the manufacturer's protocol (Nahata and Dixit, 2012). The PSA ELISA kit is intended for the quantitative determination of total PSA. Briefly, 100 µL of tissue supernatants, diluted standards, quality controls, and dilution buffer (blank) were added to a pre-coated plate with monoclonal anti-PSA for 2 h. After washing, 100 µL of biotin labeled Ab was added for 1 h. The plate was washed and 100 µL of streptavidin - HRP conjugate was added, and the plate was incubated for a further 30 min period in the dark. The addition of 100 µL of the substrate and stop solution represented the last steps before the reading of absorbance (measured at 450 nm) on a microplate reader. Antigen levels in the samples were determined using a standard curve of PSA and expressed as ng/mL.

3.5.5. Cytokine and Chemokine Protein Array

All mice were sacrificed at indicated time-point, and prostates and seminal vesicles were immediately removed and collected into a 2 mL tube for immediate preservation in liquid nitrogen and successive storage at −80 °C. The isolated tissues were homogenized in ice-chilled Tris–HCl buffer (20 mM, pH 7.4) containing 1 mM EDTA, 1 mM EGTA, 1 mM PMSF, 1 mM sodium orthovanadate, and one protease inhibitor tablet per 50 mL of buffer. According to the manufacturer's instructions, equal volumes (1.5 mL) of the pulled prostate or seminal vesicle homogenates from all experimental conditions were then incubated with the pre-coated proteome profiler array membranes. Dot plots were detected by using the enhanced chemiluminescence detection kit and Image Quant 400 GE Healthcare software (GE Healthcare, Italy) and successively quantified using GS 800 imaging densitometer software (Biorad, Italy) (Saviano *et al.*, 2022).

3.5.6. Data and Statistical Analysis

Statistical analysis complies with international recommendations on experimental design and analysis in pharmacology (Curtis *et al.*, 2015) and data sharing and presentation in preclinical pharmacology (Alexander *et al.*, 2018; George *et al.*, 2017). All data are presented as the mean ± S.D. and were analyzed using one or two-way ANOVA followed by Bonferroni's or Dunnett's for multiple comparisons. GraphPad Prism 8.0 software (San Diego, CA, USA) was used for analysis. Differences among groups were considered significant when $p \leq 0.05$ was achieved. The sample size was chosen to ensure alpha 0.05 and power 0.8. Animal weight was used for randomization and group allocation to reduce unwanted sources of variations by data normalization. No animals and related *ex vivo* samples were excluded from the analysis. *In vivo* study was carried out to generate groups of equal size (n=6 of independent values), using randomization and blinded analysis.

Chapter 4

Evaluation of Antibacterial Activity of GSE and ATGSE against Escherichia coli in Bladder Epithelial Cell Cultures

4.1. Introduction

Uropathogenic *Escherichia coli* (UPEC) is the main etiological agent of urinary tract infections (UTIs), causing approximately 85% of bladder infections recorded in a year worldwide (Gajdács *et al.*, 2019). UTIs are gender-specific diseases, with a higher incidence in women (Haider *et al.*, 2010). They occur when pathogenic enterobacteria, penetrating through the urethra, proliferate in the lower urinary tract and cause urethritis or cystitis. If not properly treated, urinary tract infections can spread to the upper urinary tract, including ureters and kidneys, causing ureteritis and pyelonephritis. The attack of bacterial pathogens on urothelial cells is regulated by specific interactions between surface bacterial components (adhesins) and receptors of the host cell. The adhesins are found on superficial filamentous organelles (called pili or fimbriae). These structures allow bacteria to climb up to the bladder, adhere to the epithelial cells, and colonize the tissues (Wilnes *et al.*, 2008). The treatment of UTIs consists of the administration of antibacterial drugs (trimethoprim/sulfamethoxazole, nitrofurantoin, and fluoroquinolones), but due to the dramatic increase in antimicrobial resistance (AMR), this strategy has partially lost its therapeutic efficacy (Chibeleano *et al.*, 2020; Petca *et al.*, 2021). For this reason, the search for natural alternatives for the treatment of UTIs is a topic of current research. In particular, in recent years, much attention has been paid to the identification and selection of natural bioactive molecules, in particular polyphenols, effective in the prevention and treatment of urinary tract infections. In this regard, natural products based on proanthocyanidins (PACs), such as A-type PACs from

cranberry products, are widely known in the literature (Cimolai N., and Cimolai T., 2007). However, studies on the efficacy of B-type PACs in the treatment of UTIs are very poor and often contradictory. The main sources of B-type PACs are grape seeds, blueberries, cocoa, and apples, while plums, avocados, peanuts, curry, and cinnamon (Gu *et al.*, 2003). Among these, grape seeds are being studied extensively for their antibacterial properties (Jayaprakasha *et al.*, 2003; Chedea *et al.*, 2011) and could be potential therapeutic candidates for the health of the urogenital tract. However, the bioactivity of PACs may vary depending on their molecular structure and size (Zheng *et al.*, 2020). In this regard, this chapter investigated the antibacterial effect of grape seed extract (GSE) and its version processed under alkaline conditions (ATGSE), with a different composition in PACs, against UPEC in bladder epithelial cells. Then, the activity of the two extracts to inhibit bacterial growth and their ability to inhibit bacterial invasion were evaluated.

4.2. Results and Discussion

Grape seed extract (GSE) is a product of the wine industry rich in polyphenolic compounds, especially proanthocyanidins (PACs), which have been shown to have health-promoting effects (Sci *et al.*, 2003). Many literature studies attribute an antibacterial effect to GSE (Chedea *et al.*, 2011; Baydar *et al.*, 2006), which provides the opportunity to develop GSE as a natural additive to improve food safety and quality. However, studies related to its potential antimicrobial effects on urinary tract health are very poor. Conversely, studies on the effects of cranberry, rich in A-type PACs, in the treatment of urinary tract infections are widely known in the literature (Jepson *et al.*, 2012). However, as discussed in detail in previous chapters, the activity of PACs-based products can vary greatly depending on their molecular structure and size. In this context, our research was focused on investigating the potential antibacterial activity of GSE and ATGSE against UPEC in bladder epithelial cells. Firstly, to assess the effect of GSE and ATGSE on the proliferation

of urinary bladder cells, an MTT assay was performed. The results obtained showed that none of the tested concentrations of the two extracts affected cell proliferation (**Figure 21**).

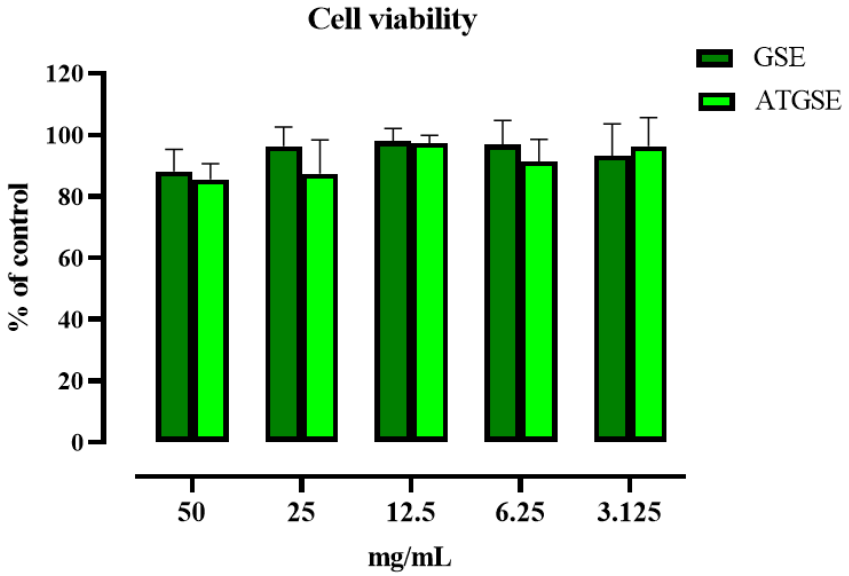

Figure 21. Cell viability (% of control) of GSE and ATGSE. Statistical analysis was conducted by one-way ANOVA followed by Bonferroni's for multiple comparisons, but no significant data were found compared to the control.

Then, to evaluate the effect of GSE and ATGSE on bacteria growth, a Minimum Inhibitory Concentration (MIC) assay was performed. The results demonstrated that ATGSE showed a significant ability to modulate the growth of *E.coli* compared to GSE ($p<0.01$), with an inhibition rate of 50% and 35% at a concentration of 50mg/mL and 25mg/mL, respectively. (**Figure 22**). The sub-inhibitory concentration (sub-MIC) of 25 mg/mL was used as the starting concentration for the bacterial invasion assay. The UTIs are mediated by the interaction between the pathogen and the bladder epithelium, so the first phase to counteract infection could be to modulate the colonization of the bacteria and their ability to invade the tissue (Wiles *et al.*, 2008). To this end, the inhibitory capacity of GSE and ATGSE against

the invasion of *E.coli* in bladder epithelial cells was investigated. This inhibitory effect was determined by pre-treatment of cells with the extracts and subsequently infection with *E.coli* and by simultaneous treatment of cells treated with *E.coli* and the extracts. The co-treatment showed no effect on inhibiting bacterial growth, while pre-treatment showed significant modulation of bacterial invasion. **Table 7** shows the results of the invasion assay expressed as CFU/mL. In particular, a significant reduction in the number of internalized microorganisms was observed after treatment with ATGSE 25 mg/mL compared to control (cells without treatment), showing a CFU/mL of 4.4×10^5 and 6.4×10^8 respectively. In addition, ATGSE showed a significant inhibitory effect on bacterial invasion compared to GSE (1.8×10^7 CFU/mL). **Figure 23** shows the results of cells infected with *E.coli* after treatment with GSE and ATGSE at the concentration of 25 mg/mL.

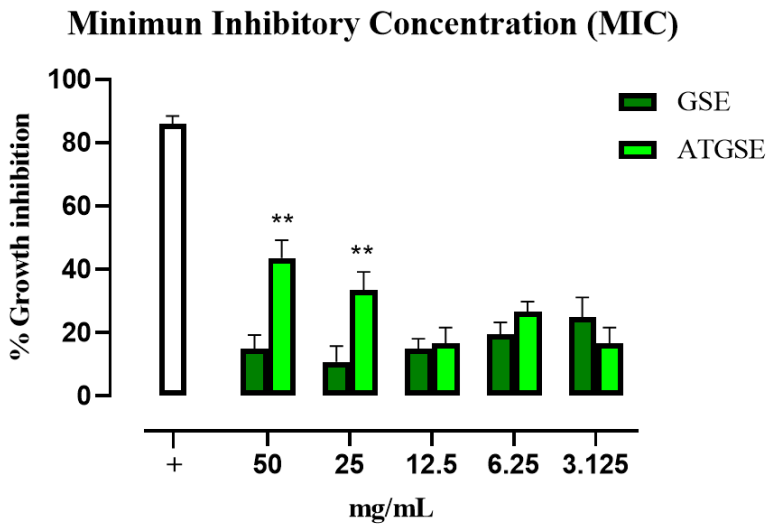

Figure 22. Minimum inhibitory concentration (MIC) of GSE and ATGSE expressed as percentage (%) of growth inhibitory activity compared to untreated control. Ampicillin was used as a positive control. Statistical significance is calculated by Student's t-test analysis: $^{**}p < 0.01$ GSE *vs* ATGSE

Table 7. Invasion assay of GSE and ATGSE compared to control (HT-1376 cells infected with *E.coli*) and expressed as colony forming unit (CFU)/mL.

Sample	CFU/mL	CFU/mL (25 mg/mL)	CFU/mL (12.5 mg/mL)	CFU/mL (6.25 mg/mL)	CFU/mL (3.125 mg/mL)
Control	6.4×10^8	-	-	-	-
GSE	-	1.8×10^7	5.4×10^7	3.2×10^7	2.1×10^7
ATGSE	-	4.4×10^5	5.8×10^7	9.1×10^7	2.1×10^8

(a) **(b)** **(c)**

Figure 23. Microplates used for the invasion assay of cells infected with *E. coli* and treated with GSE and ATGSE. Figure (a) shows cells infected with *E.coli* (control), while figures (b) and (c) show cells infected with *E.coli* treated with GSE and ATGSE at the concentration of 25 mg/mL.

4.3. Conclusions

In conclusion, our research showed that ATGSE at a concentration of 25 mg/mL proved to be more effective than GSE in inhibiting bacterial invasion. This effect could be due to its high content in oligomeric PACs. These preliminary results suggest that ATGSE could be a potential candidate for the management of UTIs. However, further studies will be needed to investigate the molecular mechanisms underlying these activities.

4.4. Experimental Section

4.4.1. Materials

The cells used in this experiment HT-1376 CRL-1472TM cells (ATCC) were grown and maintained in ATCC-formulated Eagle's Minimum Essential Medium, supplemented with antibiotic solution 100X and 10% Fetal Bovine Serum (FBS) (Microgem, Naples, Italy). The bacteria strain used was *Escherichia coli* (*E.coli*) (ATCC 700928/ UPEC). *E.coli* was grown in Luria–Bertani (LB) medium (Difco, Sparks, MD, USA). Grape seed extract (GSE) 95% proanthocyanidins from *Vitis vinifera* L. used for analyses was purchased from MB-Med S.r.l (Turin, Italy).

4.4.2. Determination of Cell Viability by MTT Assay

The cytotoxicity of GSE and ATGSE against HT-1376 cells was determined using the colorimetric 3-[4,5-dimethylthiazol-2-yl]-2,5 diphenyl tetrazolium bromide (MTT) assay (Mosmann, 1983). Cells were seeded at a density of 2 x 10^4 cells/well in 96-well microliter plates and incubated at 37 °C with 5% CO_2 in a humid environment. Concentrations ranging from 50 to 3.125 mg/mL were used for cell treatment for 20 hours. After incubation, 100 µL of MTT (Sigma-Aldrich, St. Louis, Missouri, USA) solution (0.3 mg/mL) was added to each well for 3 hours at 37 °C. The solution was removed from each well and 100 µl of DMSO (100%) was added to solubilize the formazan crystals. Lastly, the absorbance at 570 nm was measured using a microplate reader (Tecan, Männedorf, Swiss). Three independent experiments were performed. The absorbance ratio between the cell culture treated with the extracts and the untreated control (ctrl) multiplied by 100 represents cell viability (percentage of control).

4.4.3. Minimum Inhibitory Concentration (MIC)

MIC assay was obtained through the plate microdilution assay, following the guidelines of the Clinical and Laboratory Standards Institute (CLSI). Briefly, GSE

and ATGSE were serially diluted to obtain concentrations in the range from 50 mg/mL to 3.125 mg/mL at a final volume of 100 µL/well. Ampicillin (20 µg/mL) was used as a positive control. *E. coli* was grown in Luria–Bertani (LB) medium (Difco, Sparks, MD, USA) at 37 °C in aerobic conditions with orbital shaking (180 rpm). A volume of 50 µL of the bacterial suspension was added to each well, achieving a final density of 5×10^5 CFU/well. Thereafter, the plate was incubated at 37 °C and the turbidity was measured after 20 hours of incubation, using a microplate reader (Tecan, Männedorf, Swiss). The assay was performed in biological triplicate. Growth inhibitory activity was expressed as a mean percentage (%) of growth inhibition with respect to control without antimicrobial extract (untreated bacteria) (de Llano *et al.*, 2015).

4.4.4. Invasion Assay

To evaluate the capability of GSE and ATGSE to modulate invasion of *E.coli*, urinary bladder cells (HT-1376) were grown in Eagle's Minimum Essential Medium, supplemented with antibiotic solution 100X and 10% Fetal Bovine Serum (FBS) to reach 70% of confluence. *E. coli* was grown in Luria–Bertani (LB) medium (Difco, Sparks, MD, USA) at 37 °C in aerobic conditions with orbital shaking (180 rpm). Then cells were pretreated for 24 h with GSE and ATGSE extracts, separately, at the following concentrations: 25 mg/ml, 12.5 mg/ml, 6.25 mg/ml, and 3.125 mg/mL. Then, cells were infected with the uropathogenic E. coli (UPEC) for 4h (MOI 10^5 CFU/mL). The experiments were conducted at the same time with the two different treatments. At the end of the treatments, cells were washed three times with PBS and treated with gentamycin (Merck; Italy) at a bactericidal concentration (10 µg/mL) for 4 h at 37 °C. Then, cells were detached with trypsin and lysed with 0.1% Triton-X100 at 4 °C. Finally, cells were diluted in PBS and plated using Luria–Bertani (LB) medium, and the bacterial colonies were counted after 24 h at 30 °C in triplicate

using 10 μL to evaluate the CFU/mL (colony-forming unit/mL) (Brannon *et al.*, 2020; Martinez *et al.*, 2000; Schilling *et al.*, 2001).

4.4.5. Statistical Analysis

Each experiment was performed in triplicate. Values were expressed as mean ± standard deviation. Graphs were determined using GraphPad Prism 8 software. Student's t-test to assess significant differences between a pair of variables. The statistical significance of the data was tested by one-way analysis of variance (ANOVA), followed by the Bonferroni test to assess significant differences between more pairs of variables. p values below 0.05 were considered significant.

Chapter 5

Development of a Potential Nutraceutical Formulation for the Treatment of Urogenital Diseases

5.1. Introduction

In the previous chapters, it was shown that the development of a food-grade depolymerization method for a grape seed extract (GSE) (*Vitis vinifera L.*) rich in polymeric proanthocyanidins (PACs), allowed the production of a nutraceutical formulation (ATGSE) with a high content of oligomeric PACs, which are more bioavailable and bioactive. Specifically, the high intestinal bioavailability of ATGSE was discussed in Chapter 2, while in Chapters 3 and 4, it was shown that ATGSE could have a potentially beneficial effect in the treatment of urogenital diseases. Furthermore, as reported in Chapter 1, ATGSE production was characterized by a final freeze-drying step. From a technological point of view, this lyophilized appears as a high-volume and high-density powder, which as such is difficult to use for the development of a nutraceutical formulation. For this reason, it is necessary to add the appropriate excipients and use the appropriate technologies that allow the production of the most suitable pharmaceutical form for human intake. Therefore, this chapter analyzes the technological process carried out in the Department of Galenic Technique of the company S.I.I.T. S.R.L.-INNOVATIVE HEALTHCARE PRODUCTS in Milan (Italy), to develop a potential nutraceutical formulation for the treatment of urogenital diseases. The common food supplements useful in this type of pathology are generally administered orally. Although studies in the literature are often contradictory, some of them report that polyphenols are particularly sensitive to the gastric environment. In this regard, our results have shown that the total polyphenol content (TPC) in ATGSE is significantly reduced after *in vitro* gastrointestinal digestion (Chapter 2). For this reason, the preparation of a gastro-

resistant tablet proved to be the most appropriate dose form to ensure a greater fraction of bioactive PACs at the systemic level.
The phases leading to the development of this formulation were:

- Granulation and subsequent addition of the appropriate excipients
- Formation of the tablet core
- Gastro-resistant coating of the tablet
- Coating Colored Film of the tablet

In the development of the gastro-resistant tablet, various technological processes had to be applied to find the most suitable method for the controlled release of the active ingredient (ATGSE) in the small intestine. The experimental tests carried out concerned the choice of granulation method, excipients and the quantity of gastro-resistant coating to be used to promote the correct release of the active ingredient. This chapter describes the final technological process that proved to be the most suitable to achieve the objectives set.

5.2. Granulation

ATGSE lyophilized was subjected to a wet granulation process using alcohol and a high-speed granulator called Diosna. The amount of active ingredient (ATGSE) and excipients used during the granulation process are shown in **Figure 24**. The choice of 500 mg of active ingredient was derived from our *in viv*o results, which showed that the dose of ATGSE 250 mg/kg was most effective in the treatment of benign prostatic hypertrophy in animal models (Chapter 3). With a corresponding conversion to humans, the daily dose would correspond to about 1 g with an intake of two tablets per day. First, the density of ATGSE was measured, which was 0.055 g/mL. Furthermore, the flowability of the powder, which is an important parameter for volumetric distribution (to form capsules and tablets), was evaluated using a suitable instrument reported in the European Pharmacopoeia (Ph.

Eur.) based on the passage of the powder through a funnel with a hole of known diameter. This measurement takes into account the time required for the powder to flow through the funnel. The measurement carried out showed that ATGSE does not flow through the funnel. To increase the density of the lyophilized, microcrystalline cellulose, an excipient dilution function, was added and the density was measured again (0.12 g/mL). Then, the mixture obtained was placed in the Diosna and mixed with a solution of alcohol and binder (polyvinylpyrrolidone PVP K30) to obtain solid granules formed by the compaction of the powder particles. The granulate powder was placed in the oven at 45°C for 6 hours. At the end of the treatment, the granulate was sieved and the density was measured (0.45 g/mL).

Name	mg/tablet	%
Lyophilized ATGSE	500,00 mg	44,84
Mycrocrystalline cellulose	600,00 mg	53,81
Polyvinylpyrrolidone PVP K30	15,00 mg	1,35
Ethyl Alcohol 96°C	470,00 mg	42,15
Total	1115,00 mg	

Figure 24. Quantity (expressed in mg/tablet or percentage) of active ingredient (ATGSE) and excipients used for the granulation process.

Figure 25 shows the excipients added to the granulate to obtain the final mixture used to form the tablet core. Vitamins such as zinc, vitamin D3, and selenium were added, which according to the literature are effective in the treatment of urogenital diseases (Vastalova *et al.*, 2013; Das and Buchholz (2019); Deng *et al.*, 2019; Elfakharany *et al.*, 2022; Ali *et al.*, 2020; Mohsenpour *et al.*, 2019). Excipients have been added according to their activity: croscarmellose sodium and polyplasdone XL with a disintegrating function to facilitate the disintegration of the tablet after contact

with water, and magnesium stearate with a lubricating and anti-friction function to prevent friction and wear of the machinery.

Name	mg/tablet	%
Granulate	1115,00 mg	87,80
Zinc	20,58 mg	1,62
Vitamin D3	1,20 mg	0,09
Selenium	0,06 mg	0,0048
Croscarmellose sodium	35,00 mg	2,76
Polysplasone XL	85,66 mg	6,75
Magnesium stearate	12,50 mg	0,98
	1270,00 mg	

Figure 25. Final mixture of ingredients for the formation of the tablet core.

Then, the density and flowability of the mixture obtained were re-evaluated, important parameters to ensure correct compression. A density of 50 g/mL was found. Therefore, the technological process carried out allowed a significant improvement in the density of the matrix. The evaluation of the flowability showed that the powder flows quickly and easily through the funnel (19 seconds).

5.3. Formation of the Core

In the previous paragraphs, the most important properties of a compressible powder were evaluated: sufficient flowability, high density, and rapid release (disintegration) of the active ingredients by using appropriate excipients. In the next phase, the core of the tablets was formed using a tablet press. Some indications of the specifications adopted for tablet production are a dosing chamber of 13.7 mm; thickness of 2.10 mm and kilonewton 25-27. A format of 21.4 × 10 was chosen for the tablet.

5.3.1. European Pharmacopoeia Test for Uncoated Tablets

The core of the uncoated tablet was subjected to the controls required by the Ph. Eur. to avoid any defects in the manufacture of the pharmaceutical forms. The control test carried out were:

- **uniformity of mass**: 20 units taken at random from the same batch are weighed individually and the average mass is determined. No more than two of these individual masses may deviate from the average by more than 5% and no unit by more than twice this percentage.
- **fracture strength of tablets**: measures of the force required to cause the fracture of the tablets by axial resistance (thickness) obtained by pressure in the center of one of the two sides of the tablet and radial resistance (hardness) obtained by pressure along the tablet diameter.
- **friability of uncoated tablets**: place 10 weighed tablets in a suitable instrument described in the Ph. Eur. (drum) which rotates about 100 times. At the end of the process, remove the tablets from the instrument, discard the released powder, and re-weigh them. The weight loss should not exceed 1%.
- **disaggregation**: the test determines whether the tablets disaggregate within the prescribed time when they are placed in a liquid medium, usually water at the temperature of 36-38°C. For this test, a specific container described in Ph. Eur is used, which is alternately lowered and raised in a different solution (to simulate the peristaltic movements of the stomach) depending on the type of tablet (for uncoated tablets, this is usually water). The tablets should dissolve within the prescribed time (usually 15 minutes). This test was performed on six tablets taken from a sample representative of the entire batch.

5.4. Gastro-resistant Coating

Once the core of the tablets conformed to the texts reported by the Ph. Eur, the tablets were gastro-resistant coated in the tablet coating machine to ensure release in the intestine. The materials and excipients used in this phase are shown in **Figure 26**. Shellac is the most commonly used material for the enteric coating of nutraceuticals, pesticides, and food additives, as it is of natural origin and has good resistance to gastric fluids. It is derived from the hardened secretion of the insect *Kerria lacca*. Other excipients used were: an aqueous solution of ammonium carbonate to facilitate the solubilization of the shellac; triethyl citrate a plasticizer agent used to improve the mechanical properties of shellac films and to prevent cracking and breaking; methocel is a non-gastro-resistant filming agent used to allow the disintegration of the tablet at intestinal pH (pH=6.8).

Name	mg/tablet	%
Shellac	38,15 mg	8,55
Ammonium carbonate	2,86 mg	0,64
Methocel	12,69 mg	2,84
Triethyl citrate	4,30 mg	0,96
Purified water	388,16 mg	87,00
Total wet weight:	446,16 mg	
Total dry weight:	58,00	

Figure 26. Materials and excipients used for gastro-resistant coating.

5.4.1. European Pharmacopoeia Test for Coated Tablets

The tablets covered with a gastro-resistant coating must comply with the following test:

- **disaggregation:** the same apparatus is used for uncoated tablets, but the liquid medium used changed. Firstly, the tablets are placed in 0.1 M hydrochloric acid (HCl) solution for 2 hours. No tablet should show signs of disintegration that would allow the contents to escape. Then, the liquid medium is replaced by a phosphate buffer solution pH 6.8 and the apparatus is operated for 1 hour. During this time, the tablets should dissolve. This test was performed on 6 tablets taken from a sample representative of the entire batch.

5.5. Coating Colored Film

In the final phase, the coated tablets were filmed with a dye in the tablet coating machine. The materials and excipients used are shown in **Figure 27**. An aqueous solution of Sepifilm (filming agent) is used in which colored excipients (cochineal carmine dye and indigo carmine blu dye) are dissolved.

Name	mg/tablet	%
Sepifilm lp 700 white	23,97 mg	11,99
Cochineal carmine dye	0,03 mg	0,01260
Indigo carmine blu dye	0,0014 mg	0,00072
Purified water	176,00 mg	87,99997

Total wet weight:	200,00 mg
Total dry weight:	24,00
Total weight tablet:	1352,00

Figure 27. Materials and excipients used for coating colored film.

5.6. Conclusions

In conclusion, the technological process allowed to significant increase the density of ATGSE and turn it into a compressible powder. Considering the nature of this PAC-rich food matrix and its sensitivity to gastric pH, the gastro-resistant tablet proved to be the most appropriate choice to increase the bioaccessibility of the active ingredient in the small intestine. Such this formulation could improve the beneficial effects of pathologies affecting the urogenital system, as shown by our previous results.

General Conclusions

This Ph.D. thesis focused on the study of proanthocyanidins (PACs), bioactive molecules found in a variety of plants and foods with numerous beneficial effects on human health. In particular, the food matrix of our interest was a grape seed extract (GSE) (*Vitis vinifera* L.), an abundant waste product obtained from the agri-food industry, that is particularly rich in PACs. The choice of this raw material was driven by the growing interest of the food and nutraceutical industries in the valorization and functional reuse of agri-food waste products as an alternative raw material for the extraction of bioactive compounds to be included in nutraceuticals and food supplements. However, the main limitation of PACs is related to their degree of polymerization (DP) and molecular size which influence their absorption and bioavailability. Therefore, this Ph.D. thesis aimed to develop a food-grade, as well as, rapid and economical method for the large-scale production of PACs with high bioavailability and bioaccessibility from GSE. This extract was subjected to alkaline treatment to depolymerize PAC polymers into low molecular weight monomers and oligomers. The results showed that both GSE and ATGSE, obtained by alkaline treatment of GSE, exhibited high antioxidant and anti-inflammatory activity *in vitro*. Therefore, no variations in the biological activity were detected before and after treatment. After *in vitro* gastrointestinal digestion, the bioaccessible polyphenol fraction and antioxidant capacity were higher in ATGSE than in GSE, while this trend was reversed after in vitro fermentation. Therefore, the food-grade alkaline treatment performed on GSE could be considered a suitable and reliable method to favor a better intestinal bioavailability of ATGSE, due to its high content of oligomeric PACs. Moreover, ATGSE proved to be a bioactive product with a high antioxidant activity at the intestinal level, and, specifically, with a high capacity to increase short-chain fatty acid (SCFA) concentration at the colonic level. In view of

the obtained results, the second part of my Ph.D. project aimed to investigate ATGSE potential beneficial effects on human health. In particular, the interest was directed toward diseases of the urogenital system. Therefore, a first evaluation of the different bioactivity of the two extracts was performed through a study on an animal model of benign prostatic hyperplasia (BPH) induced by subcutaneous administration of testosterone. Data showed that the oral administration of ATGSE (250 mg/kg), rich in oligomeric PACs, showed a significant decrease in prostate and seminal vesicle weights, and PSA levels. Furthermore, ATGSE also revealed a protective effect against the inflammatory process triggered during the development of the pathology, by reducing the expression of pro-inflammatory cyto-chemokines in the involved anatomical districts. In addition, the different bioactivity of the two extracts was tested in an *in vitro* model to evaluate their ability to inhibit the invasion of uropathogenic *Escherichia Coli* (UPEC) in human bladder cells. Our research showed that ATGSE at a concentration of 25 mg/mL proved to be more effective than GSE in inhibiting bacterial invasion. Considering these promising biological effects of ATGSE, the most appropriate technological process was developed to obtain a nutraceutical formulation based on ATGSE. In particular, the gastro-resistant tablet proved to be the most appropriate choice to increase the bioaccessibility of the active ingredient in the small intestine. This formulation could guarantee beneficial effects on pathologies affecting the urogenital system, demonstrated by our previous results. In conclusion, our data reasonably support ATGSE as a source of innovative and promising nutraceutical formulations with beneficial effects on human health. According to the observed results, these beneficial activities may be attributed to the high content of oligomeric PACs in ATGSE extract. Undoubtedly, the results obtained highlight the need for further *in vitro* and *in vivo* studies aimed at clarifying the mechanism of action underlying the beneficial effects of ATGSE in humans.

Appendix

Figure A1. LC-MS/MS-based Molecular Networking of compounds clustered together and detected in GSE and ATGSE. Blue and green nodes were identified in GSE and ATGSE extracts, respectively. Instead, red nodes represented compounds in common in the two extracts. The proanthocyanidin (PAC) cluster in the red box was the one identified and discussed in this article.

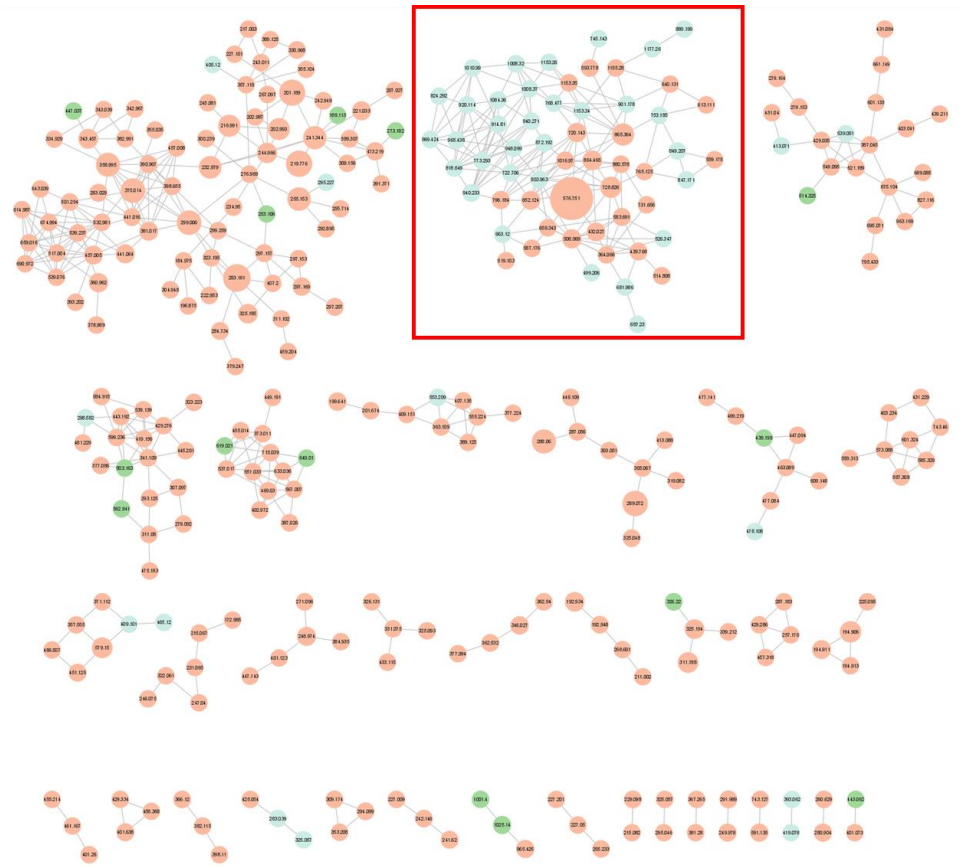

Table A1. UHPLC-ESI HRMS/MS analysis of proanthocyanidin (PAC) compounds present in GSE and ATGSE.

Compound	Charge	m/z	Formula	R_t	Fragment ions	Reference
Procyanidin trimer B-type isomer 1	$[M-H]^-$	865.2012	$C_{45}H_{37}O_{18}$	1.33	695.1379 (-$C_8H_{10}O_4$), 577.1376 (-$C_{15}H_{12}O_6$), 451.1054 (-$C_{21}H_{18}O_9$), 425.0871 (-$C_{23}H_{20}O_9$), 407.0779 (-$C_{23}H_{22}O_{10}$), 289.0716 (-$C_{30}H_{24}O_{12}$), 287.0554 (-$C_{30}H_{26}O_{12}$), 125.0231 (-$C_{39}H_{31}O_{15}$)	(Lin *et al.*, 2014)
Procyanidin trimer B-type isomer 2	$[M-H]^-$	865.2012	$C_{45}H_{37}O_{18}$	1.85	739.1673 (-$C_6H_6O_3$), 695.1412 (-$C_8H_{10}O_4$), 577.1353 (-$C_{15}H_{12}O_6$), 575.1199 (-$C_{15}H_{14}O_6$), 451.1039 (-$C_{21}H_{18}O_9$), 449.0876 (-$C_{21}H_{20}O_9$), 425.0884 (-$C_{23}H_{20}O_9$), 423.0718 (-$C_{23}H_{22}O_9$), 407.0772 (-$C_{23}H_{22}O_{10}$), 405.0613 (-$C_{23}H_{24}O_{10}$), 289.0719 (-$C_{30}H_{24}O_{12}$), 287.0562 (-$C_{30}H_{26}O_{12}$), 125.0233 (-$C_{39}H_{31}O_{15}$)	(Lin *et al.*, 2014)
(Epi)gallocatechin	$[M-H]^-$	305.0667	$C_{15}H_{13}O_7$	2.13	287.0562 (-H_2O), 179.0342 (-$C_6H_6O_3$), 137.0234 (-$C_8H_8O_4$), 125.0233 (-$C_9H_8O_4$)	(Yuzuak *et al.*, 2018)
(Epi)gallocatechin-(Epi)catechin isomer 1	$[M-H]^-$	593.1290	$C_{30}H_{25}O_{13}$	2.57	467.0984 (-$C_6H_6O_3$), 441.0836 (-$C_8H_8O_3$), 425.0883 (-$C_8H_8O_4$), 407.0775 (-$C_8H_{10}O_5$), 305.0674 (-$C_{15}H_{12}O_6$), 303.0512 (-$C_{15}H_{14}O_6$), 289.0720 (-$C_{15}H_{12}O_7$), 125.0233 (-$C_{24}H_{20}O_{10}$)	(Singh *et al.*, 2018)
(Epi)catechin-(Epi)gallocatechin isomer 1	$[M-H]^-$	593.1303	$C_{30}H_{25}O_{13}$	3.03	467.0976 (-$C_6H_6O_3$), 441.0839 (-$C_8H_8O_3$), 423.0728 (-$C_8H_{10}O_4$), 305.0668 (-$C_{15}H_{12}O_6$), 289.0710 (-$C_{15}H_{12}O_7$), 287.0563 (-$C_{15}H_{14}O_7$), 269.0452 (-$C_{15}H_{16}O_8$), 125.0234	(Singh *et al.*, 2018)

					($-C_{24}H_{20}O_{10}$)	
Procyanidin trimer B-type isomer 3	$[M-H]^-$	865.2004	$C_{45}H_{37}O_{18}$	3.15	713.1530 ($-C_8H_8O_3$), 695.1426 ($-C_8H_{10}O_4$), 577.1340 ($-C_{15}H_{12}O_6$), 575.1193 ($-C_{15}H_{14}O_6$), 451.1029 ($-C_{21}H_{18}O_9$), 449.0889 ($-C_{21}H_{20}O_9$), 425.0869 ($-C_{23}H_{20}O_9$), 423.0710 ($-C_{23}H_{22}O_9$), 407.0778 ($-C_{23}H_{22}O_{10}$), 405.0618 ($-C_{23}H_{24}O_{10}$), 289.0722 ($-C_{30}H_{24}O_{12}$), 287.0563 ($-C_{30}H_{26}O_{12}$), 125.0233 ($-C_{39}H_{31}O_{15}$)	(Lin *et al.*, 2014)
(Epi)gallocatechin-(Epi)gallocatechin B-type linkage isomer 1	$[M-H]^-$	609.1226	$C_{30}H_{25}O_{14}$	3.22	591.1151 ($-H_2O$) 423.0742 ($-C_8H_{10}O_5$), 303.0509 ($-C_{15}H_{14}O_7$), 285.0410 ($-C_{15}H_{16}O_8$), 125.0232 ($-C_{24}H_{20}O_{11}$)	(Singh *et al.*, 2018)
Procyanidin pentamer B-type linkage isomer 1	$[M-2H]^{2-}$	720.1550	$C_{75}H_{60}O_{30}$	3.70	1315.2996 ($-C_6H_5O_3$), 865.2018 ($-C_{30}H_{23}O_{12}$), 577.1329($-C_{45}H_{35}O_{18}$), 575.1212 ($-C_{45}H_{37}O_{18}$), 449.0874 ($-C_{51}H_{43}O_{21}$), 407.0786($-C_{53}H_{45}O_{22}$), 289.0720 ($-C_{60}H_{47}O_{24}$), 287.0568 ($-C_{60}H_{49}O_{24}$)	(Lin *et al.*, 2014)
(Epi)gallocatechin-(Epi)catechin isomer 2	$[M-H]^-$	593.1300	$C_{30}H_{25}O_{13}$	3.78	467.0998 ($-C_6H_6O_3$), 441.0807 ($-C_8H_8O_3$), 425.0880 ($-C_8H_8O_4$), 407.0772 ($-C_8H_{10}O_5$), 305.0664 ($-C_{15}H_{12}O_6$), 303.0513 ($-C_{15}H_{14}O_6$), 289.0720 ($-C_{15}H_{12}O_7$), 125.0233 ($-C_{24}H_{20}O_{10}$)	(Singh *et al.*, 2018)
(Epi)catechin *O*-hexoside isomer 1	$[M-H]^-$	451.1232	$C_{21}H_{23}O_{11}$	3.79	289.0719 ($-C_6H_{10}O_5$), 205.0500 ($-C_{10}H_{14}O_7$), 151.0391 ($-C_{13}H_{16}O_8$), 125.0235 ($-C_{15}H_{18}O_8$)	(Šukovic *et al.*, 2020)
Procyanidin dimer B-type isomer 1	$[M-H]^-$	577.1354	$C_{30}H_{25}O_{12}$	3.87	559.1238 ($-H_2O$), 451.1039 ($-C_6H_6O_3$), 425.0880 ($-C_8H_8O_3$), 407.0775 ($-C_8H_{10}O_4$), 289.0719	(Lin *et al.*, 2014)

					(-$C_{15}H_{12}O_6$), 287.0566 (-$C_{15}H_{14}O_6$), 125.0233 (-$C_{24}H_{20}O_9$)	
Catechin	[M-H]-	289.0718	$C_{15}H_{13}O_6$	4.34	271.0615 (-H_2O), 245.0818 (-CO_2),179.0342 (-$C_6H_6O_2$), 125.0233 (-$C_9H_8O_3$)	(Yuzuak *et al.*, 2018)]
(Epi)catechin-(Epi)catechin-(Epi)gallocatechin isomer 1	[M-H]$^-$	881.1949	$C_{45}H_{37}O_{19}$	4.42	577.1337 (-$C_{15}H_{12}O_7$), 451.1018 (-$C_{21}H_{18}O_{19}$), 425.0869(-$C_{23}H_{20}O_{10}$), 407.0777 (-$C_{23}H_{22}O_{11}$), 303.0509 (-$C_{30}H_{26}O_{12}$), 289.0719(-$C_{30}H_{24}O_{13}$), 287.0565 (-$C_{30}H_{26}O_{13}$), 125.0233 (-$C_{39}H_{32}O_{16}$)	(Singh *et al.*, 2018)
Procyanidin trimer B-type isomer 4	[M-H]$^-$	865.2007	$C_{45}H_{37}O_{18}$	4.60	739.1646 (-$C_6H_6O_3$), 713.1530 (-$C_8H_8O_3$), 695.1365 (-$C_8H_{10}O_4$), 577.1365(-$C_{15}H_{12}O_6$), 575.1216 (-$C_{15}H_{14}O_6$), 451.1031 (-$C_{21}H_{18}O_9$), 449.0869 (-$C_{21}H_{20}O_9$), 425.0869 (-$C_{23}H_{20}O_9$), 423.0721 (-$C_{23}H_{22}O_9$), 407.0778(-$C_{23}H_{22}O_{10}$), 405.0604 (-$C_{23}H_{24}O_{10}$), 289.0722 (-$C_{30}H_{24}O_{12}$), 287.0564 (-$C_{30}H_{26}O_{12}$), 125.0233 (-$C_{39}H_{31}O_{15}$)	(Lin *et al.*, 2014)
Procyanidin dimer A-type	[M-H]$^-$	575.1196	$C_{30}H_{23}O_{12}$	4.62	557.1055 (-H_2O), 449.0876 (-$C_6H_6O_3$), 423.0724 (-$C_8H_8O_3$), 407.0773 (-$C_8H_8O_4$), 289.0719 (-$C_{15}H_{10}O_6$),285.0406(-$C_{15}H_{14}O_6$), 125.0233 (-$C_{24}H_{18}O_9$)	(Rue and Rush, 2018)
Procyanidin dimer B-type isomer 2	[M-H]$^-$	577.1356	$C_{30}H_{25}O_{12}$	4.65	559.1265 (-H_2O), 451.1039 (-$C_6H_6O_3$), 425.0881 (-$C_8H_8O_3$), 407.0772 (-$C_8H_{10}O_4$), 289.0718 (-$C_{15}H_{12}O_6$), 287.0563 (-$C_{15}H_{14}O_6$), 125.0233 (-$C_{24}H_{20}O_9$)	(Lin *et al.*, 2014)
(Epi)Gallocatechin-(Epi)catechin-	[M-H]$^-$	879.1812	$C_{45}H_{35}O_{19}$	4.66	709.1220 (-$C_8H_{10}O_4$), 577.1347	(de Souza *et al.*, 2008)

(Epi)catechin AB-type linkage					(-$C_{15}H_{10}O_7$), 451.1039 (-$C_{21}H_{16}O_{10}$), 449.0872 (-$C_{21}H_{18}O_{10}$), 465.0805 (-$C_{21}H_{18}O_9$), 447.0722 (-$C_{21}H_{20}O_{10}$), 421.0562 (-$C_{23}H_{22}O_{10}$), 303.0510 (-$C_{30}H_{24}O_{12}$), 289.0719(-$C_{30}H_{22}O_{13}$), 287.0563 (-$C_{30}H_{24}O_{13}$), 178.9978 (-$C_{36}H_{28}O_{15}$), 161.0237(-$C_{36}H_{30}O_{16}$), 125.0233 (-$C_{39}H_{30}O_{16}$)	
(Epi)catechin-(Epi)gallocatechin isomer 2	$[M-H]^-$	593.1315	$C_{30}H_{25}O_{13}$	4.81	467.0982 (-$C_6H_6O_3$), 441.0831 (-$C_8H_8O_3$), 423.0721 (-$C_8H_{10}O_4$), 305.0667(-$C_{15}H_{12}O_6$), 289.0725 (-$C_{15}H_{12}O_7$), 287.0556 (-$C_{15}H_{14}O_7$), 269.0456 (-$C_{15}H_{16}O_8$), 125.0233 (-$C_{24}H_{20}O_{10}$)	(Singh *et al.*, 2018)
(Epi)gallocatechin-(Epi)gallocatechin B-type linkage isomer 2	$[M-H]^-$	609.1204	$C_{30}H_{25}O_{14}$	4.92	591.1160 (-H_2O), 441.0835 (-$C_8H_8O_4$), 423.0669 (-$C_8H_{10}O_5$), 303.0516 (-$C_{15}H_{14}O_7$), 285.0410 (-$C_{15}H_{16}O_8$), 125.0233 (-$C_{24}H_{20}O_{11}$)	(Singh *et al.*, 2018)
(Epi)catechin-(Epi)catechin-(Epi)catechin-(Epi)gallocatechin B-type linkage	$[M-2H]^{2-}$	584.1285	$C_{60}H_{48}O_{25}$	4.98	879.1683 (-$C_{15}H_{13}O_6$), 591.1125 (-$C_{30}H_{25}O_{12}$), 577.1360(-$C_{30}H_{23}O_{13}$), 575.1193 (-$C_{30}H_{25}O_{13}$), 449.0891 (-$C_{24}H_{17}O_9$), 407.0772 (-$C_{26}H_{19}O_{10}$), 303.0508 (-$C_{33}H_{23}O_{11}$), 289.0719 (-$C_{33}H_{21}O_{12}$), 287.0563(-$C_{33}H_{23}O_{12}$), 285.0399 (-$C_{33}H_{25}O_{12}$),125.0233 (-$C_{55}H_{43}O_{22}$)	(Singh *et al.*, 2018)
Procyanidin trimer B-type isomer 5	$[M-H]^-$	865.1970	$C_{45}H_{37}O_{18}$	4.98	739.1647 (-$C_6H_6O_3$), 713.1519 (-$C_8H_8O_3$), 695.1406 (-$C_8H_{10}O_4$), 577.1354(-$C_{15}H_{12}O_6$), 575.1194 (-$C_{15}H_{14}O_6$), 559.1254 (-$C_{15}H_{24}O_7$), 451.1035(-$C_{21}H_{18}O_9$), 449.0879 (-$C_{21}H_{20}O_9$), 425.0880 (-$C_{23}H_{20}O_9$), 423.0715(-$C_{23}H_{22}O_9$), 407.0770	(Lin *et al.*, 2014)

					($-C_{23}H_{22}O_{10}$), 405.0609($-C_{23}H_{24}O_{10}$), 289.0719($-C_{30}H_{24}O_{12}$), 287.0562 ($-C_{30}H_{26}O_{12}$), 125.0233 ($-C_{39}H_{31}O_{15}$)	
(Epi)catechin-(Epi)catechin-(Epi)gallocatechin isomer 2	$[M-H]^-$	881.1962	$C_{45}H_{37}O_{19}$	5.03	425.0887 ($-C_{23}H_{20}O_{10}$), 407.0779 ($-C_{23}H_{22}O_{11}$), 303.0500($-C_{30}H_{26}O_{12}$), 289.0725 ($-C_{30}H_{24}O_{13}$), 287.0551 ($-C_{30}H_{26}O_{13}$), 125.0235 ($-C_{39}H_{32}O_{16}$)	(Singh *et al.*, 2018)
(Epi)Catechin-(Epi)Gallocatechin-(Epi)catechin AB-type linkage	$[M-H]^-$	879.1799	$C_{45}H_{35}O_{19}$	5.30	727.1334 ($-C_8H_8O_3$), 709.1212 ($-C_8H_{10}O_4$), 591.1157 ($-C_{15}H_{12}O_6$), 573.1049 ($-C_{15}H_{13}O_7$), 441.0834 ($-C_{23}H_{18}O_9$), 439.0663 ($-C_{23}H_{20}O_9$), 423.0735 ($-C_{23}H_{20}O_{10}$), 421.0562 ($-C_{23}H_{22}O_{10}$), 403.0458($-C_{23}H_{24}O_{11}$), 303.0507 ($-C_{30}H_{24}O_{12}$), 289.0720 ($-C_{30}H_{22}O_{13}$), 287.0559($-C_{30}H_{24}O_{13}$), 178.9964 ($-C_{36}H_{28}O_{15}$), 161.0234 ($-C_{36}H_{30}O_{16}$), 125.0232 ($-C_{39}H_{30}O_{16}$)	(de Souza *et al.*, 2008)
(Epi)catechin *O*-hexoside isomer 2	$[M-H]^-$	415.1259	$C_{21}H_{23}O_{11}$	5.40	289.0719 ($-C_6H_{10}O_5$), 271.0607 ($-C_6H_{12}O_6$), 205.0504 ($-C_{10}H_{14}O_7$), 151.0386 ($-C_{13}H_{16}O_8$), 125.0234 ($-C_{15}H_{18}O_8$)	(Šukovic *et al.*, 2020)
(Epi)catechin-(Epi)gallocatechin A-type linkage isomer 1	$[M-H]^-$	591.1163	$C_{30}H_{23}O_{13}$	5.41	573.1061 ($-H_2O$), 465.0833 ($-C_6H_6O_3$), 441.0819 ($-C_8H_6O_3$), 423.0730($-C_8H_8O_4$), 303.0513 ($-C_{15}H_{12}O_6$), 289.0731($-C_{15}H_{10}O_7$), 285.0399 ($-C_{15}H_{14}O_{17}$), 125.0233 ($-C_{24}H_{18}O_{10}$)	(Singh *et al.*, 2018)
Procyanidin trimer B-type isomer 6	$[M-H]^-$	865.2004	$C_{45}H_{37}O_{18}$	5.55	739.1671 ($-C_6H_6O_3$), 713.1512 ($-C_8H_8O_3$), 695.1417 ($-C_8H_{10}O_4$), 577.1357($-C_{15}H_{12}O_6$), 575.1198 ($-C_{15}H_{14}O_6$), 559.1269 ($-C_{15}H_{24}O_7$), 451.1040($-C_{21}H_{18}O_9$), 449.0880	(Lin *et al.*, 2014)

					(-$C_{21}H_{20}O_9$), 425.0881 (-$C_{23}H_{20}O_9$), 423.0717(-$C_{23}H_{22}O_9$), 407.0771 (-$C_{23}H_{22}O_{10}$), 405.0614(-$C_{23}H_{24}O_{10}$), 289.0719(-$C_{30}H_{24}O_{12}$), 287.0562 (-$C_{30}H_{26}O_{12}$), 125.0233 (-$C_{39}H_{31}O_{15}$)	
(Epi)afzelechin-(Epi)catechin linkage B-type isomer 1	[M-H]$^-$	561.1415	$C_{30}H_{26}O_{11}$	5.94	435.1078 (-$C_6H_6O_3$), 409.0907 (-$C_8H_8O_3$), 407.0760 (-$C_8H_{10}O_3$), 289.0719(-$C_{15}H_{12}O_5$), 273.0775 (-$C_{15}H_{12}O_6$), 271.0619 (-$C_{15}H_{11}O_5$), 125.0234(-$C_{24}H_{20}O_8$)	
Procyanidin tetramer B-type isomer 1	[M-H]$^-$	1153.2637	$C_{60}H_{49}O_{24}$	5.95	1027.2397 (-$C_7H_6O_3$), 1001.2159 (-$C_8H_8O_3$), 983.2043 (-$C_8H_{10}O_4$), 865.2009 (-$C_{15}H_{12}O_6$), 863.1835 (-$C_{15}H_{14}O_6$), 739.1674 (-$C_{21}H_{18}O_9$), 713.1521 (-$C_{23}H_{20}O_9$), 577.1359 (-$C_{30}H_{24}O_{12}$), 575.1198(-$C_{30}H_{26}O_{12}$), 451.1044 (-$C_{36}H_{30}O_{15}$), 425.0883 (-$C_{38}H_{32}O_{15}$), 407.0772(-$C_{38}H_{34}O_{16}$), 289.0719 (-$C_{45}H_{36}O_{18}$), 287.0562 (-$C_{45}H_{38}O_{18}$), 125.0233 (-$C_{54}H_{44}O_{21}$)	(Rue and Rush, 2018; Rush *et al.*, 2018)
(Epi)catechin-(Epi)catechin-(Epi)gallocatechin isomer 3	[M-H]$^-$	881.1945	$C_{45}H_{37}O_{19}$	5.99	425.0885 (-$C_{23}H_{20}O_{10}$), 407.0767 (-$C_{23}H_{22}O_{11}$), 303.0528(-$C_{30}H_{26}O_{12}$), 289.0726 (-$C_{30}H_{24}O_{13}$), 287.0559 (-$C_{30}H_{26}O_{13}$), 125.0234 (-$C_{39}H_{32}O_{16}$)	(Singh *et al.*, 2018)
Procyanidin dimer B-type isomer 3	[M-H]$^-$	577.1356	$C_{30}H_{25}O_{12}$	6.11	559.1255 (-H_2O), 451.1037 (-$C_6H_6O_3$), 425.0881 (-$C_8H_8O_3$), 407.0772(-$C_8H_{10}O_4$), 289.0719 (-$C_{15}H_{12}O_6$), 287.0562 (-$C_{15}H_{14}O_6$), 125.0233(-$C_{24}H_{20}O_9$)	(Lin *et al.*, 2014)
Epicatechin	[M-H]-	289.0718	C15H13O6	6.15	271.0610 (-H_2O), 245.0818 (-CO_2), 179.0342 (-$C_6H_6O_2$), 125.0233 (-$C_9H_8O_3$)	(Yuzuak *et al.*, 2018)

(Epi)catechin *O*-hexoside isomer 3	$[M-H]^-$	451.1251	$C_{21}H_{23}O_{11}$	6.26	289.0719 ($-C_6H_{10}O_5$), 205.0505 ($-C_{10}H_{14}O_7$), 151.0392 ($-C_{13}H_{16}O_8$), 125.0233 ($-C_{15}H_{18}O_8$)	(Šukovic *et al.*, 2020)
Galloyl procyanidin tetramer B-type linkage isomer 1	$[M-2H]^{2-}$	652.1343	$C_{67}H_{52}O_{28}$	6.26	1179.2426 ($-C_6H_5O_3$), 1135.2598 ($-C_7H_5O_5$), 865.1956 ($-C_{22}H_{15}O_{10}$), 863.1781 ($-C_{22}H_{17}O_{10}$), 577.1347 ($-C_{37}H_{27}O_{16}$), 575.1189($-C_{37}H_{29}O_{16}$), 449.0880 ($-C_{43}H_{35}O_{19}$), 407.0766 ($-C_{45}H_{37}O_{20}$), 289.0719($-C_{52}H_{39}O_{22}$), 287.0562 ($-C_{52}H_{41}O_{22}$), 269.0445 ($-C_{52}H_{43}O_{23}$), 125.0233 ($-C_{62}H_{47}O_{25}$)	(Singh *et al.*, 2018)
Procyanidin trimer B-type isomer 7	$[M-H]^-$	865.1996	$C_{45}H_{37}O_{18}$	6.32	739.1678 ($-C_6H_6O_3$), 713.1520 ($-C_8H_8O_3$), 695.1417 ($-C_8H_{10}O_4$), 677.1328($-C_8H_{12}O_5$), 577.1356 ($-C_{15}H_{12}O_6$), 575.1199 ($-C_{15}H_{14}O_6$), 559.1253($-C_{15}H_{24}O_7$), 557.1091 ($-C_{30}H_{26}O_7$), 451.1039 ($-C_{21}H_{18}O_9$), 449.0878($-C_{21}H_{20}O_9$), 425.0880 ($-C_{23}H_{20}O_9$), 423.0719 ($-C_{23}H_{22}O_9$), 407.0774($-C_{23}H_{22}O_{10}$), 405.0611 ($-C_{23}H_{24}O_{10}$), 289.0718($-C_{30}H_{24}O_{12}$), 287.0562($-C_{30}H_{26}O_{12}$), 125.0233 ($-C_{39}H_{31}O_{15}$)	(Lin *et al.*, 2014)
(Epi)afzelechin-(Epi)catechin-(Epi)catechin linkage B-type isomer 1	$[M-H]^-$	849.2068	$C_{45}H_{37}O_{17}$	6.39	679.2460 ($-C_8H_{10}O_4$), 561.1423 ($-C_{15}H_{12}O_6$), 559.1234 ($-C_{15}H_{14}O_6$), 435.1065 ($-C_{24}H_{19}O_8$), 407.0779 ($-C_{23}H_{22}O_9$), 389.0660 ($-C_{23}H_{24}O_{10}$), 289.0724 ($-C_{30}H_{24}O_{11}$), 287.0559 ($-C_{30}H_{26}O_{11}$), 273.0766($-C_{30}H_{24}O_{12}$), 271.0618 ($-C_{30}H_{26}O_{12}$), 125.0234 ($-C_{39}H_{32}O_{14}$)	(de Souza *et al.*, 2008)
(Epi)gallocatechin-(Epi)gallocatechin	$[M-H]^-$	609.1262	$C_{30}H_{25}O_{14}$	6.52	591.1136 ($-H_2O$), 423.0738	(Singh *et al.*, 2018)

B-type linkage isomer 3					(-$C_8H_{10}O_5$), 303.0513 (-$C_{15}H_{14}O_7$), 285.0395(-$C_{15}H_{16}O_8$), 125.0236 (-$C_{24}H_{20}O_{11}$)	
O-Galloyl Procyanidin hexamer B-type linkage isomer 1	$[M-2H]^{2-}$	940.7023	$C_{97}H_{76}O_{40}$	6.54	1305.2651 (-$C_{30}H_{23}O_{12}$), 865.1904 (-$C_{52}H_{39}O_{22}$), 864.1947 (-$C_7H_4O_4$), 863.1749 (-$C_{52}H_{41}O_{22}$), 796.1590 (-$C_{15}H_{12}O_6$), 577.1367 (-$C_{67}H_{51}O_{28}$), 576.1234 (-$C_{37}H_{28}O_{16}$), 575.1205 (-$C_{67}H_{53}O_{28}$), 449.0889(-$C_{73}H_{59}O_{31}$), 407.0765 (-$C_{75}H_{61}O_{32}$), 289.0723 (-$C_{82}H_{63}O_{34}$), 287.0561(-$C_{82}H_{65}O_{34}$), 269.0461 (-$C_{82}H_{67}O_{35}$)	(Singh *et al.*, 2018)
(Epi)catechin-(Epi)gallocatechin A-type linkage isomer 2	$[M-H]^-$	591.1140	$C_{30}H_{23}O_{13}$	6.56	573.1031 (-H_2O), 465.0839 (-$C_6H_6O_3$), 441.0826 (-$C_8H_6O_3$), 423.0736 (-$C_8H_8O_4$), 303.0515 (-$C_{15}H_{12}O_6$), 289.0713(-$C_{15}H_{10}O_7$), 285.0403 (-$C_{15}H_{14}O_{17}$), 125.0234 (-$C_{24}H_{18}O_{10}$)	(Singh *et al.*, 2018)
(Epi)catechin-(Epi)catechin *O*-hexoside B-type linkage	$[M-H]^-$	739.1827	$C_{36}H_{35}O_{17}$	6.61	587.1391 (-$C_8H_8O_3$), 577.1337 (-$C_6H_{10}O_5$), 451.1058 (-$C_{12}H_{16}O_8$), 425.0865 (-$C_{16}H_{18}O_8$), 407.0762 (-$C_{24}H_{20}O_9$), 289.0721 (-$C_{21}H_{22}O_{11}$), 287.0558 (-$C_{21}H_{24}O_{11}$), 125.0233 (-$C_{30}H_{30}O_{14}$)	(Singh *et al.*, 2018)
Procyanidin pentamer B-type linkage isomer 2	$[M-2H]^{2-}$	720.1590	$C_{75}H_{60}O_{30}$	6.65	1315.2932 (-$C_6H_5O_3$), 1153.2604 (-$C_{15}H_{11}O_6$), 1151.2479(-$C_{15}H_{13}O_6$), 865.2001 (-$C_{30}H_{23}O_{12}$), 863.1839 (-$C_{30}H_{25}O_{12}$), 577.1355(-$C_{45}H_{35}O_{18}$), 576.1245 (-$C_{15}H_{12}O_6$), 575.1201 (-$C_{45}H_{37}O_{18}$), 449.0882(-$C_{51}H_{43}O_{21}$), 407.0774 (-$C_{53}H_{45}O_{22}$), 289.0719 (-$C_{60}H_{47}O_{24}$), 287.0562(-$C_{60}H_{49}O_{24}$), 269.0457 (-$C_{60}H_{51}O_{25}$)	(Lin *et al.*, 2014)

Epigallocatechin gallate isomer 1	$[M-H]^-$	457.0777	$C_{22}H_{17}O_{11}$	6.84	305.0668 ($-C_7H_5O_4$), 287.0567 ($-C_7H_7O_5$), 169.0134 ($-C_{15}H_{13}O_6$), 125.0234($-C_{16}H_{13}O_8$)	(de Souza *et al.*, 2008)
O-Galloyl-(Epi)catechin-(Epi)gallocatechin B-type linkage	$[M-H]^-$	745.1462	$C_{37}H_{29}O_{17}$	6.86	593.1268 ($-C_7H_4O_4$), 575.1175 ($-C_7H_6O_5$), 449.0873 ($-C_{13}H_{12}O_8$), 441.0821($-C_{15}H_{12}O_7$), 423.0722 ($-C_{15}H_{14}O_8$), 405.0622 ($-C_{15}H_{16}O_9$), 305.0672($-C_{22}H_{16}O_{10}$), 289.0719 ($-C_{22}H_{16}O_{11}$), 287.0568($-C_{22}H_{18}O_{11}$), 271.0621($-C_{22}H_{18}O_{12}$), 269.0453 ($-C_{22}H_20O_{12}$), 169.0135 ($-C_{20}H_{24}O_{12}$), 125.0233 ($-C_{31}H_{24}O_{14}$)	(Singh *et al.*, 2018)
(Epi)afzelechin-(Epi)catechin linkage B-type isomer 2	$[M-H]^-$	561.1427	$C_{30}H_{26}O_{11}$	6.96	435.1092 ($-C_6H_6O_3$), 409.0923 ($-C_8H_8O_3$), 289.0719 ($-C_{15}H_{12}O_5$), 273.0771($-C_{15}H_{12}O_6$), 125.0233 ($-C_{24}H_20O_8$)	(Enomoto *et al.*, 2019)
O-Galloyl-(Epi)catechin-(Epi)catechin-(Epi)catechin B-type linkage isomer 1	$[M-H]^-$	1017.2130	$C_{52}H_{41}O_{22}$	7.02	891.1765 ($-C_6H_6O_3$), 865.1951 ($-C_7H_4O_4$), 739.1642 ($-C_{13}H_{10}O_7$), 729.1482 ($-C_{15}H_{12}O_6$), 727 .1343 ($-C_{15}H_{14}O_6$), 721.1598 ($-C_{13}H_{12}O_8$), 577.1361 ($-C_{22}H_{16}O_{10}$), 575.1200($-C_{22}H_{18}O_{10}$), 559.1251 ($-C_{22}H_{18}O_{11}$), 557.1102 ($-C_{22}H_20O_{11}$), 541.1157 ($-C_{22}H_20O_{12}$), 451.1063 ($-C_{28}H_{22}O_{13}$), 433.0923 ($-C_{28}H_{24}O_{14}$), 425.0894 ($-C_{30}H_{24}O_{13}$), 423.0738 ($-C_{30}H_{26}O_{13}$), 405.0738 ($-C_{30}H_{28}O_{14}$), 387.0535 ($-C_{30}H_{30}O_{15}$), 289.0721 ($-C_{37}H_{28}O_{16}$), 287.0563 ($-C_{37}H_{30}O_{16}$), 269.0451 ($-C_{37}H_{32}O_{17}$), 169.0135 ($-C_{45}H_{36}O_{17}$), 125.0233 ($-C_{46}H_{36}O_{19}$)	(Singh *et al.*, 2018)
Procyanidin pentamer	$[M-2H]^{2-}$	720.1595	$C_{75}H_{60}O_{30}$	7.03	1315.2858 ($-C_6H_5O_3$), 1153.2686	(Lin *et al.*, 2014)

B-type linkage isomer 3					(-$C_{15}H_{11}O_6$), 1151.2473(-$C_{15}H_{13}O_6$), 865.1996 (-$C_{30}H_{23}O_{12}$), 863.1844 (-$C_{30}H_{25}O_{12}$), 577.1355(-$C_{45}H_{35}O_{18}$), 576.1236 (-$C_{15}H_{12}O_6$), 575.1198 (-$C_{45}H_{37}O_{18}$), 449.0882(-$C_{51}H_{43}O_{21}$), 407.0775 (-$C_{53}H_{45}O_{22}$), 289.0719 (-$C_{60}H_{47}O_{24}$), 287.0563(-$C_{60}H_{49}O_{24}$), 269.0465 (-$C_{60}H_{51}O_{25}$)	
Procyanidin octamer B-type linkage isomer 1	$[M-2H]^{2-}$	1153.2638	$C_{120}H_{96}O_{48}$	7.09	865.2005 (-$C_{75}H_{59}O_{30}$), 863.1827 (-$C_{75}H_{61}O_{30}$), 577.1363(-$C_{90}H_{71}O_{36}$), 575.1202 (-$C_{90}H_{73}O_{36}$), 449.0887 (-$C_{96}H_{79}O_{39}$), 407.0785(-$C_{98}H_{81}O_{40}$), 289.0717 (-$C_{105}H_{83}O_{42}$), 287.0562 (-$C_{105}H_{85}O_{42}$)	(Lin *et al.*, 2014)
(Epi)catechin-(Epi)catechin-(Epi)gallocatechin isomer 4	$[M-H]^{-}$	881.1956	$C_{45}H_{37}O_{19}$	7.11	577.1344 (-$C_{15}H_{12}O_7$), 425.0880 (-$C_{23}H_{20}O_{10}$), 407.0766(-$C_{23}H_{22}O_{11}$), 303.0508 (-$C_{30}H_{26}O_{12}$), 289.0721 (-$C_{30}H_{24}O_{13}$), 287.0567(-$C_{30}H_{26}O_{13}$), 125.0234 (-$C_{39}H_{32}O_{16}$)	(Singh *et al.*, 2018)
O-Galloyl Procyanidin pentamer B-type linkage isomer 1	$[M-2H]^{2-}$	796.1651	$C_{82}H_{54}O_{34}$	7.11	1303.2593 (-$C_{15}H_{13}O_6$), 863.1856 (-$C_{37}H_{29}O_{16}$), 652.1348 (-$C_{15}H_{12}O_6$), 577.1374 (-$C_{52}H_{39}O_{22}$), 576.1221 (-$C_{22}H_{16}O_{10}$), 575.1192(-$C_{52}H_{41}O_{22}$), 449.0874 (-$C_{58}H_{47}O_{25}$), 407.0775 (-$C_{60}H_{49}O_{26}$), 289.0721(-$C_{67}H_{51}O_{28}$), 287.0565 (-$C_{67}H_{53}O_{28}$), 269.0458 (-$C_{67}H_{55}O_{29}$)	(Singh *et al.*, 2018)
Procyanidin eptamer B-type linkage isomer 1	$[M-2H]^{2-}$	1008.7339	$C_{105}H_{84}O_{42}$	7.14	865.2001 (-$C_{60}H_{47}O_{24}$), 864.1851 (-$C_{15}H_{12}O_6$), 863.1862 (-$C_{60}H_{49}O_{24}$), 577.1368 (-$C_{75}H_{59}O_{30}$), 576.1262 (-$C_{45}H_{36}O_{18}$), 575.1204(-$C_{75}H_{61}O_{30}$), 449.0887 (-$C_{81}H_{67}O_{33}$), 407.0781	(Lin *et al.*, 2014)

					(-$C_{83}H_{69}O_{34}$), 289.0720(-$C_{90}H_{71}O_{36}$), 287.0563 (-$C_{90}H_{73}O_{36}$)	
Galloyl-(Epi)catechin-(Epi)catechin B-type linkage isomer 1	$[M-H]^-$	729.1472	$C_{37}H_{29}O_{16}$	7.24	577.1361 (-$C_7H_4O_4$), 559.1251 (-$C_7H_6O_5$), 541.1135 (-$C_7H_8O_6$), 451.1045 (-$C_{13}H_{10}O_7$), 433.0930 (-$C_{13}H_{12}O_8$), 425.0881 (-$C_{15}H_{12}O_7$), 407.0774 (-$C_{15}H_{14}O_8$), 289.0720 (-$C_{22}H_{16}O_{10}$), 287.0563(-$C_{22}H_{18}O_{10}$), 269.0458 (-$C_{22}H_{20}O_{11}$), 169.0134 (-$C_{30}H_{24}O_{11}$), 125.0233 (-$C_{31}H_{24}O_{13}$)	(Singh *et al.*, 2018)
(Epi)afzelechin	$[M-H]^-$	273.0771	$C_{15}H_{13}O_5$	7.40	255.0660 (-H_2O), 179.0343 (-C_6H_6O), 151.0387 (-$C_7H_6O_2$), 125.0236(-$C_9H_8O_2$), 93.0333 (-$C_9H_8O_4$)	(Lin *et al.*, 2014)
Procyanidin pentamer B-type linkage isomer 4	$[M-2H]^{2-}$	720.1589	$C_{75}H_{60}O_{30}$	7.42	1315.2917 (-$C_6H_5O_3$), 1153.2653 (-$C_{15}H_{11}O_6$), 1151.2482(-$C_{15}H_{13}O_6$), 865.2023 (-$C_{30}H_{23}O_{12}$), 863.1846 (-$C_{30}H_{25}O_{12}$), 577.1354(-$C_{45}H_{35}O_{18}$), 576.1253 (-$C_{15}H_{12}O_6$), 575.1204 (-$C_{45}H_{37}O_{18}$), 449.0880(-$C_{51}H_{43}O_{21}$), 407.0773 (-$C_{53}H_{45}O_{22}$), 289.0719 (-$C_{60}H_{47}O_{24}$), 287.0563(-$C_{60}H_{49}O_{24}$), 269.0446 (-$C_{60}H_{51}O_{25}$)	(Lin *et al.*, 2014)
(Epi)catechin-(Epi)catechin-(Epi)catechin-(Epi)catechin-(Epi)catechin-(Epi)gallocatechin B-type linkage isomer 1	$[M-2H]^{2-}$	872.1936	$C_{90}H_{72}O_{37}$	7.56	879.1846 (-$C_{45}H_{37}O_{18}$), 865.1959 (-$C_{45}H_{35}O_{19}$), 863.1832(-$C_{45}H_{37}O_{19}$), 577.1350 (-$C_{60}H_{47}O_{25}$), 576.1230 (-$C_{30}H_{22}O_{13}$), 575.1196(-$C_{60}H_{49}O_{25}$), 449.0880 (-$C_{66}H_{55}O_{28}$), 407.0758 (-$C_{68}H_{57}O_{29}$), 303.0506(-$C_{75}H_{61}O_{30}$), 289.0721 (-$C_{75}H_{59}O_{31}$), 287.0564 (-$C_{75}H_{61}O_{31}$), 125.0234 (-$C_{85}H_{67}O_{34}$)	(Singh *et al.*, 2018)
(Epi)afzelechin-(Epi)catechin linkage	$[M-H]^-$	561.1382	$C_{30}H_{26}O_{11}$	7.57	435.1098 (-$C_6H_6O_3$), 425.0867	(Enomoto *et al.*, 2019)

B-type isomer 3					(-$C_8H_9O_2$), 407.0768 (-$C_8H_{10}O_3$), 289.0721 (-$C_{15}H_{12}O_5$), 273.0775 (-$C_{15}H_{12}O_6$), 271.0616 (-$C_{15}H_{11}O_5$), 125.0234 (-$C_{24}H_{20}O_8$)	
(Epi)catechin-(Epi)gallocatechin A-type linkage isomer 3	$[M-H]^-$	591.1144	$C_{30}H_{23}O_{13}$	7.71	573.1004 (-H_2O), 465.0847 (-$C_6H_6O_3$), 441.0826 (-$C_8H_6O_3$), 423.0701(-$C_8H_8O_4$), 303.0515 (-$C_{15}H_{12}O_6$), 289.0717 (-$C_{15}H_{10}O_7$), 285.0403(-$C_{15}H_{14}O_{17}$), 125.0234 (-$C_{24}H_{18}O_{10}$)	(Singh *et al.*, 2018)
(Epi)catechin-(Epi)catechin-(Epi)gallocatechin ABB linkage isomer 1	$[M-H]^-$	879.1793	$C_{45}H_{35}O_{19}$	7.83	753.1492 (-$C_6H_6O_3$), 727.1321 (-$C_8H_8O_3$), 709.1210 (-$C_8H_{10}O_4$), 591.1136 (-$C_{15}H_{12}O_6$), 577.1367 (-$C_{15}H_{10}O_7$), 575.1226 (-$C_{15}H_{12}O_7$), 573.1046 (-$C_{15}H_{14}O_7$), 555.0909 (-$C_{15}H_{16}O_8$), 465.0786 (-$C_{21}H_{18}O_9$), 441.0829 (-$C_{23}H_{18}O_9$), 423.0731 (-$C_{23}H_{20}O_{10}$), 413.0861 (-$C_{24}H_{18}O_{10}$), 289.0718 (-$C_{30}H_{22}O_{13}$), 287.0563 (-$C_{30}H_{24}O_{13}$), 125.0233 (-$C_{39}H_{30}O_{16}$)	(Singh *et al.*, 2018)
Procyanidin trimer B-type isomer 8	$[M-H]^-$	865.1998	$C_{45}H_{37}O_{18}$	7.85	739.1682 (-$C_6H_6O_3$), 713.1520 (-$C_8H_8O_3$), 695.1414 (-$C_8H_{10}O_4$), 677.1316 (-$C_8H_{12}O_5$), 577.1356 (-$C_{15}H_{12}O_6$), 575.1200 (-$C_{15}H_{14}O_6$), 559.1235 (-$C_{15}H_{24}O_7$), 557.1100 (-$C_{30}H_{26}O_7$), 451.1039 (-$C_{21}H_{18}O_9$), 449.0879 (-$C_{21}H_{20}O_9$), 425.0881 (-$C_{23}H_{20}O_9$), 423.0721 (-$C_{23}H_{22}O_9$), 407.0773 (-$C_{23}H_{22}O_{10}$), 405.0612 (-$C_{23}H_{24}O_{10}$), 289.0719 (-$C_{30}H_{24}O_{12}$), 287.0562 (-$C_{30}H_{26}O_{12}$), 125.0233 (-$C_{39}H_{31}O_{15}$)	(Lin *et al.*, 2014)

O-Galloyl-(Epi)catechin-(Epi)catechin-(Epi)catechin B-type linkage isomer 2	$[M-H]^-$	1017.2077	$C_{52}H_{41}O_{22}$	7.87	891.1791 (-$C_6H_6O_3$), 729.1473 (-$C_{15}H_{12}O_6$), 577.1353 (-$C_{22}H_{16}O_{10}$), 575.1180 (-$C_{22}H_{18}O_{10}$), 559.1224 (-$C_{22}H_{18}O_{11}$), 451.1049(-$C_{28}H_{22}O_{13}$), 425.0902 (-$C_{30}H_{24}O_{13}$), 423.0724 (-$C_{30}H_{26}O_{13}$), 407.0767(-$C_{30}H_{26}O_{14}$), 405.0604 (-$C_{30}H_{28}O_{14}$), 289.0725 (-$C_{37}H_{28}O_{16}$), 287.0563(-$C_{37}H_{30}O_{16}$), 269.0446 (-$C_{37}H_{32}O_{17}$), 169.0136 (-$C_{45}H_{36}O_{17}$), 125.0234 (-$C_{46}H_{36}O_{19}$)	(Singh *et al.*, 2018)
O-Galloyl Procyanidin pentamer B-type linkage isomer 2	$[M-2H]^{2-}$	796.1649	$C_{82}H_{54}O_{34}$	7.89	865.1914 (-$C_{37}H_{27}O_{16}$), 863.1806 (-$C_{37}H_{29}O_{16}$), 652.1351 (-$C_{15}H_{12}O_6$), 577.1359 (-$C_{52}H_{39}O_{22}$), 575.1196 (-$C_{52}H_{41}O_{22}$), 449.0878(-$C_{58}H_{47}O_{25}$), 407.0773 (-$C_{60}H_{49}O_{26}$), 289.0720 (-$C_{67}H_{51}O_{28}$), 287.0562 (-$C_{67}H_{53}O_{28}$), 269.0454 (-$C_{67}H_{55}O_{29}$)	(Singh *et al.*, 2018)
O-Galloyl Procyanidin tetramer B-type linkage	$[M-H]^-$	1305.2733	$C_{67}H_{53}O_{28}$	7.90	1153.2560 (-$C_7H_4O_4$), 1017.2159 (-$C_{15}H_{12}O_6$), 865.1931(-$C_{22}H_{16}O_{10}$), 863.1788 (-$C_{22}H_{18}O_{10}$), 739.1690 (-$C_{28}H_{22}O_{13}$),729.1462(-$C_{30}H_{24}O_{12}$), 727.1279 (-$C_{30}H_{26}O_{12}$), 713.1484 (-$C_{30}H_{24}O_{13}$),695.1437(-$C_{30}H_{26}O_{14}$), 577.1382 (-$C_{37}H_{28}O_{16}$), 575.1196 (-$C_{37}H_{30}O_{16}$), 451.1048(-$C_{43}H_{34}O_{19}$), 449.0887 (-$C_{43}H_{36}O_{19}$), 439.0651 (-$C_{45}H_{38}O_{19}$), 425.0886(-$C_{45}H_{36}O_{19}$), 423.0718 (-$C_{45}H_{38}O_{19}$), 407.0782 (-$C_{45}H_{38}O_{20}$), 405.0635(-$C_{45}H_{40}O_{20}$), 289.0726 (-$C_{52}H_{40}O_{22}$), 287.0563 (-$C_{52}H_{42}O_{22}$), 269.0460 (-$C_{52}H_{44}O_{23}$), 125.0234 (-$C_{61}H_{48}O_{25}$)	(Singh *et al.*, 2018)

Epigallocatechin gallate isomer 2	$[M-H]^-$	457.0771	$C_{22}H_{17}O_{11}$	7.98	305.0671 (-$C_7H_5O_4$), 287.0563 (-$C_7H_7O_5$), 169.0134 (-$C_{15}H_{13}O_6$), 125.0233 (-$C_{16}H_{13}O_8$)	(Yuzuak *et al.*, 2018)
Galloyl procyanidin tetramer B-type linkage isomer 2	$[M-2H]^{2-}$	652.1336	$C_{67}H_{52}O_{28}$	8.01	1179.2415 (-$C_6H_5O_3$), 865.2000 (-$C_{22}H_{15}O_{10}$), 863.1835(-$C_{22}H_{17}O_{10}$), 577.1359 (-$C_{37}H_{27}O_{16}$), 575.1201 (-$C_{37}H_{29}O_{16}$), 449.0881(-$C_{43}H_{35}O_{19}$), 407.0772 (-$C_{45}H_{37}O_{20}$), 289.0718 (-$C_{52}H_{39}O_{22}$), 287.0562(-$C_{52}H_{41}O_{22}$), 269.0445 (-$C_{52}H_{43}O_{23}$), 125.0233 (-$C_{62}H_{47}O_{25}$)	(Singh *et al.*, 2018)
Procyanidin eptamer B-type linkage isomer 2	$[M-2H]^{2-}$	1008.7310	$C_{105}H_{84}O_{42}$	8.06	865.1953 (-$C_{60}H_{47}O_{24}$), 864.1882 (-$C_{15}H_{12}O_6$), 863.1870 (-$C_{60}H_{49}O_{24}$), 577.1364 (-$C_{75}H_{59}O_{30}$), 576.1213 (-$C_{45}H_{36}O_{18}$), 575.1207(-$C_{75}H_{61}O_{30}$), 449.0874 (-$C_{81}H_{67}O_{33}$), 407.0774 (-$C_{83}H_{69}O_{34}$), 289.0721(-$C_{90}H_{71}O_{36}$), 287.0562 (-$C_{90}H_{73}O_{36}$), 269.0461 (-$C_{90}H_{75}O_{37}$)	(Lin *et al.*, 2014)
Procyanidin octamer B-type linkage isomer 2	$[M-2H]^{2-}$	1153.2635	$C_{120}H_{96}O_{48}$	8.08	865.1980 (-$C_{75}H_{59}O_{30}$), 864.1849 (-$C_{30}H_{24}O_{12}$), 863.1844(-$C_{75}H_{61}O_{30}$), 577.1356 (-$C_{90}H_{71}O_{36}$), 575.1198 (-$C_{90}H_{73}O_{36}$), 449.0884(-$C_{96}H_{79}O_{39}$), 407.0774 (-$C_{98}H_{81}O_{40}$),289.0718 (-$C_{105}H_{83}O_{42}$),287.0563 (-$C_{105}H_{85}O_{42}$),269.0459(-$C_{105}H_{87}O_{43}$)	(Lin *et al.*, 2014)
Galloyl-(Epi)catechin-(Epi)catechin B-type linkage isomer 2	$[M-H]^-$	729.1468	$C_{37}H_{29}O_{16}$	8.09	577.1392 (-$C_7H_4O_4$), 541.1155 (-$C_7H_8O_6$), 451.1039 (-$C_{13}H_{10}O_7$), 441.0831 (-$C_{15}H_{12}O_6$), 433.0932 (-$C_{13}H_{12}O_8$), 425.0880 (-$C_{15}H_{12}O_7$), 407.0774 (-$C_{15}H_{14}O_8$), 289.0719 (-$C_{22}H_{16}O_{10}$), 287.0563(-$C_{22}H_{18}O_{10}$), 269.0457 (-$C_{22}H_{20}O_{11}$), 169.0134	(Singh *et al.*, 2018)

					($-C_{30}H_{24}O_{11}$), 125.0233 ($-C_{31}H_{24}O_{13}$)	
Procyanidin dimer B-type isomer 4	$[M-H]^-$	577.1352	$C_{30}H_{25}O_{12}$	8.11	559.1257 ($-H_2O$), 451.1038 ($-C_6H_6O_3$), 425.0880 ($-C_8H_8O_3$), 407.0772 ($-C_8H_{10}O_4$), 289.0719 ($-C_{15}H_{12}O_6$), 287.0562 ($-C_{15}H_{14}O_6$), 125.0233 ($-C_{24}H_{20}O_9$)	(Lin *et al.*, 2014)
Galloyl-(Epi)catechin-(Epi)catechin A-type linkage isomer 1	$[M-H]^-$	727.1342	$C_{37}H_{27}O_{16}$	8.14	575.1203 ($-C_7H_4O_4$), 539.0983 ($-C_7H_8O_6$), 449.0894 ($-C_{13}H_{10}O_7$), 441.0815 ($-C_{15}H_{10}O_6$), 439.0669 ($-C_{15}H_{12}O_6$), 431.0779 ($-C_{13}H_{12}O_8$), 425.0886 ($-C_{15}H_{10}O_7$), 407.0772 ($-C_{15}H_{12}O_8$), 389.0672 ($-C_{15}H_{14}O_9$), 289.0719 ($-C_{22}H_{14}O_{10}$), 287.0563 ($-C_{22}H_{16}O_{10}$), 271.0617($-C_{22}H_{16}O_{11}$), 269.0455 ($-C_{22}H_{18}O_{11}$), 169.0134 ($-C_{30}H_{22}O_{11}$), 125.0233($-C_{31}H_{22}O_{13}$)	(Singh *et al.*, 2018)
O-Galloyl Procyanidin hexamer B-type linkage isomer 2	$[M-2H]^{2-}$	940.7009	$C_{97}H_{76}O_{40}$	8.30	1305.2760 ($-C_{30}H_{23}O_{12}$), 1303.2544 ($-C_{30}H_{25}O_{12}$), 865.1932($-C_{52}H_{39}O_{22}$), 863.1824 ($-C_{52}H_{41}O_{22}$), 796.1659 ($-C_{15}H_{12}O_6$), 577.1346($-C_{67}H_{51}O_{28}$), 576.1235 ($-C_{37}H_{28}O_{16}$), 575.1202 ($-C_{67}H_{53}O_{28}$), 449.0894($-C_{73}H_{59}O_{31}$), 407.0770 ($-C_{75}H_{61}O_{32}$), 289.0720 ($-C_{82}H_{63}O_{34}$), 287.0561($-C_{82}H_{65}O_{34}$), 269.0454 ($-C_{82}H_{67}O_{35}$)	(Singh *et al.*, 2018)
Procyanidin tetramer B- type isomer 2	$[M-H]^-$	1153.2655	$C_{60}H_{49}O_{24}$	8.37	1027.2325 ($-C_7H_6O_3$) , 1001.2158 ($-C_8H_8O_3$) , 983.2032 ($-C_8H_{10}O_4$), 865.2002 ($-C_{15}H_{12}O_6$) , 863.1830 ($-C_{15}H_{14}O_6$) , 739.1667 ($-C_{21}H_{18}O_9$) , 713.1518 ($-C_{23}H_{20}O_9$) , 577.1355 ($-C_{30}H_{24}O_{12}$),575.1201($-C_{30}H_{26}O_{12}$), 451.1040 ($-C_{36}H_{30}O_{15}$) ,425.0879	(Rue and Rush, 2018; Rush *et al.*, 2018)

					($-C_{38}H_{32}O_{15}$) , 407.0772 ($-C_{38}H_{34}O_{16}$), 289.0720 ($-C_{45}H_{36}O_{18}$) , 287.0562 ($-C_{45}H_{38}O_{18}$) ,125.0233 ($-C_{54}H_{44}O_{21}$)	
(Epi)catechin-(Epi)catechin-(Epi)catechin-(Epi)catechin-(Epi)catechin-(Epi)gallocatechin B-type linkage isomer 2	$[M-2H]^{2-}$	872.1816	$C_{90}H_{72}O_{37}$	8.43	879.1789 ($-C_{45}H_{37}O_{18}$), 863.1887 ($-C_{45}H_{37}O_{19}$), 720.1511($-C_{15}H_{12}O_7$), 577.1359 ($-C_{60}H_{47}O_{25}$), 576.1225 ($-C_{30}H_{22}O_{13}$), 575.1169 ($-C_{60}H_{49}O_{25}$), 449.0862($-C_{66}H_{55}O_{28}$), 407.0771 ($-C_{68}H_{57}O_{29}$), 303.0509 ($-C_{75}H_{61}O_{30}$), 289.0721($-C_{75}H_{59}O_{31}$), 287.0562 ($-C_{75}H_{61}O_{31}$), 125.0234 ($-C_{85}H_{67}O_{34}$)	(Singh *et al.*, 2018)
O-Galloyl-(Epi)catechin-(Epi)gallocatechin A-type linkage isomer 1	$[M-H]^-$	743.1285	$C_{37}H_{27}O_{17}$	8.43	591.1195($-C_7H_4O_4$), 573.1058 ($-C_7H_6O_5$), 555.0934 ($-C_7H_8O_6$), 441.0810 ($-C_{15}H_{12}O_7$), 439.0671 ($-C_{15}H_{12}O_7$), 423.0724 ($-C_{15}H_{14}O_8$), 421.0567 ($-C_{15}H_{14}O_8$), 405.0625 ($-C_{15}H_{16}O_9$), 403.0455 ($-C_{15}H_{16}O_9$), 289.0712 ($-C_{22}H_{14}O_{11}$), 169.0134 ($-C_{20}H_{22}O_{12}$), 125.0234 ($-C_{31}H_{22}O_{14}$)	(Singh *et al.*, 2018)
(Epi)catechin-(Epi)catechin-(Epi)gallocatechin ABB linkage isomer 2	$[M-H]^-$	879.1736	$C_{45}H_{35}O_{19}$	8.46	753.1474 ($-C_6H_6O_3$), 727.1279 ($-C_8H_8O_3$), 709.1221 ($-C_8H_{10}O_4$), 591.1120 ($-C_{15}H_{12}O_6$), 575.1223 ($-C_{15}H_{12}O_7$), 573.1007 ($-C_{15}H_{14}O_7$), 465.0789 ($-C_{21}H_{18}O_9$), 441.0752 ($-C_{23}H_{18}O_9$), 423.0729 ($-C_{23}H_{20}O_{10}$), 413.0830 ($-C_{24}H_{18}O_{10}$), 289.0718 ($-C_{30}H_{22}O_{13}$), 287.0563($-C_{30}H_{24}O_{13}$), 125.0233 ($-C_{39}H_{30}O_{16}$)	(Singh *et al.*, 2018)
Procyanidin pentamer B-type linkage isomer 5	$[M-2H]^{2-}$	720.1594	$C_{75}H_{60}O_{30}$	8.66	1315.2996 ($-C_6H_5O_3$), 1153.2644 ($-C_{15}H_{11}O_6$), 1151.2490 $-C_{15}H_{13}O_6$), 865.2009 ($-C_{30}H_{23}O_{12}$), 863.1850 ($-C_{30}H_{25}O_{12}$), 577.1356($-C_{45}H_{35}O_{18}$), 576.1249 ($-C_{15}H_{12}O_6$), 575.1199	(Lin *et al.*, 2014)

					(-$C_{45}H_{37}O_{18}$), 449.0884(-$C_{51}H_{43}O_{21}$), 407.0773 (-$C_{53}H_{45}O_{22}$), 289.0719 (-$C_{60}H_{47}O_{24}$), 287.0563 (-$C_{60}H_{49}O_{24}$), 269.0450 (-$C_{60}H_{51}O_{25}$)	
Digalloyl procyanidin trimer B-type linkage isomer 1	$[M-2H]^{2-}$	584.1113	$C_{59}H_{44}O_{26}$	8.68	577.1360 (-$C_{29}H_{19}O_{14}$), 575.1181 (-$C_{29}H_{21}O_{14}$), 508.1024 (-$C_7H_4O_4$), 449.0898 (-$C_{35}H_{27}O_{17}$), 441.0815 (-$C_{37}H_{27}O_{16}$), 407.0780(-$C_{37}H_{29}O_{18}$), 289.0720 (-$C_{44}H_{31}O_{20}$), 287.0720 (-$C_{44}H_{33}O_{20}$), 269.0457(-$C_{44}H_{35}O_{21}$), 169.0133 (-$C_{52}H_{39}O_{21}$), 125.0233 (-$C_{54}H_{39}O_{23}$)	(Singh *et al.*, 2018)
Galloyl procyanidin tetramer B-type linkage isomer 3	$[M-2H]^{2-}$	652.1326	$C_{67}H_{52}O_{28}$	8.68	1179.2493 (-$C_6H_5O_3$), 865.1957 (-$C_{22}H_{15}O_{10}$), 863.1774(-$C_{22}H_{17}O_{10}$), 577.1362 (-$C_{37}H_{27}O_{16}$), 575.1204 (-$C_{37}H_{29}O_{16}$),449.0882(-$C_{43}H_{35}O_{19}$), 407.0772 (-$C_{45}H_{37}O_{20}$), 289.0719 (-$C_{52}H_{39}O_{22}$), 287.0563(-$C_{52}H_{41}O_{22}$), 269.0453 (-$C_{52}H_{43}O_{23}$), 125.0233 (-$C_{62}H_{47}O_{25}$)	(Singh *et al.*, 2018)
O-Galloyl Procyanidin pentamer B-type linkage isomer 3	$[M-2H]^{2-}$	796.1674	$C_{82}H_{54}O_{34}$	8.74	1305.2805 (-$C_{15}H_{11}O_6$), 1303.2512 (-$C_{15}H_{13}O_6$), 865.1991 (-$C_{37}H_{27}O_{16}$), 863.1835 (-$C_{37}H_{29}O_{16}$), 652.1334 (-$C_{15}H_{12}O_6$), 577.1368 (-$C_{52}H_{39}O_{22}$), 576.1223 (-$C_{22}H_{16}O_{10}$), 575.1195 (-$C_{52}H_{41}O_{22}$), 449.0877(-$C_{58}H_{47}O_{25}$), 407.0774 (-$C_{60}H_{49}O_{26}$), 289.0720 (-$C_{67}H_{51}O_{28}$), 287.0564 (-$C_{67}H_{53}O_{28}$), 269.0458 (-$C_{67}H_{55}O_{29}$)	(Singh *et al.*, 2018)
O-Galloyl-(Epi)catechin-(Epi)catechin-(Epi)catechin B-type linkage isomer 3	$[M-H]^{-}$	1017.2114	$C_{52}H_{41}O_{22}$	8.76	891.1774 (-$C_6H_6O_3$), 729.1465 (-$C_{15}H_{12}O_6$), 727 .1293 (-$C_{15}H_{14}O_6$), 577.1373 (-$C_{22}H_{16}O_{10}$), 575.1215	(Singh *et al.*, 2018)

					(-$C_{22}H_{18}O_{10}$), 557.1100(-$C_{22}H_{20}O_{11}$), 451.1045 (-$C_{28}H_{22}O_{13}$), 433.0935 (-$C_{28}H_{24}O_{14}$), 425.0887 (-$C_{30}H_{24}O_{13}$), 423.0725(-$C_{30}H_{26}O_{13}$), 407.0772(-$C_{30}H_{26}O_{14}$), 405.0609 (-$C_{30}H_{28}O_{14}$), 289.0721(-$C_{37}H_{28}O_{16}$), 287.0564(-$C_{37}H_{30}O_{16}$), 269.0458 (-$C_{37}H_{32}O_{17}$), 169.0135(-$C_{45}H_{36}O_{17}$), 125.0234(-$C_{46}H_{36}O_{19}$)	
Galloyl (Epi)catechin-(Epi)catechin-(Epi)catechin-(Epi)catechin-(Epi)catechin-(Epi)gallocatechin B-type linkage	$[M-2H]^{2-}$	948.2001	$C_{97}H_{76}O_{41}$	8.84	1131.1815 (-$C_{45}H_{35}O_{18}$), 577.1333 (-$C_{67}H_{51}O_{29}$), 576.1255(-$C_{37}H_{28}O_{17}$), 575.1218 (-$C_{67}H_{53}O_{29}$), 449.0910 (-$C_{73}H_{59}O_{32}$), 407.0784(-$C_{75}H_{61}O_{33}$), 303.0524 (-$C_{82}H_{65}O_{34}$), 289.0717 (-$C_{82}H_{63}O_{35}$), 287.0567 (-$C_{82}H_{65}O_{35}$)	(Singh *et al.*, 2018)
(Epi)catechin gallate isomer 1	$[M-H]^{-}$	441.0829	$C_{22}H_{17}O_{10}$	8.98	331.0462 (-$C_{6}H_{6}O_{2}$), 303.0511 (-$C_{7}H_{6}O_{3}$), 289.0718 (-$C_{7}H_{4}O_{4}$), 271.0613 (-$C_{7}H_{6}O_{5}$), 169.0134 (-$C_{15}H_{12}O_{5}$), 125.0233 (-$C_{18}H_{7}O_{7}$)	(Yuzuak *et al.*, 2018)
Galloyl-(Epi)catechin-(Epi)catechin B-type linkage isomer 3	$[M-H]^{-}$	729.1413	$C_{37}H_{29}O_{16}$	9.03	577.1323 (-$C_{7}H_{4}O_{4}$), 451.1046 (-$C_{13}H_{10}O_{7}$), 441.0832 (-$C_{15}H_{12}O_{6}$), 433.0953 (-$C_{13}H_{12}O_{8}$), 425.0890 (-$C_{15}H_{12}O_{7}$), 407.0777 (-$C_{15}H_{14}O_{8}$), 289.0719 (-$C_{22}H_{16}O_{10}$), 287.0556 (-$C_{22}H_{18}O_{10}$), 271.0611(-$C_{22}H_{18}O_{12}$), 269.0466 (-$C_{22}H_{20}O_{11}$), 169.0133 (-$C_{30}H_{24}O_{11}$), 125.0233 (-$C_{31}H_{24}O_{13}$)	(Singh *et al.*, 2018)
O-Galloyl Procyanidin pentamer B-type linkage isomer 4	$[M-2H]^{2-}$	796.1658	$C_{82}H_{54}O_{34}$	9.22	1305.2817 (-$C_{15}H_{11}O_{6}$), 1303.2562 (-$C_{15}H_{13}O_{6}$), 865.1967 (-$C_{37}H_{27}O_{16}$), 863.1857 (-$C_{37}H_{29}O_{16}$), 652.1328 (-$C_{15}H_{12}O_{6}$), 577.1358 (-$C_{52}H_{39}O_{22}$), 576.1236 (-$C_{22}H_{16}O_{10}$), 575.1200	(Singh *et al.*, 2018)

					($-C_{52}H_{41}O_{22}$), 449.0878 ($-C_{58}H_{47}O_{25}$), 407.0774($-C_{60}H_{49}O_{26}$), 289.0720($-C_{67}H_{51}O_{28}$), 287.0563 ($-C_{67}H_{53}O_{28}$), 269.0457 ($-C_{67}H_{55}O_{29}$)	
(Epi)afzelechin-(Epi)catechin-(Epi)catechin linkage B-type isomer 2	$[M-H]^-$	849.2043	$C_{45}H_{37}O_{17}$	9.23	561.1411 ($-C_{15}H_{12}O_6$), 559.1271 ($-C_{15}H_{14}O_6$), 407.0786 ($-C_{23}H_{22}O_9$), 289.0717 ($-C_{30}H_{24}O_{11}$), 287.0565 ($-C_{30}H_{26}O_{11}$), 271.0614 ($-C_{30}H_{26}O_{12}$), 125.0235 ($-C_{39}H_{32}O_{14}$)	(de Souza *et al.*, 2008)
Procyanidin octamer B-type linkage isomer 3	$[M-2H]^{2-}$	1153.2633	$C_{120}H_{96}O_{48}$	9.23	865.1973 ($-C_{75}H_{59}O_{30}$), 864.1902 ($-C_{30}H_{24}O_{12}$), 863.1861($-C_{75}H_{61}O_{30}$), 577.1356 ($-C_{90}H_{71}O_{36}$), 576.1217 ($-C_{60}H_{48}O_{24}$), 575.1205($-C_{90}H_{73}O_{36}$), 449.0890 ($-C_{96}H_{79}O_{39}$), 407.0770 ($-C_{98}H_{81}O_{40}$), 289.0721 ($-C_{105}H_{83}O_{42}$), 287.0563 ($-C_{105}H_{85}O_{42}$),269.0455 ($-C_{105}H_{87}O_{43}$)	(Lin *et al.*, 2014)
O-Galloyl Procyanidin hexamer B-type linkage isomer 3	$[M-2H]^{2-}$	940.6982	$C_{97}H_{76}O_{40}$	9.25	1305.2638 ($-C_{30}H_{23}O_{12}$), 1303.2577 ($-C_{30}H_{25}O_{12}$), 865.1923($-C_{52}H_{39}O_{22}$), 863.1843 ($-C_{52}H_{41}O_{22}$), 796.1611 ($-C_{15}H_{12}O_6$), 577.1355($-C_{67}H_{51}O_{28}$), 576.1249 ($-C_{37}H_{28}O_{16}$), 575.1207 ($-C_{67}H_{53}O_{28}$), 449.0883($-C_{73}H_{59}O_{31}$), 407.0773 ($-C_{75}H_{61}O_{32}$), 289.0721 ($-C_{82}H_{63}O_{34}$), 287.0563($-C_{82}H_{65}O_{34}$), 269.0459 ($-C_{82}H_{67}O_{35}$)	(Singh *et al.*, 2018)
Digalloyl procyanidin pentamer B-type linkage isomer 1	$[M-2H]^{2-}$	872.1750	$C_{89}H_{68}O_{38}$	9.27	865.1940 ($-C_{44}H_{31}O_{20}$), 863.1796 ($-C_{44}H_{33}O_{20}$), 796.1599 ($-C_7H_4O_4$), 729.1506 ($-C_{52}H_{39}O_{22}$), 577.1368 ($-C_{59}H_{43}O_{26}$), 576.1249($-C_{29}H_{20}O_{14}$), 575.1205 ($-C_{59}H_{45}O_{26}$), 449.0881 ($-C_{65}H_{51}O_{29}$), 407.0778($-C_{67}H_{53}O_{30}$), 289.0721 ($-C_{74}H_{55}O_{32}$), 287.0563	(Singh *et al.*, 2018)

					(-$C_{74}H_{57}O_{32}$), 269.0459 (-$C_{74}H_{59}O_{33}$)	
Procyanidin hexamer B-type linkage	$[M-2H]^{2-}$	864.1895	$C_{90}H_{72}O_{36}$	9.28	1153.2609 (-$C_{30}H_{23}O_{12}$), 1151.2482 (-$C_{30}H_{25}O_{12}$), 1135.2483 (-$C_{30}H_{25}O_{13}$), 865.2001(-$C_{45}H_{35}O_{18}$), 863.1826(-$C_{45}H_{37}O_{18}$), 720.1568 (-$C_{15}H_{12}O_6$), 577.1359 (-$C_{60}H_{47}O_{24}$), 576.1241(-$C_{30}H_{24}O_{12}$), 575.1200 (-$C_{60}H_{49}O_{24}$), 449.0878(-$C_{66}H_{55}O_{27}$), 407.0774(-$C_{68}H_{57}O_{28}$), 289.0719 (-$C_{75}H_{59}O_{30}$), 287.0562(-$C_{75}H_{61}O_{30}$), 269.0452 (-$C_{75}H_{63}O_{31}$)	(Lin *et al.*, 2014)
(Epi)catechin-(Epi)catechin-(Epi)gallocatechin ABB linkage isomer 3	$[M-H]^-$	879.1769	$C_{45}H_{35}O_{19}$	9.34	727.1299 (-$C_8H_8O_3$), 709.1227 (-$C_8H_{10}O_4$), 591.1163 (-$C_{15}H_{12}O_6$), 577.1340 (-$C_{15}H_{10}O_7$), 575.1220 (-$C_{15}H_{12}O_7$), 573.1053 (-$C_{15}H_{14}O_7$), 423.0715 (-$C_{23}H_{20}O_{10}$), 413.0905 (-$C_{24}H_{18}O_{10}$), 289.0721(-$C_{30}H_{22}O_{13}$), 287.0561 (-$C_{30}H_{24}O_{13}$), 125.0233 (-$C_{39}H_{30}O_{16}$)	(Singh *et al.*, 2018)
O-Galloyl-(Epi)catechin-(Epi)gallocatechin A-type linkage isomer 2	$[M-H]^-$	743.1255	$C_{37}H_{27}O_{17}$	9.41	573.1044 (-$C_7H_6O_5$), 455.0634 (-$C_{15}H_{12}O_7$), 439.0658 (-$C_{15}H_{12}O_7$), 421.0565 (-$C_{15}H_{14}O_8$), 303.0514 (-$C_{22}H_{16}O_{10}$), 289.0731(-$C_{22}H_{14}O_{11}$), 287.0562 (-$C_{22}H_{16}O_{11}$), 285.0406 (-$C_{22}H_{18}O_{11}$), 169.0127(-$C_{20}H_{22}O_{12}$), 125.0233 (-$C_{31}H_{22}O_{14}$)	(Singh *et al.*, 2018)
(Epi)catechin-(Epi)gallocatechin A-type linkage isomer 4	$[M-H]^-$	591.1123	$C_{30}H_{23}O_{13}$	9.49	573.1034 (-H_2O), 465.0840 (-$C_6H_6O_3$), 423.0727 (-$C_8H_8O_4$), 303.0511(-$C_{15}H_{12}O_6$), 289.0719 (-$C_{15}H_{10}O_7$), 285.0403 (-$C_{15}H_{14}O_{17}$), 125.0234 (-$C_{24}H_{18}O_{10}$)	(Singh *et al.*, 2018)
(Epi)afzelechin-(Epi)catechin linkage	$[M-H]^-$	561.1401	$C_{30}H_{26}O_{11}$	9.51	435.1064 (-$C_6H_6O_3$), 409.0901	(Enomoto *et al.*, 2019)

B-type isomer 4					(-$C_8H_8O_3$), 407.0785 (-$C_8H_{10}O_3$), 289.0720 (-$C_{15}H_{12}O_5$), 273.0770 (-$C_{15}H_{12}O_6$), 271.0613 (-$C_{15}H_{11}O_5$), 125.0281 (-$C_{24}H_{20}O_8$)	
O-Galloyl procyanidin octamer B-type linkage isomer 1	$[M-3H]^{3-}$	819.1783	$C_{127}H_{101}O_{52}$	9.70	865.2010 (-$C_{82}H_{64}O_{34}$), 863.1857 (-$C_{82}H_{66}O_{34}$), 577.1355(-$C_{97}H_{76}O_{40}$), 575.1202 (-$C_{97}H_{78}O_{40}$), 449.0881 (-$C_{103}H_{84}O_{43}$), 407.0772 (-$C_{105}H_{86}O_{44}$), 289.0717 (-$C_{112}H_{88}O_{46}$), 287.0564 (-$C_{112}H_{90}O_{46}$), 269.0449 (-$C_{112}H_{92}O_{47}$)	(Singh *et al.*, 2018)
O-Galloyl Procyanidin eptamer B-type linkage isomer 1	$[M-2H]^{3-}$	722.8196	$C_{112}H_{87}O_{46}$	9.71	865.1950 (-$C_{82}H_{64}O_{34}$), 863.1845 (-$C_{82}H_{66}O_{34}$), 577.1353(-$C_{97}H_{76}O_{40}$), 575.1203 (-$C_{97}H_{78}O_{40}$), 449.0874 (-$C_{103}H_{84}O_{43}$), 407.0770 (-$C_{105}H_{86}O_{44}$), 289.0719 (-$C_{112}H_{88}O_{46}$), 287.0562 (-$C_{112}H_{90}O_{46}$), 269.0458 (-$C_{112}H_{92}O_{47}$)	(Singh *et al.*, 2018)
Trigalloyl procyanidin tetramer B-type linkage isomer 1	$[M-2H]^{2-}$	804.1475	$C_{81}H_{60}O_{36}$	9.78	1169.2173 (-$C_{22}H_{15}O_{10}$), 1167.2109 (-$C_{22}H_{17}O_{10}$), 729.1448(-$C_{44}H_{31}O_{20}$), 728.1385 (-$C_7H_4O_4$), 727.1270 (-$C_{44}H_{33}O_{20}$), 577.1387(-$C_{51}H_{35}O_{24}$), 575.1208 (-$C_{51}H_{37}O_{24}$), 449.0878 (-$C_{57}H_{43}O_{27}$), 441.0818(-$C_{59}H_{43}O_{26}$), 407.0766 (-$C_{59}H_{45}O_{28}$), 289.0723 (-$C_{66}H_{47}O_{30}$),287.0563(-$C_{66}H_{49}O_{30}$), 269.0451(-$C_{66}H_{51}O_{31}$), 169.0135 (-$C_{74}H_{55}O_{31}$), 125.0234 (-$C_{76}H_{55}O_{33}$)	(Singh *et al.*, 2018)
Digalloyl procyanidin trimer B-type linkage isomer 2	$[M-2H]^{2-}$	584.1073	$C_{59}H_{44}O_{26}$	9.84	881.1605 (-$C_{15}H_{11}O_6$), 577.1368 (-$C_{29}H_{19}O_{14}$), 575.1204(-$C_{29}H_{21}O_{14}$), 508.0984 (-$C_7H_4O_4$), 449.0883 (-$C_{35}H_{27}O_{17}$), 441.0832(-$C_{37}H_{27}O_{16}$), 407.0775 (-$C_{37}H_{29}O_{18}$), 289.0720 (-$C_{44}H_{31}O_{20}$), 287.0564 (-$C_{44}H_{33}O_{20}$), 269.0458(-$C_{44}H_{35}O_{21}$), 169.0134	(Singh *et al.*, 2018)

					(-$C_{52}H_{39}O_{21}$), 125.023 (-$C_{54}H_{39}O_{23}$)	
(Epi)catechin gallate isomer 2	$[M-H]^-$	441.0826	$C_{22}H_{17}O_{10}$	9.88	331.0454 (-$C_6H_6O_2$), 303.0510 (-$C_7H_6O_3$), 289.0719 (-$C_7H_4O_4$), 271.0610 (-$C_7H_6O_5$), 169.0134 (-$C_{15}H_{12}O_5$), 125.0233 (-$C_{18}H_7O_7$)	(Yuzuak *et al.*, 2018)
Digalloyl procyanidin pentamer B-type linkage isomer 2	$[M-2H]^{2-}$	872.1754	$C_{89}H_{68}O_{38}$	9.95	1017.2163 (-$C_{37}H_{27}O_{16}$), 796.1569 (-$C_7H_4O_4$), 729.1451 (-$C_{52}H_{39}O_{22}$), 577.1370 (-$C_{59}H_{43}O_{26}$), 576.1243 (-$C_{29}H_{20}O_{14}$), 575.1195(-$C_{59}H_{45}O_{26}$), 449.0890 (-$C_{65}H_{51}O_{29}$), 407.0770 (-$C_{67}H_{53}O_{30}$), 289.0721(-$C_{74}H_{55}O_{32}$), 287.0564 (-$C_{74}H_{57}O_{32}$), 269.0454 (-$C_{74}H_{59}O_{33}$)	(Singh *et al.*, 2018)
Digalloyl (Epi)catechin-(Epi)catechin B-type linkage	$[M-2H]^{2-}$	440.0744	$C_{44}H_{32}O_{20}$	10.05	711.1374 (-$C_7H_5O_5$), 449.0877 (-$C_{20}H_{15}O_{11}$), 407.0774 (-$C_{22}H_{17}O_{12}$), 364.0699 (-$C_7H_4O_4$), 289.0720 (-$C_{29}H_{19}O_{14}$), 287.0564(-$C_{29}H_{21}O_{14}$), 269.0458 (-$C_{29}H_{23}O_{15}$), 169.0134 (-$C_{37}H_{27}O_{15}$), 125.0233 (-$C_{39}H_{27}O_{17}$)	(Singh *et al.*, 2018)
Procyanidin octamer B-type linkage isomer 4	$[M-2H]^{2-}$	1153.2639	$C_{120}H_{96}O_{48}$	10.05	1008.1849 (-$C_{15}H_{12}O_6$), 865.2004 (-$C_{75}H_{59}O_{30}$), 864.1948(-$C_{30}H_{24}O_{12}$), 863.1862 (-$C_{75}H_{61}O_{30}$), 577.1352 (-$C_{90}H_{71}O_{36}$), 576.1220(-$C_{60}H_{48}O_{24}$), 575.1198 (-$C_{90}H_{73}O_{36}$), 449.0873 (-$C_{96}H_{79}O_{39}$), 407.0768(-$C_{98}H_{81}O_{40}$), 289.0722 (-$C_{105}H_{83}O_{42}$), 287.0564 (-$C_{105}H_{85}O_{42}$), 269.0466 (-$C_{105}H_{87}O_{43}$)	(Lin *et al.*, 2014)
Digallate (Epi)catechin-(Epi)catechin B-type linkage	$[M-H]^-$	881.1589	$C_{44}H_{33}O_{20}$	10.06	729.1482 (-$C_7H_4O_4$), 711.1340 (-$C_7H_6O_5$), 603.1172 (-$C_{13}H_{10}O_7$), 577.1380 (-$C_{14}H_8O_8$), 559.1274 (-$C_{14}H_{10}O_9$), 541.1144 (-$C_{14}H_{12}O_{10}$), 451.1057 (-$C_{20}H_{14}O_{11}$), 433.0934	(Singh *et al.*, 2018)

					(-$C_{20}H_{16}O_{12}$), 425.0875(-$C_{22}H_{16}O_{11}$), 407.0774 (-$C_{22}H_{18}O_{12}$), 389.0681 (-$C_{22}H_{20}O_{13}$), 289.0720(-$C_{29}H_{20}O_{14}$), 287.0564 (-$C_{29}H_{22}O_{14}$), 271.0616 (-$C_{29}H_{22}O_{15}$), 269.0457(-$C_{29}H_{24}O_{15}$), 169.0134 (-$C_{37}H_{28}O_{15}$), 125.0233 (-$C_{38}H_{28}O_{17}$)	
Trigalloyl procyanidin octamer B-type linkage	$[M-3H]^{3-}$	930.1877	$C_{141}H_{107}O_{60}$	10.10	864.1874 (-$C_{51}H_{35}O_{24}$), 577.1361 (-$C_{111}H_{82}O_{48}$), 575.1218 (-$C_{111}H_{84}O_{48}$), 449.0882 (-$C_{117}H_{90}O_{51}$), 441.0847 (-$C_{119}H_{90}O_{50}$), 407.0786 (-$C_{119}H_{92}O_{52}$), 289.0720 (-$C_{126}H_{94}O_{54}$), 287.0565 (-$C_{126}H_{96}O_{54}$), 269.0462 (-$C_{126}H_{98}O_{55}$)	(Singh *et al.*, 2018)
(Epi)afzelechin-(Epi)catechin linkage B-type isomer 5	$[M-H]^{-}$	561.1411	$C_{30}H_{26}O_{11}$	10.22	435.1067 (-$C_6H_6O_3$), 425.0861 (-$C_8H_9O_2$), 409.0935 (-$C_8H_8O_3$), 289.0725 (-$C_{15}H_{12}O_5$), 273.0768 (-$C_{15}H_{12}O_6$), 271.0609 (-$C_{15}H_{11}O_5$), 125.0234 (-$C_{24}H_{20}O_8$)	(Enomoto *et al.*, 2019)
Procyanidin dimer B-type isomer 5	$[M-H]^{-}$	577.1354	$C_{30}H_{25}O_{12}$	10.22	559.1273 (-H_2O), 451.1038 (-$C_6H_6O_3$), 425.0882 (-$C_8H_8O_3$), 407.0773 (-$C_8H_{10}O_4$), 289.0719 (-$C_{15}H_{12}O_6$), 287.0563 (-$C_{15}H_{14}O_6$), 125.0233 (-$C_{24}H_{20}O_9$)	(Lin *et al.*, 2014)
O-Galloyl-(Epi)catechin-(Epi)catechin-(Epi)catechin) B-type linkage isomer 4	$[M-H]^{-}$	1017.2136	$C_{52}H_{41}O_{22}$	10.34	891.1794 (-$C_6H_6O_3$), 729.1474 (-$C_{15}H_{12}O_6$), 575.1193 (-$C_{22}H_{18}O_{10}$), 557.1069 (-$C_{22}H_{20}O_{11}$), 541.1155 (-$C_{22}H_{20}O_{12}$), 451.1039(-$C_{28}H_{22}O_{13}$), 433.0954 (-$C_{28}H_{24}O_{14}$), 425.0879 (-$C_{30}H_{24}O_{13}$), 423.0721(-$C_{30}H_{26}O_{13}$), 407.0771 (-$C_{30}H_{26}O_{14}$), 405.0621 (-$C_{30}H_{28}O_{14}$), 289.0719 (-$C_{37}H_{28}O_{16}$), 287.0564(-$C_{37}H_{30}O_{16}$), 271.0605	

					(-$C_{37}H_{30}O_{17}$), 269.0446 (-$C_{37}H_{32}O_{17}$), 169.0134 (-$C_{45}H_{36}O_{17}$), 125.0234 (-$C_{46}H_{36}O_{19}$)	
Digalloyl procyanidin eptamer B-type linkage	$[M-3H]^{3-}$	773.4949	$C_{119}H_{91}O_{50}$	10.38	865.2014 (-$C_{74}H_{54}O_{32}$), 846.1640 (-$C_{29}H_{19}O_{14}$), 722.4777 (-$C_{7}H_{4}O_{4}$), 577.1332 (-$C_{89}H_{66}O_{38}$), 576.1224 (-$C_{59}H_{43}O_{26}$), 575.1207 (-$C_{89}H_{68}O_{38}$), 449.0888(-$C_{95}H_{74}O_{41}$), 407.0759 (-$C_{97}H_{76}O_{42}$), 289.0721 (-$C_{104}H_{78}O_{44}$), 287.0563 (-$C_{104}H_{90}O_{44}$), 269.0452 (-$C_{104}H_{82}O_{45}$)	
(Epi)catechin-(Epi)catechin-(Epi)afzelechin AB-type linkage	$[M-H]^{-}$	847.1937	$C_{45}H_{35}O_{17}$	10.48	695.1470 (-$C_{8}H_{8}O_{3}$), 577.1416 (-$C_{15}H_{10}O_{5}$), 557.1088 (-$C_{15}H_{14}O_{6}$), 425.0902 (-$C_{23}H_{18}O_{8}$), 407.0770 (-$C_{23}H_{20}O_{9}$), 289.0713 (-$C_{30}H_{22}O_{11}$), 287.0566 (-$C_{30}H_{24}O_{11}$), 269.0454 (-$C_{30}H_{26}O_{12}$), 125.0234(-$C_{39}H_{30}O_{14}$)	
(Epi)catechin-(Epi)catechin-(Epi)catechin-(Epi)catechin-(Epi)catechin-(Epi)catechin-(Epi)catechin-(Epi)gallocatechin B-type linkage isomer 1	$[M-3H]^{3-}$	869.1913	$C_{135}H_{107}O_{55}$	10.54	865.1903 (-$C_{90}H_{70}O_{37}$), 864.1877 (-$C_{45}H_{35}O_{19}$), 863.1887(-$C_{90}H_{72}O_{37}$), 591.1143 (-$C_{105}H_{84}O_{42}$), 577.1374 (-$C_{105}H_{82}O_{43}$), 575.1216 (-$C_{105}H_{84}O_{43}$), 467.0970 (-$C_{111}H_{88}O_{45}$), 449.0900 (-$C_{111}H_{90}O_{46}$), 441.0821 (-$C_{113}H_{90}O_{45}$), 407.0782 (-$C_{113}H_{92}O_{47}$), 303.0513 (-$C_{120}H_{96}O_{48}$), 289.0722 (-$C_{120}H_{94}O_{49}$), 287.0564 (-$C_{120}H_{96}O_{49}$), 285.0403 (-$C_{120}H_{98}O_{49}$), 269.0463 (-$C_{120}H_{98}O_{50}$)	(Singh *et al.*, 2018)
Galloyl-(Epi)catechin-(Epi)catechin B-type linkage isomer 4	$[M-H]^{-}$	729.1475	$C_{37}H_{29}O_{16}$	10.60	577.1367 (-$C_{7}H_{4}O_{4}$), 559.1242 (-$C_{7}H_{6}O_{5}$), 541.1143 (-$C_{7}H_{8}O_{6}$), 451.1056 (-$C_{13}H_{10}O_{7}$), 433.0928 (-$C_{13}H_{12}O_{8}$), 425.0887 (-$C_{15}H_{12}O_{7}$), 407.0773 (-$C_{15}H_{14}O_{8}$), 289.0719	(Singh *et al.*, 2018)

					(-$C_{22}H_{16}O_{10}$), 287.0565(-$C_{22}H_{18}O_{10}$), 271.0620 (-$C_{22}H_{18}O_{12}$), 269.0461 (-$C_{22}H_{20}O_{11}$), 169.0134(-$C_{30}H_{24}O_{11}$), 125.0233 (-$C_{31}H_{24}O_{13}$)	
Procyanidin eptamer B-type linkage isomer 3	$[M-2H]^{2-}$	1008.7337	$C_{105}H_{84}O_{42}$	10.66	865.1964 (-$C_{60}H_{47}O_{24}$), 864.1894 (-$C_{15}H_{12}O_6$), 863.1843 (-$C_{60}H_{49}O_{24}$), 577.1338 (-$C_{75}H_{59}O_{30}$), 576.1224 (-$C_{45}H_{36}O_{18}$), 575.1203 (-$C_{75}H_{61}O_{30}$), 449.0881(-$C_{81}H_{67}O_{33}$), 407.0770(-$C_{83}H_{69}O_{34}$), 289.0719 (-$C_{90}H_{71}O_{36}$), 287.0563 (-$C_{90}H_{73}O_{36}$)	(Lin *et al.*, 2014)
Digalloyl procyanidin pentamer B-type linkage isomer 3	$[M-2H]^{2-}$	872.1744	$C_{89}H_{68}O_{38}$	10.71	1017.2058 (-$C_{37}H_{27}O_{16}$), 865.2001 (-$C_{44}H_{31}O_{20}$), 863.1843(-$C_{44}H_{33}O_{20}$), 796.1594 (-$C_7H_4O_4$), 729.1429 (-$C_{52}H_{39}O_{22}$), 577.1368(-$C_{59}H_{43}O_{26}$), 576.1241 (-$C_{29}H_{20}O_{14}$), 575.1201 (-$C_{59}H_{45}O_{26}$), 449.0895(-$C_{65}H_{51}O_{29}$), 407.0775 (-$C_{67}H_{53}O_{30}$), 289.0720 (-$C_{74}H_{55}O_{32}$), 287.0563(-$C_{74}H_{57}O_{32}$), 269.0458 (-$C_{74}H_{59}O_{33}$)	(Singh *et al.*, 2018)
Trigalloyl procyanidin pentamer B-type linkage	$[M-2H]^{2-}$	948.1808	$C_{96}H_{72}O_{42}$	10.71	872.1625 (-$C_7H_4O_4$), 577.1359 (-$C_{96}H_{70}O_{42}$), 576.1261(-$C_{66}H_{47}O_{30}$), 575.1202 (-$C_{96}H_{72}O_{42}$), 449.0871 (-$C_{102}H_{78}O_{45}$), 407.0770 (-$C_{104}H_{80}O_{46}$), 289.0725 (-$C_{111}H_{82}O_{49}$), 287.0564 (-$C_{111}H_{84}O_{49}$), 269.0459 (-$C_{111}H_{86}O_{50}$)	(Singh *et al.*, 2018)
Procyanidin trimer B-type isomer 9	$[M-H]^{-}$	865.1956	$C_{45}H_{37}O_{18}$	10.74	577.1349 (-$C_{15}H_{12}O_6$), 575.1188 (-$C_{15}H_{14}O_6$), 451.1035 (-$C_{21}H_{18}O_9$), 449.0885 (-$C_{21}H_{20}O_9$), 425.0867 (-$C_{23}H_{20}O_9$), 423.0733 (-$C_{23}H_{22}O_9$), 407.0770 (-$C_{23}H_{22}O_{10}$), 405.0609 (-$C_{23}H_{24}O_{10}$), 289.0720 (-$C_{30}H_{24}O_{12}$), 287.0564 (-$C_{30}H_{26}O_{12}$), 125.0234	(Lin *et al.*, 2014)

					($-C_{39}H_{31}O_{15}$)	
O-Galloyl Procyanidin nonamer B-type linkage isomer 1	$[M-3H]^{3-}$	915.1989	$C_{142}H_{113}O_{58}$	10.78	1303.2610 ($-C_{75}H_{62}O_{30}$), 1151.2389 ($-C_{82}H_{66}O_{34}$), 865.1985($-C_{97}H_{76}O_{40}$), 864.1826 ($-C_{7}H_{5}O_{4}$), 864.1826 ($-C_{52}H_{41}O_{22}$), 863.1846($-C_{97}H_{78}O_{40}$), 720.1542 ($-C_{67}H_{53}O_{28}$), 577.1345 ($-C_{112}H_{88}O_{46}$), 575.1201 ($-C_{112}H_{90}O_{46}$), 449.0893 ($-C_{118}H_{96}O_{49}$), 407.0787 ($-C_{120}H_{98}O_{50}$), 289.0721($-C_{127}H_{100}O_{52}$), 287.0562 ($-C_{127}H_{102}O_{52}$), 269.0445 ($-C_{127}H_{104}O_{53}$)	(Singh *et al.*, 2018)
O-Galloyl Procyanidin eptamer B-type linkage isomer 2	$[M-2H]^{3-}$	722.8196	$C_{112}H_{87}O_{46}$	11.01	865.1907 ($-C_{67}H_{50}O_{28}$), 864.1947 ($-C_{22}H_{15}O_{10}$), 863.1754 ($-C_{67}H_{52}O_{28}$), 577.1349($-C_{97}H_{76}O_{40}$), 576.1264 ($-C_{52}H_{29}O_{22}$), 575.1216 ($-C_{97}H_{78}O_{40}$), 449.0881 ($-C_{103}H_{84}O_{43}$), 407.0770 ($-C_{105}H_{86}O_{44}$), 289.0720 ($-C_{112}H_{88}O_{46}$), 287.0564 ($-C_{112}H_{90}O_{46}$), 269.0462 ($-C_{112}H_{92}O_{47}$)	(Singh *et al.*, 2018)
Digalloyl procyanidin trimer B-type linkage isomer 3	$[M-2H]^{2-}$	584.1075	$C_{59}H_{44}O_{26}$	11.05	577.1293 ($-C_{29}H_{19}O_{14}$), 575.1221 ($-C_{29}H_{21}O_{14}$), 508.1018 ($-C_{7}H_{4}O_{4}$), 449.0897 ($-C_{35}H_{27}O_{17}$), 441.0821 ($-C_{37}H_{27}O_{16}$), 407.0782($-C_{37}H_{29}O_{18}$), 289.0721 ($-C_{44}H_{31}O_{20}$), 287.0563 ($-C_{44}H_{33}O_{20}$), 269.0457($-C_{44}H_{35}O_{21}$), 169.0135 ($-C_{52}H_{39}O_{21}$), 125.0234 ($-C_{54}H_{39}O_{23}$)	(Singh *et al.*, 2018)
O-Galloyl procyanidin octamer B-type linkage isomer 2	$[M-3H]^{3-}$	819.1696	$C_{127}H_{101}O_{52}$	11.09	1152.2498 ($-C_{7}H_{5}O_{4}$), 865.1938 ($-C_{97}H_{76}O_{40}$), 863.1829($-C_{97}H_{78}O_{40}$), 577.1364 ($-C_{97}H_{76}O_{40}$), 575.1222 ($-C_{97}H_{78}O_{40}$), 449.0861 ($-C_{103}H_{84}O_{43}$), 407.0785 ($-C_{105}H_{86}O_{44}$), 289.0719	(Singh *et al.*, 2018)

					(-$C_{112}H_{88}O_{46}$), 287.0562 (-$C_{112}H_{90}O_{46}$), 269.0461 (-$C_{112}H_{92}O_{47}$)	
O-Galloyl Procyanidin hexamer B-type linkage isomer 4	$[M-2H]^{2-}$	940.7008	$C_{97}H_{76}O_{40}$	11.36	1305.2745 (-$C_{30}H_{23}O_{12}$), 1303.2551 (-$C_{30}H_{25}O_{12}$) 863.1827(-$C_{52}H_{41}O_{22}$), 796.1663 (-$C_{15}H_{12}O_{6}$), 577.1394 (-$C_{67}H_{51}O_{28}$), 576.1237(-$C_{37}H_{28}O_{16}$), 575.1199 (-$C_{67}H_{53}O_{28}$), 449.0879 (-$C_{73}H_{59}O_{31}$), 407.0775(-$C_{75}H_{61}O_{32}$), 289.0717 (-$C_{82}H_{63}O_{34}$), 287.0564 (-$C_{82}H_{65}O_{34}$), 269.0455 (-$C_{82}H_{67}O_{35}$)	
(Epi)catechin-(Epi)catechin-(Epi)catechin-(Epi)catechin-(Epi)catechin-(Epi)catechin-(Epi)catechin-(Epi)gallocatechin B-type linkage isomer 2	$[M-3H]^{3-}$	869.1787	$C_{135}H_{107}O_{55}$	11.38	1153.2574 (-$C_{75}H_{58}O_{31}$), 865.1953 (-$C_{90}H_{70}O_{37}$), 864.1877(-$C_{45}H_{35}O_{19}$), 863.1802 (-$C_{90}H_{72}O_{37}$), 577.1380 (-$C_{105}H_{82}O_{43}$), 575.1204 (-$C_{105}H_{84}O_{43}$), 449.0885 (-$C_{111}H_{90}O_{46}$), 441.0773 (-$C_{113}H_{90}O_{45}$), 407.0750 (-$C_{113}H_{92}O_{47}$), 303.0511 (-$C_{120}H_{96}O_{48}$), 289.0722 (-$C_{120}H_{94}O_{49}$), 287.0562 (-$C_{120}H_{96}O_{49}$), 285.0404 (-$C_{120}H_{98}O_{49}$), 269.0467 (-$C_{120}H_{98}O_{50}$)	(Singh *et al.*, 2018)
Trigalloyl procyanidin tetramer B-type linkage isomer 2	$[M-2H]^{2-}$	804.1484	$C_{81}H_{60}O_{36}$	11.63	881.1562 (-$C_{37}H_{27}O_{16}$), 729.1483 (-$C_{44}H_{31}O_{20}$), 728.1401 (-$C_{7}H_{4}O_{4}$), 727.1401 (-$C_{44}H_{33}O_{20}$), 652.1304 (-$C_{14}H_{8}O_{8}$), 577.1293 (-$C_{51}H_{35}O_{24}$), 575.1191 (-$C_{51}H_{37}O_{24}$), 449.0881 (-$C_{57}H_{43}O_{27}$), 441.0818 (-$C_{59}H_{43}O_{26}$), 407.0768(-$C_{59}H_{45}O_{28}$), 289.0722 (-$C_{66}H_{47}O_{30}$), 287.0563 (-$C_{66}H_{49}O_{30}$), 269.0457(-$C_{66}H_{51}O_{31}$), 169.0134 (-$C_{74}H_{55}O_{31}$), 125.0234 (-$C_{76}H_{55}O_{33}$)	(Singh *et al.*, 2018)
Digalloyl procyanidin octamer B-type linkage	$[M-3H]^{3-}$	869.8469	$C_{134}H_{103}O_{56}$	11.94	1152.2460 (-$C_{14}H_{7}O_{8}$), 863.1775 (-$C_{89}H_{68}O_{38}$), 818.8378 (-$C_{7}H_{4}O_{4}$), 577.1349 (-$C_{104}H_{78}O_{44}$), 576.1218	(Singh *et al.*, 2018)

					(-$C_{74}H_{55}O_{32}$), 575.1218 (-$C_{104}H_{80}O_{44}$), 449.0897 (-$C_{110}H_{86}O_{47}$), 407.0765 (-$C_{112}H_{88}O_{48}$), 289.0721 (-$C_{119}H_{90}O_{50}$), 287.0721 (-$C_{119}H_{92}O_{50}$), 285.0415 (-$C_{119}H_{94}O_{50}$), 269.0464 (-$C_{119}H_{94}O_{51}$)	
O-Galloyl procyanidin octamer B-type linkage isomer 3	$[M-3H]^{3-}$	819.1705	$C_{127}H_{101}O_{52}$	11.96	1153.2711 (-$C_{67}H_{52}O_{28}$), 865.2057 (-$C_{82}H_{64}O_{34}$), 863.1875 (-$C_{82}H_{66}O_{34}$), 577.1321(-$C_{97}H_{76}O_{40}$), 575.1207 (-$C_{97}H_{78}O_{40}$), 449.0870 (-$C_{103}H_{84}O_{43}$), 407.0770 (-$C_{105}H_{86}O_{44}$), 289.0719 (-$C_{112}H_{88}O_{46}$), 287.0565 (-$C_{112}H_{90}O_{46}$), 269.0458 (-$C_{112}H_{92}O_{47}$)	
Procyanidin trimer B-type isomer 10	$[M-H]^{-}$	865.2017	$C_{45}H_{37}O_{18}$	12.01	577.1280 (-$C_{15}H_{12}O_{6}$), 449.0901 (-$C_{21}H_{20}O_{9}$), 407.0771(-$C_{23}H_{22}O_{10}$), 289.0723 (-$C_{30}H_{24}O_{12}$), 287.0565 (-$C_{30}H_{26}O_{12}$), 125.0233(-$C_{39}H_{31}O_{15}$)	(Lin *et al.*, 2014)
(Epi)catechin-(Epi)catechin-(Epi)catechin-(Epi)catechin-(Epi)catechin-(Epi)catechin-(Epi)catechin-(Epi)catechin-(Epi)gallocatechin B-type linkage	$[M-3H]^{3-}$	965.5389	$C_{150}H_{119}O_{61}$	12.07	864.1818 (-$C_{60}H_{47}O_{25}$), 863.1837 (-$C_{105}H_{84}O_{43}$), 577.1330 (-$C_{120}H_{94}O_{49}$), 576.1245 (-$C_{90}H_{71}O_{37}$), 575.1207 (-$C_{120}H_{96}O_{49}$),449.0891 (-$C_{126}H_{102}O_{52}$), 441.0853 (-$C_{128}H_{102}O_{51}$), 407.0771 (-$C_{128}H_{104}O_{53}$),303.0511(-$C_{135}H_{108}O_{54}$), 289.0720 (-$C_{135}H_{106}O_{55}$), 287.0560 (-$C_{135}H_{108}O_{55}$), 285.0425 (-$C_{135}H_{110}O_{55}$), 269.0450 (-$C_{135}H_{110}O_{56}$)	(Singh *et al.*, 2018)
O-Galloyl Procyanidin decamer B-type linkage	$[M-3H]^{3-}$	1010.8876	$C_{157}H_{121}O_{64}$	12.20	1303.2552 (-$C_{90}H_{70}O_{36}$), 1151.2513 (-$C_{97}H_{74}O_{40}$), 863.1835 (-$C_{18}H_{16}O_{10}$), 577.1340 (-$C_{127}H_{96}O_{52}$), 575.1202 (-$C_{127}H_{98}O_{52}$), 449.0876 (-$C_{133}H_{104}O_{55}$), 407.0767 (-$C_{135}H_{106}O_{56}$), 289.0726	(Singh *et al.*, 2018)

					(-$C_{142}H_{108}O_{58}$), 287.0565 (-$C_{142}H_{110}O_{58}$), 269.0466 (-$C_{142}H_{112}O_{59}$)	
O-Galloyl-(Epi)catechin-(Epi)catechin-(Epi)catechin B-type linkage isomer 5	$[M-H]^-$	1017.2135	$C_{52}H_{41}O_{22}$	12.23	891.1757 (-$C_6H_6O_3$), 729.1478 (-$C_{15}H_{12}O_6$), 577.1303(-$C_{22}H_{16}O_{10}$), 575.1201 (-$C_{22}H_{18}O_{10}$), 451.1046 (-$C_{28}H_{22}O_{13}$), 433.0941 (-$C_{28}H_{24}O_{14}$), 407.0777(-$C_{30}H_{26}O_{14}$), 405.0586(-$C_{30}H_{28}O_{14}$), 289.0720 (-$C_{37}H_{28}O_{16}$), 287.0562 (-$C_{37}H_{30}O_{16}$), 269.0454 (-$C_{37}H_{32}O_{17}$), 169.0133(-$C_{45}H_{36}O_{17}$), 125.0234 (-$C_{46}H_{36}O_{19}$)	(Singh *et al.*, 2018)
Trigalloyl procyanidin trimer B-type linkage	$[M-2H]^{2-}$	660.1140	$C_{66}H_{48}O_{30}$	12.33	729.1481 (-$C_{29}H_{19}O_{14}$), 584.1064 (-$C_7H_4O_4$), 575.1143 (-$C_{36}H_{25}O_{18}$), 449.0884 (-$C_{42}H_{31}O_{21}$), 407.0785 (-$C_{44}H_{33}O_{22}$), 289.0723(-$C_{51}H_{35}O_{24}$), 287.0564 (-$C_{51}H_{37}O_{24}$), 269.0439 (-$C_{51}H_{39}O_{25}$), 169.0134(-$C_{59}H_{43}O_{25}$), 125.0233 (-$C_{61}H_{41}O_{27}$)	(Singh *et al.*, 2018)
O-Galloyl Procyanidin nonamer B-type linkage isomer 2	$[M-3H]^{3-}$	915.2023	$C_{142}H_{113}O_{58}$	12.35	865.1936 (-$C_{97}H_{76}O_{40}$), 863.1855 (-$C_{97}H_{78}O_{40}$), 577.1354 (-$C_{112}H_{88}O_{46}$), 575.1206 (-$C_{112}H_{90}O_{46}$), 449.0875 (-$C_{118}H_{96}O_{49}$), 407.0771 (-$C_{120}H_{98}O_{50}$), 289.0721 (-$C_{127}H_{100}O_{52}$), 287.0563 (-$C_{127}H_{102}O_{52}$), 269.0464 (-$C_{127}H_{104}O_{53}$)	(Singh *et al.*, 2018)
Digalloyl procyanidin nonamer B-type linkage	$[M-3H]^{3-}$	965.5285	$C_{149}H_{115}O_{62}$	12.40	914.8511 (-$C_7H_4O_4$), 865.1961 (-$C_{104}H_{78}O_{44}$), 864.1833 (-$C_{14}H_8O_8$), 577.1349 (-$C_{119}H_{90}O_{50}$), 575.1204 (-$C_{119}H_{92}O_{50}$), 449.0895 (-$C_{125}H_{98}O_{53}$), 407.0786 (-$C_{127}H_{100}O_{54}$), 289.0719 (-$C_{134}H_{102}O_{56}$), 287.0565 (-$C_{134}H_{104}O_{56}$), 269.0470 (-$C_{134}H_{106}O_{57}$)	(Singh *et al.*, 2018)

O-Galloyl Procyanidin hexamer B-type linkage isomer 5	$[M-2H]^{2-}$	940.7065	$C_{97}H_{76}O_{40}$	12.42	1305.2733 ($-C_{30}H_{23}O_{12}$), 863.1790 ($-C_{52}H_{41}O_{22}$), 577.1319 ($-C_{67}H_{51}O_{28}$), 576.1246($-C_{37}H_{28}O_{16}$), 575.1220 ($-C_{67}H_{53}O_{28}$), 449.0874 ($-C_{73}H_{59}O_{31}$), 407.0775($-C_{75}H_{61}O_{32}$), 289.0721 ($-C_{82}H_{63}O_{34}$), 287.0564 ($-C_{82}H_{65}O_{34}$), 269.0457 ($-C_{82}H_{67}O_{35}$)	(Singh *et al.*, 2018)
(Epi)catechin *O*-coumarate isomer 1	$[M-H]^{-}$	453.1088	$C_{24}H_{19}O_{8}$	12.47	341.0670 ($-C_{6}H_{6}O$), 289.0709 ($-C_{9}H_{7}O_{2}$), 125.0233 ($-C_{18}H_{14}O_{5}$)	(Šukovic *et al.*, 2020)
Galloyl-(Epi)catechin-(Epi)catechin B-type linkage isomer 5	$[M-H]^{-}$	729.1458	$C_{37}H_{29}O_{16}$	12.52	541.1138 ($-C_{7}H_{8}O_{6}$), 451.1042 ($-C_{13}H_{10}O_{7}$), 433.0936 ($-C_{13}H_{12}O_{8}$), 425.0887 ($-C_{15}H_{12}O_{7}$), 407.0776 ($-C_{15}H_{14}O_{8}$), 289.0721 ($-C_{22}H_{16}O_{10}$), 287.0563 ($-C_{22}H_{18}O_{10}$), 271.0616 ($-C_{22}H_{18}O_{12}$), 269.0461($-C_{22}H_{20}O_{11}$), 169.0135 ($-C_{30}H_{24}O_{11}$), 125.0234 ($-C_{31}H_{24}O_{13}$)	
(Epi)catechin-(Epi)catechin-(Epi)catechin-(Epi)catechin-(Epi)catechin-(Epi)catechin-(Epi)catechin-(Epi)catechin-(Epi)gallocatechin B-type linkage isomer 3	$[M-3H]^{3-}$	869.1905	$C_{135}H_{107}O_{55}$	12.53	863.1798($-C_{90}H_{72}O_{37}$), 577.1362 ($-C_{105}H_{82}O_{43}$), 575.1206 ($-C_{105}H_{84}O_{43}$), 449.0882 ($-C_{111}H_{90}O_{46}$), 441.0789 ($-C_{113}H_{90}O_{45}$), 407.0763 ($-C_{113}H_{92}O_{47}$), 303.0503 ($-C_{120}H_{96}O_{48}$), 289.0721 ($-C_{120}H_{94}O_{49}$), 287.0565 ($-C_{120}H_{96}O_{49}$), 285.0401 ($-C_{120}H_{98}O_{49}$), 269.0457 ($-C_{120}H_{98}O_{50}$)	(Singh *et al.*, 2018)
Galloyl-(Epi)catechin-(Epi)catechin A-type linkage isomer 2	$[M-H]^{-}$	727.1348	$C_{37}H_{27}O_{16}$	12.53	575.1212 ($-C_{7}H_{4}O_{4}$), 557.1100 ($-C_{7}H_{6}O_{5}$), 539.1041 ($-C_{7}H_{8}O_{6}$), 449.0873 ($-C_{13}H_{10}O_{7}$), 431.0801 ($-C_{13}H_{12}O_{8}$), 407.0775 ($-C_{15}H_{12}O_{8}$), 389.0672 ($-C_{15}H_{14}O_{9}$), 289.0719	(Singh *et al.*, 2018)

					($-C_{22}H_{14}O_{10}$), 287.0563($-C_{22}H_{16}O_{10}$), 271.0617 ($-C_{22}H_{16}O_{11}$), 269.0455 ($-C_{22}H_{18}O_{11}$), 169.0134($-C_{30}H_{22}O_{11}$), 125.0233 ($-C_{31}H_{22}O_{13}$)	
(Epi)catechin-(Epi)catechin-(Epi)catechin AB-type linkage	$[M-H]^-$	863.1827	$C_{45}H_{35}O_{18}$	12.62	737.1558 ($-C_6H_6O_3$), 711.1359 ($-C_8H_8O_3$), 577.1359 ($-C_{15}H_{10}O_6$), 575.1192 ($-C_{15}H_{12}O_6$), 573.1013 ($-C_{15}H_{14}O_6$), 449.0872 ($-C_{21}H_{18}O_9$), 425.0855 ($-C_{23}H_{18}O_9$), 407.0755 ($-C_{23}H_{20}O_{10}$), 289.0722($-C_{30}H_{22}O_{12}$), 287.0562 ($-C_{30}H_{24}O_{12}$), 269.0451 ($-C_{30}H_{26}O_{13}$)	(Lin *et al.*, 2014)
Galloyl-(Epi)catechin-(Epi)catechin-(Epi)catechin AB-type linkage	$[M-H]^-$	863.2051	$C_{52}H_{39}O_{22}$	13.09	863.1784 ($-C_7H_4O_4$), 575.1194 ($-C_{22}H_{16}O_{10}$), 449.0875($-C_{28}H_{22}O_{13}$), 407.0768 ($-C_{30}H_{24}O_{14}$), 289.0720 ($-C_{37}H_{26}O_{16}$), 287.0564($-C_{37}H_{28}O_{16}$), 269.0458 ($-C_{37}H_{30}O_{17}$)	(Singh *et al.*, 2018)
(Epi)catechin-(Epi)afzelechin-(Epi)catechin AB-type linkage isomer 1	$[M-H]^-$	847.1932	$C_{45}H_{35}O_{17}$	13.20	559.1289 ($-C_{15}H_{12}O_6$), 433.0930 ($-C_{21}H_{18}O_9$), 407.0790 ($-C_{23}H_{20}O9$), 289.0717 ($-C_{30}H_{22}O_{11}$), 287.0543 ($-C_{30}H_{24}O_{11}$), 269.0454($-C_{30}H_{26}O_{12}$), 125.0235 ($-C_{39}H_{30}O_{14}$)	(Singh *et al.*, 2018)
(Epi)catechin ethyl dimer isomer 1	$[M-H]^-$	605.1677	$C_{32}H_{29}O_{12}$	13.38	453.1169 ($-C_8H_8O_3$), 315.0879 ($-C_{15}H_{15}O_6$), 289.0722 ($-C_{17}H_{16}O_6$), 125.0235 ($-C_{26}H_{24}O_9$)	(Rockenbach *et al.*, 2012)
(Epi)catechin-(Epi)afzelechin A-type linkage isomer 1	$[M-H]^-$	559.1250	$C_{30}H_{23}O_{11}$	13.78	433.0931 ($-C_6H_6O_3$), 407.0775 ($-C_8H_8O_3$), 289.0720 ($-C_{15}H_{10}O_5$), 269.0458 ($-C_{15}H_{14}O_6$), 125.0231 ($-C_{24}H_{18}O_8$)	(Singh *et al.*, 2018)
(Epi)catechin *O*-coumarate isomer 2	$[M-H]^-$	453.1101	$C_{24}H_{19}O_8$	14.26	341.0669 ($-C_6H_6O$), 289.0721 ($-C_9H_7O_2$), 165.0186 ($-C_{16}H_{14}O_4$), 125.0231 ($-C_{18}H_{14}O_5$)	(Šukovic *et al.*, 2020)

(Epi)catechin-(Epi)afzelechin-(Epi)catechin AB-type linkage isomer 2	$[M-H]^-$	847.1944	$C_{45}H_{35}O_{17}$	14.64	559.1257 ($-C_{15}H_{12}O_6$), 433.0933 ($-C_{21}H_{18}O_9$), 407.0786 ($-C_{23}H_{20}O_9$), 289.0721 ($-C_{30}H_{22}O_{11}$), 287.0561 ($-C_{30}H_{24}O_{11}$), 269.0450 ($-C_{30}H_{26}O_{12}$), 125.0234 ($-C_{39}H_{30}O_{14}$)	(Singh *et al.*, 2018)
(Epi)catechin ethyl dimer isomer 2	$[M-H]^-$	605.1677	$C_{32}H_{29}O_{12}$	14.96	453.1224 ($-C_8H_8O_3$), 315.0877 ($-C_{15}H_{15}O_6$), 289.0721 ($-C_{17}H_{16}O_6$), 125.0232 ($-C_{26}H_{24}O_9$)	(Rockenbach *et al.*, 2012)
(Epi)catechin-(Epi)afzelechin A-type linkage isomer 2	$[M-H]^-$	559.1266	$C_{30}H_{23}O_{11}$	15.29	433.0932 ($-C_6H_6O_3$), 407.0785 ($-C_8H_8O_3$), 289.0718 ($-C_{15}H_{10}O_5$), 269.0457 ($-C_{15}H_{14}O_6$), 125.0228 ($-C_{24}H_{18}O_8$)	(Singh *et al.*, 2018)
(Epi)catechin *O*-coumarate isomer 3	$[M-H]^-$	453.1053	$C_{24}H_{19}O_8$	16.42	289.0720 ($-C_9H_7O_2$), 165.0189 ($-C_{16}H_{14}O_4$), 125.0231 ($-C_{18}H_{14}O_5$)	(Šukovic *et al.*, 2020)

Figure A2. Full MS chromatograms of GSE (A) and ATGSE (B) obtained by UHPLC-ESI HRMS/MS analysis.

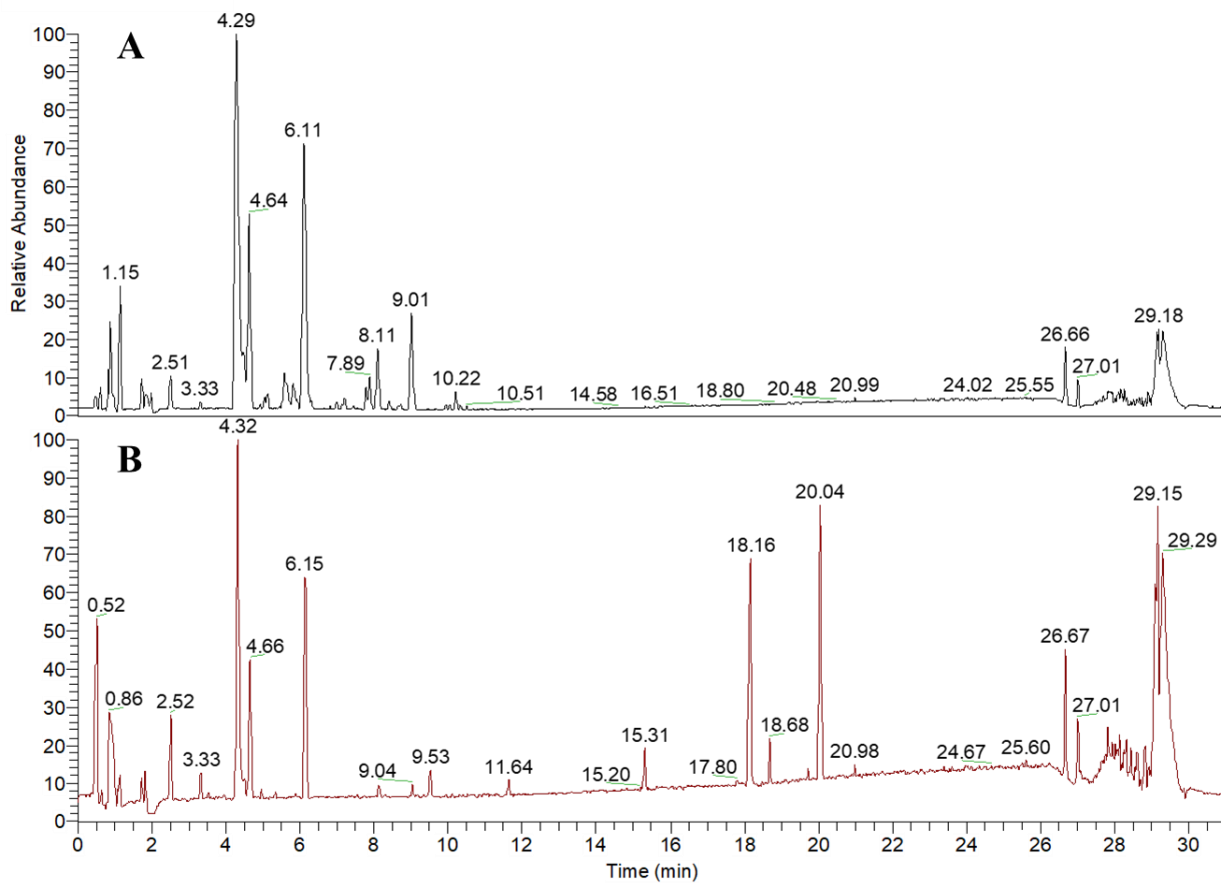

Table A2. Determination of the concentration (mM) of SCFA in healthy and pathological subjects. Values are mean ± standard deviation (SD) of three replications. Statistical significance was calculated by ANOVA and Bonferroni post-hoc analysis: $^{*}p< 0.05$, $^{**}p< 0.01$, $^{***}p< 0.005$, $^{****}p< 0.001$ *vs* control; $^{\#}p< 0.05$, $^{\#\#}p< 0.01$, $^{\#\#\#}p< 0.005$, $^{\#\#\#\#}p< 0.001$ *vs* GSE.

Subjects	Sample	Lactic acid (mM)	Acetic acid (mM)	Succinic acid (mM)	Propionic acid (mM)	Butyric acid (mM)
Healthy adults	GSE	$1.72 \pm 0.26^{*}$	$1.80 \pm 0.22^{***}$	1.74 ± 0.03	$0.97 \pm 0.05^{**}$	0.393 ± 0.004
	ATGSE	$7.54 \pm 0.05^{****\#\#\#\#}$	$3.38 \pm 0.15^{****\#\#\#\#}$	$2.08 \pm 0.05^{***\#\#\#}$	1.12 ± 0.02	0.465 ± 0.001
	Control	0.93 ± 0.37	0.72 ± 0.06	1.73 ± 0.07	1.78 ± 0.14	0.4614 ± 0.0003
Healthy children	GSE	$1.82 \pm 0.03^{**}$	$2.31 \pm 0.51^{***}$	1.55 ± 0.14	$0.73 \pm 0.06^{****}$	$0.300 \pm 0.006^{*}$
	ATGSE	$100.0 \pm 0.6^{****\#\#\#\#}$	$3.28 \pm 0.06^{****\#}$	$4.1 \pm 0.2^{****\#\#\#\#}$	$0.72\pm 0.01^{****}$	$0.356 \pm 0.008^{****\#\#\#\#}$
	Control	0.63 ± 0.06	0.23 ± 0.04	1.385 ± 0.001	1.18 ± 0.02	0.2508 ± 0.0005
Allergic children	GSE	$7.61 \pm 0.02^{****}$	$3.41 \pm 0.05^{****}$	$4.23 \pm 0.08^{****}$	0.694 ± 0.002	$0.375 \pm 0.006^{****}$
	ATGSE	$40.76 \pm 0.72^{****\#\#\#\#}$	$5.92 \pm 0.24^{****\#\#\#\#}$	$4.49 \pm 0.04^{****}$	0.447 ± 0.001	$0.37 \pm 0.01^{****}$
	Control	1.21 ± 0.12	0.38 ± 0.01	1.11 ± 0.21	0.88 ± 0.60	0.2843 ± 0.0008
Obese children	GSE	5.73 ± 0.04	$3.53 \pm 0.12^{****}$	$3.008 \pm 0.025^{****}$	$0.71 \pm 0.01^{****}$	$0.255 \pm 0.006^{****}$
	ATGSE	$19.85 \pm 0.54^{****\#\#\#\#}$	$7.38 \pm 0.30^{****\#\#\#\#}$	$1.64 \pm 0.07^{**\#\#\#}$	$1.79 \pm 0.02^{****\#\#\#\#}$	$0.267 \pm 0.005^{****}$
	Control	0.2060 ± 0.0002	0.25 ± 0.12	0.97 ± 0.06	0.41 ± 0.04	0.136 ± 0.003
Celiac children	GSE	$45.34 \pm 0.07^{****}$	$8.210 \pm 0.009^{****}$	$4.83 \pm 0.06^{****}$	$0.4798 \pm 0.0002^{***}$	$0.1558 \pm 0.0002^{****}$
	ATGSE	$80.58 \pm 0.69^{****\#\#\#\#}$	$4.41 \pm 0.20^{****\#\#\#\#}$	$4.42 \pm 0.02^{****\#}$	$0.515 \pm 0.003^{***}$	$0.156 \pm 0.009^{****}$
	Control	0.99 ± 0.08	1.34 ± 0.19	1.36 ± 0.23	1.20 ± 0.18	0.07 ± 0.01

Figure A3. Chromatogram of SCFA determination by UHPLC-RID analysis. As an example, the chromatogram of SCFA detected in the ATGSE fermentation supernatant of the obese children was shown. The SCFA identified and quantified are lactic acid, acetic acid, succinic acid, propionic acid, and butyric acid.

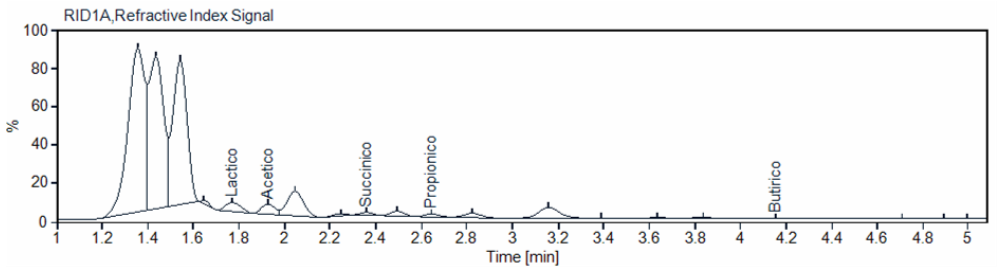

Figure A4. Monitoring the body weight of the animal during four weeks of treatment. Values are presented as the mean ± S.D. (n = 6 for each experimental group). Statistical significance was calculated by one- or two-way ANOVA followed by Bonferroni's or Dunnett's for multiple comparisons, but no significant data were found.

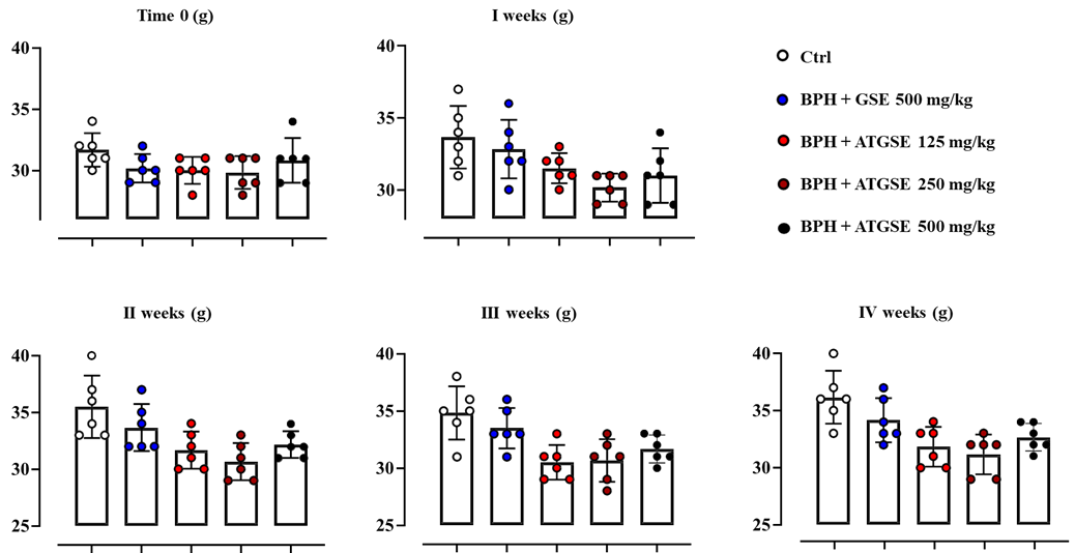

Bibliography

Ahmad, B., Yadav, V., Yadav, A., Rahman, M.U., Yuan, W.Z., Li, Z., Wang, X. Integrated biorefinery approach to valorize winery waste: A review from waste to energy perspectives. *Science of the Total Environment.* **2020**, 719, 137315.

Alexander, S.P.H., Roberts, R.E., Broughton, B.R.S., Sobey, C.G., George, C.H., Stanford, S.C., Cirino, G., Docherty, J.R., Giembycz, M.A., Hoyer, D., Insel, P.A., Izzo, A.A., Ji, Y., MacEwan, D.J., Mangum, J., Wonnacott, S., Ahluwalia, A. Goals and Practicalities of Immunoblotting and Immunohistochemistry: A Guide for Submission to the British Journal of Pharmacology: Editorial. *British Journal of Pharmacology.* **2018**, 175, 407–411.

Ali, S. B., Perdawood, D., Abdulrahman, R., Al Farraj, D. A. and Alkubaisi, N.A. Vitamin D deficiency as a risk factor for urinary tract infection in women at reproductive age. *Saudi Journal of Biological Sciences.* **2020**, 27(11), 2942-2947.

Amayo, A., and Obara, W. Serum Prostate Specific Antigen Levels in Men with Benign Prostatic Hyperplasia and Cancer of the Prostate. *East African Medical Journal.* **2004**, 81, 22–26.

Andersen-Civil, A.I.S., Arora, P., Williams, A.R. Regulation of Enteric Infection and Immunity by Dietary Proanthocyanidins. *Frontiers in Immunology.* **2021**, 12, 637603.

Andriambeloson, E., Magnier, C., Haan-Archipoff, G., Lobstein, A., Anton, R., Beretz, A., Stoclet, J.C., Andriantsitohaina, R. Natural dietary polyphenolic compounds cause endothelium-dependent vasorelaxation in rat thoracic aorta. *Journal of Nutrition.* **1998**, 128(12), 2324-2333.

Andriole, G., Bruchovsky, N., Chung, L.W.K., Matsumoto, A.M., Rittmaster, R., Roehrborn, C., Russell, D., Tindall, D. Dihydrotestosterone and the prostate: the scientific rationale for 5α-reductase inhibitors in the treatment of benign prostatic hyperplasia. *Journal of Urology.* **2004**, 172, 1399–1403.

Appeldoorn, M.M., Vincken, J.P., Aura, A.M., Hollman, P.C., Gruppen, H. Procyanidin dimers are metabolized by human microbiota with 2-(3, 4-dihydroxyphenyl) acetic acid and 5-(3, 4-dihydroxyphenyl)-γ-valerolactone as the

major metabolites. *Journal of agricultural and food chemistry.* **2009**, 57(3), 1084-1092.

Arimboor, R., and Arumughan, C. Effect of polymerization on antioxidant and xanthine oxidase inhibitory potential of sea buckthorn (*H. rhamnoides*) proanthocyanidins. *Journal of Food Science.* **2012**, 77(10), C1036-C1041.

Aron, A.T., Gentry, E.C., McPhail, K.L., Nothias, L.-F., Nothias-Esposito, M., Bouslimani, A., Petras, D., Gauglitz, J.M., Sikora, N., Vargas, F., *et al*. Reproducible Molecular Networking of Untargeted Mass Spectrometry Data Using GNPS. *Nature Protocols.* **2020**, 15, 1954–1991.

Astudillo, A.M., Balgoma, D., Balboa, M.A., Balsinde, J. Dynamics of Arachidonic Acid Mobilization by Inflammatory Cells. Biochim. Biophys. *Acta—Molecular and Cell Biology of Lipids*. **2012**, 1821, 249–256.

Aydin, B., Leme-Kraus, A.A., Vidal, C.M.P., Aguiar, T.R., Phansalkar, R.S., Nam, J.-W., McAlpine, J.B., Chen, S.-N., Pauli, G.F., Bedran-Russo, A.K. Evidence to the Role of Interflavan Linkages and Galloylation of Proanthocyanidins at Sustaining Long-Term Dentin Biomodification. *Dental Materials.* **2019**, 35, 328–334.

Baba, S., Osakabe, N., Natsume, M., Terao, J. Absorption and urinary excretion of procyanidin B2 [epicatechin-(4β-8)-epicatechin] in rats. *Free Radical Biology and Medicine.* **2002**, 33(1), 142-148.

Bagchi, D., Swaroop, A., Preuss, H.G., Bagchi, M. Free Radical Scavenging, Antioxidant and Cancer Chemoprevention by Grape Seed Proanthocyanidin: An Overview. *Mutation Research.* **2014**, 768, 69–73.

Bandini, E., Wicht, K., Ampe, A., Baert, M., Eghbali, H., Lynen, F. Hyphenating Temperature Gradient Elution with Refractive Index Detection through Temperature-Responsive Liquid Chromatography. *Analytica Chimica Acta.* **2022**, 1231, 340441.

Barkin, J. Benign Prostatic Hyperplasia and Lower Urinary Tract Symptoms: Evidence and Approaches for Best Case Management. Canadian Journal of Urology. **2011**, 18(1), 14.

Baroi, A.M., Popitiu, M., Fierascu, I., Sărdărescu, I.-D., Fierascu, R.C. Grapevine Wastes: A Rich Source of Antioxidants and Other Biologically Active Compounds. *Antioxidants*. **2022**, 11, 393.

Baydar, N. G., Sagdic, O., Ozkan, G., Cetin, S. Determination of antibacterial effects and total phenolic contents of grape (Vitis vinifera L.) seed extracts. *International Journal of Food Science & Technology*. **2006**, 41(7), 799-804.

Bearelly, P., and Avellino, G.J. The Role of Benign Prostatic Hyperplasia Treatments in Ejaculatory Dysfunction. *Fertility and Sterility*. **2021**, 116, 611–617.

Beecher, G.R. Proanthocyanidins: Biological Activities Associated with Human Health. *Pharmaceutical Biology*. **2004**, 42, 2–20.

Begley, L.A.; Kasina, S.; MacDonald, J.; Macoska, J.A. The Inflammatory Microenvironment of the Aging Prostate Facilitates Cellular Proliferation and Hypertrophy. *Cytokine*. **2008**, 43, 194–199.

Belcaro, G., Ledda, A., Hu, S., Cesarone, M. R., Feragalli, B., Dugall, M. Grape seed procyanidins in pre- and mild hypertension: A registry study. *Evidence-based Complementary and Alternative Medicine* **2013**.

Beres, C., Costa, G.N.S., Cabezudo, I., da Silva-James, N.K., Teles, A.S.C., Cruz, A.P.G., Mellinger-Silva, C., Tonon, R.V., Cabral, L.M.C., Freitas, S.P. Towards integral utilization of grape pomace from winemaking process: A review. *Waste Management.* **2017**, 68, 581–594.

Bisha, B., Weinsetel, N., Brehm-Stecher, B.F., Mendonca, A. Antilisterial effects of gravinol-s grape seed extract at low levels in aqueous media and its potential application as a produce wash. *Journal of Food Protection.* **2010**, 73(2), 266-273.

Bittner, K., Kemme, T., Peters, K., Kersten, S., Danicke, S., Humpf, H.U. Systemic absorption and metabolism of dietary procyanidin B4 in pigs. *Molecular Nutrition and Food Research.* **2014**, 58(12), 2261-2273.

Bitzer, Z.T., Glisan, S.L., Dorenkott, M.R., Goodrich, K.M., Ye, L., O'Keefe, S.F., Lambert, J.D., Neilson, A. P. Cocoa procyanidins with different degrees of polymerization possess distinct activities in models of colonic inflammation. *Journal of Nutritional Biochemistry*. **2015**, 26(8), 827–831.

Blaak, E.E.; Canfora, E.E.; Theis, S.; Frost, G.; Groen, A.K.; Mithieux, G.; Nauta, A.; Scott, K.; Stahl, B.; van Harsselaar, J.; *et al.* Short Chain Fatty Acids in Human Gut and Metabolic Health. *Beneficial Microbes*. **2020**, 11, 411–455.

Borish, L.C., and Steinke, J.W. 2. Cytokines and Chemokines. *Journal of Allergy and Clinical Immunology*. **2003**, 111, S460–S475.

Bowser, S. M., Moore, W.T., McMillan, R.., Dorenkott, M. R., Goodrich, K.M., Ye, L., O'Keefe, S.F., Hulver, M.W., Neilson, A. P. High-molecular-weight cocoa procyanidins possess enhanced insulin-enhancing and insulin mimetic activities in human primary skeletal muscle cells compared to smaller procyanidins. *Journal of Nutritional Biochemistry*. **2017**, 39, 48–58.

Brannon, J.R., Dunigan, T.L., Beebout, C.J., Ross, T., Wiebe, M.A., Reynolds, W. S., Hadjifrangiskou, M. Invasion of vaginal epithelial cells by uropathogenic Escherichia coli. *Nature communications.* **2020**, 11(1), 1-11.

Briganti, A., Capitanio, U., Suardi, N., Gallina, A., Salonia, A., Bianchi, M., Tutolo, M., Di Girolamo, V., Guazzoni, G., Rigatti, P., *et al.* Benign Prostatic Hyperplasia and Its Aetiologies. *European Urology Supplements.* **2009**, 8, 865–871.

Busserolles, J., Gueux, E., Balasinska, B., Piriou, Y., Rock, E., Rayssiguier, Y., Mazur, A. *In Vivo* Antioxidant Activity of Procyanidin-Rich Extracts from Grape Seed and Pine (Pinus Maritima) Bark in Rats. *International Journal for Vitamin and Nutrition Research.* **2006**, 76, 22–27.

Byun, E.B., Ishikawa, T., Suyama, A., Kono, M., Nakashima, S., *et al.* A procyanidin trimer, C1, promotes NO production in rat aortic endothelial cells via both hyperpolarization and PI3K/Akt pathways. *European Journal of Pharmacology*. **2012**, 692(1-3), 52-60.

Cedo, L., Castell-Auví, A., Pallares, V., Blay, M., Ardevol, A., Pinent, M. Grape seed procyanidin extract improves insulin production but enhances Bax protein expression in cafeteria-treated male rats. *International Journal of Food Science*, **2013**.

Chedea, V.S., Braicu, C., Chirilă, F., Ober, C., Socaciu, C. Antibacterial action of an aqueous grape seed polyphenolic extract. *African Journal of Biotechnology*. **2011**, 10(33), 6276-6280.

Chen, L., Deng, H., Cui, H., Fang, J., Zuo, Z., Deng, J., Li, Y., Wang, X., Zhao, L. Inflammatory Responses and Inflammation- Associated Diseases in Organs. *Oncotarget.* **2018**, 9, 7204.

Chen, L., Sun, P., Wang, T., Chen, K.X., Jia, Q., *et al.* Diverse mechanisms of antidiabetic effects of the different procyanidin oligomer types of two different cinnamon species on db/db mice. *Journal of Agricultural and Food Chemistry*. **2012**, 60(36), 9144-9150.

Chen, Y., Robles, A.I., Martinez, L.A., Liu, F., Gimenez-Conti, I.B., Conti, C.J. Expression of G1 Cyclins, Cyclin-Dependent Kinases, and Cyclin-Dependent Kinase Inhibitors in Androgen-Induced Prostate Proliferation in Castrated Rats. *Cell Growth and Differentiation.* **1996**, 7, 1571–1578.

Chen, Y., Wang, J., Zou, L., Cao, H., Ni, X., Xiao, J. Dietary Proanthocyanidins on Gastrointestinal Health and the Interactions with Gut Microbiota. *Critical Reviews in Food Science and Nutrition.* **2022**, 1–24.

Chen, Y., Wen, J., Deng, Z., Pan, X., Xie, X., Peng, C. Effective utilization of food wastes: Bioactivity of grape seed extraction and its application in food industry. *Journal of Functional Foods*. **2020**, 73, 104113.

Chibelean, C.B., Petca, R.C., Mareș, C., Popescu, R.I., Enikő, B., Mehedințu, C., Petca, A. A Clinical Perspective on the Antimicrobial Resistance Spectrum of Uropathogens in a Romanian Male Population. *Microorganisms.* **2020**, 8(6), 848.

Choi, H.-M., Jung, Y., Park, J., Kim, H.-L., Youn, D.-H., Kang, J., Jeong, M.-Y., Lee, J.-H., Yang, W.M., Lee, S.-G., *et al.* Cinnamomi Cortex (Cinnamomum Verum) Suppresses Testosterone-Induced Benign Prostatic Hyperplasia by Regulating 5α-Reductase. *Scientific Reports.* **2016**, 6, 31906.

Cimolai, N., and Cimolai, T. The cranberry and the urinary tract. *European Journal of Clinical Microbiology and Infectious Diseases.* **2007**, 26(11), 767-776.

Cires, M.J., Navarrete, P., Pastene, E., Carrasco-Pozo, C., Valenzuela, R., Medina, D.A., Andriamihaja, M., Beaumont, M., Blachier, F., Gotteland, M. Effect of a Proanthocyanidin-Rich Polyphenol Extract from Avocado on the Production of Amino Acid-Derived Bacterial Metabolites and the Microbiota Composition in Rats Fed a High-Protein Diet. *Food and Function.* **2019**, 10, 4022–4035.

Cires, M.J., Wong, X., Carrasco-Pozo, C., Gotteland, M. The gastrointestinal tract as a key target organ for the health-promoting effects of dietary proanthocyanidins. *Frontiers in nutrition*. **2017**, 3, 57.

Cory, H., Passarelli, S., Szeto, J., Tamez, M., Mattei, J. The role of polyphenols in human health and food systems: A mini-review. *Frontiers in nutrition.* **2018**, 5, 87.

Csikós, E., Horváth, A., Ács, K., Papp, N., Balázs, V.L., Dolenc, M.S., Kenda, M., Kočevar Glavač, N., Nagy, M., Protti, M.; *et al.* Treatment of Benign Prostatic Hyperplasia by Natural Drugs. *Molecules.* **2021**, 26, 7141.

Cueva, C., Sanchez-Patan, F., Monagas, M., Walton, G.E., Gibson, G.R.,Martin-Alvarez, P.J., *et al. In vitro* fermentation of grape seed flavan-3-ol fractions by human faecal microbiota: changes in microbial groups and phenolic metabolites. *FEMS Microbiology Ecology*. **2013**, 83(3), 792-805.

Curtis, M.J., Bond, R.A., Spina, D., Ahluwalia, A., Alexander, S.P.A., Giembycz, M.A., Gilchrist, A., Hoyer, D., Insel, P.A., Izzo, A.A., *et al.* Experimental Design and Analysis and Their Reporting: New Guidance for Publication in BJP. *British Journal of Pharmacology.* **2015**, 172(14), 3461.

Das, K., and Buchholz, N. Benign prostate hyperplasia and nutrition. *Clinical nutrition ESPEN*. **2019**, 33, 5-11.

de Llano, D.G., Esteban-Fernández, A., Sánchez-Patán, F., Martín-Álvarez, P.J., Moreno-Arribas, M.V., Bartolomé, B. Anti-adhesive activity of cranberry phenolic compounds and their microbial-derived metabolites against uropathogenic Escherichia coli in bladder epithelial cell cultures. *International journal of molecular sciences*. **2015**, 16(6), 12119-12130.

de Souza, L.M., Cipriani, T.R., Iacomini, M., Gorin, P.A.J., Sassaki, G.L. HPLC/ESI-MS and NMR Analysis of Flavonoids and Tannins in Bioactive Extract from Leaves of *Maytenus ilicifolia*. *Journal of Pharmaceutical and Biomedical Analysis.* **2008**, 47, 59–67.

Deprez, S., Brezillon, C., Rabot, S., Philippe, C., Mila, I., Lapierre, C., Scalbert, A. Polymeric proanthocyanidins are catabolized by human colonic microflora into low-molecular weight phenolic acids. *The Journal of Nutrition.* **2000**, 130, 2733–2738.

Di Silverio, F., Gentile, V., De Matteis, A., Mariotti, G., Giuseppe, V., Antonio Luigi, P., Sciarra, A. Distribution of Inflammation, Pre-Malignant Lesions, Incidental Carcinoma in Histologically Confirmed Benign Prostatic Hyperplasia: A Retrospective Analysis. *European Urology.* **2003**, 43, 164–175.

Ding, Y., Zhang, Z., Dai, X., Jiang, Y., Bao, L., Li, Y., Li, Y. Grape seed proanthocyanidins ameliorate pancreatic beta-cell dysfunction and death in low-dose streptozotocin-and high-carbohydrate/high-fat diet-induced diabetic rats partially by regulating endoplasmic reticulum stress. *Nutrition and metabolism.* **2013**, 10(1), 1-12.

Dixon, R.A., Xie, D., Sharma, S.B. Proanthocyanidins—A Final Frontier in Flavonoid Research? *New Phytologist.* **2005**, 165, 9–28.

Djavan, B., Eckersberger, E., Espinosa, G., Kramer, G., Handisurya, A., Lee, C., Marberger, M., Lepor, H., Steiner, G.E. Complex Mechanisms in Prostatic Inflammatory Response. *European Urology Supplements.* **2009**, 8, 872–878.

Donovan, J.L., Lee, A., Manach, C., Rios, L., Morand, C., Scalbert, A., Rémésy, C. Procyanidins Are Not Bioavailable in Rats Fed a Single Meal Containing a Grapeseed Extract or the Procyanidin Dimer B3. *British Journal of Nutrition.* **2002**, 87, 299–306.

Dorenkott, M.R., Griffin, L.E., Goodrich, K.M., Thompson-Witrick, K.A., Fundaro, G., *et al.* Oligomeric cocoa procyanidins possess enhanced bioactivity compared to monomeric and polymeric cocoa procyanidins for preventing the development of obesity, insulin resistance, and impaired glucose tolerance during high-fat feeding. *Journal of Agricultural and Food Chemistry.* **2014**, 62(10), 2216-2227.

Draijer, R., de Graaf, Y., Slettenaar, M., de Groot, E., Wright, C.I. Consumption of a polyphenol-rich grape-wine extract lowers ambulatory blood pressure in mildly hypertensive subjects. *Nutrients.* **2015**, 7(5), 3138–3153.

Dwyer, K., Hosseinian, F., Rod, M.R. The market potential of grape waste alternatives. *Journal of Food Research.* **2014**, 3, 91–106.

Eleazu, C., Eleazu, K., Kalu, W. Management of Benign Prostatic Hyperplasia: Could Dietary Polyphenols Be an Alternative to Existing Therapies? *Frontiers in Pharmacology.* **2017**, 8, 234.

Elfakharany, W.A., Safwat, M.M., Essawy, A.S. Possible protective and curative effects of selenium nanoparticles on testosterone-induced benign prostatic hyperplasia rat model. *Folia Morphologica*. **2022**, 81(4), 942-955.

Elzanaty, S., Rezanezhad, B., Borgquist, R. Association between PSA Levels and Biomarkers of Subclinical Systemic Inflammation in Middle-Aged Healthy Men from the General Population. *Current Urology.* **2016**, 9, 148–152.

Enomoto, H., Takahashi, S., Takeda, S., Hatta, H. Distribution of Flavan-3-Ol Species in Ripe Strawberry Fruit Revealed by Matrix-Assisted Laser Desorption/Ionization-Mass Spectrometry Imaging. *Molecules* **2019**, 25, 103.

Epasinghe, D.J., Yiu, C.K.Y., Burrow, M.F., Hiraishi, N., Tay, F.R. The inhibitory effect of proanthocyanidin on soluble and collagen-bound proteases. *Journal of Dentistry.* **2013**, 41(9), 832-839.

Esposito, M., Nothias, L.-F., Retailleau, P., Costa, J., Roussi, F., Neyts, J., Leyssen, P., Touboul, D., Litaudon, M., Paolini, J. Isolation of Premyrsinane, Myrsinane, and Tigliane Diterpenoids from Euphorbia Pithyusa Using a Chikungunya Virus Cell-Based Assay and Analogue Annotation by Molecular Networking. *Journal of Natural Products.* **2017**, 80, 2051–2059.

Feldman, M., Tanabe, S., Howell, A., Grenier, D. Cranberry proanthocyanidins inhibit the adherence properties of Candida albicans and cytokine secretion by oral epithelial cells. *BMC Complementary and Alternative Medicine.* **2012**, 12(1), 1-12.

Ferreira, Y.A.M., Jamar, G., Estadella, D., Pisani, L.P. Proanthocyanidins in Grape Seeds and Their Role in Gut Microbiota-White Adipose Tissue Axis. *Food Chemistry*. **2023**, 404, 134405.

Fitzpatrick, D.F., Fleming, R.C., Bing, B., Maggi, D.A., O'Malley, R.M. Isolation and characterization of endothelium-dependent vasorelaxing compounds from grape seeds. *Journal of Agricultural and Food Chemistry.* **2000**, 48(12), 6384-6390.

Foo, L.Y., Lu, Y., Howell, A.B., Vorsa, N. A-type proanthocyanidin trimers from cranberry that inhibit adherence of uropathogenic P-fimbriated Escherichia coli. *Journal of Natural Products.* **2000**, 63(9), 1225-1228.

Forbes, A.M., Meier, G.P., Haendiges, S., Taylor, L.P. Structure–activity relationship studies of flavonol analogues on pollen germination. *Journal of Agricultural and Food Chemistry*. **2014**, 62(10), 2175-2181.

Forrester, S.J., Kikuchi, D.S., Hernandes, M.S., Xu, Q. Griendling, K.K. Reactive Oxygen Species in Metabolic and Inflammatory Signaling. *Circulation Research.* **2018**, 122, 877–902.

Gajdács, M., Ábrók, M., Lázár, A., Burián, K. Comparative Epidemiology and Resistance Trends of Common Urinary Pathogens in a Tertiary-Care Hospital: A 10-Year Surveillance Study. *Medicina (Lithuania).* **2019**, 55.

Ganesan, K., Quiles, J.L., Daglia, M., Xiao, J., Xu, B. Dietary Phytochemicals Modulate Intestinal Epithelial Barrier Dysfunction and Autoimmune Diseases. *Food Frontiers.* **2021**, 2, 357–382.

García-Conesa, M.T., Tribolo, S., Guyot, S., Tomás-Barberán, F.A., Kroon, P.A. Oligomeric procyanidins inhibit cell migration and modulate the expression of migration and proliferation associated genes in human umbilical vascular endothelial cells. *Molecular Nutrition and Food Research.* **2009**, 53(2), 266-276.

Garrido, M.D., Auqui, M., Martí, N., Linares, M.B. Effect of two different red grape pomace extracts obtained under different extraction systems on meat quality of pork burgers. *LWT Food Science and Technology.* **2011**, 44, 2238–2243.

Gentile, C., Allegra, M., Angileri, F., Pintaudi, A.M., Livrea, M.A., Tesoriere, L. Polymeric proanthocyanidins from Sicilian pistachio (Pistacia vera L.) nut extract inhibit lipopolysaccharide-induced inflammatory response in RAW 264.7 cells. *European Journal of Nutrition.* **2012**, 51, 353-363.

Gentile, C.L., and Weir, T.L. The Gut Microbiota at the Intersection of Diet and Human Health. *Science.* **2018**, 362, 776–780.

George, C.H., Stanford, S.C., Alexander, S., Cirino, G., Docherty, J.R., Giembycz, M.A., Hoyer, D., Insel, P.A., Izzo, A.A., Ji, Y., *et al.* Updating the Guidelines for Data Transparency in the British Journal of Pharmacology - Data Sharing and the Use of Scatter Plots Instead of Bar Charts. *British Journal of Pharmacology*. **2017**, 174(17), 2801.

Ghouila, Z., S. Laurent, S. Boutry, L. Vander Elst, F. Nateche, R.N. Muller, A. Baaliouamer. Antioxidant, antibacterial and cell toxicity effects of polyphenols *Fromahmeur bouamer* grape seed extracts. *Journal of Fundamental and Applied* Sciences. **2017**, 9(1), 392-420.

Girardot, M., Guerineau, A., Boudesocque, L., Costa, D., Bazinet, L., *et al.* Promising results of cranberry in the prevention of oral Candida biofilms. *Pathogens and Disease.* **2014**, 70(3), 432-439.

Gonthier, M.P., Donovan, J. L., Texier, O., Felgines, C., Remesy, C., Scalbert, A. Metabolism of dietary procyanidins in rats. *Free Radical Biology and Medicine*. **2003**, 35(8), 837–844.

Goodrich, K.M., Smithson, A.T., Ickes, A.K., Neilson, A.P. Pan-colonic pharmacokinetics of catechins and procyanidins in male Sprague–Dawley rats. *Journal of Nutritional Biochemistry*. **2015**, 26(10), 1007-1014.

Gu, L., Kelm, M.A., Hammerstone, J.F., Beecher, G., Holden, J., Haytowitz, D., Prior, R. L. Screening of foods containing proanthocyanidins and their structural characterization using LC-MS/MS and thiolytic degradation. *Journal of Agricultural and Food Chemistry*. **2003**, 51(25), 7513–7521.

Gu, L., Kelm, M.A., Hammerstone, J.F., Beecher, G., Holden, J., Haytowitz, D., Gebhardt, S., Prior, R.L. Concentrations of Proanthocyanidins in Common Foods and Estimations of Normal Consumption. *Journal of Nutrition.* **2004**, 134, 613–617.

Gupta, K., Chou, M. Y., Howell, A., Wobbe, C., Grady, R., Stapleton, A. E. Cranberry products inhibit adherence of p-fimbriated Escherichia coli to primary cultured bladder and vaginal epithelial cells. *Journal of Urology*. **2007**, 177(6), 2357-2360.

Haider, G., Zehra, N., Munir, A.A., Haider, A. Risk Factors of Urinary Tract Infection in Pregnancy. *Journal of the Pakistan Medical Association.* **2010**, 60, 213–216.

Hamid, A.R.A.H., Umbas, R., Mochtar, C.A. Recent Role of Inflammation in Prostate Diseases: Chemoprevention Development Opportunity. *Acta Medica Indonesiana.* **2011**, 43, 59–65.

Han, M., Song, P., Huang, C., Rezaei, A., Farrar, S., Brown, M.A., Ma, X. Dietary Grape Seed Proanthocyanidins (GSPs) Improve Weaned Intestinal Microbiota and Mucosal Barrier Using a Piglet Model. *Oncotarget*. **2016**, 7, 80313–80326.

Hellstrom, J. K., Torronen, A.R., Mattila, P.H. Proanthocyanidins in common food products of plant origin. *Journal of Agricultural and Food Chemistry.* **2009**, 57(17), 7899-7906.

Hemmersbach, S., Brauer, S.S., Huwel, S., Galla, H.J., Humpf, H.U. Transepithelial permeability studies of flavan-3-ol-C-glucosides and procyanidin dimers and trimers across the Caco-2 cell monolayer. *Journal of Agricultural and Food Chemistry*. **2013**, 61(33), 7932-7940.

Hernes, P.J., and Hedges, J.I. Determination of Condensed Tannin Monomers in Environmental Samples by Capillary Gas Chromatography of Acid Depolymerization Extracts. *Analytical Chemistry.* **2000**, 72, 5115–5124.

Holt, R.R., Lazarus, S.A., Sullards, M.C., Zhu, Q.Y., Schramm, D.D., Hammerstone, J.F., Fraga, C.G., Schmitz, H.H., Keen, C.L. Procyanidin Dimer B2 [Epicatechin-(4β-8)-Epicatechin] in Human Plasma after the Consumption of a Flavanol-Rich Cocoa. *American Journal of Clinical Nutrition.* **2002**, 76, 798–804.

Howell, A.B. Bioactive compounds in cranberries and their role in prevention of urinary tract infections. *Molecular Nutrition and Food Research.* **2007**, 51(6), 732-737.

Howell, A.B., Reed, J.D., Krueger, C.G., Winterbottom, R., Cunningham, D.G., Leahy M. A-type cranberry proanthocyanidins and uropathogenic bacterial anti-adhesion activity. *Phytochemistry*. **2005**, 66(18), 2281-2291.

Huang, Y., Chen, H., Zhou, X., Wu, X., Hu, E., Jiang, Z. Inhibition Effects of Chlorogenic Acid on Benign Prostatic Hyperplasia in Mice. *European Journal of Pharmacology*. **2017**, 809, 191–195.

Hummer, W., and Schreier, P. Analysis of Proanthocyanidins. *Molecular Nutrition and Food Research.* **2008**, 52, 1381–1398.

Iacob, S., Iacob, D.G., Luminos, L.M. Intestinal Microbiota as a Host Defense Mechanism to Infectious Threats. *Frontiers in Microbiology.* **2019**, 9, 3328.

Iannuzzo, F., Piccolo, V., Novellino, E., Schiano, E., Salviati, E., Summa, V., Campiglia, P., Tenore, G.C., Maisto, M. A Food-Grade Method for Enhancing the Levels of Low Molecular Weight Proanthocyanidins with Potentially High Intestinal Bioavailability. *Internation Journal of Molecular Science.* **2022**, 23, 13557.

Imran, I.B., Karonen, M., Salminen, J.-P., Engström, M.T. Modification of Natural Proanthocyanidin Oligomers and Polymers Via Chemical Oxidation under Alkaline Conditions. *ACS Omega.* **2021**, 6, 4726–4739.

Izumi, T., and Terauchi, M. The Diverse Efficacy of Food-Derived Proanthocyanidins for Middle-Aged and Elderly Women. *Nutrients.* **2020**, 12, 3833.

Jayaprakasha, G.K., Selvi, T., Sakariah, K.K. Antibacterial and antioxidant activities of grape (*Vitis vinifera*) seed extracts. *Food research international.* **2003**, 36(2), 117-122.

Jepson, R.G., Williams, G., Craig, J.C. Cranberries for preventing urinary tract infections. *Cochrane database of systematic reviews*. **2012**, 10.

Kalli, E., Lappa, I., Bouchagier, P., Tarantilis, P.A., Skotti, E. Novel application and industrial exploitation of winery by-products. *Journal of Bioresources and Bioproducts.* **2018**, 5, 46.

Karami, S., Rahimi, M., Babaei, A. An Overview on the Antioxidant, Anti-Inflammatory, Antimicrobial and Anti-Cancer Activity of Grape Extract. *Biomedical Research and Clinical Practice.* **2018**, 3, 1–4.

Kim, S.K., Seok, H., Park, H.J., Jeon, H.S., Kang, S.W., Lee, B.-C., Yi, J., Song, S.Y., Lee, S.H., Kim, Y.O., *et al.* Inhibitory Effect of Curcumin on Testosterone Induced Benign Prostatic Hyperplasia Rat Model. *BMC Complementary and Alternative Medicine.* **2015**, 15, 380.

Kim, Y., Choi, Y., Ham, H., Jeong, H.S., Lee J. Protective effects of oligomeric and polymeric procyanidin fractions from defatted grape seeds on tert-butyl hydroperoxide-induced oxidative damage in HepG2 cells. *Food Chemistry.* **2013**, 137(1-4), 136-141.

Koh, A., De Vadder, F., Kovatcheva-Datchary, P., Bäckhed, F. From Dietary Fiber to Host Physiology: Short-Chain Fatty Acids as Key Bacterial Metabolites. *Cell.* **2016**, 165, 1332–1345.

Koo, H., Duarte, S., Murata, R.M., Scott-Anne, K., Gregoire, S., *et al.* Influence of cranberry proanthocyanidins on formation of biofilms by Streptococcus mutans on saliva-coated apatitic surface and on dental caries development *in vivo. Caries Research.* **2010**, 44(2), 116-126.

Koutsos, A., M. Lima, L. Conterno, M. Gasperotti, M. Bianchi, F. Fava, U. Vrhovsek, J.A. Lovegrove, K.M. Tuohy. Effects of commercial apple varieties on human gut microbiota composition and metabolic output using an in vitro colonic model. *Nutrients.* **2017**, 9(6), 533.

Krenn, L., Steitz, M., Schlicht, C., Kurth, H., Gaedcke, F. Anthocyanin-and proanthocyanidin-rich extracts of berries in food supplements–analysis with problems. Die Pharmazie-An *International Journal of Pharmaceutical Sciences.* **2007**, 62(11), 803-812.

Kumar Singh, A., Cabral, C., Kumar, R., Ganguly, R., Kumar Rana, H., Gupta, A., Rosaria Lauro, M., Carbone, C., Reis, F., Pandey, A.K. Beneficial Effects of Dietary Polyphenols on Gut Microbiota and Strategies to Improve Delivery Efficiency. *Nutrients.* **2019**, 11, 2216.

Langan, R.C. Benign Prostatic Hyperplasia. *Primary Care: Clinics in Office Practice.* **2019**, 46, 223–232.

Laparra, J.M., and Sanz, Y. Interactions of gut microbiota with functional food components and nutraceuticals. *Pharmacological Research.* **2010**, 61(3), 219-225.

Lee, Y.A., Kim, Y.J., Cho, E.J., Yokozawa, T. Ameliorative effects of proanthocyanidin on oxidative stress and inflammation in streptozotocin-induced diabetic rats. *Journal of Agricultural and Food Chemistry.* **2007**, 55(23), 9395-9400.

Leeuwendaal, N.K., Stanton, C., O'Toole, P.W., Beresford, T.P. Fermented Foods, Health and the Gut Microbiome. *Nutrients.* **2022**, 14, 1527.

Lei, Y., Liu, D., Ren, X., Chen, J. Potential of Grape Seed-Derived Polyphenols Extract for Protection against Testosterone-Induced Benign Prostatic Hyperplasia in Castrated Rats. *RSC Advances.* **2014a**, 4, 62996–63004.

Lei, Y., Ren, X., Chen, J., Liu, D., Ruan, J. Protective Effects of Grape Seed-Derived Procyanidin Extract against Carrageenan-Induced Abacterial Prostatitis in Rats. *Journal of Functional Foods*. **2014b**, 7, 416–424

Levitt, J.M., and Slawin, K.M. Prostate-Specific Antigen and Prostate-Specific Antigen Derivatives as Predictors of Benign Prostatic Hyperplasia Progression. *Current Urology Report.* **2007**, 8, 269–274.

Li, J., Tian, Y., Guo, S., Gu, H., Yuan, Q., Xie, X. Testosterone-Induced Benign Prostatic Hyperplasia Rat and Dog as Facile Models to Assess Drugs Targeting Lower Urinary Tract Symptoms. *PLOS ONE.* **2018**, 13, e0191469.

Li, S., Xiao, J., Chen, L., Hu, C., Chen, P., Xie, B., Sun, Z. Identification of Aseries oligomeric procyanidins from pericarp of *Litchi chinensis* by FT-ICR-MS and LC-MS. *Food Chemistry.* **2012**, 135(1), 31–38.

Li, X., Sui, Y., Li, S., Xie, B., Sun, Z. A-type procyanidins from litchi pericarp ameliorate hyperglycaemia by regulating hepatic and muscle glucose metabolism in streptozotocin (STZ)-induced diabetic mice fed with high fat diet. *Journal of Functional Foods*. **2016**, 27, 711–722.

Liang, N.-N., He, F., Pan, Q.-H., Wang, J., Reeves, M.J., Duan, C.-Q. Optimization of Sample Preparation and Phloroglucinol Analysis of Marselan Grape Skin Proanthocyanidins Using HPLC-DADESI- MS/MS. *South African Journal of Enology and Viticulture.* **2016**, 33, 122–131.

Lin, L.-Z., Sun, J., Chen, P., Monagas, M.J., Harnly, J.M. UHPLC-PDA-ESI/HRMS n Profiling Method to Identify and Quantify Oligomeric Proanthocyanidins in Plant Products. *Journal of Agricultural and Food Chemistry.* **2014**, 62, 9387–9400.

Liu, H., Zou, T., Gao, J., Gu, L. Depolymerization of Cranberry Procyanidins Using (+)-Catechin, (-)-Epicatechin, and (-)- Epigallocatechin Gallate as Chain Breakers. *Food Chemistry*. **2013**, 141, 488–494.

Lizarraga, D., Lozano, C., Briedé, J.J., van Delft, J.H., Touriño, S., Centelles, J.J., Torres, J.L., Cascante, M. The importance of polymerization and galloylation for the antiproliferative properties of procyanidin-rich natural extracts. *FEBS Journal*. **2007**, 274(18), 4802-4811.

Lotito, S.B., Actis-Goretta, L., Renart, M.L., Caligiuri, M., Rein, D., Schmitz, H.H., Steinberg, F.M., Keen, C.L., Fraga, C.G. Influence of oligomer chain length on the antioxidant activity of procyanidins. *Biochemical and Biophysical Research Communications*. **2000**, 276(3), 945–951.

Luca, S.V., Bujor, A., Miron, A., Aprotosoaie, A.C., Skalicka-Wozniak, K., Trifan, A. Preparative Separation and Bioactivity of Oligomeric Proanthocyanidins. *Phytochemistry Reviews.* **2020**, 19, 1093–1140.

Ma, X., Wang, R., Yu, S., Lu, G., Yu, Y., Jiang, C. Anti-Inflammatory Activity of Oligomeric Proanthocyanidins Via Inhibition of NF-KB and MAPK in LPS-Stimulated MAC-T Cells. *Journal of Microbiology and Biotechnology.* **2020**, 30, 1458–1466.

Maisto, M., Annunziata, G., Schiano, E., Piccolo, V., Iannuzzo, F., Santangelo, R., Ciampaglia, R., Tenore, G.C., Novellino, E., Grieco, P. Potential Functional Snacks: Date Fruit Bars Supplemented by Different Species of Lactobacillus spp. *Foods.* **2021**, 10, 1760.

Maisto, M., Piccolo, V., Novellino, E., Schiano, E., Iannuzzo, F., Ciampaglia, R., Summa, V., Tenore, G.C. Optimization of Phlorizin Extraction from Annurca Apple Tree Leaves Using Response Surface Methodology. *Antioxidants*. **2022a**, 11, 1933.

Maisto, M., Schiano, E., Novellino, E., Piccolo, V., Iannuzzo, F., Salviati, E., Summa, V., Annunziata, G., Tenore, G.C. Application of a Rapid and Simple Technological Process to Increase Levels and Bioccessibility of Free Phenolic Compounds in Annurca Apple Nutraceutical Product. *Foods*. **2022b**, 11, 1453.

Mansoor, K.A., Matalka, K.Z., Qdan, F.S., Awad, R., Schmidt, M. Two New Proanthocyanidin Trimers Isolated from *Cistus incanus* L. Demonstrate Potent Anti-Inflammatory Activity and Selectivity to Cyclooxygenase Isoenzymes Inhibition. *Natural Product Research.* **2016**, 30, 1919–1926.

Mao, J. T., Lu, Q. Y., Xue, B., Neis, P., Zamora, F.D., Lundmark, L., Qualls, C., Massie, L. A pilot study of a grape seed procyanidin extract for lung cancer chemoprevention. *Cancer Prevention Research.* **2019**, 12(8), 557–565.

Mao, T., Powell, J., Van de Water, J., Keen, C., Schmitz, H., Gershwin, M. Effect of cocoa procyanidins on the secretion of interleukin-4 in peripheral blood mononuclear cells. *Journal of Medicinal Food.* **2000**, 3(2), 107-114.

Martinez, J.J., Mulvey, M.A., Schilling, J.D., Pinkner, J.S, Hultgren, S.J. Type 1 pilus-mediated bacterial invasion of bladder epithelial cells. *EMBO Journal.* **2000**, 19, 2803–2812.

Masumoto, S., Terao, A., Yamamoto, Y., Mukai, T., Miura, T., Shoji, T. Nonabsorbable apple procyanidins prevent obesity associated with gut microbial and metabolomic changes. *Scientific Reports.* **2016**, 6(1), 1-10.

Meeran, S.M., and Katiyar, S.K. Grape Seed Proanthocyanidins Promote Apoptosis in Human Epidermoid Carcinoma A431 Cells through Alterations in Cdki-Cdk-Cyclin Cascade, and Caspase-3 Activation via Loss of Mitochondrial Membrane Potential. *Experimental Dermatology.* **2007**, 16, 405–415.

Mirone, V., Fusco, F., Verze, P., Schulman, C., Debruyne, F., Imbimbo, C. Androgens and Benign Prostatic Hyperplasia. *European Urology Supplements.* **2006**, 5, 410–417.

Mitsunari, K., Miyata, Y., Matsuo, T., Mukae, Y., Otsubo, A., Harada, J., Kondo, T., Matsuda, T., Ohba, K., Sakai, H. Pharmacological Effects and Potential Clinical Usefulness of Polyphenols in Benign Prostatic Hyperplasia. *Molecules.* **2021**, 26, 450.

Mizuno, M., Nakanishi, I., Matsubayashi, S., Imai, K., Arai, T., Matsumoto, K.I., Fukuhara, K. Synthesis and antioxidant activity of a procyanidin B3 analogue. *Bioorganic & medicinal chemistry letters.* **2007**, 27(4), 1041-1044.

Mohsenpour, B., Ahmadi, A., Baneh, A.M., Hajibagheri, K., Ghaderi, E., Afrasiabian, S., Azizi, S. Relation between serum zinc levels and recurrent urinary tract infections in female patients: A case-control study. *Medical Journal of the Islamic Republic of Iran.* **2019**, 33, 33.

Monagas, M., Quintanilla-López, J.E., Gómez-Cordovés, C., Bartolomé, B., Lebrón-Aguilar, R. MALDI-TOF MS Analysis of Plant Proanthocyanidins. *Journal of Pharmaceutical and Biomedical Analysis.* **2010a**, 51, 358–372.

Monagas, M., Urpi-Sarda, M., Sánchez-Patán, F., Llorach, R., Garrido, I., Gómez-Cordovés, C., Andres-Lacueva, C., Bartolomé, B. Insights into the Metabolism and Microbial Biotransformation of Dietary Flavan-3-Ols and the Bioactivity of Their Metabolites. *Food and Function.* **2010b**, 1, 233–253.

Mosmann, T. Rapid colorimetric assay for cellular growth and survival: application to proliferation and cytotoxicity assays. *Journal of Immunological Methods*. **1983**, 65(1-2), 55-63.

Musto, G., Laurenzi, V., Annunziata, G., Novellino, E., Stornaiuolo, M. Genotoxic Assessment of Nutraceuticals Obtained from Agricultural Biowaste: Where Do We "AMES"?. *Antioxidants*. **2022**, 11, 1197

Nahata, A., and Dixit, V.K. Ameliorative Effects of Stinging Nettle (Urtica Dioica) on Testosterone-Induced Prostatic Hyperplasia in Rats: Urtica Dioica Attenuates Prostatic Hyperplasia. *Andrologia.* **2012**, 44, 396–409.

Navajas-Porras, B., Pérez-Burillo, S., Hinojosa-Nogueira, D., Douros, K., Pastoriza, S., Rufián-Henares, J.Á. The Gut Microbiota of Obese Children Releases Lower Antioxidant Capacity from Food than That of Lean Children. *Nutrients.* **2022a**, 14, 2829.

Navajas-Porras, B., Pérez-Burillo, S., Hinojosa-Nogueira, D., Douros, K., Pastoriza, S., Rufián-Henares, J.Á. The Intake of Antioxidant Capacity of Children Depends on Their Health Status. *Nutrients.* **2022b**, 14, 3965.

Nicolosi, D., Tempera, G., Genovese, C., Furneri, P.M. Anti-Adhesion Activity of A2-Type Proanthocyanidins (a Cranberry Major Component) on Uropathogenic *E. Coli* and *P. Mirabilis Strains*. *Antibiotics.* **2014**, 3, 143–154.

Nie, Y., and Stürzenbaum, S.R. Proanthocyanidins of Natural Origin: Molecular Mechanisms and Implications for Lipid Disorder and Aging-Associated Diseases. *Advances in Nutrition.* **2019**, 10, 464–478.

Nunes, C., Figueiredo, R., Laranjinha, J., da Silva, G.J. Intestinal Cytotoxicity Induced by Escherichia Coli Is Fully Prevented by Red Wine Polyphenol Extract: Mechanistic Insights in Epithelial Cells. *Chemico-Biological Interactions.* **2019**, 310, 108711.

Nunes, M.A., Pimentel, F., Costa, A.S.G., Alves, R.C., Oliveira, M.B.P.P. Cardioprotective Properties of Grape Seed Proanthocyanidins: An Update. *Trends in Food Science and Technology.* **2016**, 57, 31–39.

Oelke, M., and Martinelli, E. Medikamentöse Therapie des benignen Prostatasyndroms. *Urologe.* **2016**, 55, 81–96.

Okudan, N., Barışkaner, H., Gökbel, H., şahin, A. S., Belviranlı, M., Baysal, H. The effect of supplementation of grape seed proanthocyanidin extract on vascular dysfunction in experimental diabetes. *Journal of Medicinal Food.* **2011**, 14(11), 1298-1302.

Olivas, A., and Price, R.S. Obesity, Inflammation, and Advanced Prostate Cancer. *Nutrition and Cancer*. **2021**, 73, 2232–2248.

Ottaviani, J.I., Kwik-Uribe, C., Keen, C.L., Schroeter, H. Intake of dietary procyanidins does not contribute to the pool of circulating flavanols in humans. *American Journal of Clinical Nutrition.* **2012**, 95(4), 851-858.

Ou, K., and Gu, L. Absorption and Metabolism of Proanthocyanidins. *Journal of Functional Foods*. **2014**, 7, 43–53.

Pandey, K.B., and Rizvi, S.I. Plant polyphenols as dietary antioxidants in human health and disease. *Oxidative Medicine and Cellular Longevity.* **2009**, 2(5), 270-278.

Parkar, S.G., Trower, T.M., Stevenson, D.E. Fecal Microbial Metabolism of Polyphenols and Its Effects on Human Gut Microbiota. *Anaerobe.* **2013**, 23, 12–19.

Patel, S. Rose hip as an underutilized functional food: Evidence-based review. *Trends in Food Science & Technology.* **2017**, 63, 29-38.

Pejčić, T., Tosti, T., Džamić, Z., Gašić, U., Vuksanović, A., Dolićanin, Z., Tešić, Ž. The Polyphenols as Potential Agents in Prevention and Therapy of Prostate Diseases. *Molecules*. **2019**, 24, 3982.

Pejčić, T., Tosti, T., Tešić, Ž., Milković, B., Dragičević, D., Kozomara, M., Čekerevac, M., Džamić, Z. Testosterone and Dihydrotestosterone Levels in the Transition Zone Correlate with Prostate Volume. *Prostate.* **2017**, 77, 1082–1092.

Pereira-Caro, G., Gaillet, S., Ordóñez, J.L., Mena, P., Bresciani, L., Bindon, K.A., Del Rio, D., Rouanet, J.-M., Moreno-Rojas, J.M., Crozier, A. Bioavailability of Red

Wine and Grape Seed Proanthocyanidins in Rats. *Food and Function.* **2020**, 11, 3986–4001.

Pérez-Burillo, S., Rufián-Henares, J.A., Pastoriza, S. Towards an Improved Global Antioxidant Response Method (GAR+): Physiological-Resembling *in Vitro* Digestion-Fermentation Method. *Food Chemistry*. **2018**, 239, 1253–1262.

Petca, R.C., Negoiță, S., Mareș, C., Petca, A., Popescu, R.I., Chibelean, C.B. Heterogeneity of Antibiotics Multidrug-Resistance Profile of Uropathogens in Romanian Population. *Antibiotics*. **2021**, 10(5), 523.

Porter, L.J., Hrstich, L.N., Chan, B.G. The conversion of procyanidins and prodelphinidins to cyanidin and delphinidin. *Phytochemistry*. **1986**, 25, 223-230.

Prasad, K.N., and Bondy, S.C. Dietary Fibers and Their Fermented Short-Chain Fatty Acids in Prevention of Human Diseases. *Bioactive Carbohydrates and Dietary Fibre*. **2019**, 17, 100170.

Qin, Y., Che, F., Li, J., Hu, B. Analysis of content of proanthocyanidin from featured fruit of Xinjiang. *Xinjiang Agricultural Sciences*. **2009**, 46(3), 484-487.

Raina, K., Singh, R.P., Agarwal, R., Agarwal, C. Oral Grape Seed Extract Inhibits Prostate Tumor Growth and Progression in TRAMP Mice. *Cancer Research*. **2007**, 67, 5976–5982.

Rauf, A., Imran, M., Abu-Izneid, T., Iahtisham-Ul-Haq, Patel, S., Pan, X., Naz, S., Sanches Silva, A., Saeed, F., Rasul Suleria, H.A. Proanthocyanidins: A Comprehensive Review. *Biomedicine & Pharmacotherapy* **2019**, 116, 108999.

Ravindranathan, P., Pasham, D., Balaji, U., Cardenas, J., Gu, J., Toden, S., Goel, A. Mechanistic insights into anticancer properties of oligomeric proanthocyanidins from grape seeds in colorectal cancer. *Carcinogenesis.* **2018**, 39(6), 767-777.

Re, R., Pellegrini, N., Proteggente, A., Pannala, A., Yang, M., Rice-Evans, C. Antioxidant Activity Applying an Improved ABTS Radical Cation Decolorization Assay. *Free Radical Biology and Medicine.* **1999**, 26, 1231–1237.

Rigaud, J., Escribanobailon, M.T., Prieur, C., Souquet, J.M., Cheynier, V. Normal-phase high performance liquid-chromatographic separation of procyanidins from cacao beans and grape seeds. *Journal of Chromatography A.* **1993**, 654, 255-260.

Rios, L.Y., Gonthier, M.P., Rémésy, C., Mila, I., Lapierre, C., Lazarus, S.A., *et al.* Chocolate intake increases urinary excretion of polyphenol-derived phenolic acids in healthy human subjects. *American Journal of Clinical Nutrition.* **2003**, 77(4), 912-918.

Rockenbach, I.I., Jungfer, E., Ritter, C., Santiago-Schübel, B., Thiele, B., Fett, R., Galensa, R. Characterization of Flavan-3-Ols in Seeds of Grape Pomace by CE, HPLC-DAD-MSn and LC-ESI-FTICR-MS. *Food Research International.* **2012**, 48, 848–855.

Rodríguez-Daza, M.C., Pulido-Mateos, E.C., Lupien-Meilleur, J., Guyonnet, D., Desjardins, Y., Roy, D. Polyphenol-Mediated Gut Microbiota Modulation: Toward Prebiotics and Further. *Frontiers in Nutrition.* **2021**, 8, 689456.

Rodríguez-Pérez, C., García-Villanova, B., Guerra-Hernández, E., Verardo, V. Grape Seeds Proanthocyanidins: An Overview of *In Vivo* Bioactivity in Animal Models. *Nutrients*. **2019**, 11, 2435.

Roehrborn, C.G. Male Lower Urinary Tract Symptoms (LUTS) and Benign Prostatic Hyperplasia (BPH). *Medical Clinics of North America.* **2011**, 95, 87–100.

Roehrborn, C.G., Boyle, P., Nickel, J.C., Hoefner, K., Andriole, G. Efficacy and Safety of a Dual Inhibitor of 5-Alpha-Reductase Types 1 and 2 (Dutasteride) in Men with Benign Prostatic Hyperplasia. *Urology*. **2002**, 60, 434–441.

Rossi, M., Edefonti, V., Parpinel, M., Lagiou, P., Franchi, M., Ferraroni, M., Decarli, A., Zucchetto, A., Serraino, D., Dal Maso, L., Negri, E., La Vecchia, C. Proanthocyanidins and other flavonoids in relation to endometrial cancer risk: A case-control study in Italy. *British Journal of Cancer.* **2013**, 109(7), 1914–1920.

Rue, E.A., Rush, M.D., van Breemen, R.B. Procyanidins: A Comprehensive Review Encompassing Structure Elucidation via Mass Spectrometry. *Phytochemistry Reviews.* **2018**, 17, 1–16.

Rush, M.D., Rue, E.A., Wong, A., Kowalski, P., Glinski, J.A., van Breemen, R.B. Rapid Determination of Procyanidins Using MALDI-ToF/ToF Mass Spectrometry. *Journal of Agricultural and Food Chemistry*. **2018**, 66, 11355–11361.

Russell, W.R., Hoyles, L., Flint, H.J., Dumas, M.E. Colonic bacterial metabolites and human health. *Current Opinion in Microbiology.* **2013**, 16(3), 246-254.

Salvadó, M.J., Casanova, E., Fernández-Iglesias, A., Arola, L., Bladé, C. Roles of proanthocyanidin rich extracts in obesity. Food and function. 2015, 6(4), 1053-1071.

Samuelsson, B., Rouzer, C.A., Matsumoto, T. Human Leukocyte 5-Lipoxygenase: An Enzyme Possessing Dual Enzymatic Activities and a Multicomponent Regulatory System. *Advances in Prostaglandin, Thromboxane, and Leukotriene Research*. **1987**, 17, 1–11.

Sánchez-Velázquez, O.A., Mulero, M., Cuevas-Rodríguez, E.O., Mondor, M., Arcand, Y., Hernández-Álvarez, A.J. *In Vitro* Gastrointestinal Digestion Impact on Stability, Bioaccessibility and Antioxidant Activity of Polyphenols from Wild and Commercial Blackberries (*Rubus* Spp.). *Food and Function.* **2021**, 12, 7358–7378.

Sano, A., Yamakoshi, J., Tokutake, S., Tobe, K., Kubota, Y., Kikuchi, M. Procyanidin B1 is detected in human serum after intake of proanthocyanidin-rich grape seed extract. *Bioscience, Biotechnology, and Biochemistry*. **2003**, 67(5), 1140-1143.

Santos-Buelga, C., Francia-Aricha, E.M., Escribano-Bailon, M.T., Comparative flavan-3-ol composition of seeds from different grape varieties. *Food Chemistry.* **1995**, 53, 197-201.

Sarma, A.V., and Wei, J.T. Benign Prostatic Hyperplasia and Lower Urinary Tract Symptoms. *New England Journal of Medicine*. **2012**, 367, 248–257.

Saviano, A., Raucci, F., Casillo, G.M., Mansour, A.A., Piccolo, V.; Montesano, C., Smimmo, M., Vellecco, V., Capasso, G., Boscaino, A., *et al.* Anti-Inflammatory and Immunomodulatory Activity of Mangifera Indica L. Reveals the Modulation of COX-2/MPGES-1 Axis and Th17/Treg Ratio. *Pharmacological Research*. **2022**, 182, 106283.

Saylor, P.J., Kozak, K.R., Smith, M.R., Ancukiewicz, M.A., Efstathiou, J.A., Zietman, A.L., Jain, R.K., Duda, D.G. Changes in Biomarkers of Inflammation and Angiogenesis During Androgen Deprivation Therapy for Prostate Cancer. *Oncologist.* **2012**, 17, 212–219.

Schiano, E., Maisto, M., Piccolo, V., Novellino, E., Annunziata, G., Ciampaglia, R., Montesano, C., Croce, M., Caruso, G., Iannuzzo, F., *et al.* Beneficial Contribution to Glucose Homeostasis by an Agro-FoodWaste Product Rich in Abscisic Acid: Results from a Randomized Controlled Trial. *Foods.* **2022a**, 11, 2637.

Schiano, E., Piccolo, V., Novellino, E., Maisto, M., Iannuzzo, F., Summa, V., Tenore, G.C. Thinned Nectarines, an Agro-Food Waste with Antidiabetic Potential: HPLC-HESI-MS/MS Phenolic Characterization and *In Vitro* Evaluation of Their Beneficial Activities. *Foods*. **2022b**, 11, 1010.

Schilling, J.D., Mulvey, M.A., Vincent, C.D., Lorenz, R.G., Hultgren, S.J. Bacterial invasion augments epithelial cytokine responses to Escherichia coli through a lipopolysaccharide-dependent mechanism. *Journal of Immunology*. **2001**, 166(2), 1148-1155.

Schmidt, B.M., Howell, A.B., McEniry, B., Knight, C.T., Seigler, D., Erdman, J.W. Jr, Lila, M.A. Effective separation of potent antiproliferation and antiadhesion components from wild blueberry (*Vaccinium angustifolium* Ait.) fruits. *Journal of Agricultural and Food Chemistry.* **2004**, 52(21), 6433-6442.

Selma, M.V., Espín, J.C., Tomás-Barberán, F.A. Interaction between phenolics and gut microbiota: role in human health. *Journal of Agricultural and Food Chemistry.* **2009**, 57(15), 6485-6501.

Serra, A., Macià, A., Romero, M.-P., Valls, J., Bladé, C., Arola, L., Motilva, M.-J. Bioavailability of Procyanidin Dimers and Trimers and Matrix Food Effects *in Vitro* and *in Vivo* Models. *British Journal of Nutrition.* **2010**, 103, 944–952.

Sharifi-Rad, M., Tayeboon, G.S., Miri, A., Sharifi-Rad, M., Setzer, W.N., Fallah, F., Kuhestani, K., Tahanzadeh, N., Sharifi-Rad, J. Mutagenic, Antimutagenic, Antioxidant, Anti-Lipoxygenase and Antimicrobial Activities of *Scandix Pecten-veneris* L. *Molecular and Cellular Biology.* **2016**, 62, 8–16.

Shi, J., Yu, J., Pohorly, J.E., Kakuda, Y. Polyphenolics in grape seeds-biochemistry and functionality. *Journal of Medicinal Food.* **2003**, 6(4), 291-299.

Shoji, T., Masumoto, S., Moriichi, N., Akiyama, H., Kanda, T., Ohtake, Y., Goda, Y. Apple procyanidin oligomers absorption in rats after oral administration: Analysis of procyanidins in plasma using the porter method and high-performance liquid chromatography/tandem mass spectrometry. *Journal of Agricultural and Food Chemistry.* **2006**, 54(3), 884–892.

Shoji, T., Masumoto, S., Moriichi, N., Kobori, M., Kanda, T., Shinmoto, H., Tsushida, T. Procyanidin trimers to pentamers fractionated from apple inhibit melanogenesis in B16 mouse melanoma cells. *Journal of Agricultural and Food Chemistry.* **2005**, 53(15), 6105–6111.

Shrestha, S.P., Thompson, J.A., Wempe, M.F., Gu, M., Agarwal, R., Agarwal, C. Glucuronidation and methylation of procyanidin dimers b2 and 3,3''-si-o-galloyl-b2 and corresponding monomers epicatechin and 3-o-galloyl-epicatechin in mouse liver. *Pharmaceutical Research.* **2012**, 29, 856-865.

Sies, H., Schewe, T., Heiss, C., Kelm, M. Cocoa Polyphenols and Inflammatory Mediators. *American Journal of Clinical Nutrition.* **2005**, 81, 304S–312S.

Singh, A., Kumar, S., Kumar, B. LC-MS Identification of Proanthocyanidins in Bark and Fruit of Six Terminalia Species. *Natural Product Communications.* **2018**, 13, 555–560.

Skrypnik, K., and Suliburska, J. Association between the Gut Microbiota and Mineral Metabolism: Gut Microbiota and Mineral Metabolism. *Journal of the Science of Food and Agriculture*. **2018**, 98, 2449–2460.

Smeriglio, A., Barreca, D., Bellocco, E., Trombetta, D. Proanthocyanidins and Hydrolysable Tannins: Occurrence, Dietary Intake and Pharmacological Effects: Pharmacological Aspects of Tannins. *British Journal of Pharmacology*. **2017**, 174, 1244–1262.

Spencer, J.P., Schroeter, H., Shenoy, B., Srai, S.K., Debnam, E.S., Rice-Evans, C. Epicatechin is the primary bioavailable form of the procyanidin dimers B2 and B5 after transfer across the small intestine. *Biochemical and Biophysical Research Communications.* **2001**, 285(3), 588-593.

Stoupi, S., Williamson, G., Viton, F., Barron, D., King, L.J., Brown, J.E., Clifford, M.N. *In vivo* bioavailability, absorption, excretion, and pharmacokinetics of [14C] procyanidin B2 in male rats. *Drug Metabolism and Disposition.* **2010**, 38(2), 287-291.

Sugiyama, H., Akazome, Y., Shoji, T., Yamaguchi, A., Yasue, M., Kanda, T., Ohtake, Y. Oligomeric procyanidins in apple polyphenol are main active components for inhibition of pancreatic lipase and triglyceride absorption. *Journal of Agricultural and Food Chemistry*. **2007**, 55(11), 4604–4609.

Šukovic, D., Kneževic, B., Gašic, U., Sredojevic, M., Ciric, I., Todic, S., Mutic, J., Tešic, Ž. Phenolic Profiles of Leaves, Grapes and Wine of Grapevine Variety Vranac (*Vitis vinifera* L.) from Montenegro. *Foods.* **2020**, 9, 138.

Tao, W., Zhang, Y., Shen, X., Cao, Y., Shi, J., Ye, X., Chen, S. Rethinking the Mechanism of the Health Benefits of Proanthocyanidins: Absorption, Metabolism,

and Interaction with Gut Microbiota. *Comprehensive Reviews in Food Science and Food Safety.* **2019**, 18, 971–985.

Tatsuno, T., Jinno, M., Arima, Y., Kawabata, T., Hasegawa, T., *et al.* Anti-inflammatory and anti-melanogenic proanthocyanidin oligomers from peanut skin. *Biological and Pharmaceutical Bulletin.* **2012**, 35(6), 909-916.

Taubert, D., Berkels, R., Klaus, W., Roesen, R. Nitric oxide formation and corresponding relaxation of porcine coronary arteries induced by plant phenols: essential structural features. *Journal of Cardiovascular Pharmacology*. **2002**, 40(5), 701-713.

Tebib, K., Besançon, P., Rouanet, J.M. Dietary grape seed tannins affect lipoproteins, lipoprotein lipases and tissue lipids in rats fed hypercholesterolemic diets. *Journal of Nutrition.* **1994**, 124(12), 2451-2457.

Terrapon, N., and Henrissat, B. How Do Gut Microbes Break down Dietary Fiber? *Trends in Biochemical Sciences* **2014**, 39, 156–158.

Thursby, E., and Juge, N. Introduction to the Human Gut Microbiota. *Biochemical Journal.* **2017**, 474, 1823–1836.

Tomas-Barberán, F.A., Cienfuegos-Jovellanos, E., Marín, A., Muguerza, B., Gil-Izquierdo, A., Cerdá, B., Zafrilla, P., Morillas, J., Mulero, J., Ibarra, A. A New Process to Develop a Cocoa Powder with Higher Flavonoid Monomer Content and Enhanced Bioavailability in Healthy Humans. *Journal of Agricultural and Food Chemistry.* **2007**, 55, 3926–3935.

Tong, Y., and Zhou, R. Review of the Roles and Interaction of Androgen and Inflammation in Benign Prostatic Hyperplasia. *Mediators of Inflammation*. **2020**, 1–7.

Tzounis, X., Vulevic, J., Kuhnle, G.G.C., George, T., Leonczak, J., Gibson, G.R., Kwik-Uribe, C., Spencer, J.P.E. Flavanol Monomer-Induced Changes to the Human Faecal Microflora. *British Journal of Nutrition.* **2008**, 99, 782–792.

Ulrey, R.K., Barksdale, S.M., Zhou, W., van Hoek, M.L. Cranberry proanthocyanidins have anti-biofilm properties against Pseudomonas aeruginosa. *BMC Complementary and Alternative Medicine.* **2014**, 14(1), 1-12.

Unusan, N. Proanthocyanidins in Grape Seeds: An Updated Review of Their Health Benefits and Potential Uses in the Food Industry. *Journal of Functional Foods.* **2020**, 67, 103861.

Valencia-Hernandez, L.J., Wong-Paz, J.E., Ascacio-Valdés, J.A., Chávez-González, M.L., Contreras-Esquivel, J.C., Aguilar, C.N. Procyanidins: From Agro-Industrial Waste to Food as Bioactive Molecules. *Foods.* **2021**, 10, 3152.

Vostalova, J., Vidlar, A., Ulrichova, J., Vrbkova, J., Simanek, V., and Student, V. Use of selenium–silymarin mix reduces lower urinary tract symptoms and prostate specific antigen in men. *Phytomedicine*. **2013**, 21(1), 75-81.

Walle, T.W., Walgren, R.A., Walle, K., Galijatovic, A., Vaidyanathan, J. Understanding the bioavailability of flavonoids through studies in Caco-2 cells. O*xidative Stress and Disease*. **2003**, 9, 349-362.

Wang, M., Carver, J.J., Phelan, V.V., Sanchez, L.M., Garg, N., Peng, Y., Nguyen, D.D., Watrous, J., Kapono, C.A., Luzzatto-Knaan, T., *et al.* Sharing and Community Curation of Mass Spectrometry Data with Global Natural Products Social Molecular Networking. *Nature Biotechnology.* **2016**, 34, 828–837.

Wang, Y., Alkhalidy, H., Liu, D. The Emerging Role of Polyphenols in the Management of Type 2 Diabetes. *Molecules.* **2021**, 26, 703.

Weiss, E.I., Kozlovsky, A., Steinberg, D., Lev-Dor, R., Bar Ness Greenstein, R., *et al.* A high molecular mass cranberry constituent reduces mutans streptococci level in saliva and inhibits in vitro adhesion to hydroxyapatite. *FEMS Microbiology Letters.* **2004**, 232(1), 89-92.

Wen, K.-S., Ruan, X., Wang, J., Yang, L., Wei, F., Zhao, Y.-X., Wang, Q. Optimizing Nucleophilic Depolymerization of Proanthocyanidins in Grape Seeds to Dimeric Proanthocyanidin B1 or B2. *Journal of Agricultural and Food Chemistry.* **2019**, 67(21), 5978-5988.

White, B.L., Howard, L.R., Prior, R.L. Release of Bound Procyanidins from Cranberry Pomace by Alkaline Hydrolysis. *Journal of Agricultural and Food Chemistry.* **2010**, 58, 7572–7579.

Wiese, S., Esatbeyoglu, T., Winterhalter, P., Kruse, H.P., Winkler, S., Bub, A., Kulling, S.E. Comparative biokinetics and metabolism of pure monomeric, dimeric, and polymeric flavan-3-ols: a randomized cross-over study in humans. *Molecular Nutrition and Food Research*. **2015**, 59(4), 610-621.

Wiles, T.J., Kulesus, R.R., Mulvey, M.A. Origins and virulence mechanisms of uropathogenic Escherichia coli. *Experimental and Molecular Pathology.* **2008**, 85(1), 11-19.

Wu, Y., Ma, N., Song, P., He, T., Levesque, C., Bai, Y., Zhang, A., Ma, X. Grape Seed Proanthocyanidin Affects Lipid Metabolism via Changing Gut Microflora and Enhancing Propionate Production in Weaned Pigs. *Journal of Nutrition.* **2019**, 149, 1523–1532.

Xie, Q., Bedran-Russo, A.K., Wu, C.D. *In vitro* remineralization effects of grape seed extract on artificial root caries. *Journal of Dentistry.* **2008**, 36(11), 900-906.

Xing, Y.-W., Lei, G.-T., Wu, Q.-H., Jiang, Y., Huang, M.-X. Procyanidin B2 protects against diet-induced obesity and non-alcoholic fatty liver disease via the modulation of the gut microbiota in rabbits. *World Journal of Gastroenterology*. **2019**, 25(8), 955–966.

Xue, B., Lu, Q.Y., Massie, L., Qualls, C., Mao, J.T. Grape seed procyanidin extract against lung cancer: The role of microrna-106b, bioavailability, and bioactivity. *Oncotarget.* **2018**, 9(21), 15579–15590.

Yahfoufi, N., Alsadi, N., Jambi, M., Matar, C. The Immunomodulatory and Anti-Inflammatory Role of Polyphenols. *Nutrients.* **2018**, 10, 1618.

Yamashita, Y., Okabe, M., Natsume, M., Ashida, H. Cinnamtannin A2, a tetrameric procyanidin, increases GLP-1 and insulin secretion in mice. *Bioscience, Biotechnology, and Biochemistry.* **2013**, 77(4), 888-891.

Yamashita, Y., Okabe, M., Natsume, M., Ashida, H. Comparison of anti-hyperglycemic activities between low- and high-degree of polymerization procyanidin fractions from cacao liquor extract. *Journal of Food and Drug Analysis.* **2012a**, 20(1), 39.

Yamashita, Y., Okabe, M., Natsume, M., Ashida, H. Prevention mechanisms of glucose intolerance and obesity by cacao liquor procyanidin extract in high-fat diet-fed C57BL/6 mice. *Archives of Biochemistry and Biophysics.* **2012b**, 527(2), 95–104.

Yang, H., Tuo, X., Wang, L., Tundis, R., Portillo, M.P., Simal-Gandara, J., Yu, Y., Zou, L., Xiao, J., Deng, J. Bioactive Procyanidins from Dietary Sources: The Relationship between Bioactivity and Polymerization Degree. *Trends in Food Science and Technology.* **2021**, 111, 114–127.

Yemis, O., Bakkalbasi, E., Artik, N. Antioxidative Activities of Grape (*Vitis vinifera*) Seed Extracts Obtained from Different Varieties Grown in Turkey. *International Journal of Food Science Technology.* **2008**, 43, 154–159.

Yu, Z.-J., Yan, H.-L., Xu, F.-H., Chao, H.-C., Deng, L.-H., Xu, X.-D., Huang, J.-B., Zeng, T. Efficacy and Side Effects of Drugs Commonly Used for the Treatment of Lower Urinary Tract Symptoms Associated With Benign Prostatic Hyperplasia. *Frontiers in Pharmacology.* **2020**, 11, 658.

Yuzuak, S., Ballington, J., Xie, D.-Y. HPLC-QTOF-MS/MS-Based Profiling of Flavan-3-Ols and Dimeric Proanthocyanidins in Berries of Two Muscadine Grape Hybrids FLH 13-11 and FLH 17-66. *Metabolites.* **2018**, 8, 57.

Zeng, Y.X., Wang, S., Wei, L., Cui, Y.Y., Chen, Y.H. Proanthocyanidins: Components, pharmacokinetics and biomedical properties. *American Journal of Chinese Medicine*. **2020**, 48(04), 813-869.

Zhang, A., Li, J., Zhang, S., Mu, Y., Zhang, W., Li, J. Characterization and Acid-Catalysed Depolymerization of Condensed Tannins Derived from Larch Bark. *RSC Advances.* **2017**, 7, 35135–35146.

Zhang, H., Jing, Y., Wu, G. Inhibitory Effects of Crude Polysaccharides from Semen Vaccariae on Benign Prostatic Hyperplasia in Mice. *Journal of Ethnopharmacology* **2013**, 145, 667–669.

Zhang, J., Liu, D., Wang, A., Cheng, L., Wang, W., Liu, Y., Ullah, S., Yuan, Q. Production of Oligomeric Procyanidins by Mild Steam Explosion Treatment of Grape Seeds. *Bioresources and Bioprocessing.* **2021a**, 8, 23.

Zhang, J., Zhang, M., Tang, J., Yin, G., Long, Z., He, L., Zhou, C., Luo, L., Qi, L., Wang, L. Animal Models of Benign Prostatic Hyperplasia. *Prostate Cancer and Prostatic Diseases.* **2021b**, 24, 49–57.

Zhang, L., Wang, Y., Li, D., Ho, C.T., Li, J., Wan, X. The absorption, distribution, metabolism and excretion of procyanidins. *Food and Function.* **2016**, 7(3), 1273-1281.

Zheng, Z., Tang, J., Hu, Y., Zhang, W. Role of Gut Microbiota-Derived Signals in the Regulation of Gastrointestinal Motility. *Frontiers in Medicine.* **2022**, 9, 961703.

Zhou, D.D., Li, J., Xiong, R.G., Saimaiti, A., Huang, S.Y., Wu, S.X., *et al*. Bioactive compounds, health benefits and food applications of grape. *Foods.* **2022**, 11(18), 2755.

Zhou, H., Lin, Y.M., Wei, S.D., Tam, N.F.Y. Structural diversity and antioxidant activity of condensed tannins fractionated from mangosteen pericarp. *Food Chemistry.* **2011**, 129(4), 1710–1720.

Zhou, L., Wang, W., Huang, J., Ding, Y., Pan, Z., Zhao, Y., Zhang, R., Hu, B., Zeng, X. *In Vitro* Extraction and Fermentation of Polyphenols from Grape Seeds (*Vitis Vinifera*) by Human Intestinal Microbiota. *Food and Function.* **2016**, 7, 1959–1967.

Zhou, X., Chen, S., Ye, X. The anti-obesity properties of the proanthocyanidin extract from the leaves of Chinese bayberry (*Myrica rubra* Sieb.et Zucc.). *Food and Function.* **2017**, 8(9), 3259–3270.

Zhu, H., Li, P., Ren, S., Tan, W., Fang, G. Low-Cost Ru/C-Catalyzed Depolymerization of the Polymeric Proanthocyanidin-Rich Fraction from Bark to Produce Oligomeric Proanthocyanidins with Antioxidant Activity. *ACS Omega* **2019**, 4, 16471–16480.

Zielinska, E., Baraniak, B., Karas, M. Antioxidant and Anti-Inflammatory Activities of Hydrolysates and Peptide Fractions Obtained by Enzymatic Hydrolysis of Selected Heat-Treated Edible Insects. *Nutrients.* **2017**, 9, 970.

Zumdick, S., Deters, A., Hensel, A. *In vitro* intestinal transport of oligomeric procyanidins (DP 2 to 4) across monolayers of Caco-2 cells. *Fitoterapia*. **2012**, 83(7), 1210-1217.